

Institut für Organische Chemie der Justus-Liebig-Universität Gießen

**Unsaturated Nanodiamonds:
Synthesis and Functionalization of Coupled Diamondoids as a Direct Route to
Nanometer-sized Building Blocks**

Inaugural-Dissertation zur Erlangung des Doktorgrades
der Naturwissenschaftlichen Fachbereiche
(Fachbereich 08 – Biologie und Chemie)
der Justus-Liebig-Universität Giessen

Vorgelegt von Tetyana V. Koso (geb. Rodionova), M. Sc.
aus Kiev, Ukraine

2013

Die vorliegende Dissertation wurde im Zeitraum von Oktober 2005 bis Oktober 2009 am Institut für Organische Chemie der Justus Liebig-Universität und von November 2009 bis Februar 2010 am Institut für Organische Chemie und Technologie der Kiev Politechniker unter der Leitung von Herrn Prof. Dr. Peter R. Schreiner, Ph. D. angefertigt.

Ich erkläre: Ich habe die vorgelegte Dissertation selbständig und ohne unerlaubte fremde Hilfe und nur mit den Hilfen angefertigt, die ich in der Dissertation angegeben habe. Alle Textstellen, die wörtlich oder sinngemäß aus veröffentlichten Schriften entnommen sind, und alle Angaben, die auf mündlichen Auskünften beruhen, sind als solche kenntlich gemacht. Bei den von mir durchgeführten und in der Dissertation erwähnten Untersuchungen habe ich die Grundsätze guter wissenschaftlicher Praxis, wie sie in der „Satzung der Justus-Liebig-Universität Gießen zur Sicherung guter wissenschaftlicher Praxis“ niedergelegt sind, eingehalten.

An dieser Stelle möchte ich Herrn Prof. Dr. P. R. Schreiner für die Anregungen zu diesem Thema, sein stetes Interesse am Fortgang dieser Arbeit, die ausgezeichneten Arbeitsbedingungen und zahlreichen fördernden Diskussionen danken.

To my parents...

This thesis is based on the following publications and manuscripts:

I. "*Oxygen-Doped Nanodiamonds: Synthesis and Functionalizations*"

Fokin, A.A., Zhuk, T.S., Pashenko, A.E., Dral, P.O., Gunchenko, P.A., Dahl, J.E.P., Carlson, R.M.K., Koso, T.V., Serafin, M., Schreiner, P.R. *Org. Lett.* **2009**, *11*, 3068-3071.

II. "*Synthesis and Structure of C_i -trans- C_s -8-trishomocubylidene- C_s -8-trishomocubane*"

Koso, T.V., Nguyen, D.L.N., Serafin, M., Schreiner, P.R., Fokin, A.A., Rodionov, V.N.
Manuscript in preparation.

III. "*Coupled Diamondoids: Preparation and Functionalization*"

Koso, T.V., Serafin, M., Hausmann, H., Fokin, A.A., Schreiner, P.R.
Manuscript in preparation.

Poster presentations:

Zhuk T.S.; Pashchenko A.E.; Koso T.V.; Osipov V.V.; Speka A.S.; Schreiner P.R.; Fokin A.A.
Preparation of higher oxydiamondoids. // II International conference of graduate students and young scientists on chemistry and chemical technology. Kiev, 22nd–24th of April 2009, p. 81.

Koso, T.V., Kovalenko, O.V., Fokin A.A., Schreiner, P.R. Synthesis of adamantylidenediamantane by McMurry procedure. (in Russian) // III International conference of graduate students and young scientists on chemistry and chemical technology. Kiev, 21st–23rd of April 2010, p. 89.

Zhuk, T.S., Kostyanoy, M.V., Pashenko, A.E., Dral, P.O., Gunchenko, P.A., Serafin, M., Dahl, J.E.P., Carlson, R.K.M., Koso, T.V., Schreiner, P.R., Fokin, A.A. Functionalization of heterodiamantanes. (in Russian) // XXII Ukrainian conference of organic chemistry, Uzhgorod, 20th–25th of September 2010, p. 182.

Koso, T.V., Kovalenko, O.V., Hausmann, H., Schreiner, P.R., Fokin, A.A. Structure of isomeric diamantylidenediamantanes. (in Russian) // XXII Ukrainian conference of organic chemistry, Uzhgorod, 20th–25th of September 2010, p. 304.

Table of Contents

Summary	i
Keywords	ii
Chapter 1. Introduction and State-of-the-Art	1
1.1. Diamondoids in modern science	1
1.2. Methods of synthesis of sterically hindered alkenes	6
1.2.1. The main methods of synthesis of sterically hindered alkenes	6
1.2.2. Synthesis of sterically hindered alkenes by McMurry procedure	10
1.3. Reactivity and functionalization of sterically hindered cage alkenes	21
1.4. Conclusions and Outlook	25
Chapter 2. Research objectives	26
Chapter 3. Results and Discussion	27
3.1. Synthesis of diamondoidyl ketones	27
3.1.1. Synthesis of diamantanone	27
3.1.2. Synthesis of triamantanones	28
3.1.3. Synthesis of diamantanediones	29
3.1.4. Synthesis of C ₅ -trishomocubane-8-one	30
3.2. Synthesis of the coupled diamondoids	36
3.2.1. Synthesis of adamantylideneadamantane	36
3.2.2. Synthesis of <i>anti</i> - and <i>syn</i> -diamantylidenediamantanes	37
3.2.3. Synthesis of adamantylidenediamantane-3	42
3.2.4. Comparison of used McMurry reductive coupling procedures	44
3.2.5. Synthesis of adamantylidenetriamantane-8	45
3.2.6. Synthesis of di(adamantylidene-2)diamantane-3,10	49
3.2.7. Synthesis of C ₅ -8-trishomocubylidene-C ₅ -8-trishomocubanes	51
3.2.8. Dispersion forces and the structure and stability of the selected diamondoid dimers	54
3.3. Functionalization of coupled diamondoids	65
3.3.1. Functionalization of <i>anti</i> -diamantylidenediamantane under PTC conditions	65
3.3.2. Functionalization of <i>syn</i> -diamantylidenediamantane under PTC conditions	74

3.3.3. Functionalization of adamantylideneadamantane	82
3.3.4. Functionalization of <i>anti</i> -diamantylidenediamantane with NBS	83
Chapter 4. Conclusions and Outlook	84
Chapter 5. Experimental part	87
5.1. Chemicals and solvents	87
5.2. Instruments and methods	87
5.3. General procedures	88
5.4. Synthesis	89
Appendix I Spectral data of synthesized compounds	108
Appendix II Crystal structures of selected synthesized compounds	144
Appendix III Cartesian coordinates of selected compounds (M06-2X/CC-pVTZ)	154
Appendix IV List of Symbols and Abbreviations	165
References	167
Acknowledgements	177

Summary

In the present doctoral thesis, a series of novel compounds containing diamondoidyl and homocubyl moieties and unsaturated spacers were prepared from respective cage ketones. The preparative procedures for the synthesis of diamantanone, triamantanones, diamantanediones and C_5 -trishomocubanone-8 were developed, reductive McMurry coupling of these ketones was studied and the preparative procedures were optimized. The functionalization of coupled diamondoids was performed in order to create new building blocks for potential nanoelectronic devices. For some of coupled diamondoids selective functionalization at tertiary carbon atoms of cage was performed with product separation and identification. The main results of this dissertation can be summarized as follows:

- Chapter 1 describes possible applications of nanodiamonds and reviews the methods of synthesis and functionalization of sterically hindered alkenes
- Chapter 2 describes the research objectives and main research goals
- Chapter 3 describes coupling and functionalization of diamondoids
 - 3.1. reports the synthesis of diamondoidyl ketones for their further coupling as well as cross-coupling
 - 3.2. describes the choice of the reductive coupling procedure for given diamondoidyl ketones, separation and characterization of products
 - 3.3. reports about functionalization of selected coupled diamondoids, as insight into their application for nanoelectronics
- Chapter 4 consists of conclusions and outlook of the current dissertation
- Chapter 5 provides experimental methods and procedures description and full characterization of all newly synthesized compounds

Keywords:

McMurry reaction, reductive coupling, sterically hindered alkene, diamondoid, adamantanone, diamantanone, triamantanone-8, triamantanone-16, diamantanedione-3,10, C_5 -trishomocubane-8-one *anti*-diamantylidenediamantane, *syn*-diamantylidenediamantane, adamantylidenediamantane-3, adamantylidenetriamantane-8, di(adamantylidene-2)diamantane-3,10, C_i -*trans*- C_5 -8-trishomocubylidene- C_5 -8-trishomocubane, 5-bromoadamantylidenediamantane, 4-bromo-*anti*-diamantylidenediamantane, *anti*-diamantylidenediamantan-2-ol, 4-bromo-*syn*-diamantylidenediamantane, *syn*-diamantylidenediamantan-2-ol.

Chapter 1. Introduction and State-of-the-Art

1.1. Diamondoids in modern science

Nanosciences are currently targeting new materials where carbon-based structures (nanotubes, fullerenes, graphenes and nanodiamonds) are among the most promising ones. The sizes of carbon nanostructure building blocks are now approaching the 1–5 nm scale that is already at the borderline between nanoparticles and single molecules.^[1, 2] The wide range of electronic properties in combination with high chemical stability makes diamond potentially most useful material for nanoelectronics and optics, as well as other fields of material sciences.

Nanodiamond is a mixture of compounds and of particle sizes^[3, 4] and is available from detonation residues or chemical vapor deposition (CVD).^[5] Recent studies on properties of nanodiamond showed that conduction band edge shifts to higher energies with decreasing of particle size.^[6, 7] This phenomenon is caused by quantum confinement effects and the particle size influences the exciton binding energies more pronouncedly than for other IV-group elements.^[8, 9]

Although pure diamond is an insulator, impurities if present in its structure provide semiconductivity^[10] or even superconductivity^[11, 12] thus allowing to vary electronic properties widely. On the other hand, twinning and stacking faults in diamond that are the most common defects that appear at the stage of nanodiamond formation are responsible for creating electronic traps and scattering centers for transferred charge carriers and distortions within band gap, thus making industrially available diamond materials unsuitable to many intended applications.^[13, 14] However, the surface inhomogeneities owing to presence of sp^2 carbons influence the surface conductivity decisively.^[15] The sp^3/sp^2 ratio may vary from ca. 0.3 (raw detonation sooth) to 4.3 (nanodiamond purified with acid)^[16] and the properties of such hybrid material are determined by stable graphite-like structures formed due to surface internal relaxation.^[17] These unsaturations are also partially responsible for diamond clustering.^[18, 19] While it is known that the band gap for bulk diamond is about 5.4 eV,^[20] its decrease with presence of the unsaturation on the surface was experimentally shown recently.^[21] In some cases unsaturations may be introduced artificially, *e.g.*, by the surface subjection to the E-beams that generate microscopic defects, caused by atomic displacement.^[22] Those unsaturations can serve not only as rigidity relaxants, but also diamond with high amount of sp^2 carbon phase exhibit emission at low threshold fields.^[23] It was reported that relative stability of carbon compounds strongly depends on their size: sp^3 hybridized carbon materials with a size of 2–5 nm are more stable than graphites.^[5] Thus, goal-seeking synthesis of diamond-like substrates with inclusion of

unsaturations as rigidity relaxants and conductivity sources is a perspective field of research.^[24, 25]

As already mentioned above, nanodiamond is a mixture of different particles and one of the challenges of its application is purification and functionalization. Typical purifications include direct fluorination,^[26] treating the nanodiamond powder with acids at high temperatures,^[27] or reductional quench with borane or lithium aluminum hydride.^[28] Further functionalization included, *e.g.*, photolysis of nanodiamond, covered with perfluoroazooctane for keto- and carboxy group,^[29] treating with benzoyl peroxides,^[27] silanization with further linkage to amino acids,^[30] or by reacting the fluoronanodiamond precursors with alkyllithium reagents, diamines or amino acids.^[26] Despite many attempts inhomogeneous nature of diamond materials is still of a problem and hampers to control surface functionalization.^[30]

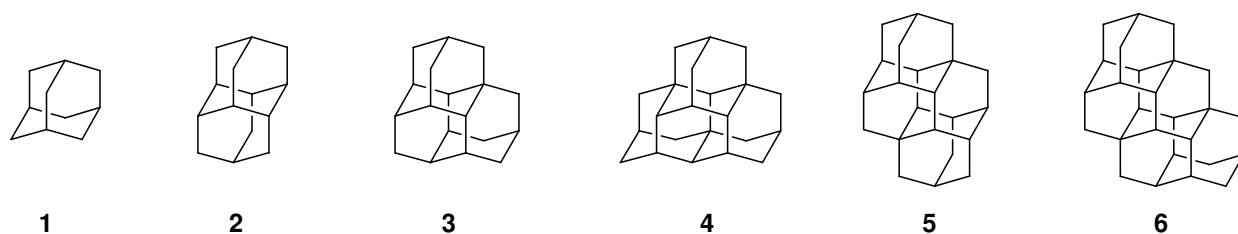


Figure 1. Selected diamondoids: adamantane (1), diamantane (2), triamantane (3), [1(2)3]tetramantane (4), [121]tetramantane (5) and [1212]pentamantane (6).

Lower (1–3) and higher diamondoids (4–6) (Fig. 1), which are now available in significant amounts from crude oil,^[31, 32] represent well-defined, monodispersed hydrogen-terminated homogenous nanodiamonds with particle sizes of 0.5–2 nm with a variety of shapes (*e.g.*, rod shaped [121]tetramantane (5), triangular [1212]pentamantane (6), etc.).^[33]

Readily available from natural sources diamondoids became objects of studies for their use for a large variety of applications. For instance, diamondoid ratios were proposed as fingerprint markers in a case of oil spills on water or land.^[34] Substituted diamondoids for application as lubricants with high viscosity index have been suggested.^[35, 36] Microelectronic devices, such as diamond-containing capacitors,^[37] diamondoid derivatives with polymerizable and hydrophilic-enhanced functionalities as photoresistants^[38] or low dielectric constant materials based on lower and higher diamondoids,^[39] which can be used as heat sinks in microelectronic packages, integrated circuit devices and multilevel interconnects have also been proposed. Such hydrocarbons also could spontaneously enter into wide diameter carbon nanotubes and, being constrained in such “containers”, they may form long “diamond wire”.^[40] Moreover, even narrow nanotubes are suitable for such purpose, as diamondoids were found to bind preferentially to its reactive open end. Perspective application of such cage hydrocarbons in

nanotechnology includes also atomic force microscope tips, signal waveform generators, molecular tachometers *etc.*^[41] Diamondoids have already found some application, for example, as templates for the crystallization of zeolite catalysts, different metal-organic frameworks and coordination polymers.^[42-44] Rigidity of the diamondoid cage made possible application of diamantane (**2**) as spacers in mechanochemical devices, like in molecular gyroscope (**7**).^[45]

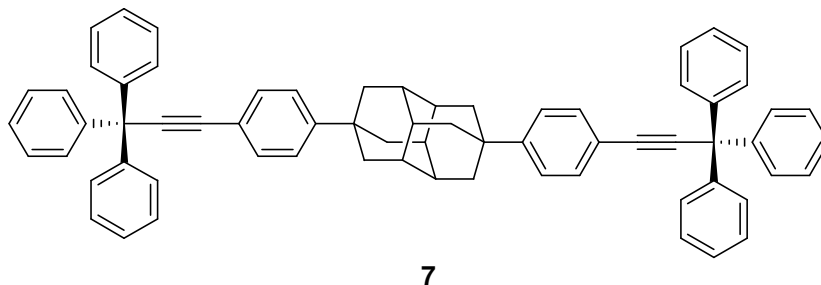


Figure 2. Molecular gyroscope (**7**) based on diamantane.

It was also reported that diamondoids with a size of less than 2 nm are used in nanooptics.^[7, 40] The host-guest complexes of functionalized diamondoids with γ -cyclodextrines recently have been investigated in detail.^[46]

Even simplest diamondoid – adamantane (**1**) – is widely used as a building block for many pharmacologically active compounds, *i.e.*, in drugs for treatment of Alzheimer's and Parkinson's diseases.^[47] Recently adamantane containing orally active drug SA13353 (**8**) was shown to exhibit inhibitory activity against lipopolysaccharide-induced TNF- α production, which plays an important role in the pathogenesis of inflammatory disease including rheumatoid arthritis, psoriasis and inflammatory bowel disease.^[48]

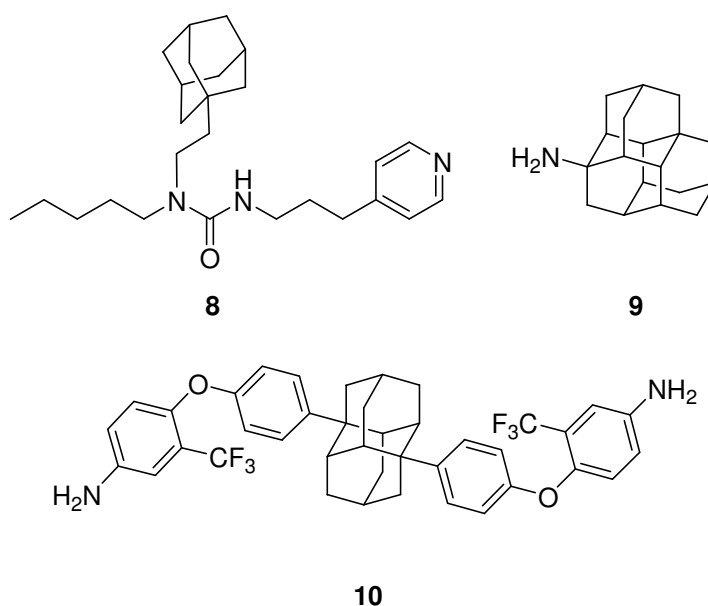
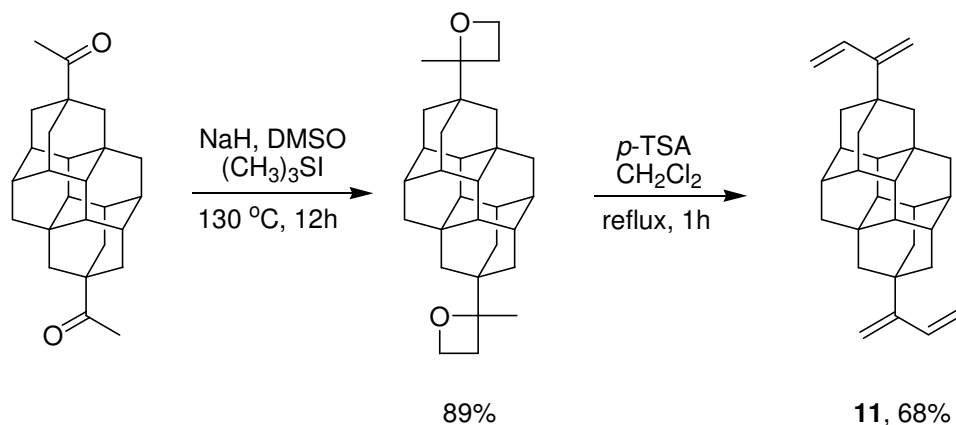


Figure 3. Example of potential diamondoid based drugs: SA13353 (**8**), 4-aminotriamantane (**9**) and 1,6-bis(4-(4-amino-2-trifluoromethylphenoxy)phenyl)diamantane (**10**).

Hypobetalipoproteinemic agents with a diamantyl moiety,^[49] as well as topological analogues of Memantine[®] – aminoderivatives of diamantane and triamantane (*e.g.*, **9**) – were obtained.^[50] Diamantane derivatives (*e.g.*, **10**) did not show anticancer activity,^[51] but further study of peptide-functionalized diamondoids is still of interest.

Copolymerization of methyl methacrylate with diamantyl methacrylate as well as homopolymerization of diamantyl methacrylate was accomplished and it was shown that introduction of diamantyl units enhances thermal stability and elevates the glass transition temperature significantly.^[52] Diamondoid-modified DNA were synthesized recently.^[53] Dithiol derivatives of diamondoids are also of interest as possible single-molecule conduction junctions and could act as switches, gates or charge-transporting elements.^[54, 55] Direct way to such dithiol derivatives would be through recently reported synthesis of diamondoids functionalized by 1,3-dienes.^[56]



Scheme 1.

Such compounds like bisdiene of [121]tetramantane (**11**) can be readily obtained from the respective ketones through oxetanes (Scheme 1). They also can be used for the formation of diamondoid self-assembling monolayers on silicon surfaces via a [4+2] cycloaddition.^[57]

Thus, there is indeed need in the diamondoid particles functionalized selectively that would serve to the growing number of purposes. As it was mentioned above, the electronic properties of nanodiamonds depend on their size.^[5] The surface of diamondoid clusters, based on sp^3 carbons, has to be stabilized by terminal groups or reconstructed into sp^2 carbon.^[58] Another limitation introduced previously showed that as the size of diamond particle reaches 2-3 nm or more, at low temperatures bucky diamonds become energetically preferred over hydrogenated nanodiamond as was shown by theoretical computations and by means of X-ray absorption.^[7] Results of modelling nanodiamonds terminated with functional groups containing oxygen^[59] and nitrogen^[60] indicated that different substituents exhibit reaction affinity to

different nanodiamond facets. Importantly, it was also found that it is likely to be possible to selectively functionalize nanodiamonds with amino groups by desorption temperature control.^[60]

Theoretical studies suggest that diamondoids possess the key spectral and electronic properties of bulk hydrogen-terminated diamond.^[40] Important characteristic of the hydrogen-terminated diamond surface is a low threshold field emission that is associated with negative electron affinity (NEA).^[61, 62] The NEA of bulk diamond is one of the key factors that determine its insulator properties and it opens up the possibility of coating surfaces with diamondoids to produce new electron-emission devices.^[63] Several theoretical predictions were verified experimentally, for instance, pronounced NEA properties were found for self-assembled monolayers of [121]tetramantane-6-thiol (**12**) on gold surfaces.^[64, 65]

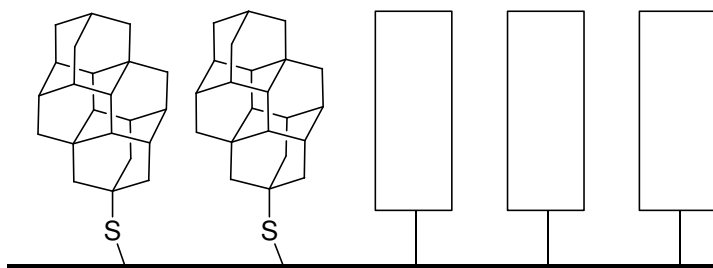


Figure 4. Schematic image of [121]tetramantane-6-thiol (**12**) monolayer on gold surface (black).

Later near-edge X-ray absorption fine structure spectroscopy was used to determine molecular orientation in such monolayers of higher diamondoids, hydrocarbon molecules with cubic-diamond-cage structures.^[66] Those monolayers have been found to be excellent source of short-termed electron bunches.^[67] However, diamondoids only up to hexamantanes (particle size of 0.6 nm) or pentamantanes (particle size of 0.75 nm for the rod-shaped [1212] isomer (**6**)) are available in sizable quantities from oil. Thus, obtaining larger diamondoid particles up to the sizes of 1–5 nm to explore the limits of diamond nanostructure applications in nanoelectronics for which theory predicts the existence of quantum confinement effects^[68] is currently problematic. This challenge may be addressed by coupling lower diamondoids with various spacers. This approach was already successfully applied for fullerene where particles of about 10 nm dimensions could be obtained by bifunctional cycloaddition of fullerene precursors.^[69] Various spacers will affect the optical and electronic properties of such diamondoid assemblies. While conjugated unsaturated spacers allow facile electron conduction, rigid saturated spacers often provide higher chemical stability.^[70] Coupling reactions with the formation of double bonds between diamondoids is a promising way of combining unsaturation with structure rigidity.

Thus, summarizing the above, diamondoid assemblies have to meet certain requirements to resemble nanodiamond particles such as: 1) sizes of several nm; 2) well-defined shapes; 3) rigidity; 4) effective communication between fragments of the structure through the spacer; 5) repeating C–H units on the surface. Thus, particular goal of our work is compilation of various diamondoid cages through certain unsaturated spacers (Fig. 5).

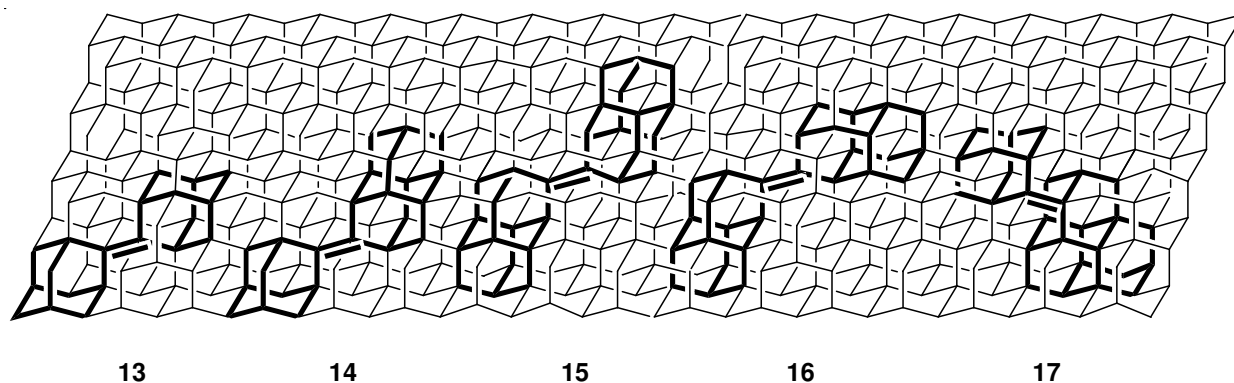


Figure 5. Examples of diamondoid assemblies.

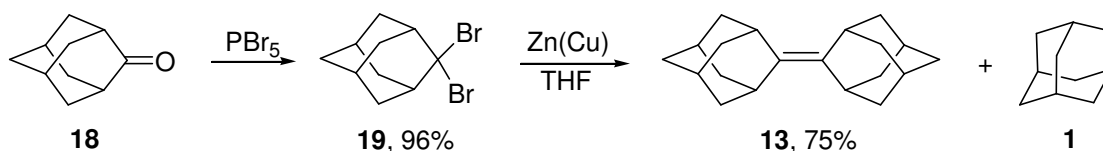
Such assemblies would represent truly new type of building blocks that bridge the gap between the sp^2 and sp^3 carbon world. Delocalization of charge through double bonds on the diamondoid cage would stabilize such compounds, comparable to the common ethylene and allene polymers. We also develop selective functionalizations of diamondoids that allow introduction of substituents.

1.2. Methods of synthesis of sterically hindered alkenes

1.2.1. Preparation of sterically hindered alkenes

Only a limited number of synthetic approaches is applicable for preparation of sterically hindered alkenes. Traditionally, those methods are based on formation of cage skeleton with simultaneous introduction of multiple bond, *i.e.*, dimerization of ketones or their derivatives. Numerous modifications of these methods expanded their applicability and made many sterically hindered alkenes available. Another way to strained alkenes is the Diels-Alder synthesis. For some others the original schemes of synthesis were developed, including elimination, usage of sulfur- and nitrogen-containing groups, involving organometallic reagents and others. Given the variety of synthetic approaches to title alkenes, this literature review will address only the most common of them.

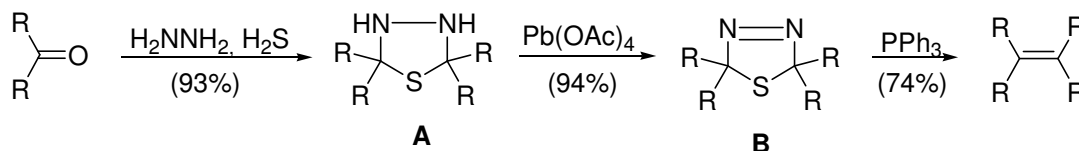
Synthesis of one of the most well-known sterically hindered cage alkene and also the simplest coupled diamondoid – adamantylideneadamantane (**13**) – was carried in two steps, based on adamantanone (**18**) (Scheme 2).^[71]



Scheme 2.

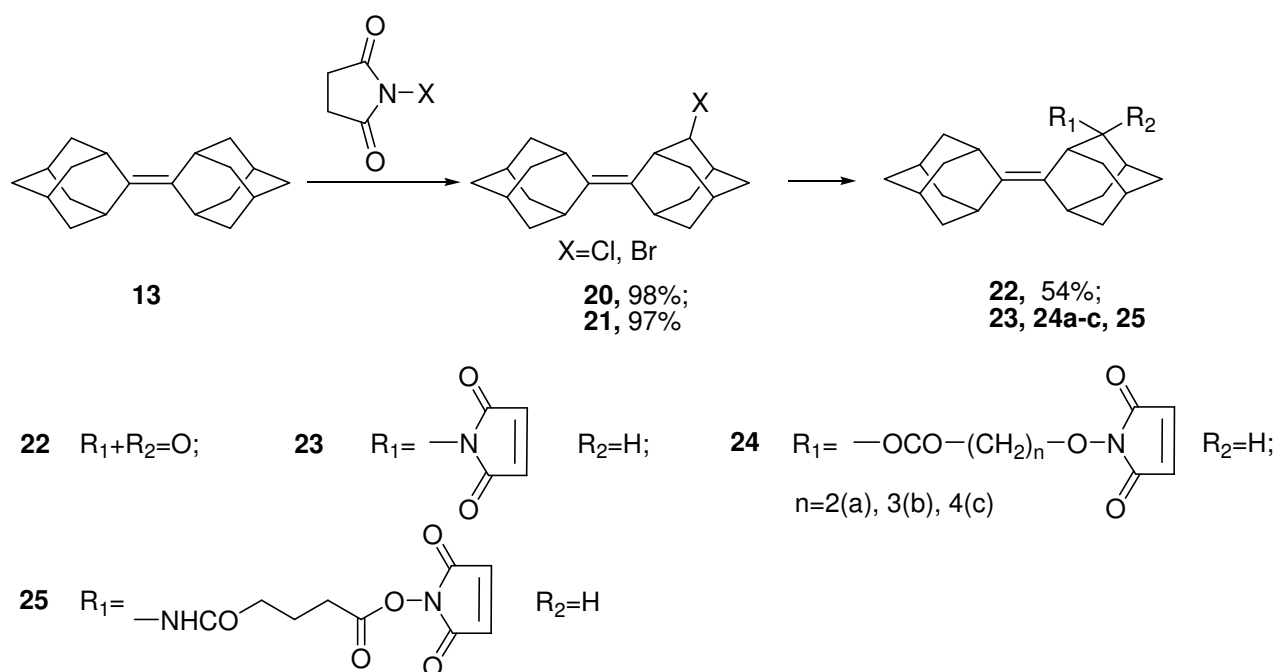
This carbenoid method was used as a preparative for a long time. The yield of **13** is lowered (60–75%) due to reduction of dibromide (**19**) to adamantane (**1**) and strongly depends on the quality of zinc and activity of the zinc-copper pair. Using magnesium instead of zinc increase the yield of alkene **13** to 83%.^[72] Through this scheme also olefin with twisted double bond, *trans*-(2-phenyladamantylidene)-2-phenyladamantane, was synthesized.^[73]

Tiadiazoline method is based on the double extrusion,^[74] – elimination of nitrogen and sulfur from various reagents with general formula **B** (Scheme 3). Yield of **13** through this method is the same as through the carbenoid one.^[75]



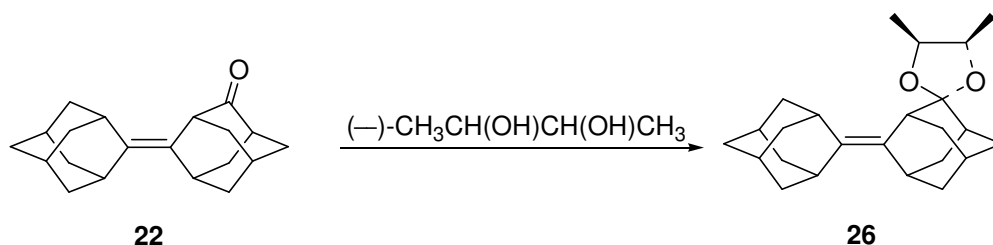
Scheme 3.

Some 4-substituted adamantylideneadamantanes were obtained from **13** by halogenation to form respective 4(e)-halogenderivatives^[76-79] and further synthetic transformations in the side chain. In this way ketoalkene **22**,^[76] maleic iminoderivatives **23**, **24 a–c** and **25**^[80] were obtained (Scheme 4).



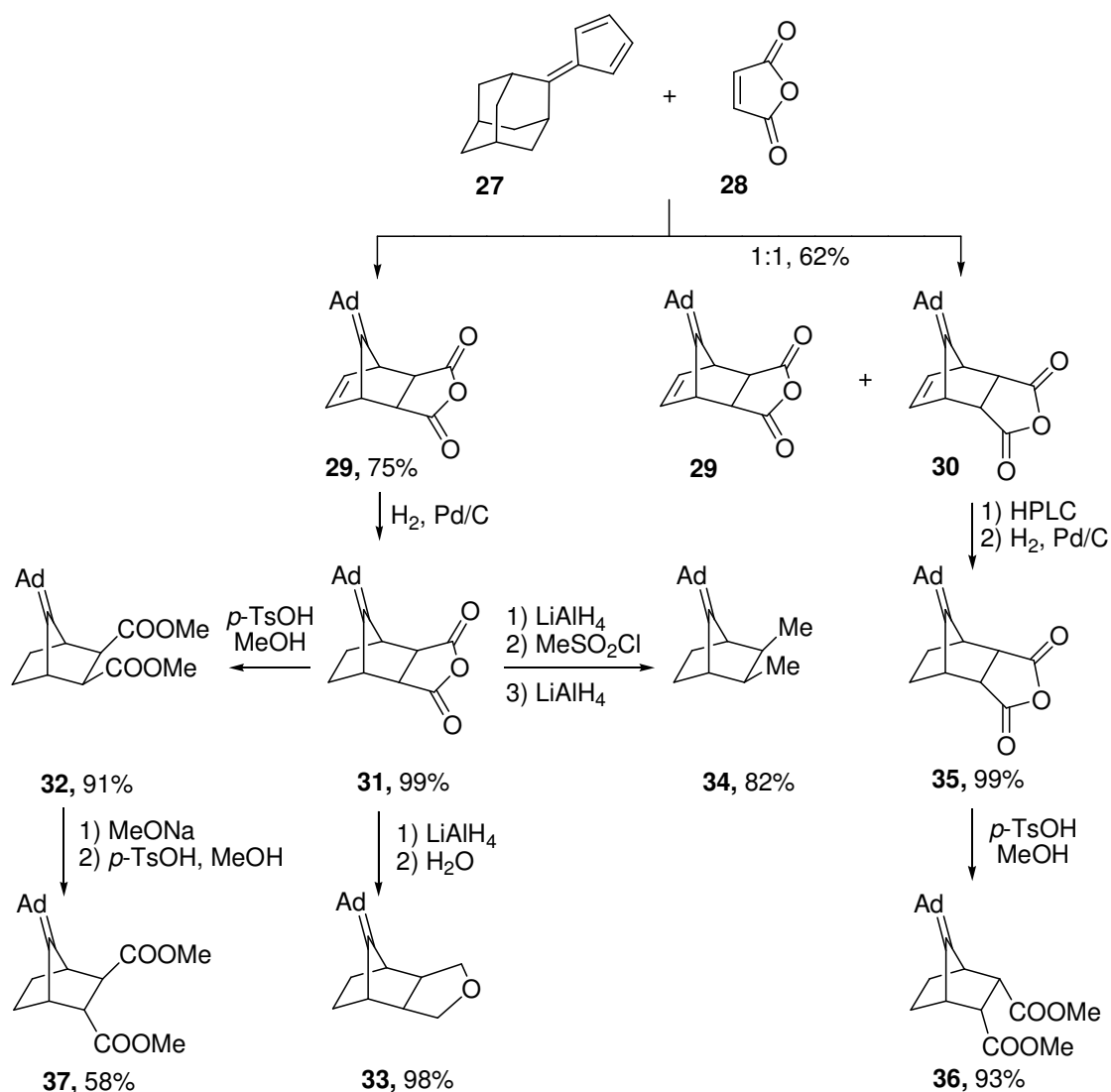
Scheme 4.

From ketoalkene **22** and optically active (–)-2,3-butanediol the mixture of diastereomeric ketals (+)-**26** and (–)-**26** was obtained. Ketal (–)-**26** was isolated, utilizing preparative GLC, with nearly quantitative yield and optical purity of 95% (Scheme 5).^[81]



Scheme 5.

The series of isomeric 2,3-disubstituted 7-adamantylenenorbornanes was synthesized as shown below, including the cycloaddition of cyclopentadienylideneadamantane (**27**) to maleic anhydride (**28**) (Scheme 6) for the further estimation of alkene structure effect on reaction of SCl_2 with sterically hindered olefins:



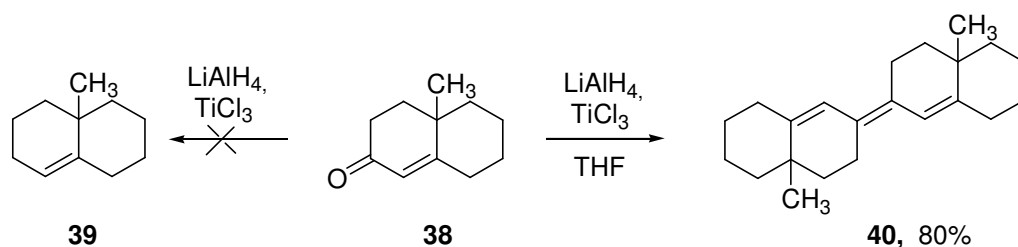
Scheme 6.

At temperature of 80 °C *exo*-adduct **29** formed exclusively whereas at 20 °C – a mixture of *exo*- and *endo*-isomers **29** and **30** form in a 1 : 1 ratio. Separation of *endo*-isomer **30** from the mixture through preparative HPLC resulted in alkenes **35** and **36**, functionalized alkenes **31-34** were obtained from *exo*-**29**. Isomerization of *exo*-diester (**32**) afforded *exo,endo*-diester (**37**).^[82] There is one drawback in the above examples of the syntheses of sterically hindered diamondoid alkenes – then involve at least two stages, include expensive reagents and characterized by low yields of target products.

1.2.2. Synthesis of sterically hindered alkenes through the McMurry procedure

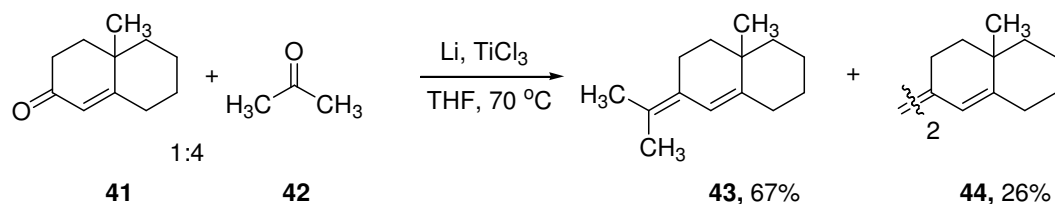
Based on the above we conclude that synthesis of coupled diamondoids from carbonyl compounds through the McMurry reaction, using titanium reagents that provide access to the target compounds, is the most promising.

Titanium-induced coupling of carbonyl compounds was accidentally found by the group of McMurry in 1974 while searching for a new method of reduction of α , β -unsaturated ketones, such as **38** to the corresponding alkene **39**.^[83, 84] Their initial idea was to conduct a hydride reduction of carbonyl group in the presence of oxophilic transition metal, which could strongly coordinate to the alkoxyl group of the intermediate and promote secondary hydride reduction to form a product that contains no oxygen. However, under these experimental conditions in the presence of lithium aluminum hydride as a strong hydride donor and titanium (III) chloride as oxophilic reagent the product of reductive coupling **40** was obtained (Scheme 7).



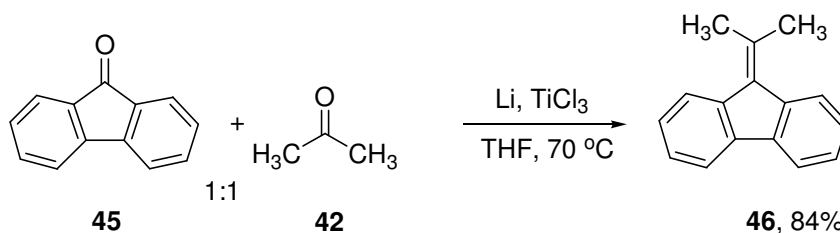
Scheme 7.

Two other research groups discovered similar transformations almost simultaneously,^[85, 86] and the potential significance of this reaction was noted immediately. The initial research in this area shows the applicability of this approach to a wide range of carbonyl compounds, including saturated, unsaturated and aryl containing aldehydes, ketones and diaryl ketones.^[87] Initially synthesis of acyclic compounds was limited to symmetric alkenes, but this was later overcome (Scheme 8):^[87]



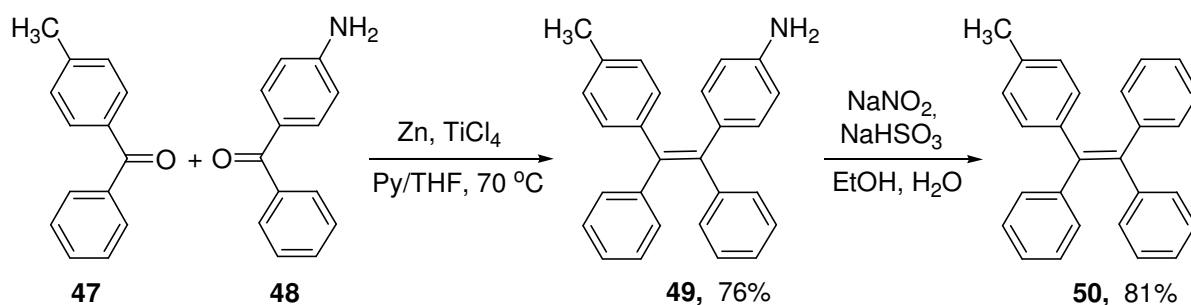
Scheme 8.

With carbonyl substrates of different redox potentials coupling products were obtained quantitatively, without excess of one of the substrates. This result was quite unexpected, on the relative ease at which bisaryl ketone must pass ketyl transformation, accompanied by an independent pinacol coupling. In fact it was one of the first results, which showed that McMurry reaction can occur through different mechanisms.^[87] In this case diaryl ketone can be selectively reduced to the dianion, which then reacts with the nucleophilic unsaturated ketone (Scheme 9):



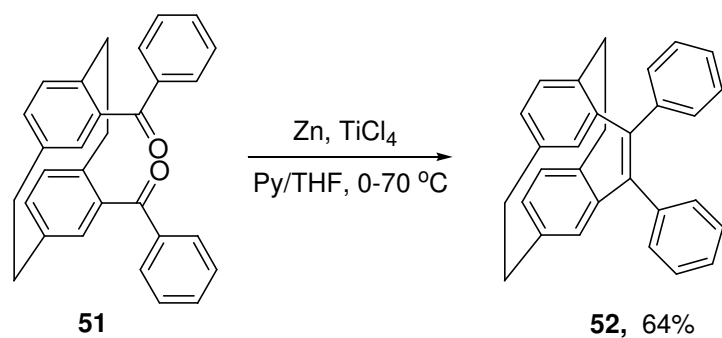
Scheme 9.

In follow-up research of heterocoupling of aryl or diaryl ketones^[88] it was suggested that the presence of heteroatoms in one of the reactants increases its affinity to the surface of titanium, where the reaction takes place. The binding of substrates deactivates the surface of titanium and inhibits homocoupling. This increases the selectivity of formation of heterocoupling product **49**. Removal of the directing groups can lead to more symmetric heterocoupling products, *e.g.*, **50** (Scheme 10).



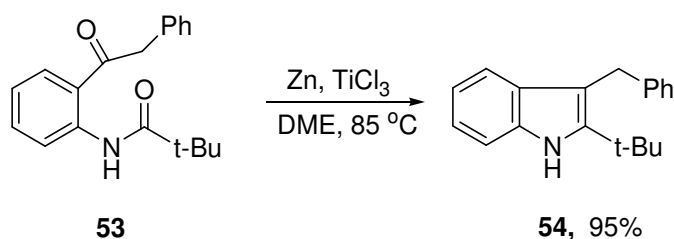
Scheme 10.

The reproducibility of the coupling reaction was repeatedly demonstrated in the synthesis of unusual ring structures, such as the key intermediate in the synthesis of three-bridged cyclophanes (Scheme 11).^[89]



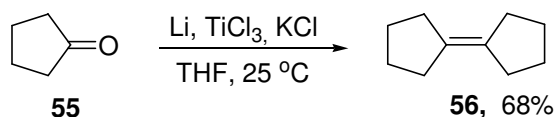
Scheme 11.

The first efforts^[90] to replace titanium for other transition metals failed. Other sources of low-valent titanium were investigated as well. Later the variations based on different combinations of this reagents, including titanium (III) chloride – potassium,^[91] titanium (III) chloride – lithium^[92] and titanium (III) chloride – zinc-copper in dimethoxyethane were suggested.^[93] In each case the reaction was carried out in two phases where the titanium chloride and reductant reacted before the introduction of the carbonyl substrate. A breakthrough in the application of low-valent titanium occurred in 1994 when one-step "instant" method of synthesis of alkylsubstituted indoles was described.^[94] In this case active titanium species are generated by the coordination of carbonyl substrate with titanium (III) chloride and subsequent reduction of this complex by zinc dust. This one-step process is effective only when the reducing agent is weak enough not to reduce the carbonyl group. By this method indole **54** has been synthesized from oxamide **53** with high preparative yield (Scheme 12). The same method was used for the synthesis of furanes and other heterocycles.^[95]



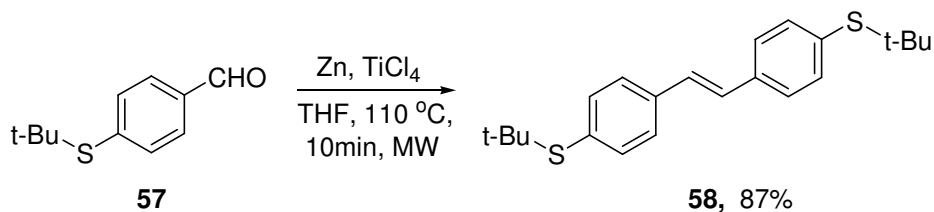
Scheme 12.

It was also discovered that the addition of salts of alkali and alkaline earth metals activates the titanium reagent.^[96] The authors suggested that the replacement of lithium with more electropositive metal cations such as potassium increases the electron density of titanium and can enhance the activity of intermetallic titanium complex (Scheme 13).



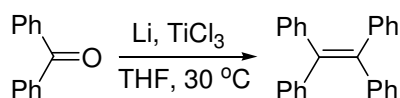
Scheme 13.

Microwave heating also reduces the time of normal McMurry reaction, which usually requires more than 2 h to complete (Scheme 14).^[97]



Scheme 14.

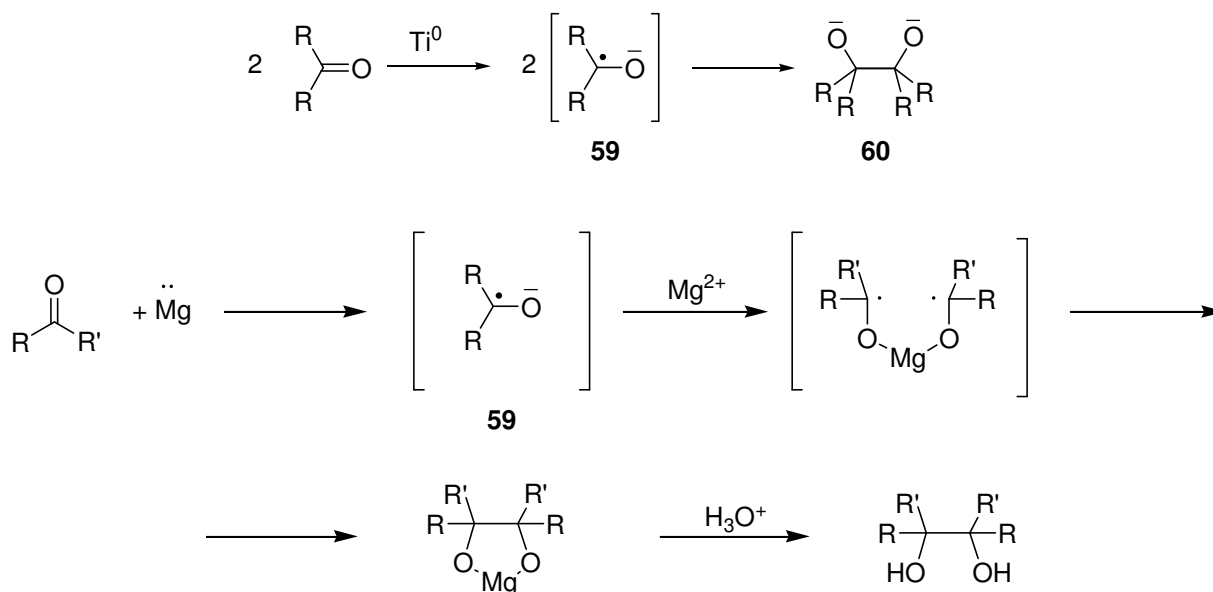
Ultrasound also promotes the coupling of aromatic aldehydes and ketones at lower temperatures (Scheme 15).^[98]



Scheme 15.

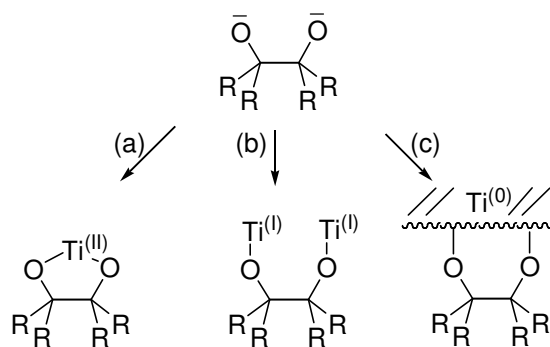
Mechanism of McMurry reaction. Combinations of reagents used for McMurry reaction in heterogeneous systems, complicate determination of the structure of intermediates and oxidation states of titanium, which changes during the reaction. However, in recent years significant progress in mechanistic studies was achieved.

Active metals are known to react with aldehydes and ketones with formation of anion-radicals, which subsequently dimerize to form pinacols. The latter may be separated as reaction products after the hydrolysis of reaction mixture. Pinacol step, which involves one-electron oxidation of titanium complex to form ketyl **59**, is followed by dimerization (formation of carbon-carbon bonds), resulting the intermediate – pinacolate dianion **60**, in contrary to classic pinacol coupling reaction, where ketyl **59** reacts with metal cation (Scheme 16).^[99]



Scheme 16.

McMurry suggested three general mechanisms: a) through cyclic transition structure (TS) with titanium; b) acyclic TS involving two titanium atoms, c) mixed mechanism, where both oxianions coordinate on the surface of fine titanium, which formed as a result of titanium (III) chloride reduction (Scheme 17).^[87]

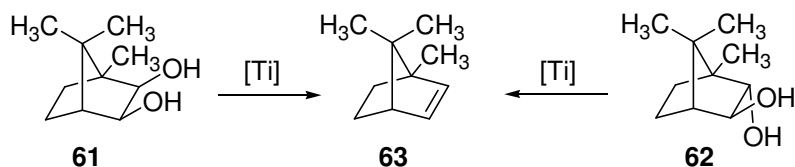


Scheme 17.

In any case, cleavage of two carbon-oxygen bonds proceeds through a radical mechanism to give alkene and titanium oxide. The fact that this mechanism could not be consistent, demonstrated by the formation of the configurationally pure diols in a mixture of *E*- and *Z*-alkenes during the reaction under such conditions.^[87]

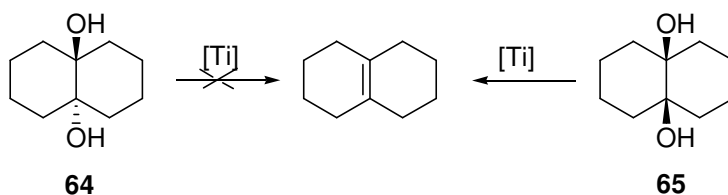
To identify possible ways a-c, two mechanistic studies were performed. It was found that both isomeric camphanediols – *cis*-camphanediol (**61**), which readily forms five-membered metallocycles and *trans*-camphanediol (**61**), which does not form them at all react under the

McMurry reaction conditions with the same rate forming camphene (**63**) (Scheme 18). This result allows to exclude path a.



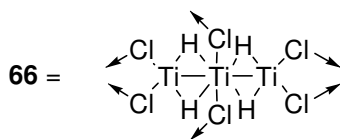
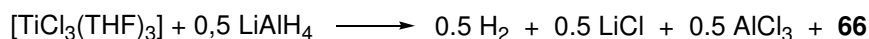
Scheme 18.

It was also found that *trans*-9,10-decalindiol (**64**) is inert to titanium under the conditions where *cis*-9,10-decalindiol (**65**) reacts easily. This result allows to exclude path b in favor of the path, that requires the participation of the surface of titanium in the reaction (Scheme 18). Path c – the only reasonable alternative, and this mechanism have found strong experimental confirmation^[100] (Scheme 19).

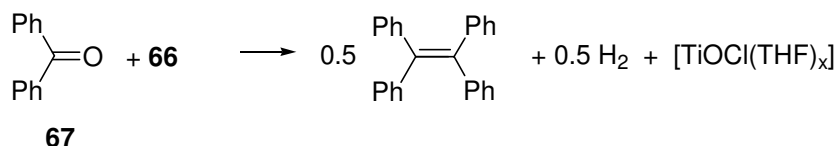


Scheme 19.

Further research showed that the presence of titanium (0) is not a requirement for the McMurry reaction. Indeed, pinacoline bonding can be conducted in the presence of titanium (II) and without the involving the complexes of titanium (0).^[101] Additionally, reductive coupling of benzaldehydes in the gas phase on the surface of titanium dioxide was carried out, where also absence of titanium (0) was proven by X-ray photoelectron spectroscopy.^[102] Finally, the hydrochloric complex of titanium (II) (**66**) was prepared independently in accordance with equation^[103] (one of possible structures shown) (Scheme 20) and was found to be active in reductive coupling of benzophenone (**67**) (Scheme 21):



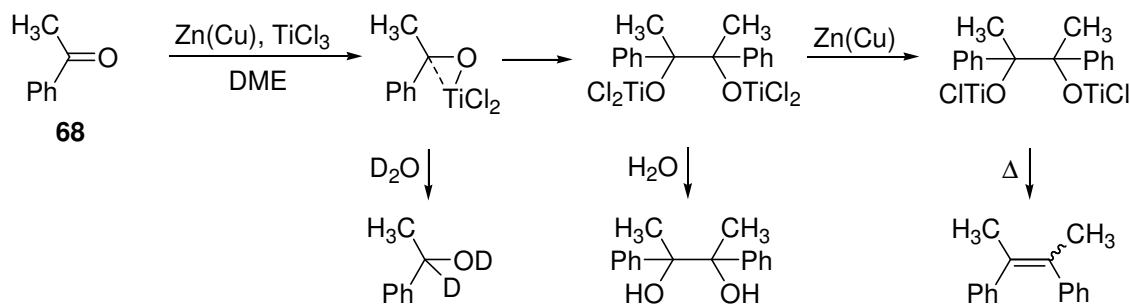
Scheme 20.



Scheme 21.

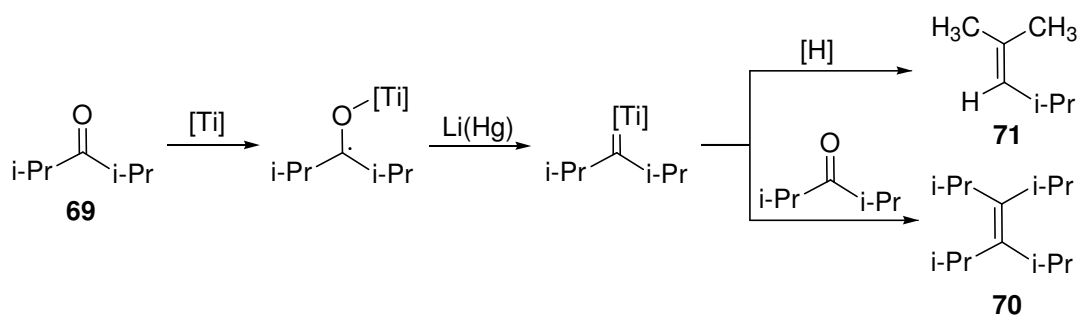
This result demonstrates that the McMurry reaction with one of the most popular sets of reagents titanium (III) chloride – lithium – tetrahydrofuran is associated with the changes in the oxidation state of titanium only between titanium (I), titanium (II) and titanium (III), and titanium (0) is not needed to be involved.^[104]

The proposed mechanism of pinacolate formation also have been doubted by analysis of the coupling reaction of acetophenone (**68**) in the presence of titanium (III) chloride – zinc (copper) in dimethoxyethane (Scheme 22).^[105]



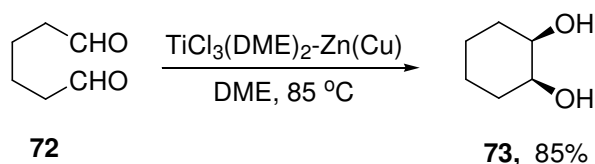
Scheme 22.

Quantum-chemical computations at the B3LYP density functional theory (DFT) level showed^[105] that this reaction path is energetically more favorable than the corresponding ketyl path. Based on the coupling of sterically hindered systems, evidence for a mechanism that does not proceed via pinacol intermediates rather through the intermediate carbenes was found.^[106] In the reaction of diisopropyl ketone (**69**) and titanium (IV) chloride – lithium (quicksilver) two products were observed: the expected alkene **70** and alkene **71**, whose formation can be explained only by intermediacy of carbenoids (Scheme 23). Lack of pinacolone product and the observation, that titanium pinacolate intermediate is unstable and readily decomposes to carbonyl compounds and titanium chloride, supports suggested mechanism. Similar evidence was obtained with di-*tert*-butylketone coupling.^[107]



Scheme 23.

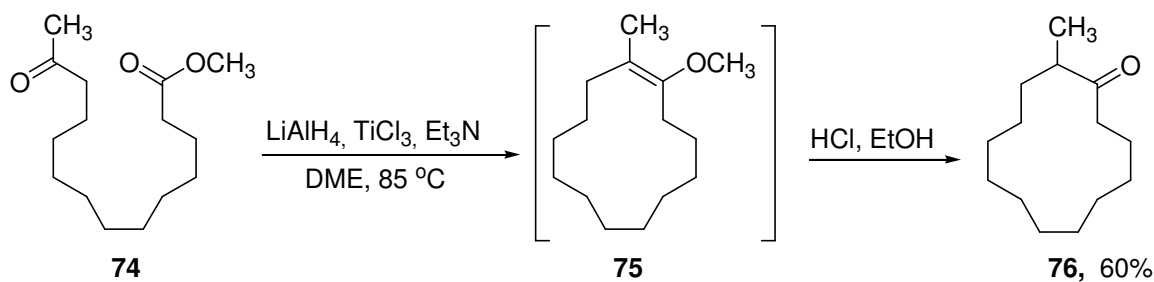
To complete the deoxygenation reaction elevated temperatures are required, *e.g.*, refluxing tetrahydrofuran. As a result at room temperature or below, pinacolone intermediates can be separated. Meanwhile, due to intermediates complex formation the intramolecular couplings are *cis*-diastereoselective (Scheme 24).^[108]



Scheme 24.

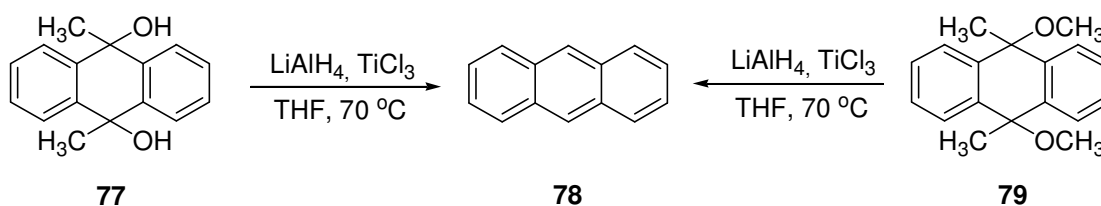
Diastereoselectivity in catalytic pinacolone coupling of aromatic aldehydes is usually much higher.^[109] In recent work on the enantioselective coupling of aromatic aldehydes enantioselectivity above 90% was observed.^[110, 111]

One of the first versions of the traditional McMurry coupling is transformation of ketoesters to enol ethers. This method can be applied for synthesis of large rings, albeit with lower yields, where the resulting cyclic enol ether **75** can hydrolyze to cyclic alkanone **76** (Scheme 25).^[112]



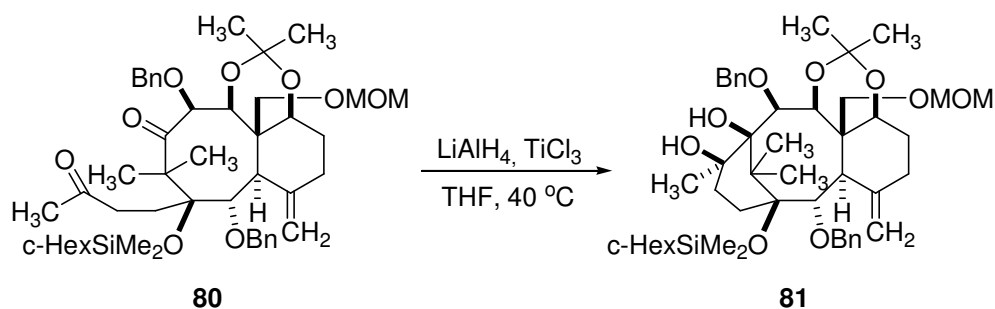
Scheme 25.

Under the McMurry reaction conditions aromatic 1,4-diol **77** and its dimethyl ether **79** give aromatic system **78** quantitatively (Scheme 26).^[113]



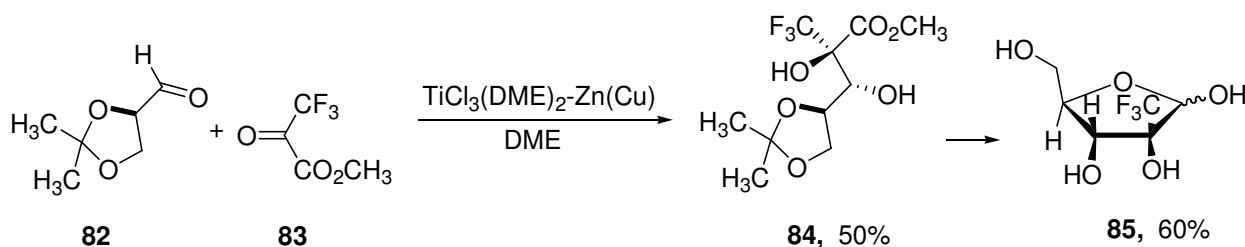
Scheme 26.

In synthesis of 19-hydroxytoxoid (**81**) – intermediate for anticancer drug 19-hydroxytoxole intramolecular pinacol coupling of diketone **80**^[114] have been performed at sufficiently low temperature to ensure separation of intermediate diol (Scheme 27).



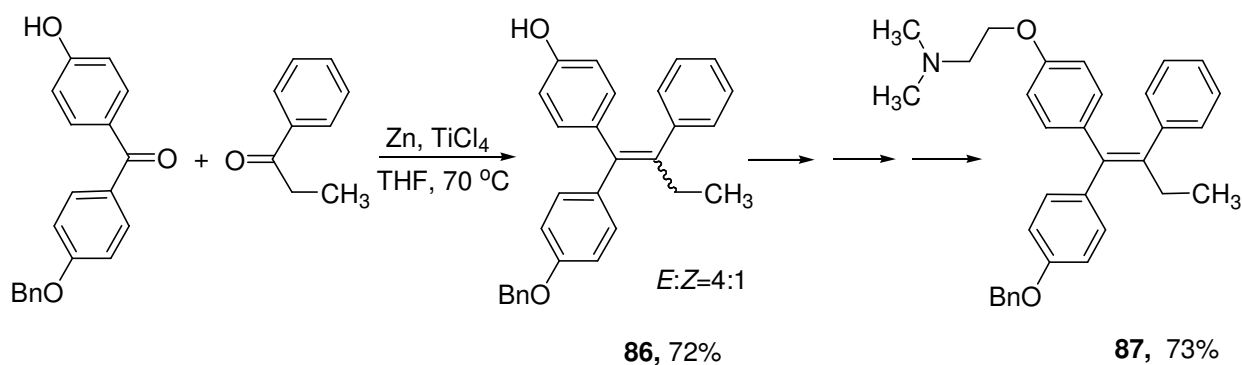
Scheme 27.

Pinacol coupling may occur with stereochemical induction on neighboring stereogenic carbon atoms. For example, the diastereomer **84** is a main product of the cross-coupling reaction of aldehyde **82** and ketone **83**^[115] along with the homocoupling product of **82**. This approach was used in the synthesis of 2-C-trifluoromethylsubstituted *D*-ribose (**85**) (Scheme 28).



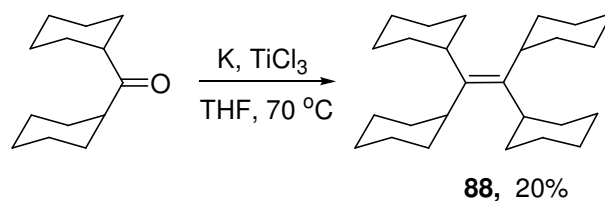
Scheme 28.

Stereoselective McMurry coupling was used in the synthesis of *E*-isomer of compound **86** – intermediate for the synthesis of *Z*-4-hydroxytamoxifen (**87**), an active metabolite of antitumor drug Tamoxifen.^[116] To control the unproductive homocoupling reduction triple molar excess of propiophenone was used (Scheme 29).



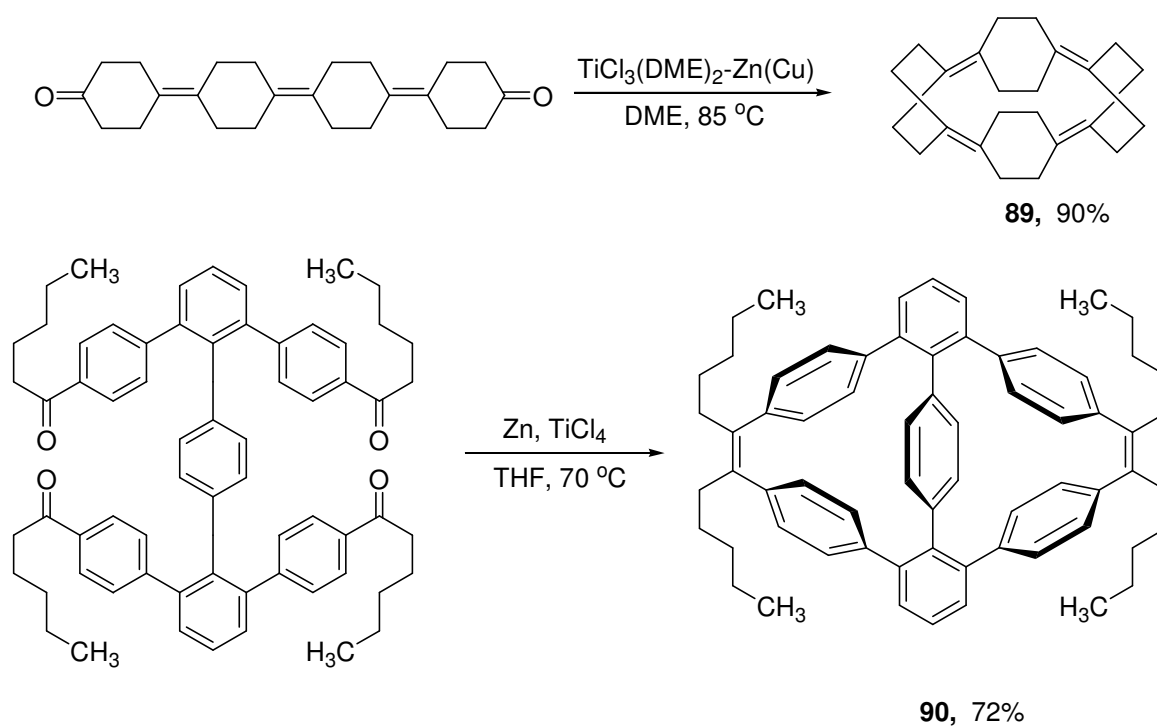
Scheme 29.

McMurry reaction is often used in the synthesis of highly strained theoretically interesting alkenes. For example, the rotational barrier of cyclohexyl rings in alkene **88** according to the dynamic NMR is 78.2 kJ•mol⁻¹ (Scheme 30).^[117]



Scheme 30.

Spherand **89** has an internal surface with a high electron density and was synthesized to bind silver ions in organometallic complexes.^[118] Receptor **90**, synthesized in accordance with Scheme 31, is able to bind the Ag(I) ion, which oscillates between two adjacent cavities in a molecule.^[119]



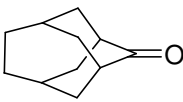
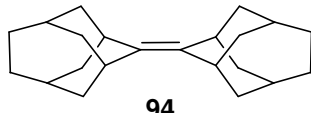
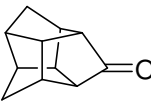
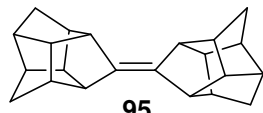
Scheme 31.

Application of McMurry reaction for synthesis of caged sterically hindered alkenes is summarized in Table 1.

Table 1.

Syntheses of sterically hindered alkenes by McMurry coupling

Reagent	Product	Titanium reagent	Yield, %
	 13	$\text{TiCl}_3\text{-LiAlH}_4$	85 ^[83]
		$\text{TiCl}_3\text{-K}$	82 ^[87]
		$\text{TiCl}_3\text{-Li}$	91 ^[87]
		$\text{TiCl}_4\text{-Zn}$	98 ^[120]
	 91	$\text{TiCl}_3\text{-K}$	52 ^[121]
	 92	$\text{TiCl}_3\text{-K}$	40 ^[122]
	 93	$\text{TiCl}_3\text{-K}$	45 ^[123, 124]

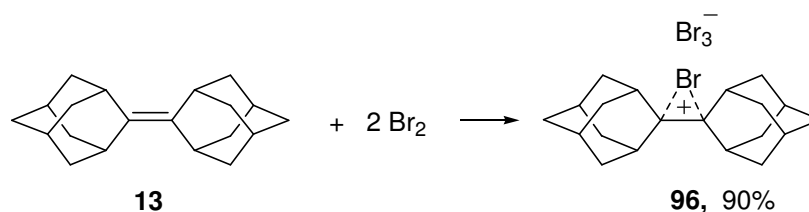
		$\text{TiCl}_3\text{-K}$	40 ^[125]
		$\text{TiCl}_4\text{-Zn}$	50 ^[126]

Note that in case of compounds **91** and **92** high stereoselectivity of reaction is observed as only *trans*-isomers are formed.

1.3. Reactivity and functionalization of sterically hindered cage alkenes

Selective functionalization of natural hydrocarbons and particularly diamondoids is often characterized by low selectivity and leads to the mixture of products. Activation of the C–H bond by different mechanisms is the key to the selectivity in formation of desired products.^[127, 128] In Nature functionalization processes are run by enzymes such as cytochrome P450,^[129] methane monooxygenase.^[130, 131] Selective functionalization in laboratory conditions was significantly developed in recent years, even is still that of a challenge.^[50, 132-136]

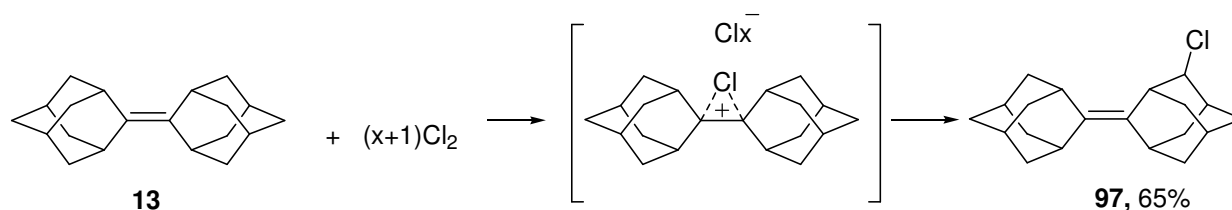
Reaction of adamantylideneadamantane (**13**) with bromine results in formation of unusual addition product – stable bromonium salt **96** (Scheme 32).^[137] Structure of **96** was confirmed by crystal X-Ray analysis^[138] and became a real scientific sensation as it confirmed existence of cyclic intermediates in the reaction of alkene bromination.^[139, 140] Later theoretical study showed that indeed the activation energy is significantly lower for the reaction of **13** with 2 Br₂ as compared to the reaction with a single Br₂, and second bromine assists the ionization of the reactant complex.^[141] The reactivity of adamantylideneadamantane towards Br₂ in solution was also studied^[142, 143] as well as the π -complexation of Br₂ with homoallylic adamantylideneadamantane derivatives.^[144, 145]



Scheme 32.

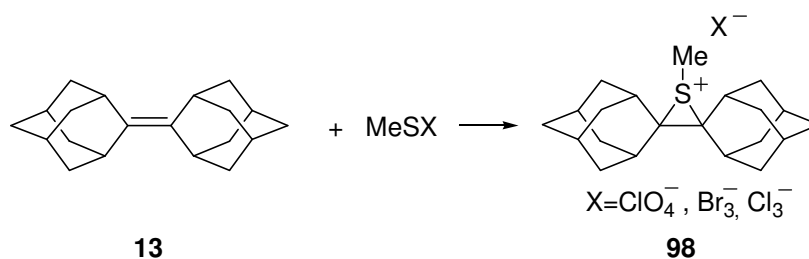
In the reaction of *trans*-1,1'-dimethyladamantylideneadamantane with bromine adduct of content $C_{11}H_{32}Br_4$ – insoluble in ether and hexane was obtained.^[121]

The reaction of chlorine with **13** afforded substituted product – chloroalkene **97** – quantitatively (Scheme 33). At the initial stage of chlorination precipitation of chloronium salt observed visually, however it's separation failed due to its instability.^[76] Later the synthesis, separation and characterization of the chloronium salt as complex with $SbCl_6^-$ or $Mo_2O_2Cl_7^-$ was performed.^[146, 147] Formation of iodonium salt in the reaction of alkene **13** with $IClN-SbF_5$ (1 : 1) in liquid sulfur oxide (IV) was confirmed spectroscopically.^[148]



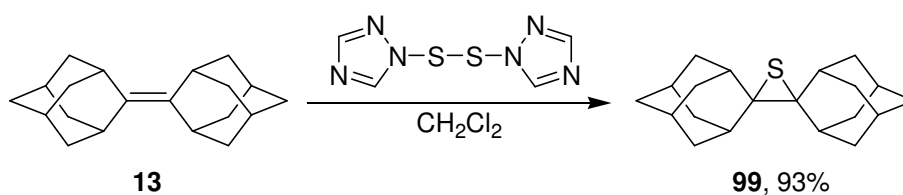
Scheme 33.

Reactions of adamantylideneadamantane (**13**) with methanesulfonylhalogenides gave stable episulfonium salts (**98**, Scheme 34).^[149] The formation of these compounds as intermediates previously was postulated in addition reactions of alkanesulfonylhalogenides to ordinary alkenes.



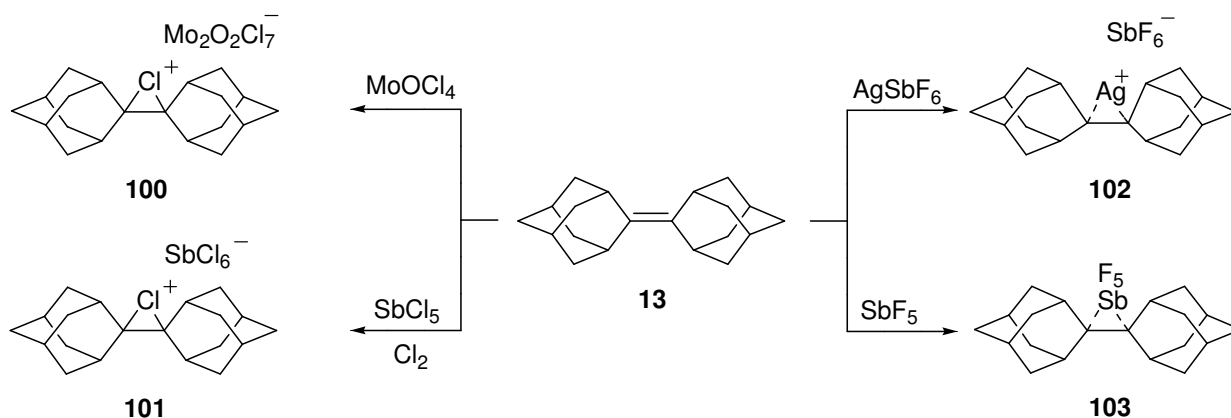
Scheme 34.

Thiirane of **13** without an activation agent under mild conditions gave the corresponding thiirane **99** in good yield (Scheme 35).^[150] Thiirane oxide of **13** generates sulfur (IV) oxide with formation of **13**,^[151, 152] *i.e.*, the reaction is reversible.^[153]



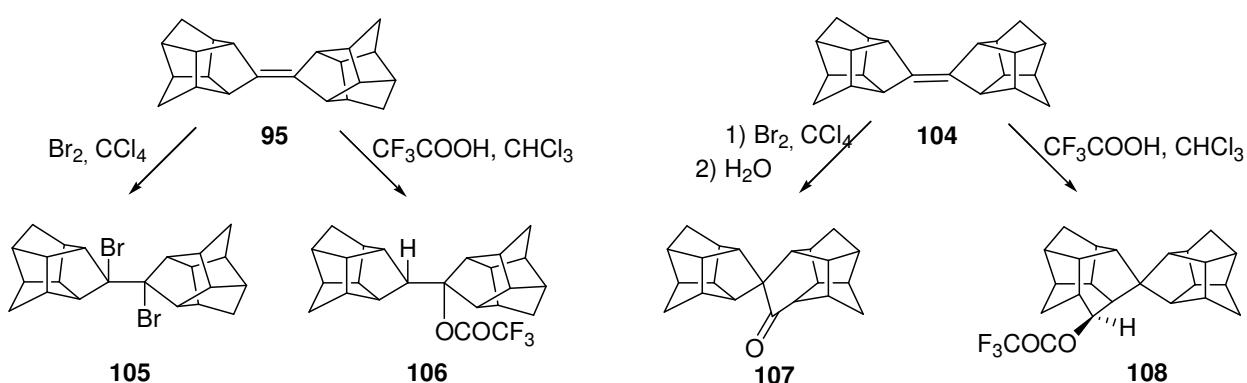
Scheme 35.

Reactions of **13** with molybdenum (IV) tetrachloride oxide and antimony pentachloride in the presence of Lewis acids leads to stable chloronium salts **100** and **101**, respectively.^[146] Through the NMR-spectra of the reaction mixture in the reaction of alkene **13** with antimony pentafluoride and silver hexafluoroantimonate – compounds **102** and **103** were observed (Scheme 36).^[148]



Scheme 36.

dl- D_3 -Trishomocubylidene- D_3 -trishomocubane (**95**) reacts with bromine and trifluoroacetic acid to give products of addition to the unsaturated bond while isomeric *meso*- D_3 -trishomocubylidene- D_3 -trishomocubane (**104**) forms oxygen-containing products with expansion of the five-membered cycle to the six-membered (Scheme 37).^[126]

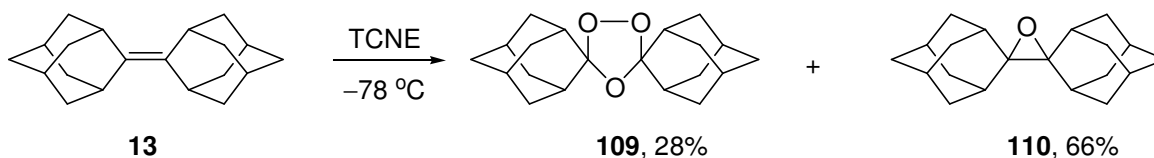


Scheme 37.

It is also worthwhile to mention that *meso*-isomer **104** reacts in a harsh environment only. Thus, addition of trifluoroacetic acid occurs within 48 hours by refluxing in chloroform, while

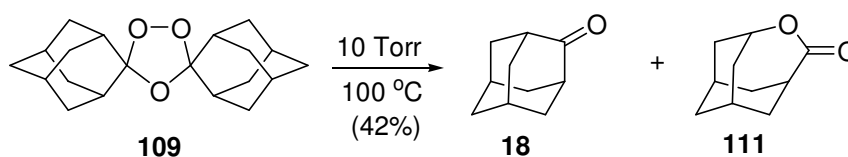
95 reacts for 2.5 hours at room temperature. Homocubylidenehomocubane reacts with the same reagents analogously to *dl*-*D*₃-trishomocubylidene-*D*₃-trishomocubane (**95**).^[154]

In the reaction of **13** with ozone in nonpolar solvents a mixture of ozonide **109** and epoxide **110** formed, in a ratio which depends on the nature of the solvent; in polar solvents exclusively epoxide **110** is formed (Scheme 38).^[155] Compound **109** was tried as antimalarial drug amongst similar ozonides, however exhibited no significant activity.^[156]



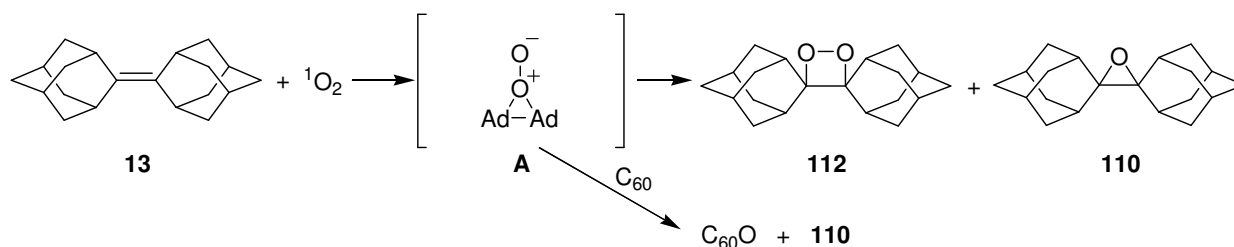
Scheme 38.

Upon the thermolysis of ozonide **109** a mixture of adamantanone (**18**) and lactone **111** is formed (Scheme 39).^[155]



Scheme 39.

For the synthesis of oxetanes from sterically hindered alkenes the oxidation by singlet oxygen, sensibilyzed by dyes is used most often. Thus, dioxetane **112** was synthesized from alkene **13** (Scheme 40). In this reaction as a sensitizer methylene blue was used.^[157] Structure of oxetane **112** was confirmed by X-Ray crystal structure analysis.^[158]



Scheme 40.

In the photooxidation of adamantylideneadamantane epoxide (**110**) also formed along with dioxetane **112**, where the ratio of products depends on the nature of dye and solvent used.

Additionally, as it was reported recently that the intermediate (**A**) behaves as a nucleophilic oxidizing agent and can react with C₆₀ and C₇₀.^[159]

Adamantylideneadamantane-1,2-dioxetane containing polymers emit visible light: mechanically induced chemiluminescence was tuned by incorporating **112** into number of polymer chains and networks. Their autoluminescent properties are an advantage over other optical mechanophores as they need no excitation light source, which greatly enhances the sensitivity.^[160]

Trapping of the adamantylideneadamantane (**13**), together with other adamantane-fragmented compounds, can template the formation of the carceplexes from deep-cavity cavitands, which are known as covalent nanoscale reactors.^[161, 162]

1.4. Conclusions and Outlook

Up-to-date reactions of sterically hindered alkenes are relatively well-studied on the example of adamantylideneadamantane (**13**) as the most suitable and easy-to-reach model compound. Synthesis and reactivity of the other alkenes of similar nature still requires deeper study. And as coupling of homocubanones by McMurry reaction was performed,^[126, 154] for higher diamondoids those studies have been completely omitted. However, the ability of diamondoids to participate in electron transfer^[163] and self-assembling on the surface^[64] or to act as good electron emitters due to stability of their radical cations on the metal surface,^[65, 164] would make synthesis of such coupled sterically hindered alkenes as highly perspective research topic.

In this work we show that this approach allows the preparation of geometrically well-defined nanodiamond particles of up to 2 nm in size from higher diamondoids starting from diamantane, which dimers are not known up to date.

Chapter 2. Research objectives

As already mentioned above, diamondoids coupled through linkers would find their own place in nano- and material sciences as a borderline between sp^2 and sp^3 carbon world. Unsaturated spacers, which connect two diamondoidyl moieties, would mimic sp^2 hybridized carbon atoms of nanodiamond and introduce conductive properties. The main target of the current work is to develop effective methods of coupling for synthesis of unsaturated sterically hindered alkenes with defined sizes and shapes.

General strategies and goals are as follows:

- development of new and optimization of the existing synthetic methods for starting ketones;
- choice of the most effective procedure for coupling of the synthesized ketones;
- coupling and cross-coupling of diamondoidyl ketones by the selected procedures in order to obtain new diamondoids with unsaturated spacers and characterization of the products by experimental and computational methods;
- functionalization of the selected coupled products and analysis in order to specify the route to possible applications as surface modifiers.

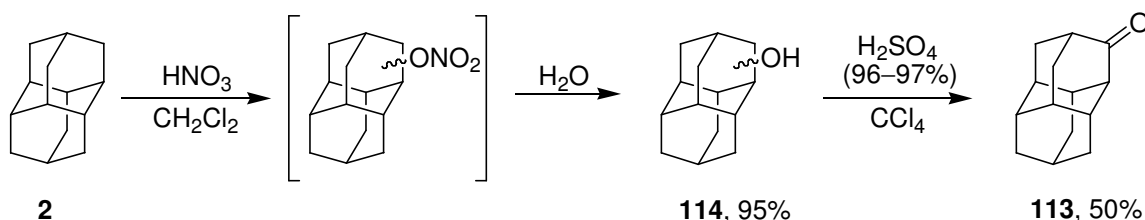
Selective functionalization of rigid diamondoids will be a starting point for construction of new nanomaterials.

Chapter 3. Results and Discussion

3.1. Synthesis of diamondoidyl ketones

3.1.1. Synthesis of diamantanone (113)

Diamantanone (**113**) was used as a starting compound for synthesis of adamantylidenediamantane-3 (**14**) and diamantylidenediamantanes (**15**, **16**). At the first step of the synthesis of **113** commercially available diamantane (**2**) was nitrated by fuming nitric acid and further nitration products were hydrolyzed to hydroxyl derivatives (Scheme 41).^[165]



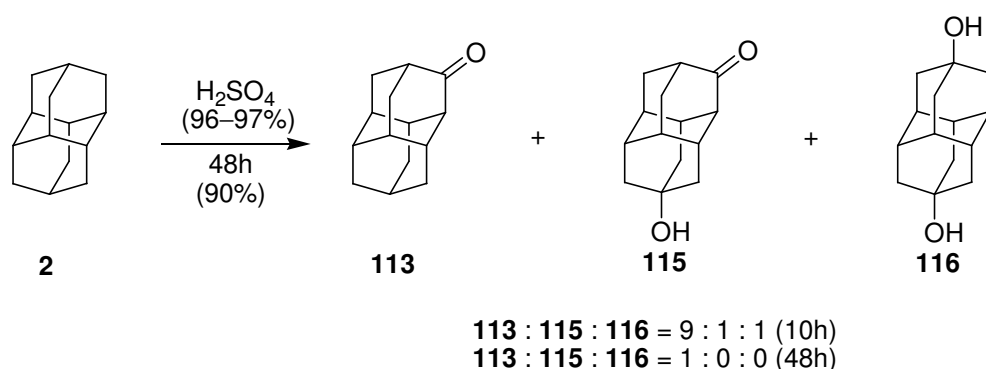
Scheme 41.

Addition of fuming nitric acid to the reaction mixture, as well as dilution of the reaction mixture with distilled water, was carried out under careful cooling. Reaction conversion did not need to be verified, as in the next step unreacted **2** may be recovered by column chromatography and reused.

Further synthesis of **113** through hydroxydiamantanes (**114**) was performed in sulfuric acid with concentration 96–97% in presence of catalytic amounts of carbon tetrachloride.^[166] The reaction mixture was placed into oil bath, heated to 75–77 °C under vigorous stirring and kept for 4 h with GC/MS control. If in 4 h reaction was not complete it was allowed to run additional time; however it had to be confirmed by GC/MS that ratio of disubstituted diamantanes was not increasing. Temperature influences decisively the oxidation of cage compounds, since lowering the temperature leads to decrease of the conversion, while increase of temperature results in dramatic increase of polyhydroxy-derivatives in reaction products. Diamantanone (**113**) was purified by column chromatography on silica gel. In case GC/MS indicated presence of diamantane (**2**) – it could be separated by column chromatography on silica gel with pentane and reused.

Although a preparative method for the synthesis of **113** via **114**^[165, 166] was successfully applied, a simplified method of direct synthesis of **113** from **2** has also been carried out (Scheme

42).^[167] As it was reported earlier in the reaction of **2** oxidation with sulfuric acid (96%) for 10 h compound **113** was obtained with 54% yield together with 6% of 9-hydroxydiamantan-3-one (**115**) and 5% of diamantane-4,9-diol (**116**).^[168] However, it was found out that increase of the reaction time reduces amount of side products and increases the yield of **113**. The reaction also was performed in the sulfuric acid with concentration 96–97% in absence of carbon tetrachloride. The reaction mixture was placed into oil bath heated to 75–77 °C under vigorous stirring and this temperature was maintained for 48 hours. Considerable increase of reaction time was completely compensated by fewer number of steps and higher purity of target compound **113**.

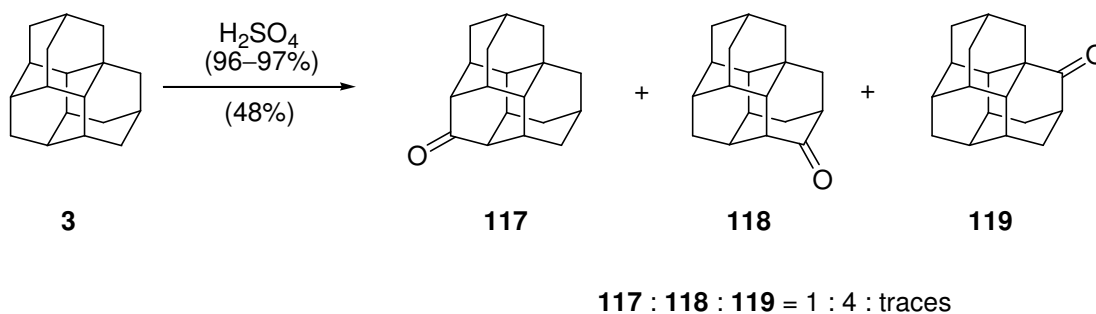


Scheme 42.

After the quenching of the reaction mixture with water, the product was separated from unreacted diamantane (**2**) by column chromatography on silica gel.

3.1.2. Synthesis of triamantanones (**117–119**)

Direct oxidation of triamantane (**3**) with sulfuric acid (96–97%) gave three products, where ketones **117** and **118** dominate (Scheme 43).^[167]



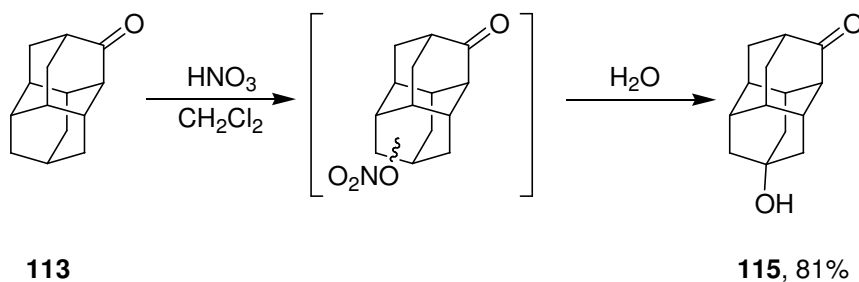
Scheme 43.

The reaction mixture was placed into an oil bath heated to 78 °C under vigorous stirring and this temperature was maintained for 4.5 hours with control of reaction mixture content by GC/MS. Crude product mixture was purified by column chromatography on silica gel and ketone **118** was obtained by recrystallization of last fractions from hexane. Ketone **119** was isolated by column chromatography on silica gel. Spectral data of triamantanone-8 (**118**) is identical to reported in literature.^[169] Triamantanone-16 (**119**) has characteristic signal of carbon atom in C=O group at 218.0 ppm in the ¹³C NMR spectrum as well as seven methine, four methylene and one signal of quaternary carbon atom at 49.4 ppm which was assigned by the APT vs DEPT spectral comprehensive analysis.

3.1.3. Preparation of diamantanediones

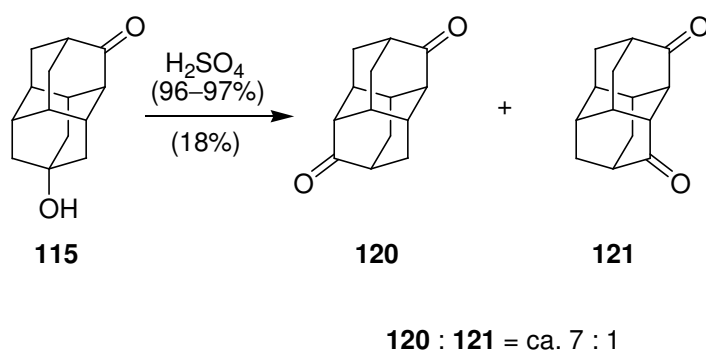
The oxidation of hydroxydiamantanes catalyzed by carbon tetrachloride in sulfuric acid (96–97%) has been carried out. However, after 6 h stirring at 77 °C, major products of the reaction mixture were identified by GC/MS as **113** (29%) and **115** (12%) together with a number of chloro-substituted side products. Those products can be easily separated by column chromatography on silica gel. Than oxidation of **116** by sulfuric acid (96–97%) was performed without carbon tetrachloride addition in order to avoid the formation of chlorinated side products. Analysis by GC/MS of the reaction mixture showed that starting material transformed into **115** (53%) together with small amounts of diketones (**120** and **121**, 6%). However, the amount of unidentified products after 6 h of reaction increases. It may be concluded, that sulfuric acid at concentration 96–97% oxidizes **115** into desired products effectively, and still another better procedure is needed.

For the synthesis of **115** we utilized a procedure, which was developed previously for preparation of hydroxydiamantanes.^[165] At first **113** was oxidized by concentrated nitric acid introducing hydroxyl substituent (Scheme 44). First step of the reaction was carried out very carefully, because of high exothermicity and foaming of the reaction mixture. After addition of whole amount of nitric acid the mixture was allowed to warm up to ambient temperature under control, with cooling on demand. During the workup of reaction mixture water layer had to be extracted with methylene chloride several times and washed with only small amounts of brine, as hydroxyketones (**115**) are readily dissolved in water. Obtained solid residue was purified by column chromatography on silica gel and crystallized from benzene to give a pure **115** in 81% yield.



Scheme 44.

Second step of synthesis of diamantanedione-3,10 (**120**) and diamantanedione-3,8 (**121**) involves an oxidation of **115** with concentrated sulfuric acid (96–97%).



Scheme 45.

Since the conversion of **115** is not high due to the tar formation, it requires permanent GC/MS control. Maximally possible conversion (35–38%) was reached on the 7th – 10th day. Product mixture was separated by column chromatography on silica gel to give ketones **120** and **121**. Recovered **115** can be used in the oxidation reaction anew.

Diamantanediones (**120**, **121**) are easily identified by their spectral data. While **121** has one characteristic signal of carbon atom of C=O group at 213.1 ppm of ¹³C NMR as well as four methine and two methylene signals of carbon atoms by the APT spectral data, **120**, aside from C=O carbon atom signal at 215.2 ppm, possesses only 3 methine and 1 methylene signals in APT spectrum. This is in a full agreement with C_{2h} and C₂ symmetries of **120** and **121**, respectively.

3.1.4. Preparation of C₅-trishomocubane-8-one (**122**)

For the synthesis of target compound – pentacyclo[5.4.0.0^{2,6}.0^{3,10}.0^{5,9}]undecane-8-one (**122**) (Fig. 6) – the synthetic route through photocyclization of tricyclic diene was chosen.^[170]

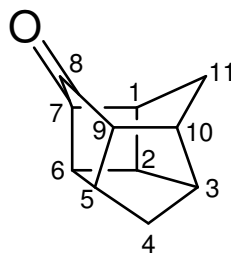
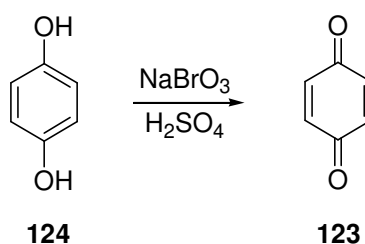


Figure 6. The structure of pentacyclo[5.4.0.0^{2,6}.0^{3,10}.0^{5,9}]undecane-8-one (**122**).

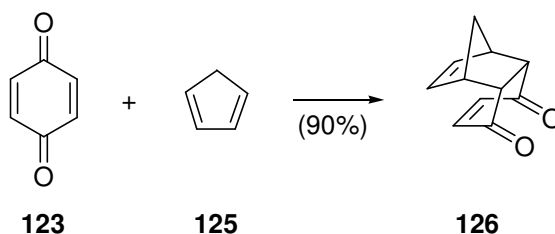
Starting compound – *p*-benzoquinone (**123**) – was obtained by oxidation of hydroquinone (**124**, Scheme 46).



Scheme 46.

Reaction proceeded through the respective quinhydrone, which at higher temperatures converts into **123** in the presence of oxidant. As the *p*-benzoquinone is photosensitive and transforms back into quinhydrone during storage, it was always used freshly prepared.

p-Benzoquinone (**123**) is extremely active as dienophile due to the activation of unsaturated bonds by β -carbonyl and easily forms Diels-Alder adducts with active dienes, *e.g.* cyclopentadiene (**125**) in our case (Scheme 47).

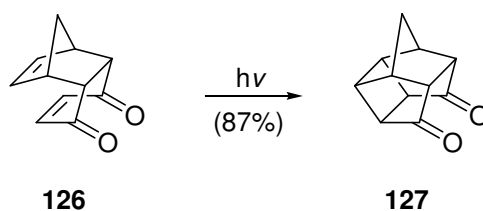


Scheme 47.

Tricyclo[6.2.1.0^{2,7}]undecadiene-4,9-dione-3,6 (**126**) thus formed contains active double bond in the quinone fragment and is able to react with another diene molecule, therefore, the reaction was performed with molar ratio diene : dienophile = 1 : 1 in methanol at $-70\text{ }^{\circ}\text{C}$. Further replacement of methanol for ethanol allowed temperature increase to $0\text{ }^{\circ}\text{C}$ without

lowering of the yield. It is worthwhile to note that literature procedure^[170] does not scale up efficiently. Considerable increase in yield of **126** was reached by running reaction overnight at 0 °C. Dione **126** thus obtained was chromatographically pure and was used in further synthesis without additional purification.

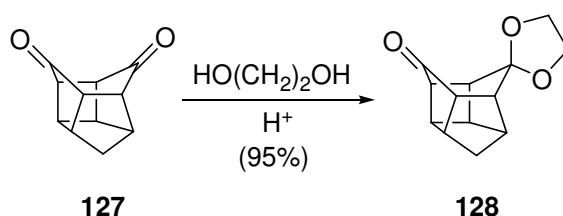
Intramolecular photochemical [2+2] cycloaddition of **126** was performed under UV irradiation of its solution in ethylacetate or acetone under argon (Scheme 48).



Scheme 48.

In order to avoid intermolecular photochemical [2+2] cycloaddition, high dilution (12–14 g of **126** in 160 mL of solvent) was used. Solution was irradiated for 6 h without additional sensibilization and yielded chromatographically pure pentacyclo[5.4.0.0^{2,6}.0^{3,10}.0^{5,9}]undecane-8,11-dione (**127**).

Pentacyclo[5.4.0.0^{2,6}.0^{3,10}.0^{5,9}]undecane-8,11-dione ethylene ketal (**128**) was synthesized in accordance with Scheme 49.

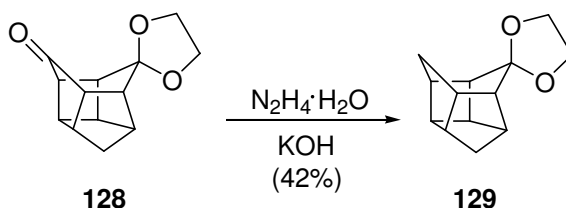


Scheme 49.

In the previously reported work^[171] on the method of **128** synthesis, key compound in the synthesis of *C*₅-trishomocubane-8-one (**122**), was proposed and included reflux of equimolar amounts of ethylene glycol and diketone **127** in benzene. However while reproducing the literature procedure we found significant tar formation after 2–3 hours of reflux. Instead refluxing of **127** in benzene with excess of ethylene glycol and 0.2–0.3 g of Dowex as catalyst was used. It was reported earlier^[172] that diketones form bisketals with great difficulties or do not form them at all due to sterical hindrance. However, in our case it was noted that significant amounts of bisketal of diketone **127** (up to 10% by GC/MS analytical data) were present in

reaction already after 1.5 h. The general recommendation for decreasing the amount of undesirable product is to preheat the reaction mixture to 110–120 °C, and use permanent stirring and reflux no longer then 75 minutes. Under these conditions monoketal **128** is formed with quantitative yield.

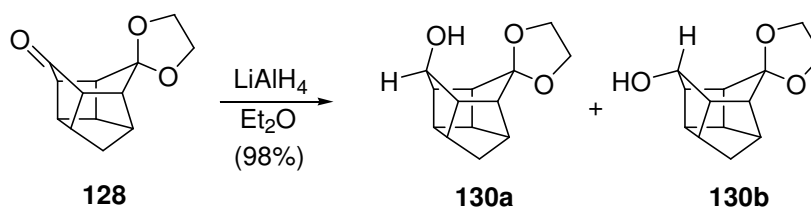
Similarly to synthesis of C_2 -bishomocubane-6-one^[173, 174] the reduction of ketal **128** to pentacyclo[5.4.0.0^{2,6}.0^{3,10}.0^{5,9}]undecane-8-one ethylene ketal (**129**) was performed utilizing the Kizhner-Wolff reaction (Huang-Minlon modification,^[173] Scheme 50).



Scheme 50.

The reaction was performed accordingly to procedure described in literature,^[173] with the same loading and the yield of desired product not exceeding 35–40%. Distilling water off from the reaction mixture has lead to side products of further reduction and destruction of trishomocubane cage. Low yields of ketal **129** in the reaction of diketone ethylene ketal **128** reduction motivated us to look up for alternative synthetic routs to **122**.

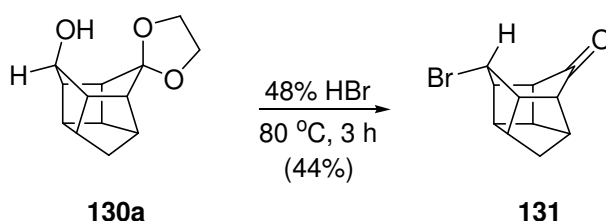
As it was reported before,^[171, 175, 176] 11-hydroxypentacyclo[5.4.0.0^{2,6}.0^{3,10}.0^{5,9}]undecane-8-one (**130**), which can be obtained from ketal **128**, is possible intermediate compound in the synthesis of trishomocubane ketones. Reduction was performed in presence of lithium aluminum hydride in diethyl ether or tetrahydrofurane. Despite reported^[171, 177] exclusive formation of *endo*-11-hydroxypentacyclo[5.4.0.0^{2,6}.0^{3,10}.0^{5,9}]undecane-8-one ethylene ketal (**130a**), actual composition of product mixture strongly depends on the method of reaction mixture workup (Scheme 51).



Scheme 51.

If reaction mixture after the reduction with excess of lithium aluminum hydride in diethyl ether was quenched by gradual addition of saturated aqueous solution of ammonium chloride, pure **130a** was formed. This product was indicated based on ^1H NMR spectrum, where the doublet signal of proton neighboring oxygen atom of hydroxyl substituent at 5.33 ppm ($J = 10$ Hz), and also two characteristic triplet signals at 3.72 and 3.56 ppm ($J = 2$ Hz), which belong to proton attached to the C-8 carbon atom of C_5 -trishomocubane cage were observed.

On contrary, if reduction was performed in tetrahydrofuran and excess of lithium aluminum hydride was destroyed by stepwise addition of water and 15% aqueous solution of sodium hydroxide to form solid precipitate of lithium/aluminum hydroxides, pure *exo*-11-hydroxypentacyclo[5.4.0.0^{2,6}.0^{3,10}.0^{5,9}]undecane-8-one ethylene ketal (**130b**) was obtained. It was characterized by presence of triplet signal of proton neighboring C-8 carbon atom, at 4.55 ppm ($J = 4$ Hz). Two triplet signals at 3.72 and 3.56 ppm ($J = 2$ Hz), that characteristic for **130a**, were absent. Many other literature methods for lithium aluminum hydride reduction reactions workup afforded mixture of **130** in different ratios. Thus, we found the only way to selective preparation of stereoisomers of **130**. Obtained **130a** was brominated by hydrobromic acid (48%) at 80 °C as shown on the Scheme 52.^[171]

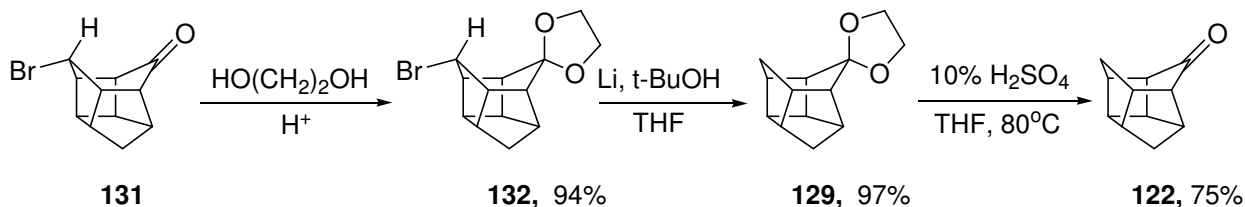


Scheme 52.

Reaction resulted in almost pure *exo*-bromoketone (**131**), which is evidenced by only one singlet signal of α -Br proton at 4.26 ppm (lit. 4.28^[171]) in ^1H NMR spectrum. Due to significant tar formation yield of **131** was not exceeding 45%. Also, **131** is quite soluble in acidic water and requires careful extraction of the target product.

Taking into consideration low yield of **131**, decreasing reaction temperature from 80 to 60 °C with simultaneous increase of reaction time to 24 h was applied. Such changes resulted increase of the product yield to 90–92%. It is worthwhile to mention that with crude hydroxyketal **130a** as starting compound the yield of the reaction significantly drops because multiple crystallization of the product **131** is required.

As direct reduction of bromoketone **131** by lithium is ineffective, ketal protection to ketone was applied (Scheme 53) by refluxing **131** in benzene with molar excess of ethylene glycol in the presence of acid catalyst.

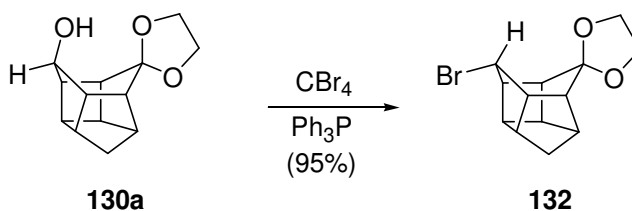


Scheme 53.

The reduction of bromoketal **132** proceeded with difficulties due to the sterical hindrance caused by spiro-ketal, thus *tert*-butanole in amounts half to starting compound was added into reaction mixture after 2 h of reaction time. In case of incomplete reduction (GLC) and presence of unreacted lithium, it is enough to add again half molar amount of *tert*-butanole and reflux the reaction mixture for 2–3 hours more to complete the reaction. If all lithium reacted but ketal **132** is still present in the reaction mixture, then additional amounts of *tert*-butanole and lithium have to be added. Process also could be followed by ^1H NMR by monitoring the singlet signal at 5.17 ppm, which belongs to C-11 carbon atom of trishomocubane cage.

Hydrolysis of ethylene ketal **129** in a mixture of 10% aqueous solution of sulfuric acid and tetrahydrofurane in ratios 4 : 1 at 80 °C gave pentacyclo[5.4.0.0^{2,6}.0^{3,10}.0^{5,9}]undecane-8-one (**122**) (Scheme 53).

Considering the low preparative yield of bromoketone **131** in the reaction of bromination of **130** we developed an alternative route. As was reported before^[178] the replacement of hydroxyl group with bromine in secondary alcohols in strained cage compounds is possible with carbon tetrabromide in presence of 2 equivalents of triphenylphosphine. This procedure was applied for the synthesis of bromoketal **132** (Scheme 54).



Scheme 54.

The reaction was carried out under reflux in dry dichloromethane, to give pure **132** with nearly quantitative yield. Further synthesis of ketone **122** was carried out in accordance with the procedures shown in the Scheme 53.

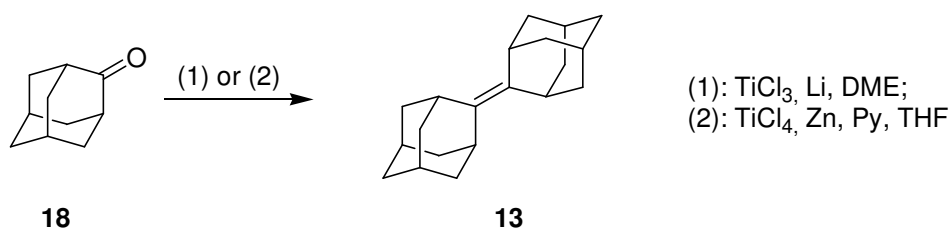
As a result we developed a synthetic route to pentacyclo[5.4.0.0^{2,6}.0^{3,10}.0^{5,9}]undecane-8-one (**122**) through the key intermediate – 11-hydroxypentacyclo[5.4.0.0^{2,6}.0^{3,10}.0^{5,9}]undecane-8-one ethylene ketal (**130**).

3.2. Synthesis of the coupled diamondoids

McMurry coupling under different conditions have been described in literature in details.^[83, 126, 179] However, as the preparation of adamantylideneadamantane (**13**)^[179] is the only known example of diamondoids coupling, we decided to test some existing methods in order to choose most efficient.

3.2.1. Synthesis of adamantylideneadamantane (**13**)

For minimizing the influence of oxygen deoxygenation of argon is needed and all preparations of the reagents were performed in argon camera. Titanium reagent was prepared *in situ* utilizing titanium (III) chloride and lithium powder and then solution of ketone **18** was added into reaction mixture. After reaction was finished the reaction mixture was quenched by pouring to water with further extraction of product. Hydrocarbon **13** was purified by column chromatography on silica gel with maximum yield of 42%.^[83]



Scheme 55.

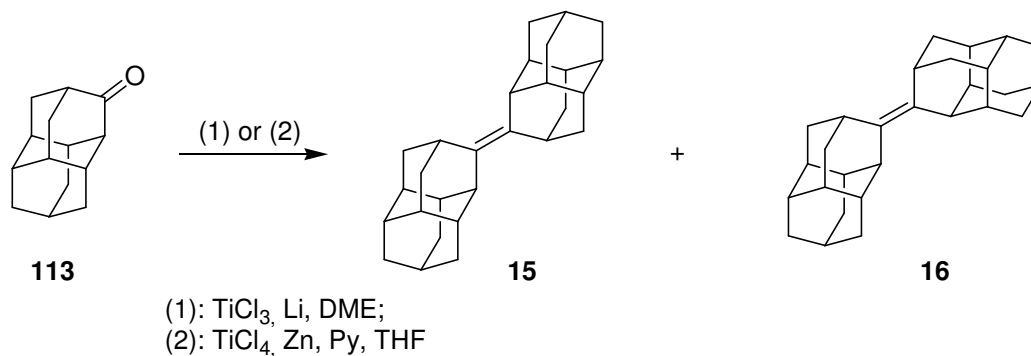
We also tested the two-step procedure when the titanium reagent was prepared under reflux from titanium tetrachloride and zinc powder in dry tetrahydrofurane, which was distilled over sodium in a stream of argon directly before the reaction. After preparation of the titanium reagent, the required amount of dry pyridine and the solution of the ketone **18** in dry THF were subsequently added into the reaction mixture. Reaction mixture was quenched with potassium

carbonate solution, and, after extraction, **13** was purified by column chromatography on silica gel by hexane, to give *ca.* 80% of analytically pure alkene.^[126]

3.2.2. Synthesis of *anti*- and *syn*-diamantylidenediamantanes (**15**, **16**)

Diamantanone (**113**) was used as a starting compound for the synthesis of diamantylidenediamantanes (**15**, **16**).

Coupling of diamantanone (**113**) to stereoisomeric diamantylidenediamantanes (**15**, **16**) occurs according to Scheme 56. The reaction was carried out in an atmosphere of argon by adding ketone **113** to firstly prepared titanium reagent as described above. The mixture of isomeric unsaturated hydrocarbons *anti*-**15** and *syn*-**16** was obtained with maximum yield 46% after purification by column chromatography on silica gel.



Scheme 56.

Coupling of ketone **113** in presence of reductive pair titanium (IV) chloride – zinc^[126] was also tested. As in the synthesis of **13** the titanium reagent was prepared *in situ* from titanium tetrachloride and fine zinc powder in tetrahydrofurane. The reaction gave mixture of **15** and **16** in preparative yield ~90%. Crude product mixture after the reaction contains traces of hydroxydiamantanes (according to GC/MS) easily separable by column chromatography on silica gel.

It is worthwhile to mention that **15/16** forms in ratio 1/1, where the peak with a lower retention time corresponds to *syn*-isomer (**16**). Taking into consideration the fact that the compounds subjected to analysis are expected to demonstrate similar properties, it was assumed that observed in GC ratio of products reflects their ratio correctly.

It was reported in the literature^[121, 122] that 1-substituted adamantane-2-one exclusively forms *trans*-products under coupling. However, in case of **113**, additional substitution of the

adamantyl cage has no influence on stereochemistry. Presumably, in *syn*- and *anti*-isomers the bulky fragments are too distant from the double bond to favor one of the stereoisomers.

The resulting mixture of alkenes **15** and **16** was recrystallized from hexane fractionally. Notably, lower solubility of more symmetrical *anti*-isomer (**15**) in hexane comparably to *syn*-alkene (**16**) allowed utilization of scheme shown on Fig. 7.

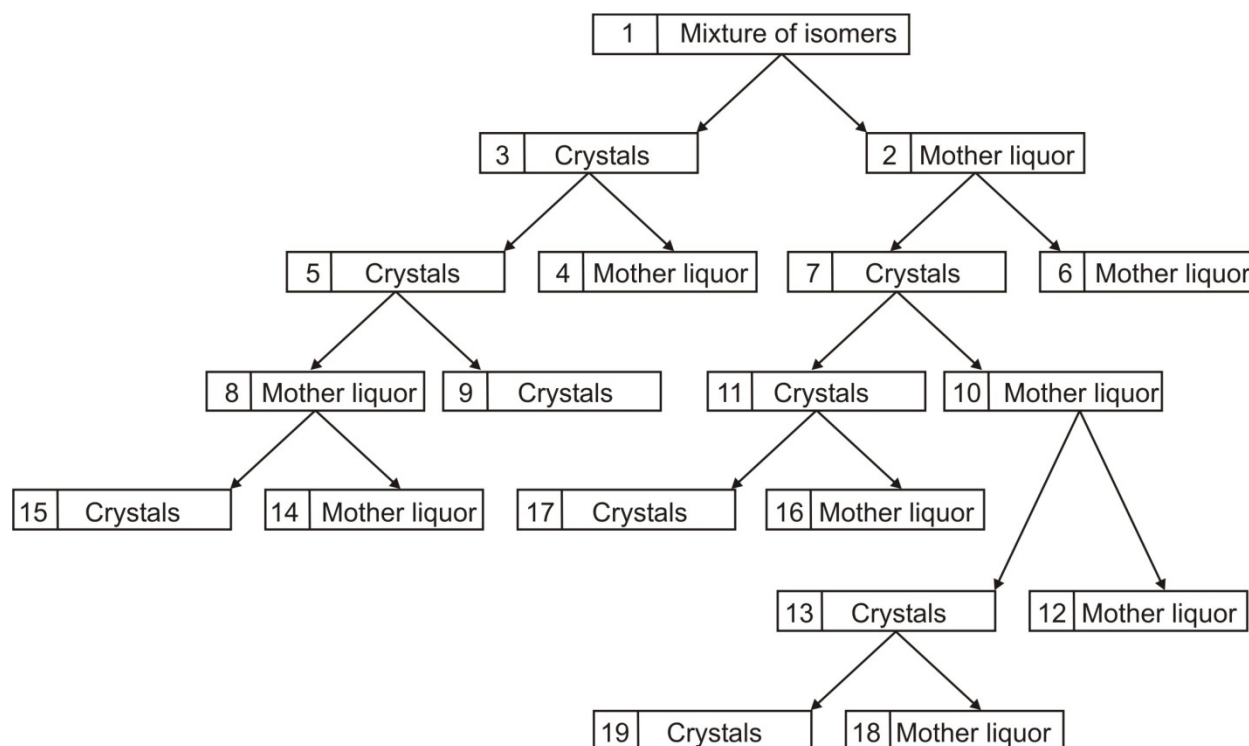


Figure 7. Fractional recrystallization of *anti*- (**15**) and *syn*-diamantylidenediamantane (**16**).

The fractional crystallization was followed by GC/MS analysis of fractions (Table 2).

Table 2.

Composition of fractions of **15** and **16** recrystallization.

№ of fraction	Named	Mixture composition and weight of sample		
		15 (<i>anti</i> -), %	16 (<i>syn</i> -), %	Weight, g
1	Mixture of isomers	53	47	1.69
2	Mother liquor	41	59	0.90
3	Crystals	61	39	0.79
4	Mother liquor	42	58	0.42
5	Crystals	78	22	0.37
6	Mother liquor	39	61	0.50
7	Crystals	70	30	0.40

8	Mother liquor	58	42	0.20
9	Crystals	100	0	0.17
10	Mother liquor	75	25	0.23
11	Crystals	62	38	0.17
12	Mother liquor	80	20	0.18
13	Crystals	8	92	0.05
14	Mother liquor	40	60	0.16
15	Crystals	100	0	0.04
16	Mother liquor	55	45	0.15
17	Crystals	100	0	0.01
18	Mother liquor	31	69	0.01
19	Crystals	0	100	0.04

As can be seen from Table 2, with three-stage crystallization of about 1.7 g of the starting mixture, pure sample of **15** at step 9 could be obtained. We conclude that the separation of the mixture by crystallization may be only performed by increasing of number of recrystallizations, and yield of the pure isomers **15** and **16** does not exceed several percent.

Structures of **15** and **16** we analyzed by the 1D NOESY NMR experiments, and pronounced NOE signals were observed for the neighboring nonequivalent H² and H⁴ of **15** (Fig. 8); for isomer **16** these interactions were absent due to the equivalence of the H² and H⁴ atoms. Thus, simple NOE analysis is able to unambiguously distinguish between the *syn*- and *anti*-isomers of coupled diamantanes.

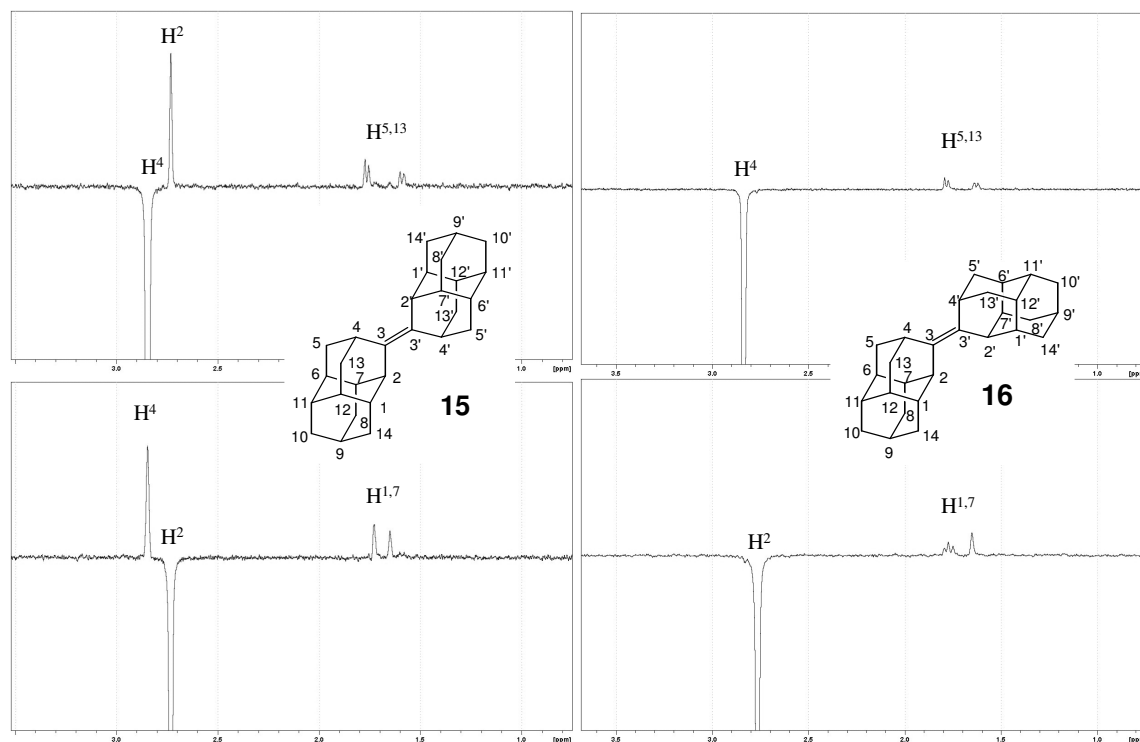


Figure 8. NOESY spectral data of **15** and **16**.

We also studied the **15** and **16** by X-Ray crystal structure analysis. Compounds **15** and **16** are comprised of two cages (*i.e.*, diamantyl moieties) that are mutually connected by a bond (Fig. 9).

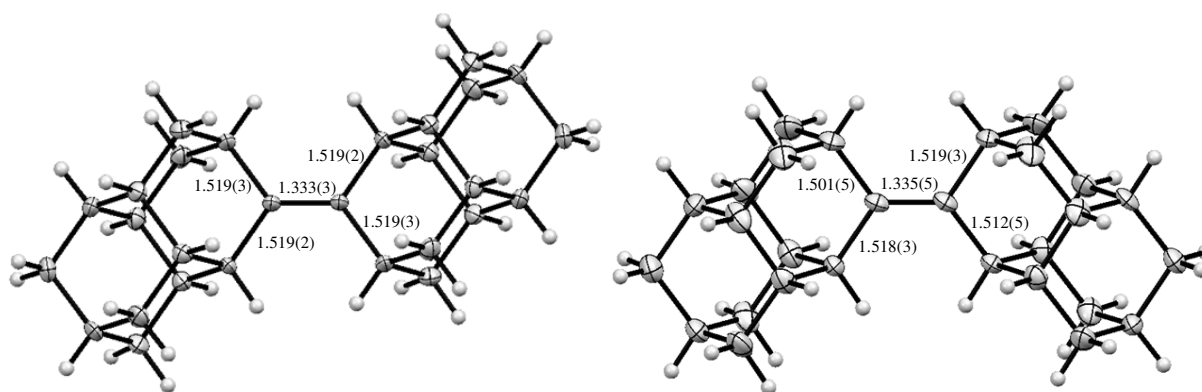


Figure 9. X-ray structure of **15** (left); X-ray structure of **16** (right).

Thus, in **15** and **16** the C(3) and C(3') methylene bridges in adjacent cage moieties are connected via a C=C double bond (numbers of carbon atoms are as on Fig. 8). Structures on Fig. 9 show that two of methylene bridge bonds that are situated adjacent to the connecting double bond are the shortest C–C bonds in molecules (in **15** all distances between corresponding carbon atoms are equal to each other and are equal to 1.519 Å whereas in **16** all such distances are different and are equal to: C(2)–C(3) – 1.518(3) Å; C(3)–C(4) – 1.501(4) Å; (C2')–C(3') – 1.512(4) Å and

C(3')–C(4') – 1.518(3) Å respectively). The carbon–carbon double bonds in both compounds are essentially planar. Analysis of X-ray crystallographic results revealed, that the twist and out-of-plane deformation in **15** are equal to 0.41° and in **16** – to 0°.

In Table 3 lengths of carbon–carbon double bonds, along with the $C(sp^3)–C(sp^2)–C(sp^3)$ internuclear angles in several sterically hindered cage olefins are given.

Table 3.

Structural features in several sterically hindered cage olefins with a planar double bond.

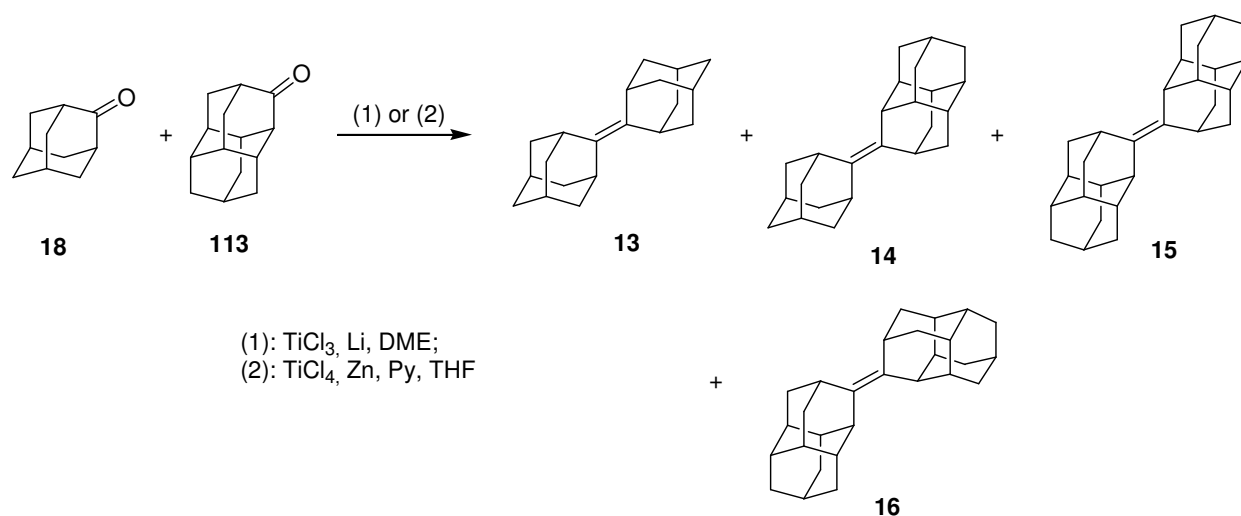
Compound	$r_{C=C}$, Å	$\angle C(sp^3)–C(sp^2)–C(sp^3)$, deg
13 ^[180]	1.336(4)	110.4(2)
14 *	1.325(3)	109.7(2)
		110.1(2)
15	1.333(4)	110.2(2)
16	1.336(4)	110.5(2)
135 *	1.326(8)	102.6(3)
104 ^[126]	1.328(3)	97.0(1)
95 ^[126]	1.322(2)	96.6

* for the synthesis of compound **14** see p. 42; ** for the synthesis of compound **135** see p. 51

The C=C bond lengths in **15** and **16** are close to normal. The data in Table 3 reveal, that these bonds are practically equal in length with the corresponding C=C bond in **13** (“normal” length). The variation among C=C bond lengths parallels the changes in the $C(sp^3)–C(sp^2)–C(sp^3)$ internuclear angles in all compounds, given in Table 3. Only cross-coupled **14** is not in agreement with this tendency, as the C=C bond length is closer to that of in compounds with five-membered cycles and internuclear angles near unsaturated bond are not equal. Additionally, while in the **13**, **15** and **16** $C(sp^3)–C(sp^2)–C(sp^3)$ internuclear angles belong to the six-membered cycles and are *ca.* 110°, in compound **135** they are only about 103°, as $C(sp^3)–C(sp^2)–C(sp^3)$ internuclear angles belong at the same time to five- and six-membered cycles. In five-membered cycles of compounds **95** and **104** those angles are *ca.* 96-97°. In general, observed variations in other carbon–carbon bond lengths and valent angles in these cage structures are in good agreement with “normal”.^[180] For more details about the structures of **15** and **16** see page 56 and Appendix II.

3.2.3. Synthesis of adamantylidenediamantane-3 (**14**)

Cross-coupling of commercially available adamantanone (**18**) and **113** to adamantylidenediamantane-3 (**14**) was carried out in accordance with the Scheme 57 in presence of reduction pair titanium (III) chloride – lithium. As it was mentioned above, the reaction of titanium agent, preparation and further ketone mixture injection were carried out in an atmosphere of deoxygenated argon. The resulting mixture of adamantylidenediamantane (**13**), **14**, and isomeric diamantylidenediamantanes **15** and **16** was isolated with maximum yield 56%.^[179]



Scheme 57.

Attempts to separate the mixture obtained from the equimolar amounts of ketones **18** and **113** by flash chromatography on silica gel with hexane were unsuccessful (see the composition of the mixture in Table 4).

As the separation of the target alkene **14** encountered difficulties, it was decided to change the ratio of the components of the reaction mixture by changing the ratio of starting ketones. The results of analysis by GC/MS of the hydrocarbon part of the reaction mixture, obtained under different **18** to **113** ratios, are listed in Table 4.

Table 4.

Ratios of starting ketones and products in synthesis of **14**.

№	Ratio 18/113	Ratios of alkenes in mixture, %				Yield, %
		13	14	15	16	
1	1:1	10	52	20	18	90

2	1:3.5	6	39	29	26	95
3	2:1	55	35	5	5	93
4	3.5:1	57	38	2,5	2,5	95
5	5:1	67	33	traces	traces	92

Table 4 shows that ketones **18** and **113** are similarly reactive, as evidenced by the relative ratio of products. Under the double molar excess of adamantanone (**18**) the total yield of diamantylidenediamantane isomers (**15**, **16**) decreased to 10% and to 5 with 3.5 excess. As even small amounts of these isomers complicate the separation of the target product the molar ratio of initial ketones of 5:1 was used to give only two products of the reaction (see Table 4).

The attempt to reduce the amount of cross coupling products in presence of diamantanone excess (3.5 mol) in order to eliminate the formation of **13** practically failed as 6% of **13** was formed.

Separation on the silica gel, impregnated with AgNO₃ also proved to be effective for separation of the reaction products obtained under the ratio of starting ketones 1 : 1 at 100 mg scale. As it was reported before^[181, 182] such method have been used for separation of hydrocarbons in general and also can be extended to homologs. For separation glass column of 1 cm in diameter was packed with 25 g of silica gel, impregnated with 5 % silver nitrate, and eluted by hexane. Low amounts of product mixture, which can be separated on such a column are determined by molar olefin/silver nitrate ratio which had to be not less than 1/10.^[182]

The structure of the molecule of **14** was confirmed by spectral data as well as X-ray crystal structure analysis. Two unequal quaternary signals in the ¹³C NMR/APT spectrum at 133.7 and 133.4 ppm indicate the product of cross-coupling. Alkene **14** also possesses nine methine and six methylene resonances of carbon atoms in APT spectra in agreement with product symmetry.

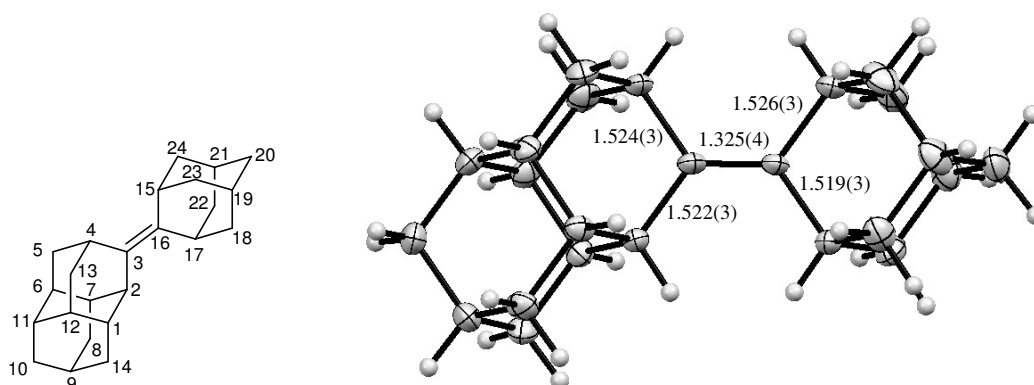


Figure 10. X-ray structure of adamantylidenediamantane-3 (**14**).

Compound **14** is comprised of two different cages (*i.e.*, adamantyl and diamantyl moieties) that are mutually connected by a bond that joins a methylene bridge in one cage with a corresponding methylene bridge in the other (Fig. 10). Thus, in **14** the C(3) and C(16) methylene bridges in adjacent cage moieties are connected via a C=C double bond (numbers of carbon atoms are as on Fig. 10). Structure on Fig. 10 shows that all methylene bridge bonds that are adjacent to the connecting double bond are the shortest C–C bonds in molecule and are equal to: C(2)–C(3) – 1.522(3) Å; C(3)–C(4) – 1.524(3) Å; C(15)–C(16) – 1.526(3) Å and C(16)–C(17) – 1.519(3) Å respectively. For more details about the structure of **14** see page 41, 54 and Appendix II.

3.2.4. Comparison of used McMurry reductive coupling procedures

As it was discussed above, both titanium (III) chloride – lithium and titanium (IV) chloride – zinc reactive systems were tested. Procedure of first choice for coupling based on the reduction pair titanium (III) chloride – lithium.^[179] Lithium was found to be less hazardous and easier to handle than potassium, used traditionally. It was found that reagent, obtained from titanium (III) chloride, as well as TiCl₃ itself, is extremely sensible to the presence of oxygen, and despite all precautions this procedure failed to give stable results.

Alternatively the reduction with titanium (IV) chloride – zinc is easier to handle, and resulted in higher yield of coupled products, as it demonstrated in Table 5.

Table 5.

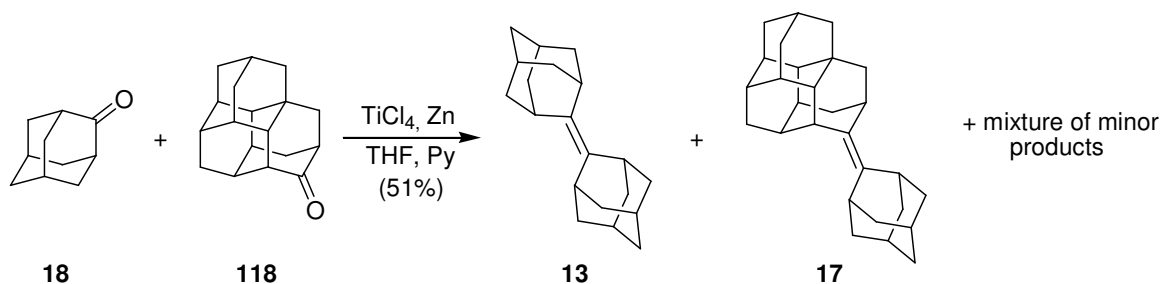
Comparative yields of McMurry coupling in different conditions.

	McMurry coupling by reductive pair	
	Titanium (III) chloride – lithium	Titanium (IV) chloride – zinc
Ti reagent : Me : ketone ratio	1 : 3 : 0.25	1 : 2.07 : 0.5
Solvent	DME	THF
Yield of olefin from coupling of 18	42% (lit. 84–87%)	85%
Yield of olefins from coupling of 113	46%	74%
Yield of olefins from coupling of 18 and 113	56%	80%

Based on comparative analysis of these two systems we then used titanium (IV) chloride – zinc pair in tetrahydrofuran for further syntheses.

3.2.5. Synthesis of adamantylidenetriamantane-8 (17)

Taking into account accessibility of starting ketones, cross coupling of **18** and **118** was performed by the Scheme 58 utilizing reductive pair titanium (IV) chloride – zinc:^[126]



Scheme 58.

Quenching of the reaction mixture and extraction of products was performed as described above and adamantylidenetriamantane-8 (**17**) was separated by column chromatography on silica gel impregnated with 5% silver nitrate. The structure of **17** was confirmed based on 2D NMR spectral data (^1H - ^1H COSY, HSQC, HMBC and HSQC-TOCSY).

The ^{13}C NMR spectrum displays 28 carbon resonances. Comparison of APT and DEPT NMR proved presence of 11 methylene, 15 methine and 3 quaternary carbon atoms, two of which were observed in the low field ($\delta_{\text{C}} = 133.5$; 133.4 ppm) and could be assigned to C-8 and C-20, while the signal of C-1 is at $\delta_{\text{C}} = 33.8$ ppm (for numbering of corresponding carbon and hydrogen atoms see Fig. 11).

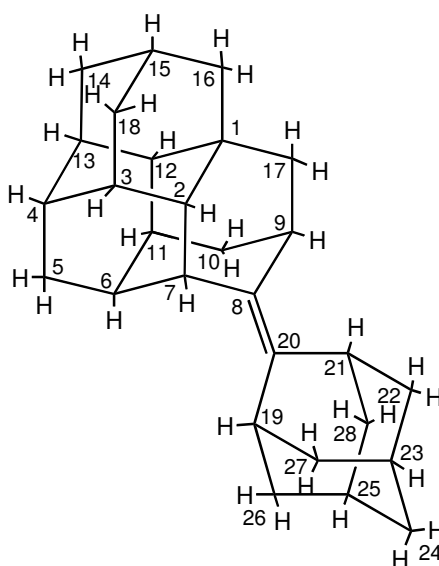


Figure 11. The structure of adamantylidenetriamantane-8 (**17**).

Characteristic features of ^1H NMR spectrum (COSY experiment) resolved the signals of protons connected to carbon atoms neighboring to the double bond. Protons H-9, H-21 and H-19 ($\delta_{\text{H}} = 2.85, 2.90, 2.94$ ppm respectively) resonate in the lower field then H-7 ($\delta_{\text{H}} = 2.64$ ppm). Final assignment of those four protons was based on NOESY experiment (Fig. 12), where H-7/H-19 and H-9/H-21 interactions were observed.

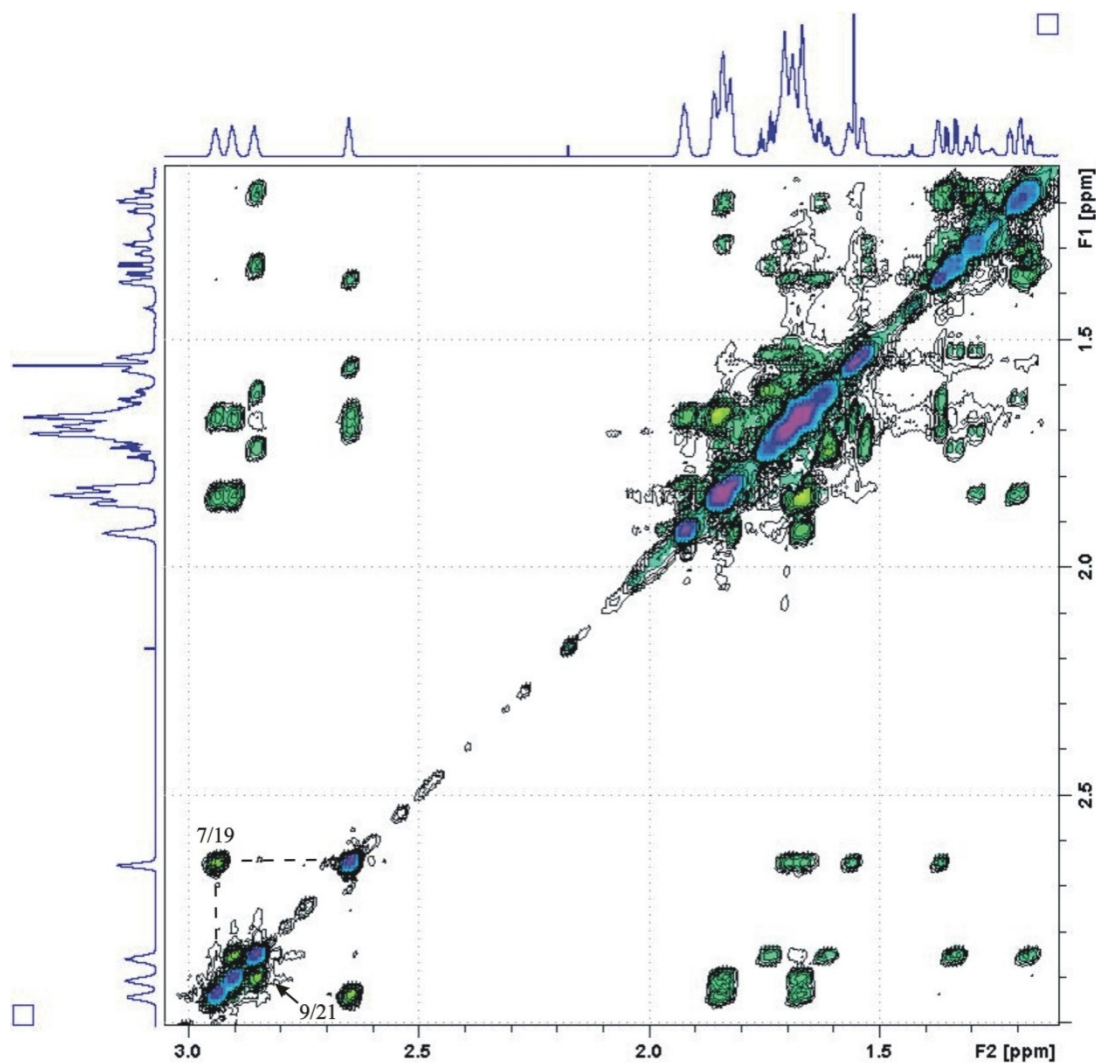


Figure 12. NOESY spectrum of **17**.

Correlations of H-21 and H-19 with H₂-28, H₂-27, H₂-22 and H₂-26 show that these protons are almost equal and give complicated resonance picture at $\delta_{\text{H}} = 1.62\text{--}1.70$ ppm and $1.80\text{--}1.88$ ppm (Fig. 13). Their correlation with peak at $\delta_{\text{H}} = 1.92$ ppm allows to identify H-25 and H-23 protons that are very close in shifts, while their correlation with protons H₂-24 is overlapping with peaks of other four CH₂ groups in the adamantylidene fragment. Resonance of proton H-9 correlates with protons H₂-17 ($\delta_{\text{H}} = 1.15\text{--}1.34$ ppm), which do not correlate with

other protons except H-9 and H₂-10 ($\delta_{\text{H}} = 1.59\text{--}1.77$ ppm). Proton H-7 correlates with H-6 and H-2. Signal of H-2 in higher field ($\delta_{\text{H}} = 1.37$), has only 2 correlations with proton H-3 (in multiplet) and H-12 ($\delta_{\text{H}} = 1.53$). In the high field another doublet of doublets is assigned to the protons attached to the quaternary carbon atom H₂-16 ($\delta_{\text{H}}=1.18\text{--}1.32$ ppm) and to assign the signal for H-15, is hidden in multiplet $\delta_{\text{H}}=1.59\text{--}1.77$ ppm).

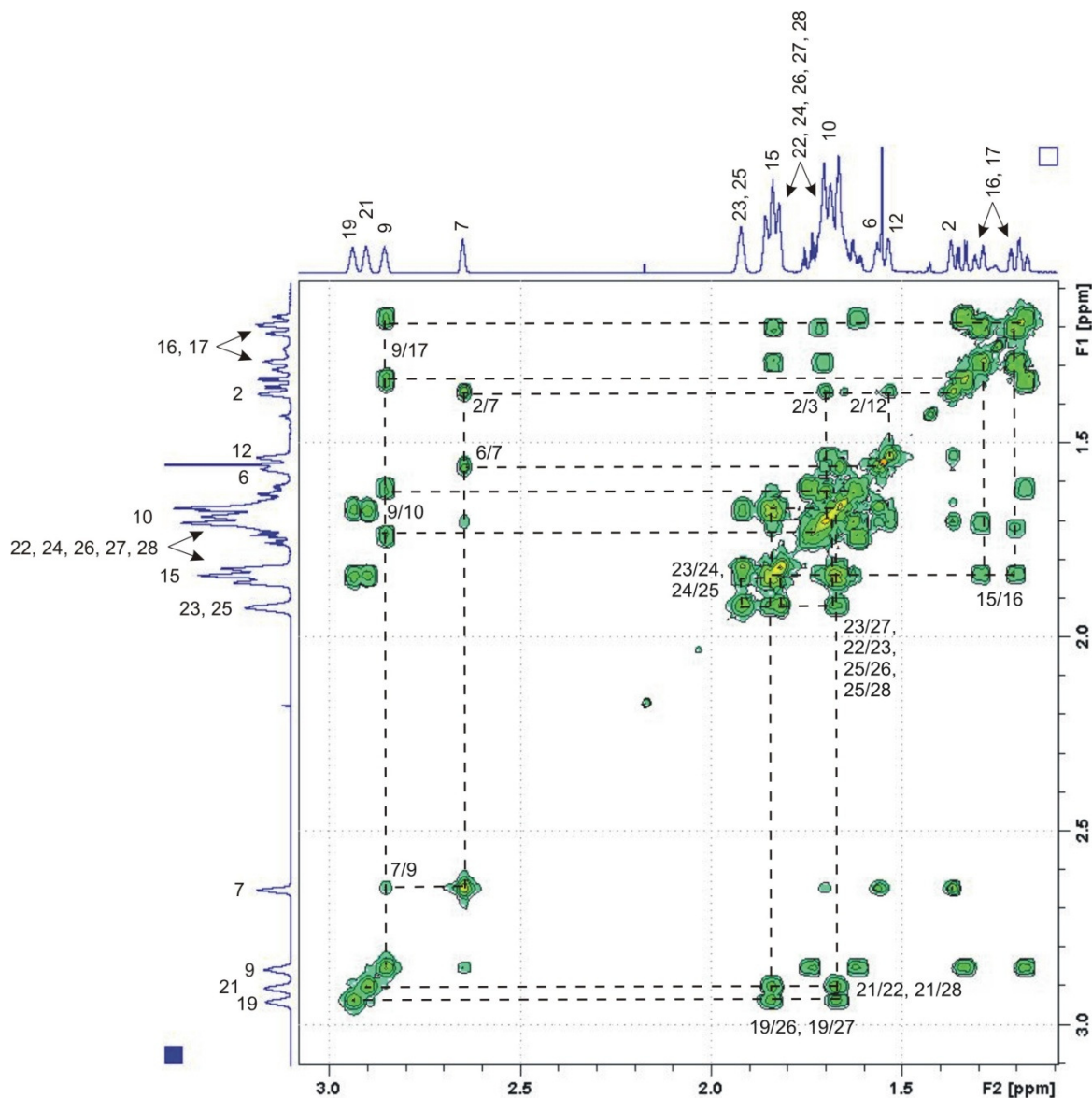


Figure 13. ^1H - ^1H COSY spectrum of **17**.

The assignment of the rest of ^1H NMR and COSY signals is possible after combined analysis of HMBC and HSQC spectra.

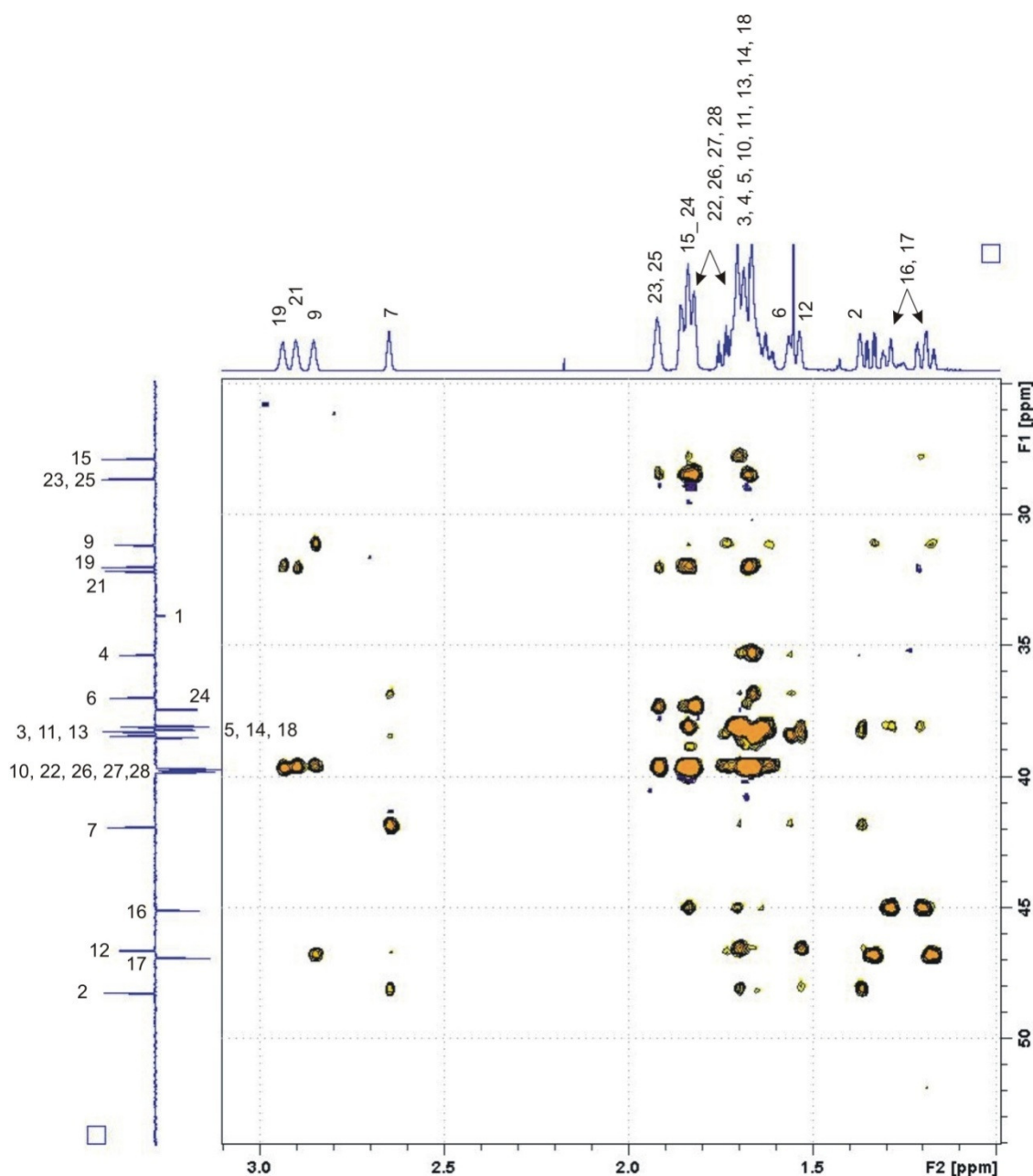


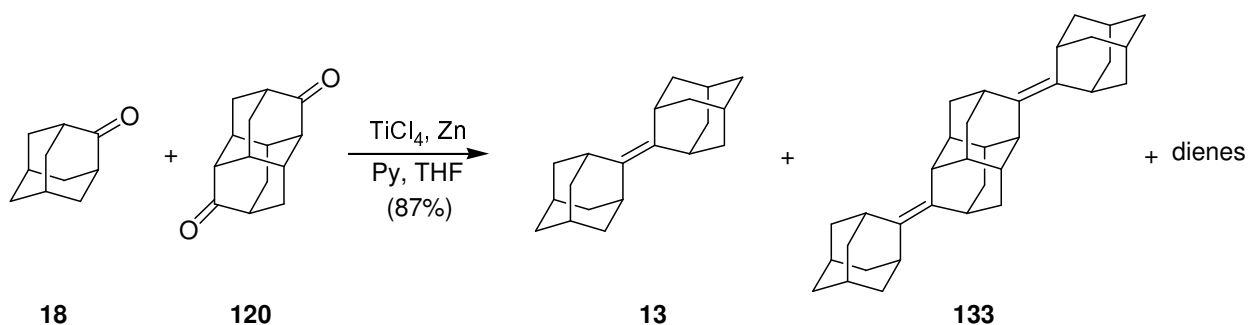
Figure 14. HSQC-TOCSY spectrum of **17**.

The signal of C-15 is defined in the higher field ($\delta_C = 27.8$) (Fig. 14). Signals of carbons C-12 and C-2 are located in the lower field of ^{13}C NMR spectrum. Proton H-7 in the low field has only one correlation with H-2 ($\delta_C = 48.2$; $\delta_H = 1.37$). Another tertiary carbon resonate in the low field (C-12 $\delta_C = 46.6$; $\delta_H = 1.53$). Correlation of H-2 shows that C-3 is located in the group of six carbon atoms ($\delta_C = 38.0\text{--}38.5$) as one of three tertiary carbons. Similarly the correlation of H-12 displays that C-11 and C-13 are in the same group as C-3. Resonance of H-7 in the higher field defines C-6 ($\delta_C = 36.9$; $\delta_H = 1.57$). Carbon atom C-17 ($\delta_C = 46.9$; $\delta_H = 1.17\text{--}1.37$) has correlation only with H-9, providing possibility to assign the C-10 as one of the signals from group of five overlapping secondary carbons, together with C-28, 27, 22 and 26 carbon atoms.

Carbon atom C-16 ($\delta_C = 45.1$; $\delta_H = 1.20$ – 1.29) is also located in the low field of ^{13}C NMR spectrum similarly to C-17, and correlates with H-15. Other correlations of H-15 allows to predict that signals of C-18 and C-14 belong to the group of six carbon atoms, together with last unidentified carbon atom C-5 ($\delta_C = 38.0$ – 38.5). Signal at $\delta_C = 35.3$ is defined as belonging to C-4, that is confirmed by characteristic correlations in the HMBC spectra with C-14/18, C-2/12 and C-6. All linkages above are also confirmed by the characteristic couplings in the HMBC spectrum.

3.2.6. Synthesis of di(adamantylidene-2)diamantane-3,10 (**133**)

In order to synthesize spatially-congested alkenes containing three cage fragments we performed coupling of **18** with **120** under the molar ratio 3 : 1 according to Scheme 59.



Scheme 59.

Since the target product is poorly soluble in hexane, benzene and many other standard organic solvents, the reaction products were extracted by carbon disulphide. In cross-coupling of **120** with **18** compounds **13** and di(adamantylidene-2)diamantane-3,10 (**133**) may form together with mixture of dione-dione coupling products. Due to low volatility of **133** the detailed analysis of the product mixture was impossible by means of GC/MS. Structure of the target product was confirmed by the combination of different 1D and 2D spectral analysis (^{13}C NMR, DEPT and HSQC-TOCSY).

Two signals of the low field in ^{13}C NMR spectrum at 133.7 and 133.5 ppm indicate that carbon atoms at double bond belong to non-equal cage fragments. Also in DEPT spectrum six methine (two of which have two-carbon intensity) and four methylene (three of which with two-carbon intensity) signals were observed.

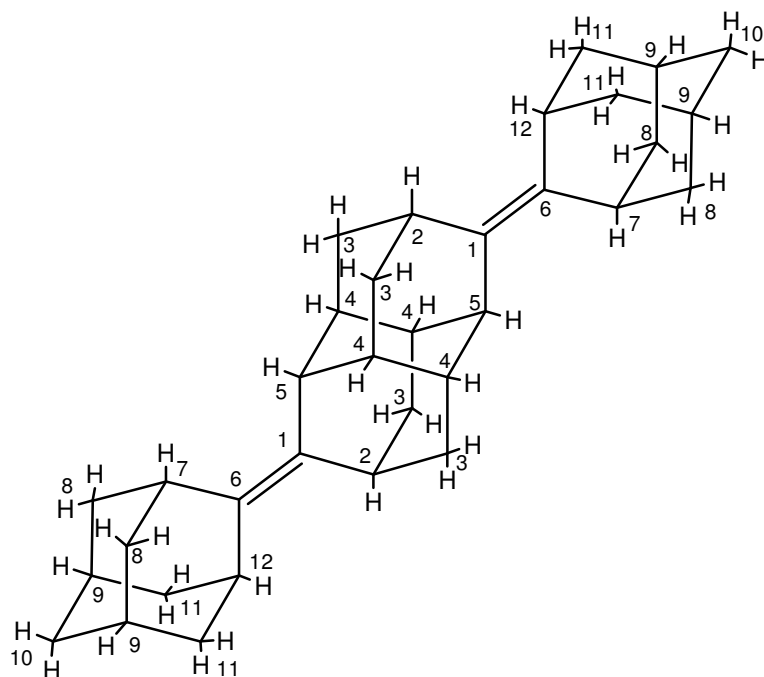


Figure 15. The structure of di(adamantylidene-2)diamantane-3,10 (**133**).

HSQC-TOCSY spectrum allows identifying all signals of methines C-4 and C-9 and methylenes C-3, C-8 and C-11 (Fig. 16) (for numbering of corresponding carbon atoms see Fig. 15)

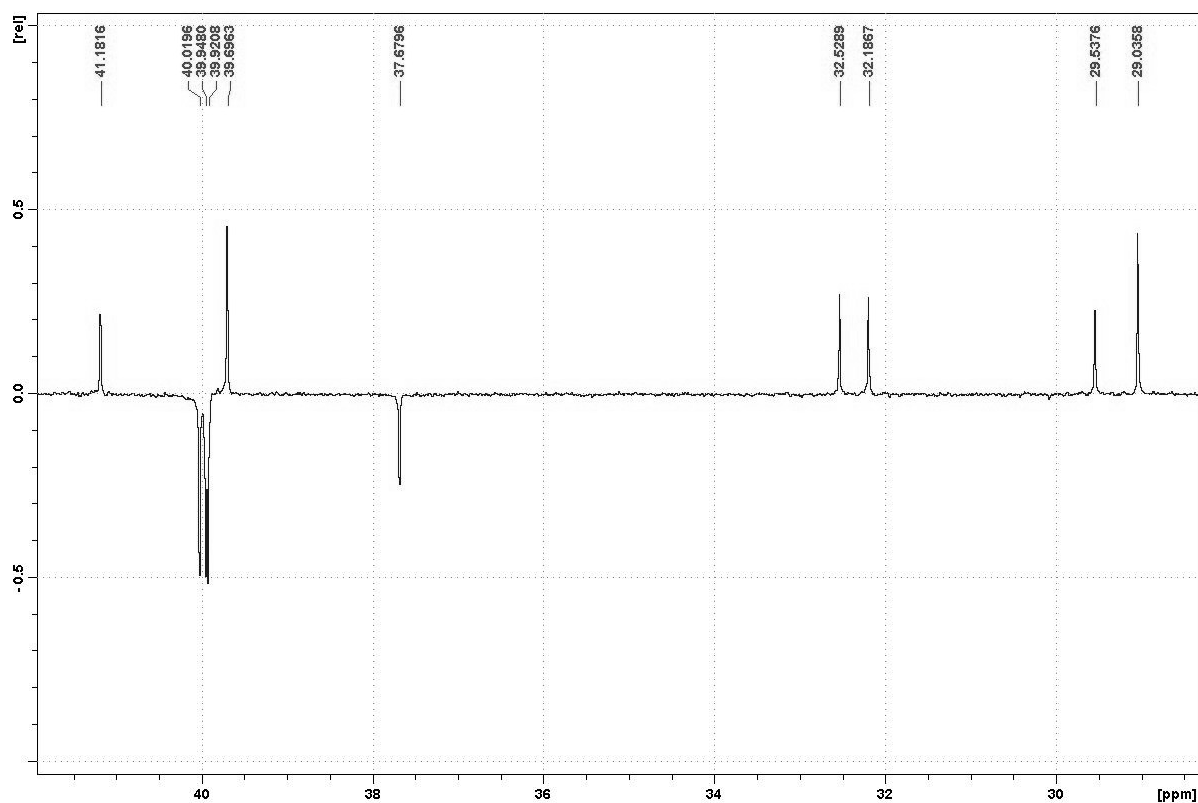
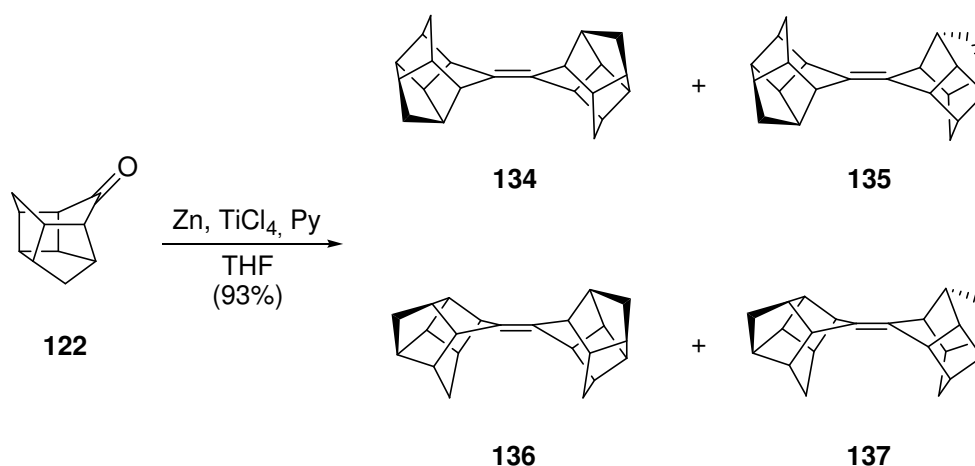


Figure 16. The part of the HSQC-TOCSY spectrum of **133**.

3.2.7. Synthesis of C_S -8-trishomocubylidene- C_S -8-trishomocubanes (134-137)

In order to study the influence of the ketone structure on stereochemistry of coupling the compound **122** was chosen. Ketone moiety in **122** located in the six- and five-membered aliphatic rings and molecule overall possesses higher strain.^[183]

Coupling of **122** into diastereomeric 8-pentacyclo[5.4.0.0^{2,6}.0^{3,10}.0^{5,9}]undecylidene-8-pentacyclo[5.4.0.0^{2,6}.0^{3,10}.0^{5,9}]undecanes (**134-137**) was performed as shown in Scheme 60.



Scheme 60.

Reaction was carried out under argon as described above in two steps: preparation of titanium (IV) chloride – zinc reagent and addition of the solution of ketone **122** into reaction mixture.^[126] After 20 hours of reflux a mixture of products formed with total yield of 80-90%. The crude product mixture contains traces of alcohols from the GC/MS analysis data, and was separated by column chromatography on silica gel. Typical chromatogram contains asymmetric and split peaks, indicating that all four diastereomers form. Two groups of the signals were observed in a ratio *ca.* 9/1. Solely for the convenience of presentation and until the proof of the structure of the compounds is complete, *trans*-structure was attributed to the reaction products with a lower retention time in the chromatogram and, consequently, *cis*-structure – to the reaction products with higher retention time. Obtained mixture of alkenes (**134-137**) was subjected to fractional crystallization from hexane (Fig. 17). GC/MS analysis of fractions displayed in Table 6.

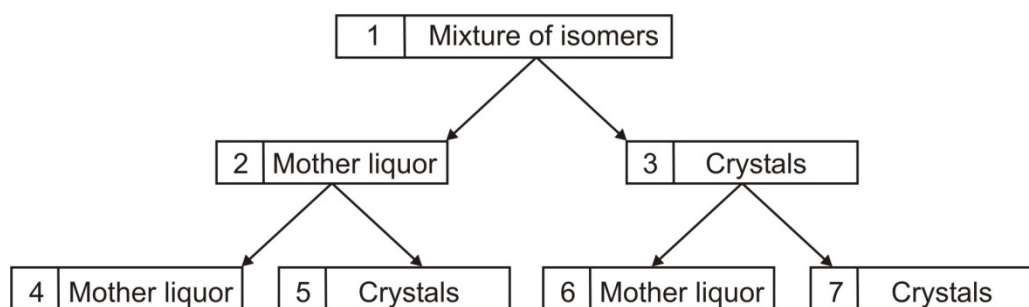


Figure 17. Fractional recrystallization of **134–137** mixture of isomers.

Table 6.

Composition of fractions of **134–137** recrystallization.

№ fraction	Named	Mixture composition and weight of sample		
		134–135, %	136–137, %	Weight, g
1	Mixture of isomers	89	11	0.98
2	Mother liquor	88	12	0.84
3	Crystals	97.6	2.4	0.14
4	Mother liquor	84.5	15.5	0.63
5	Crystals	96.2	3.82	0.21
6	Mother liquor	92.8	7.2	0.04
7	Crystals	100	0	0.10

As seen from Table 6, already after two steps of crystallization of about 1 g of the mixture pure sample of one pair of products was obtained. Considering the dynamics of enrichment of mixture with another pair of isomers (5%), it's separation by crystallization from initial mixture was not performed.

Each of the formed products (**134–137**) must possess eleven signals in the ^{13}C NMR spectrum. A fragment of ^{13}C NMR spectrum (DEPT), measured for sample 3 (Fig. 18), contains seventeen signals of carbon nuclei with different intensity (three signals of carbon nuclei with very low intensity ignored): four of those of methylene and rest – methine. In the ^{13}C NMR spectrum the signal of a carbon atom at 132.8 ppm is also present which can be attributed to the equivalent quaternary carbon atoms of the double bond. However, such amount of signals indicates mixture of isomers **134** and **135**, while some signals are overlapped and cannot be resolved.

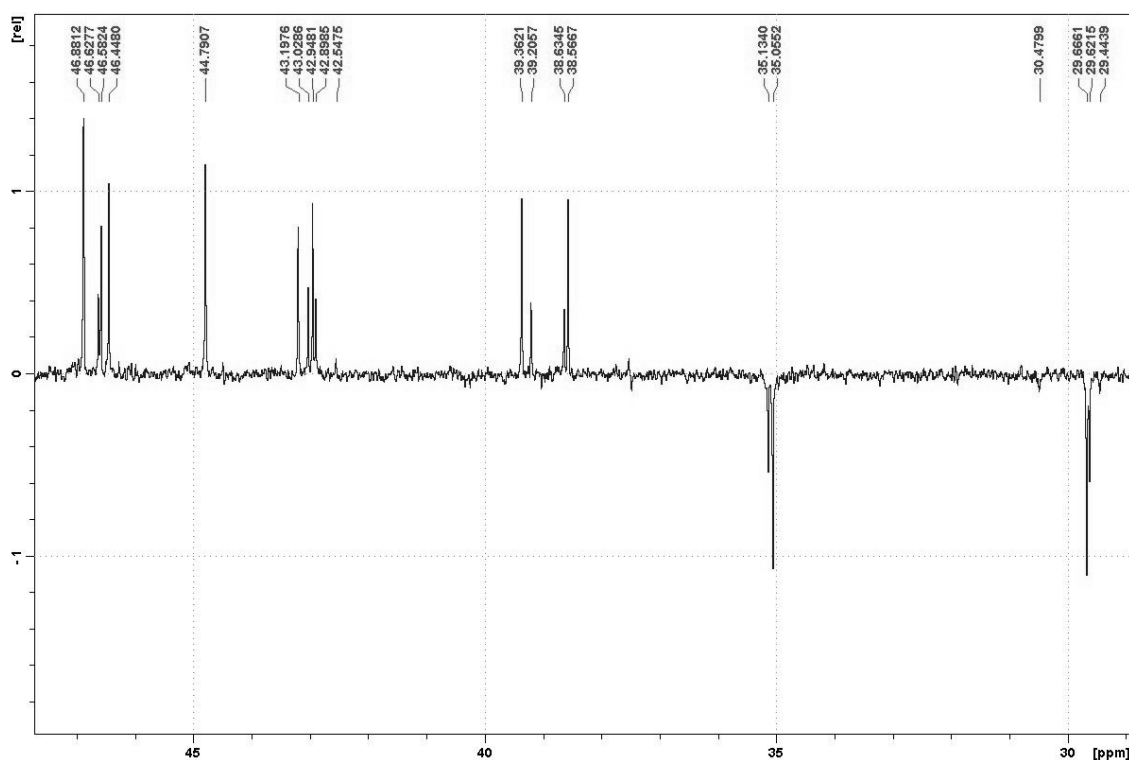


Figure 18. DEPT spectrum of sample 3.

Additional recrystallization of the sample with subsequent analysis of crystal fraction by ^{13}C NMR after three crystallizations gave a single product with observed in DEPT spectrum only ten signals of equal intensities (Fig. 19). Signal of the quaternary carbon atoms of the double bond is at 132.9 ppm of ^{13}C NMR.

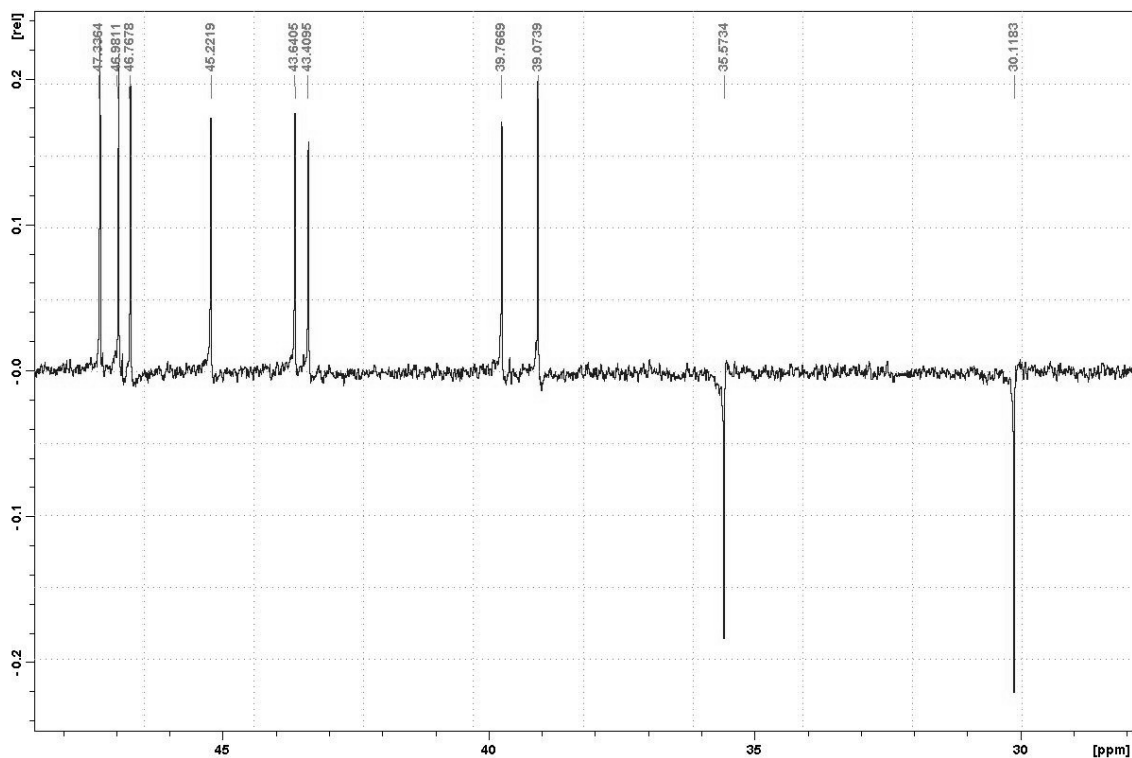


Figure 19. DEPT spectrum of sample 7 of **135**.

The X-ray crystal structure analysis allowed to identify this hydrocarbon as *C_i-trans*-C₅-8-trishomocubylidene-C₅-8-trishomocubane (**135**), which initially was a main component of the reaction mixture.

According to the X-ray crystal structure analysis, compound **135** is comprised of two cages (*i.e.*, C₅-8-trishomocubyl moieties) that are mutually connected by a bond that joins a methylene bridge in one cage with a corresponding methylene bridge in the other (Fig. 20).

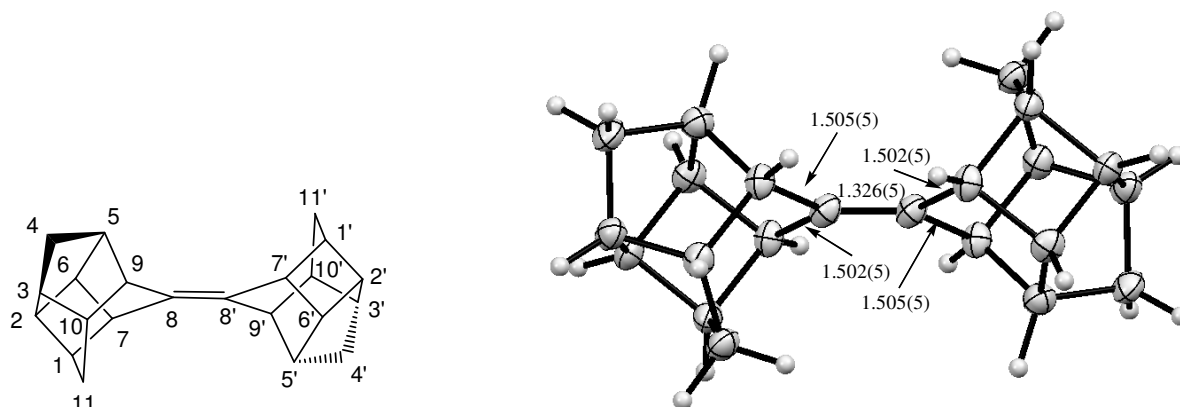


Figure 20. X-ray structure of *C_i-trans*-C₅-8-trishomocubylidene-C₅-8-trishomocubane (**135**).

In **135** the C(8) and C(8') methylene bridges in adjacent cage moieties are connected via a C=C double bond (numbers of carbon atoms are as on Fig. 20). Structure on Fig. 20 shows that all methylene bridge bonds that are situated adjacent to the connecting double bond are the shortest C–C bonds in molecule and are equal to C(8)–C(9) – 1.502(5) Å (equal to C(8') – C(9')) and C(7)–C(8) – 1.505(5) Å (equal to C(7') – C(8')) respectively). For more details about the structure of **135** see page 41, 58 and Appendix II.

3.2.8. Dispersion forces and the structure and stability of the selected diamondoid dimers

Based on X-ray crystal structure analysis we found that alkene **14** displays a double bond length of 1.325 Å and 1.976/1.981 Å for the nonbonding distances between hydrogens around the *sp*² carbon atom, as well as insignificant torsion angles 1.94/2.17° (Fig. 21). This is in agreement for **13**.^[180] Thus, the double bond is shorter than the typical 1.34 Å^[184], despite intramolecular H•••H distances are relatively short and the distortion of the structure would be expected. As was reported previously,^[185] in the construction of cage dimers with extraordinary long single carbon-carbon bond attractive dispersion interactions provide extra stabilization. Due to favorable hydrogen-hydrogen dispersion contacts around the C–C bond it would be suggested that the same applies to the sterically-congested alkenes, where intramolecular H•••H

distances are close to optimal found for molecular crystals of many organic structures (2.2–2.4 Å).^[186] For instance, intermolecular hydrogen-hydrogen bond in the crystal of **14** was found to be 2.352 Å (see App.).

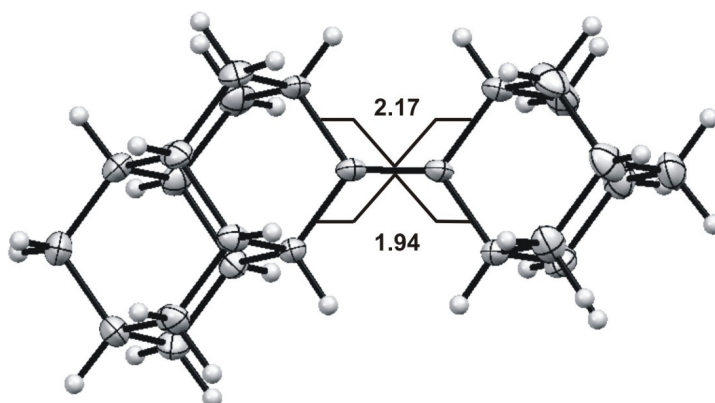


Figure 21. Torsion angles in the molecule of **14**.

For estimation of the influence of noncovalent interactions in molecules of coupled diamondoids and *C_i-trans-C₅-8-trishomocubylidene-C₅-8-trishomocubane*, we optimized their structures using various density functional theory (DFT) methods. For comparison we used B3LYP/CC-pVTZ and B3PW91/CC-pVTZ together with extensively reparametrized functionals, where dispersion correlation are incorporated *a posteriori* (B97D/CC-pVTZ)^[187] as well as *a priori* parametrized approaches (M06-2X/CC-pVTZ)^[188]. Also the B3LYP-D3/CC-pVTZ approach with dispersion corrections introduced by Grimme was applied.^[189]

Nearly in every case calculation showed systematic underestimation of the experimental values, as can be seen from selected data for **14** which is introduced on the Fig. 22.

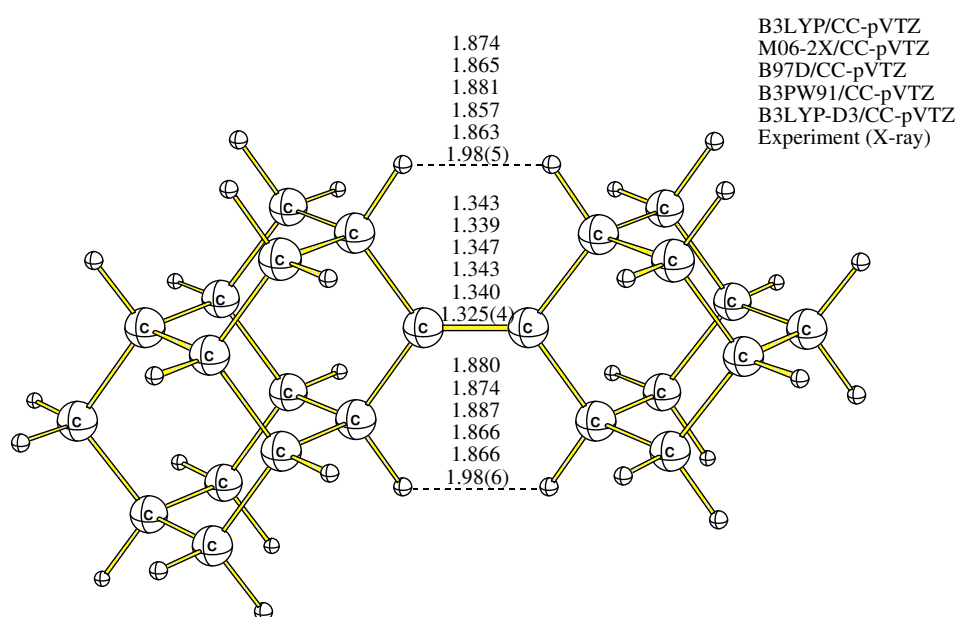


Figure 22. Selected experimental and computed bond lengths and distances in the molecule of

14.

Quantum-chemical calculations^[190] on all levels of theory showed a significant increase in length of the double bond (1.339–1.357 Å) and reducing the distance between atoms of hydrogen (1.857–1.890/1.865–1.894 Å) in comparison with the experimental data. An exact match of calculations with experiment cannot be expected due to approximations in the DFT formulations and differences which arise from gas-phase *vs* solid-phase structures, where the bond lengths usually are shorter.^[185] Also such a systematic errors in the evaluation of the distances between hydrogens can be explained by methods, used to identify positions of the hydrogen atoms by X-ray analysis. It is widely known that by X-ray data distance between hydrogens is shorter then by neutron measurements, since X-ray only determines the maximum of the electron density. At the same time electron of the hydrogen atom can be displaced from nucleus. Thus, neutron diffraction data would be needed to estimate deviations of computed data from H•••H true distances. As long it is unavailable and even we operate by coordinates of hydrogen atoms, it was decided to concentrate on the estimations of double bond length by computational methods and chose sets of data based on proximity of experimental and computed C=C values. It is also known, that one has to be cautious while comparing computed minimum with X-ray structure, as often compound during crystallization is distorted and does not retain highest possible point group of symmetry.^[191]

The structures of *anti*- (**15**) and *syn*-diadamantylidenediamantane (**16**) were also optimized at the above levels. As was found experimentally, the double bond length is 1.333 and 1.335 Å for **15** and **16** respectively (Figures 24 and 25). It is longer than in **14** but still shortened comparably to standard double bond length. The nonbonding distances between atoms of hydrogen bonded to carbon atoms around sp^2 carbon atom are 1.966 Å in **15** and 1.958/2.002 Å in *syn*-isomer **16**. Torsion angles are found to be -0.41/0.41 ° in **15** and 0.00 ° in **16** (Fig. 23).

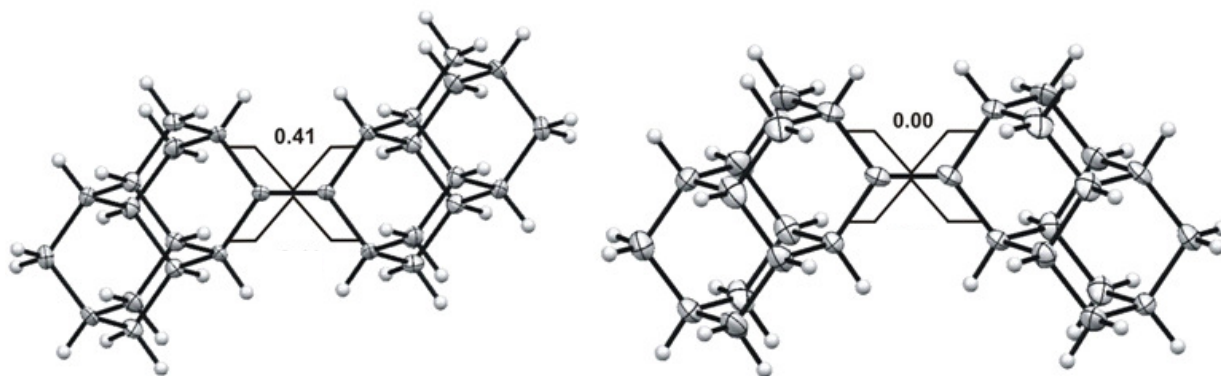


Figure 23. Torsion angles in molecules of **15** (left) and **16** (right).

The corresponding carbon-carbon bond length neighboring double bond is slightly different for each of the cages (1.518/1.501 Å and 1.512/1.519 Å, respectively) (see also page 40). Intramolecular H•••H distances here are also shorter than optimal H•••H distances and it can be explained by the same reasons. Shortest intermolecular hydrogen-hydrogen bonds in **15** and **16** are 2.248 and 2.291 Å respectively (see App. II).

Optimization of **15** also showed an increase in length of the double bond (1.340–1.358 Å) and reducing the distance between atoms of hydrogen (1.857–1.887 Å) in comparison with the experimental data (Fig. 24).

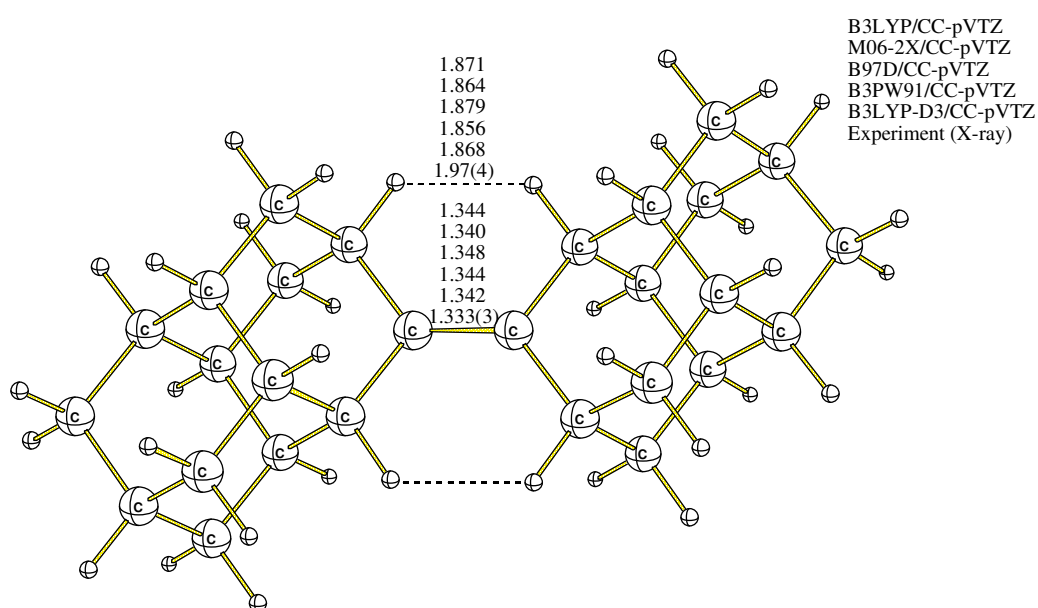


Figure 24. Selected experimental and computed bond lengths and distances in the molecule of **15**.

Similarly, for **16** computations do not agree well with the results of X-ray analysis. The computed double bond is longer than by experimental data (1.340–1.358 Å), and the intermolecular distance between atoms of hydrogen are decreased (1.861–1.895/1.851–1.879 Å). Moreover, experimental data shows that repulsion forces distort structure of *syn*-isomer **16** increasing the distance between bulky substituents, while calculations underestimate the repulsive forces between hydrogens (Fig. 25). This is a characteristic for all dimers studied.

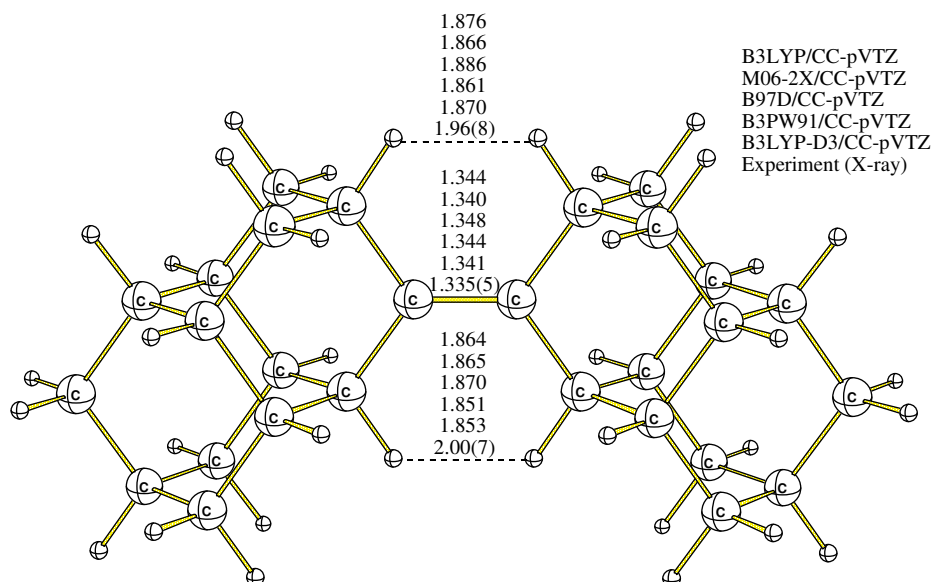


Figure 25. Selected experimental and computed bond lengths and distances in the molecule of **16**.

We conclude that in diamondoid compounds connected by unsaturated carbon-carbon bond the hydrogen-hydrogen contact around the sp^2 carbon atoms are much shorter than optimal, thus having destabilizing effect. This is in contrast to single C–C bond in diamondoid dimers,^[185] where such contacts are compensated by the number of H•••H-contacts that are close to the optimal.

However, picture is different for the product of coupling **135**. In **135** the length of the double bond is 1.326 Å and 2.310 Å for the distances between atoms of hydrogen, bonded to carbon atoms around the sp^2 carbon atoms, with small torsion angles 0.62/ –0.62 ° (Fig. 26).

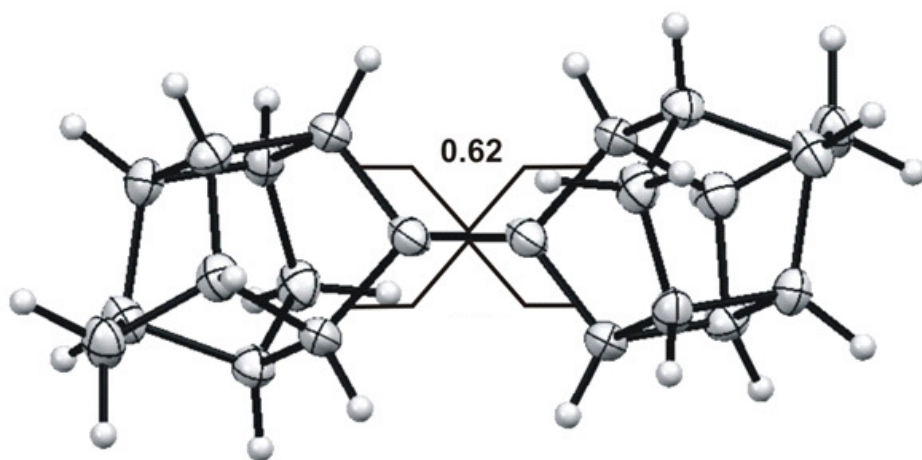


Figure 26. Torsion angles in molecule of **135**.

Those intramolecular H•••H distances are longer than in coupled diamondoids and are around the optimal values.^[186] In the crystal of **135** both intramolecular and intermolecular H•••H distances in the crystal are comparable (see App.).

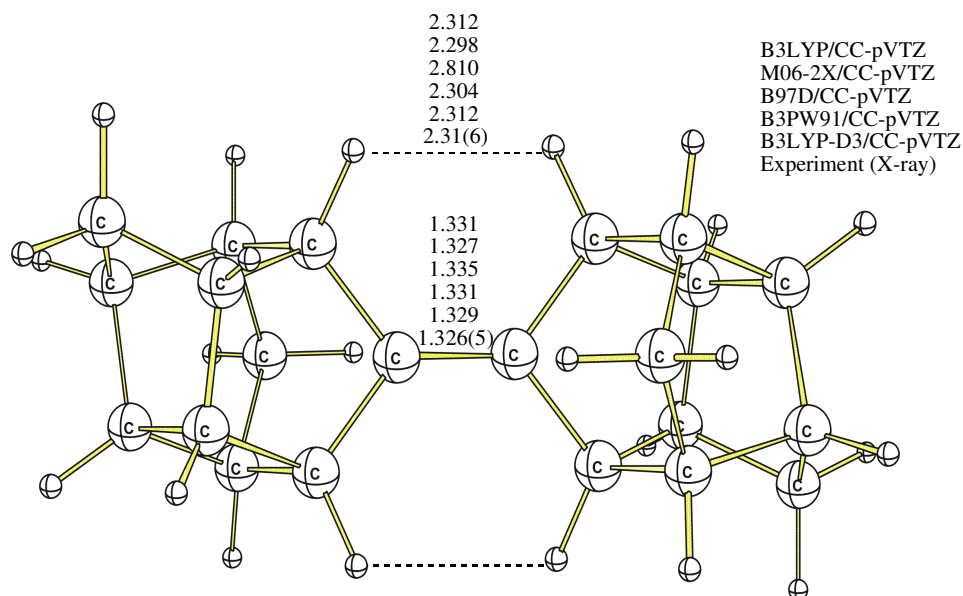


Figure 27. Selected experimental and computed bond lengths and distances in the molecule of **135**.

Computations display an increase in length of the double bond (1.327–1.345 Å) while M06-2X/CC-pVTZ and B3LYP-D3/CC-pVTZ values (1.3267 and 1.3287 Å) deviates from experimental data insignificantly. The M06-2X and B3LYP-D3 estimate the intramolecular distances between atoms of hydrogen (2.298 and 2.312 Å vs 2.310 Å). Such a match of calculations with experiment allow to assume that **135** is more “traditional” olefin, where the H•••H contacts around the C=C bond *stabilize* the molecule. Thus, we would expect slightly different electronic and chemical properties then in the case of compounds **14–16**, where hydrogen-hydrogen contacts are shorter then optimal.

The structures of the isomeric *D*₃-trishomocubylidene-*D*₃-trishomocubanes (**95**, **104**) were computed at the same levels of theory and compared with literature data. While the experimental information about H•••H distances is not available, the lengths of the C=C bond are 1.322 and 1.328 Å for **95** and **104**, respectively.^[126] Computations show similar deviations for the compound **135** described above. Carbon-carbon double bonds of **95** were found to be 1.320–1.337 Å with H•••H bonds lying in the limits 2.534–2.567 Å (Fig. 28). Similarly C=C of **104** is 1.320–1.337 Å and H•••H – 2.533–2.566 Å (Fig. 29).

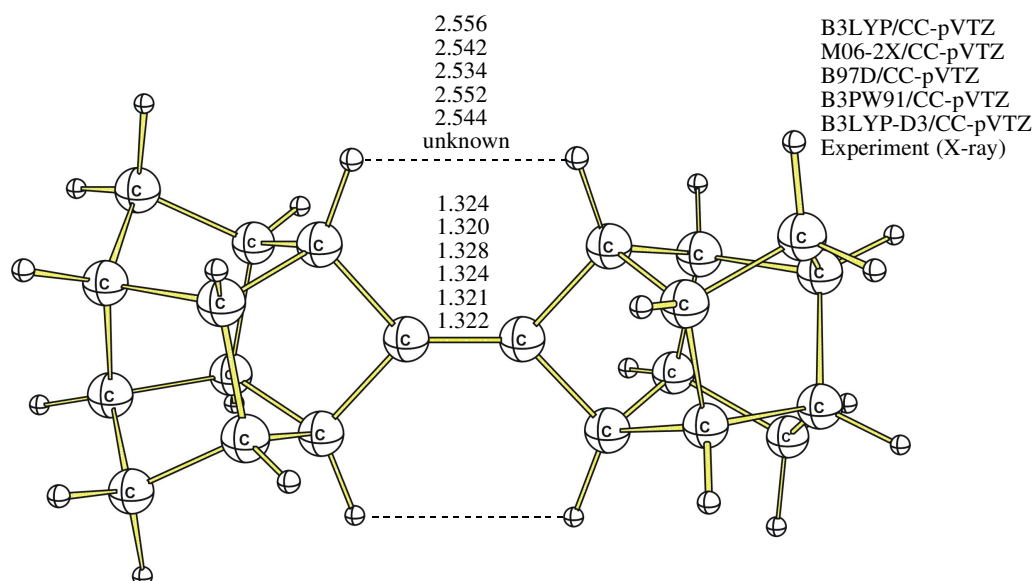


Figure 28. Selected experimental and computed bond lengths and distances in the molecule of **95**.

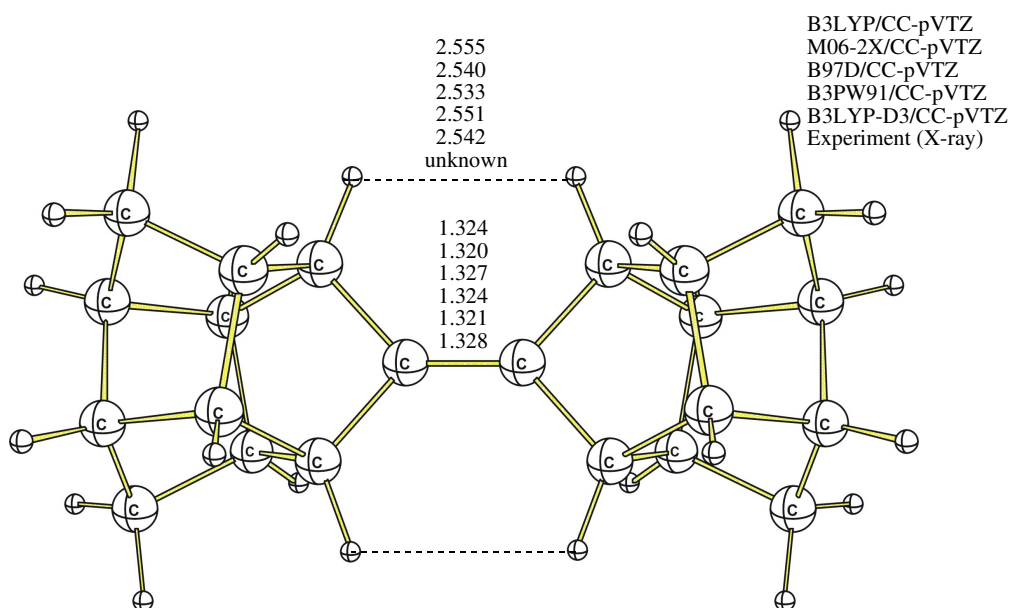


Figure 29. Selected experimental and computed bond lengths and distances in the molecule of **104**.

Picture would not be complete without smallest coupled diamondoid **13** computational analysis. While the best match with experimental value^[180] of the length of C=C bond was obtained by M06-2X and B3LYP-D3 methods (1.339 and 1.340 Å vs experimental 1.336 Å), the best estimate for H•••H distances were found at B97D (Fig. 30).

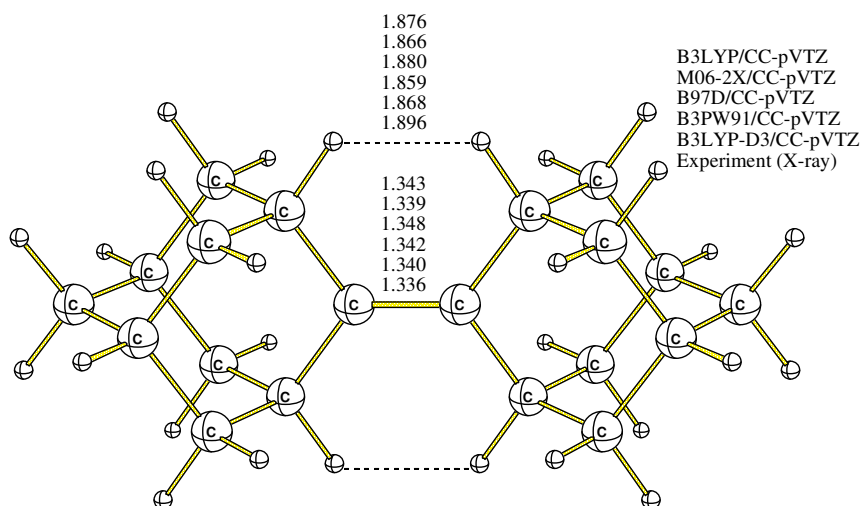


Figure 30. Selected experimental and computed bond lengths and distances in the molecule of **13**.

Since all the coupled compounds reviewed above can be considered as tetrasubstituted ethylenes, more simple structures such as unsubstituted ethylene (**138**) as well as tetramethylethylene (**139**), tetra-*iso*-propylethylene (**140**) and tetra-*tert*-butylethylene (**141**) were analysed as above. Unfortunately, reported experimental data was obtained by different methods for all the compounds, except **141**, thus forcing us to concentrate on the comparison of the different computational approaches.

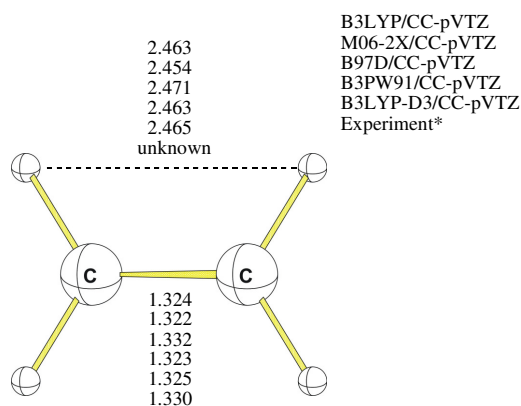


Figure 31. Selected experimental and computed bond lengths and distances in the molecule of **138**.

The carbon-carbon double bond length in **138** is 1.339 Å, however recently it was reconsidered to 1.3305 Å.^[192] In general, already B3LYP with different basis sets is sufficient (length of the C=C is 1.330 Å in B3LYP/6-31G**). It is impossible to discuss H•••H distances and torsion angles in **138** due to the rigidity of structure. For **139** in the gas phase electron

diffraction gives C=C distance of 1.351 Å.^[193] Structure of **139** with D_2 symmetry was found to be minimum, computed torsion angles are about 2 °. It is also worthwhile to note that all of the computational methods exhibited significant errors in the estimation of the unsaturated bond lengths in comparison to the experimental data (Fig. 32). Reason might be that of outdated experimental base and approach, however no up-to-date data was found.

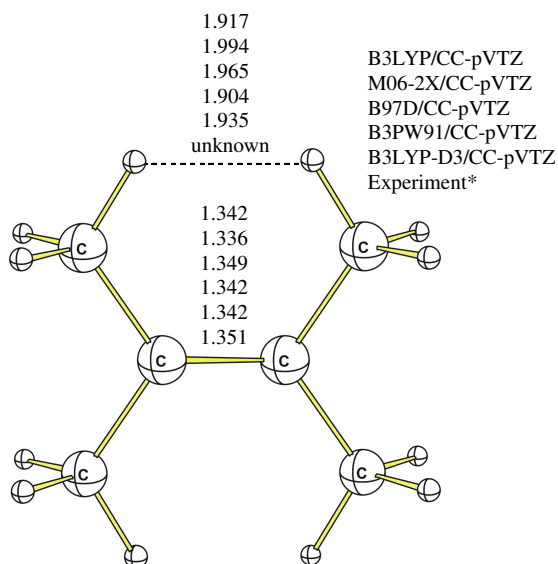


Figure 32. Selected experimental and computed bond lengths and distances in the molecule of **139**.

The only available X-ray data for tetrasubstituted ethylenes is that for tetra-*iso*-propylethylene.^[194] It was found that **140** at low temperature X-ray has C_{2h} -symmetry and it is also in agreement with other empirical data.^[195] The C=C length was determined as 1.347 Å. Hydrogen-hydrogen distances are shortened despite the rotations of *iso*-propyl groups around C–C bond, adjacent to unsaturated C=C (Fig. 33). Deviations of computed distances from experimental value are not significant and bond length of C=C best estimated at CC-pVTZ basis. Torsion angles are those of 0 °, since repulsion is compensated by *iso*-propyl group rotations.

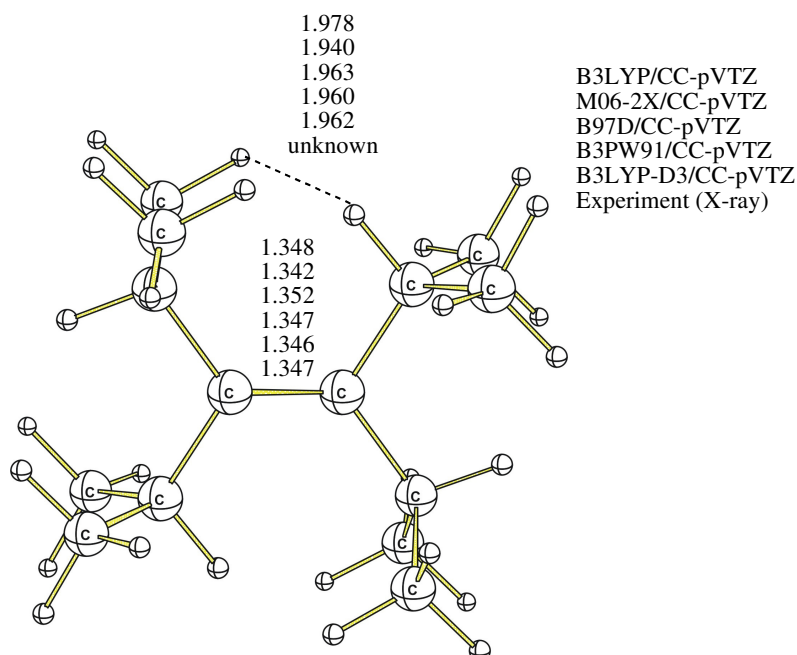


Figure 33. Selected experimental and computed bond lengths and distances in the molecule of **140**.

The next computed structure **141** was not yet synthesized despite attempts were performed quite recently.^[196] Computed results were found to be in overall agreement with previously reported calculated structures.^[197] Closely located in space hydrogen atoms are on the distances comparable to those of computed structures of coupled diamondoids. Unsaturated carbon-carbon double bond is considerably elongated due to the repulsion of the bulky substituents (Fig. 34). Torsion angles are around 46-48 ° for all methods, except B3LYP-D3, where they are close to 70 °. At the same time perfect torsion of 45 ° minimized repulsion between *tert*-butyl moieties by double bond distortion.

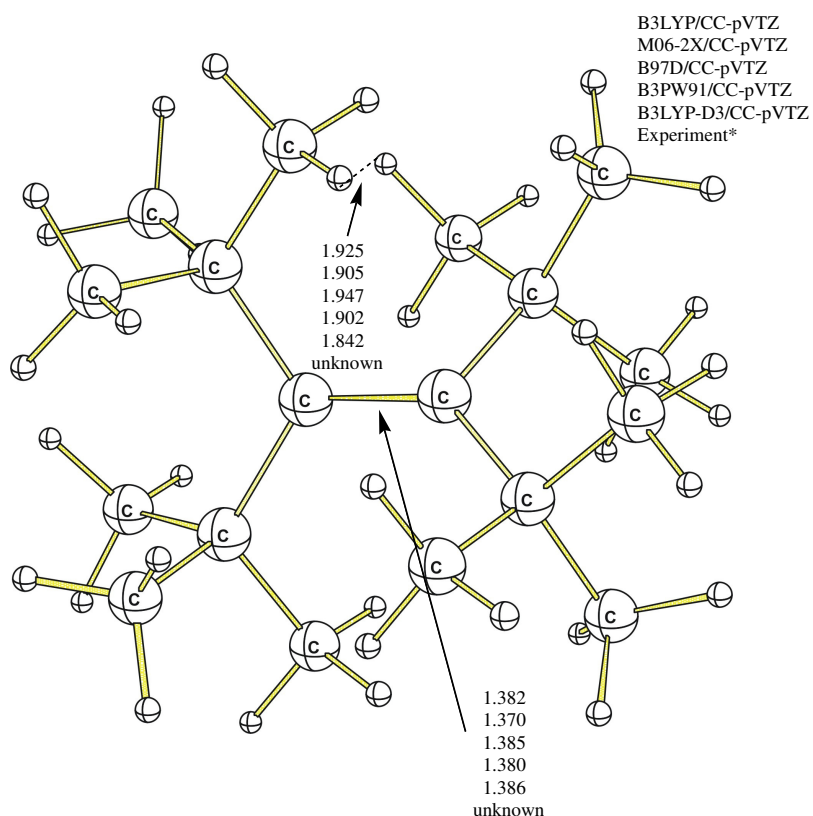


Figure 34. Selected computed bond lengths and distances in the molecule of **141**.

Overview of the proximity of the experimental and computational values is introduced in the Table 7. It is worthwhile to note, that introduction of the dispersion corrections does not improve results significantly.

Table 7.

Experimental and selected computed values of the C=C bond length.

Compound	C=C _{Exp} , Å	C=C _{Comp} , Å	
		B3LYP/CC-pVTZ	B3LYP-D3/CC-pVTZ
138	1.330	1.324	1.325
139	1.351	1.342	1.342
140	1.347	1.348	1.346
141	–	1.382	1.386
13	1.336	1.343	1.340
14	1.325(4)	1.343	1.340
15	1.333(3)	1.344	1.342
16	1.335(5)	1.344	1.341

135	1.326(5)	1.331	1.329
95	1.322	1.324	1.321
104	1.328	1.324	1.321

Comparative analysis of **13** and other coupled diamondoids **14–16** with *C_i-trans-C₅-8-trishomocubylidene-C₅-8-trishomocubane* (**135**) and isomeric *D₃-trishomocubylidene-D₃-trishomocubanes* (**95**, **104**) also can be performed for the distances between hydrogen atoms around the central C=C bond. As in **13** this distance is about 3.7 Å,^[180] while in **95** and **104** – over 5 Å.^[126] Obviously this is the explanation of the different behavior of those compounds towards electrophilic reagents *e.g.*, molecular bromine. While **13** forms stable bromonium salt **96**,^[137] **95** reacts as usual alkene with addition of bromine to double bond. For the diamondoid **14** the intramolecular contact is *ca.* 3.5 to 3.9 Å, and for **15** and **16** – 3.7 Å and 3.7–3.8 Å, respectively and close to **13**. Synthesized **135**, to our surprise, also closer to **13** than to **95** with the H•••H distance of *ca.* 3.7 Å. Thus, it can be expected that **135** will react with bromine similarly to **13**.

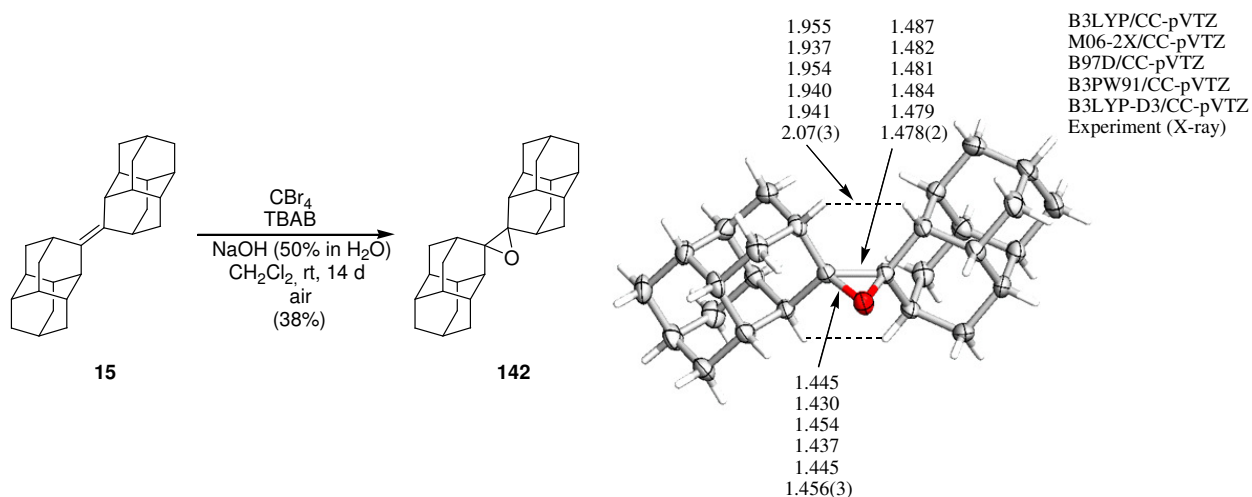
3.3. Functionalization of diamantylidenediamantanes

As it was discussed above, functionalization of diamondoids is the key to their versatile application. One of the most common and unselective radical reactions of alkenes are not widely applied up-to-date, even they represent the most direct route to functionalized hydrocarbons. Recently reported phase-transfer functionalization of alkanes introduced a new concept of combining phase-transfer catalysis with radical reactions, initialized by single-electron transfer.^[198] Functionalization of cage hydrocarbons under the phase transfer catalysis (PTC) conditions usually shows highselectivity of *tert.*-CH substitution if involved bulky radicals CHal₃•. Since the reaction proceeds in interphase zone where product concentration is low, over-functionalizations are avoided and tertiary mono-substituted products favored.^[199] We expected this method to be useful for functionalization of coupled diamondoids selectively in the cage rather than on double bond.

3.3.1. Functionalization of *anti*-diamantylidenediamantane (**15**) under PTC conditions

When **15** was brominated under the PTC conditions at room temperature, exclusively one product was formed with 38% yield (Scheme 61). Combined ¹³C NMR/APT spectral data of the obtained compound **142** indicated absence of the carbons of C=C bond and instead signal of

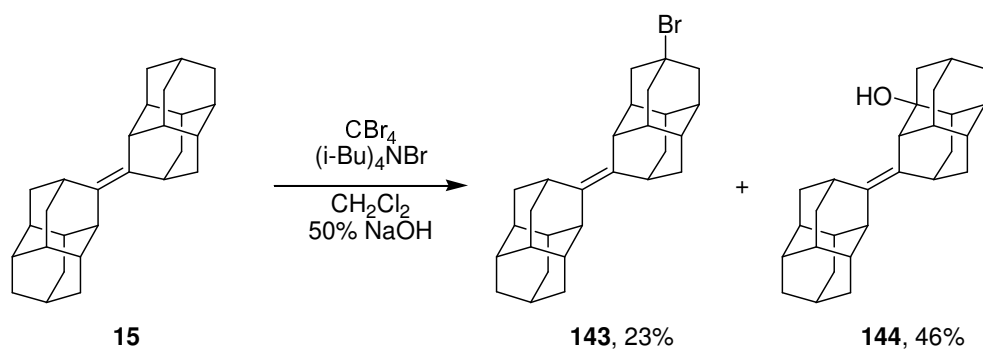
quaternary carbon at 73.7 ppm was found. Rest of the resonances belongs to 8 methines and 5 methylenes. The diamantylidenediamantane epoxide (**142**) was further subjected to the X-ray crystal structure analysis. Computation results also showed to be in the good agreement with experimental values.



Scheme 61.

The formation of **142** resulted from the addition of oxygen to central C=C bond due to inefficiency of conventional PTC halogenation procedure. In order to increase the efficiency we applied the microwave technique.

In the reaction of **15** under microwave PTC conditions^[199] a mixture of products was formed, with 4-bromo-*anti*-diamantylidenediamantane (**143**) and *anti*-diamantylidenediamantan-2-ol (**144**) as major reaction products (Scheme 62). It is also worthwhile to note that not even a trace amount of epoxide **142** was found.



Scheme 62.

The products were separated by column chromatography on silica gel. Bromide **143** was eluted by pentane and mixture of alcohols was eluted by pentane : diethyl ether 1 : 1 mixture. Pure alcohol **144** was obtained by recrystallization of last fractions from hexane.

A preliminary conclusion about the structure of isolated bromide **143** based of ^1H NMR spectrum when a complex signal in a low field (2.34–2.42 ppm) with the intensity of 6H. This signal evidences for substitution of the apical position of **15**. In the ^{13}C NMR spectrum 20 carbon resonances were found, indicating the C_s symmetry of the molecule (Fig. 35). Analysis of the DEPT spectrum displays that the signals at 135.6, 131.6 (carbons of the double bond) and 65.9 ppm belong to quaternary carbon atoms, which confirms the replacement of hydrogen by bromine neighboring the tertiary carbon atom, while the remaining resonances are six methylenes and 11 methines.

Structural assignments for the atoms C-1 – C-14 are determined by set of 2D spectral data (^1H - ^1H COSY, HSQC, HMBC and HSQC-TOCSY).

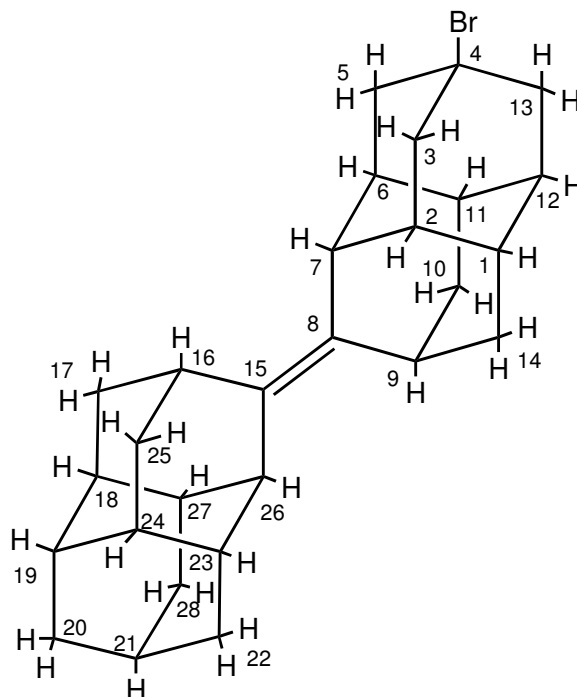


Figure 35. The structure of 4-bromo-*anti*-diamantylidenediamantane (**143**).

The multiplet at 2.34–2.42 ppm in the ^1H NMR spectrum corresponds to two signals of secondary carbon atoms at 49.6 and 49.6 ppm of data of the ^{13}C part of HSQC spectrum (Fig. 36). With high probability, these signals belong to the carbon C-3, 5 (49.6 ppm, 2C), and C-13 (49.6 ppm, 1C), as well as their corresponding hydrogen atoms (2.34–2.42 ppm). $\text{H}_2\text{-3}/\text{H}_2\text{-5}$ and $\text{H}_2\text{-13}$ correlations in the COSY spectrum indicate $\text{H-2}/\text{H-6}$ (1.85 ppm, 2H) and H-12 (1.98 ppm, 1H). Attribution of carbon signals for these protons in the HSQC-TOCSY spectrum gives C-2/C-6 at 43.3 ppm (2C) and C-12 at 41.1 ppm (1C). Correlations between resonances of protons

H-2/H-6 in the HSQC-TOCSY spectrum indicate the location of hydrogen atoms H-1/H-11 (1.88 ppm, 2H) and H-7 (2.83 ppm, 2H, one of the group).

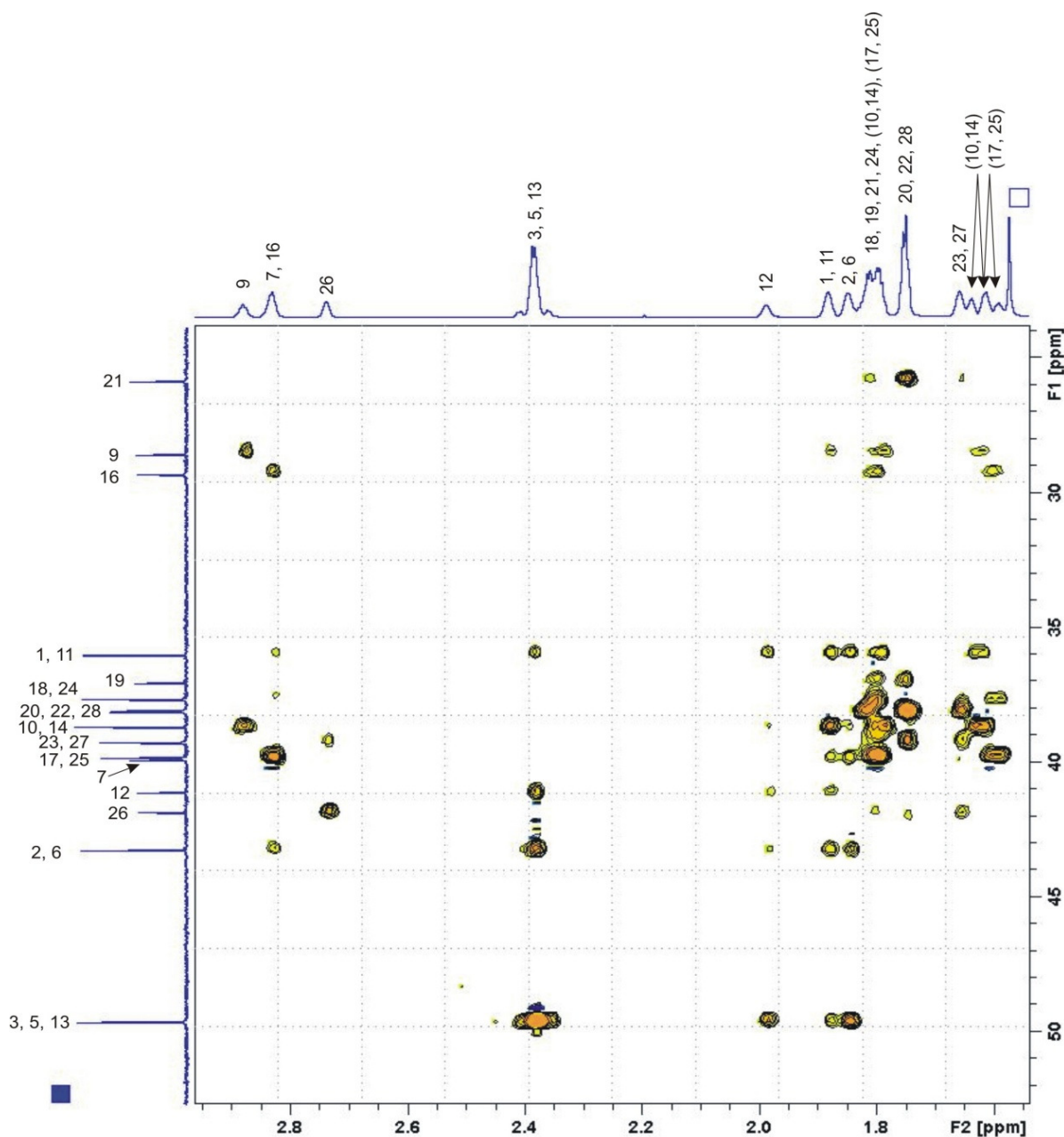


Figure 36. HSQC-TOCSY spectrum of **139**.

HSQC spectral data attributes to H-1/H-11 proton signal one of the carbon spectrum at 36.0 ppm (2C). Signals of protons at 2.83 ppm correspond with two signals of carbon atoms at 39.9 and 29.3 ppm. Observation of the H-2/H-6 correlation with the signal at 39.9 ppm indicates that this signal belongs to C-7, as is confirmed by the spectrum of HMBC, as well as a similar structure of the unsubstituted hydrocarbon.

Subsequent correlation H-1/H-11 in the spectrum of HSQC-TOSCY as a doublet of doublets at 1.65–1.82 ppm allows assignment of these signals to H₂-10/H₂-14, which carbon

resonances are located at 38.7 ppm (2C). Correlation of H₂-10/H₂-14 signal with the signal at 2.88 ppm allows assignment of this signal to H-9 (1H). The corresponding correlation in the carbon HSQC for C-9 is at 28.6 ppm (1C). The remaining signals belong to the atoms C-15 – C-28 and are identified by set of 2D spectral data (HSQC, HMBC and HSQC-TOCSY).

The remaining signals of the ¹H NMR spectrum, situated in a low field at 2.74 and 2.83 ppm, belong to H-26 and H-16, respectively. Assignment of the signal at 2.48 ppm is confirmed by the NOE between H-9 and H-26, which is observed in NOESY experiment. HSQC experiment determines the C-26 as a signal at 41.8 ppm. The correlation in HSQC-TOCSY spectrum for the signal at 2.74 ppm allows assignment of the signal C-23/C-27 as 39.2 ppm (2C). Protons H-23/H-27 are at 1.66 ppm, according to the HSQC data. HSQC-TOCSY spectral data indicates a correlation with the signal H-23/H-25 (2C at 37.6 ppm), belonging to methine, and the signal at 38.1 ppm (2C), respectively, belonging to methylene. Methylene signal of intensity 1C at 38.1, which almost overlaps with the signal of intensity 2C (38.1 ppm) belongs to the C-20. Thus, H-18/H-24 signals are located in complex multiplet with intensity 8H at 1.78–1.83 ppm, and C-18/C-24 - at 37.6 ppm; signals H₂-22/H₂-28 are located in multiplet with intensity of 6H at 1.72–1.76 ppm, C-22/C-28 – at 38.1 ppm of ¹³C NMR spectrum, according to HSQC. Correlation of signals with a signal complex H₂-22/H₂-28 8H multiplet at 1.78–1.83 ppm and 25.9 ppm of ¹³C NMR spectrum allows assignment of the apical methine CH-21. Also, by the absence of other correlations of this methine signal, it is concluded that to the CH₂-20 also belongs part of the 6H multiplet at 1.72–1.76 ppm and 38.1 ppm of carbon spectrum according to HSQC, which confirms the initial conclusion.

Correlation of the signal H₂-20 with tertiary carbon atom signal at 37.0 ppm identifies this signal as C-19, with the corresponding HSQC spectrum of the signal H-19, which is part of a complex multiplet at 1.78–1.83 ppm with intensity of 8H. Correlation of the same signal H-19 as a doublet of doublets at 1.55–1.83 ppm with the signals H₂-17/H₂-25 determines the signal C-17/C-25 at 39.83 ppm. The latter signal belongs to the methine fragment CH-16, with signals at 2.83 ppm (1H) and 29.31 ppm (1C). HMBC spectral data does not contradict to the attributed structure. COSY spectral data (Fig. 37) confirms structure of bromide **143** made on basis of HSQC-TOCSY. Key correlations of CH-7, 9, 16 and 21 with hydrogen atoms in the cage fully relate to the assignments already made, as can be seen from Fig. 37.

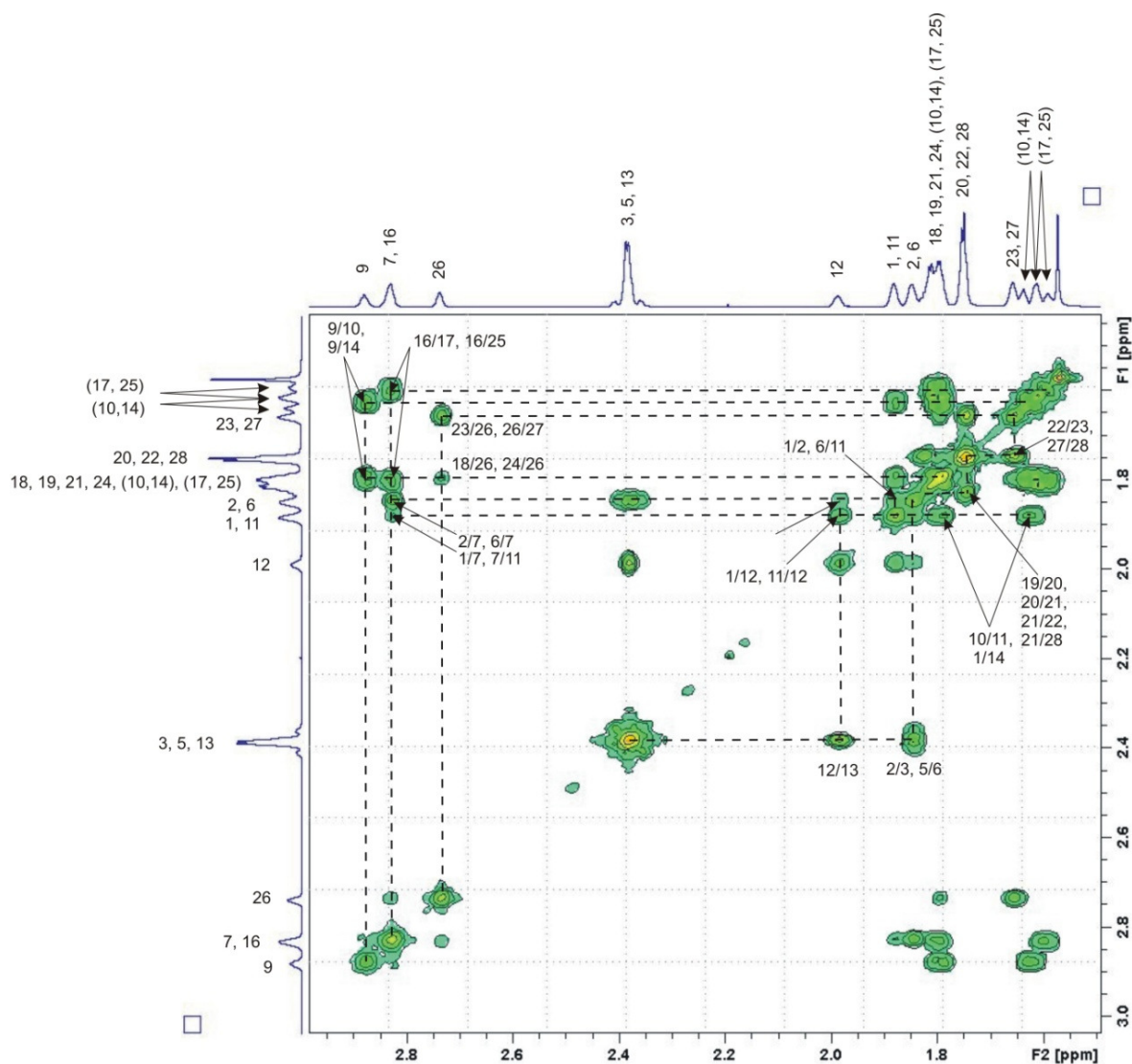


Figure 37. ^1H - ^1H COSY spectrum of **143**.

Conclusion about the structure of alcohol **144** is also based on NMR-spectral data. Comparison of the spectra ^{13}C NMR and DEPT enables to conclude the presence of three quaternary carbons, of which carbons of the double bond are in a low field (140.8 and 129.0 ppm), while the substituted carbon is in higher field (71.1 ppm). The presence of 15 methine atoms indicates C_1 symmetry substitution product (Fig. 38), although only 8 methylene signals can be observed instead of 10 due to the overlap of closely spaced resonances.

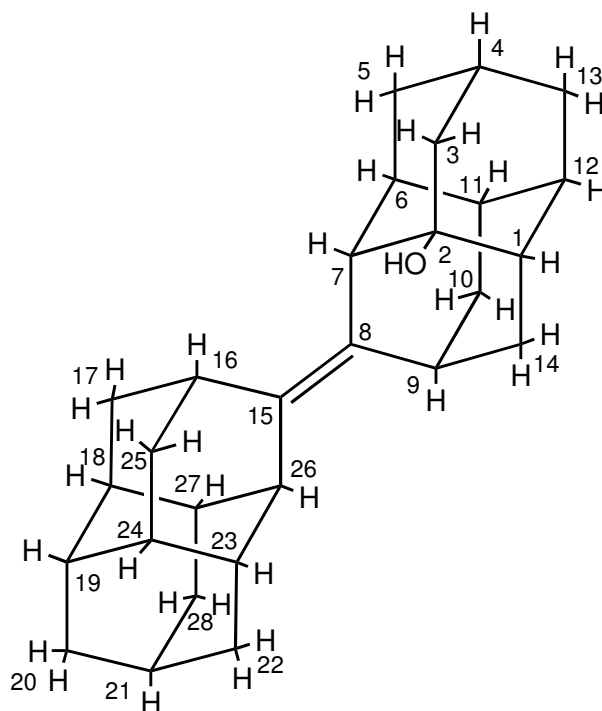


Figure 38. The structure of *anti*-diamantylidenediamantan-2-ol (**144**).

Further structure is defined by set of 2D spectral data (^1H - ^1H COSY, HSQC, HMBC, and HSQC-TOCSY).

The signals of the ^1H NMR spectrum at 2.71 and 2.82 ppm, with one-proton intensity of each, belong to methines CH-7 and CH-26, while the signals at 2.86 and 2.91 ppm, with one-proton intensity each, belong to methines CH-9 and CH-16 (Fig. 39). Such a conclusion can be made on the basis of HSQC-TOCSY spectrum, where the CH-7 and CH-26 belong to the resonances of the carbon spectrum of 48.2 and 42.1 ppm, respectively, analogously to the correlations of the spectral data of unsubstituted carbon. Similarly, carbon resonances CH-9 and CH-16 are on 28.6 and 29.2 ppm. Confirmation of assignment can be found on the HMBS spectral data, as well as final determination of the position of substitution in diamantylidenediamantane cage.

Correlations between second- and third-order α -O protons indicate quaternary carbon atom itself at which substitution take place (71.1 ppm, 1C, C-2), the signal of tertiary carbon atom at 48.2 ppm (1C, C-7) and the correlation with paired signals of methine and methylene at 43.6 ppm, which correspond to C-1 and C-3 (with one-carbon intensity each).

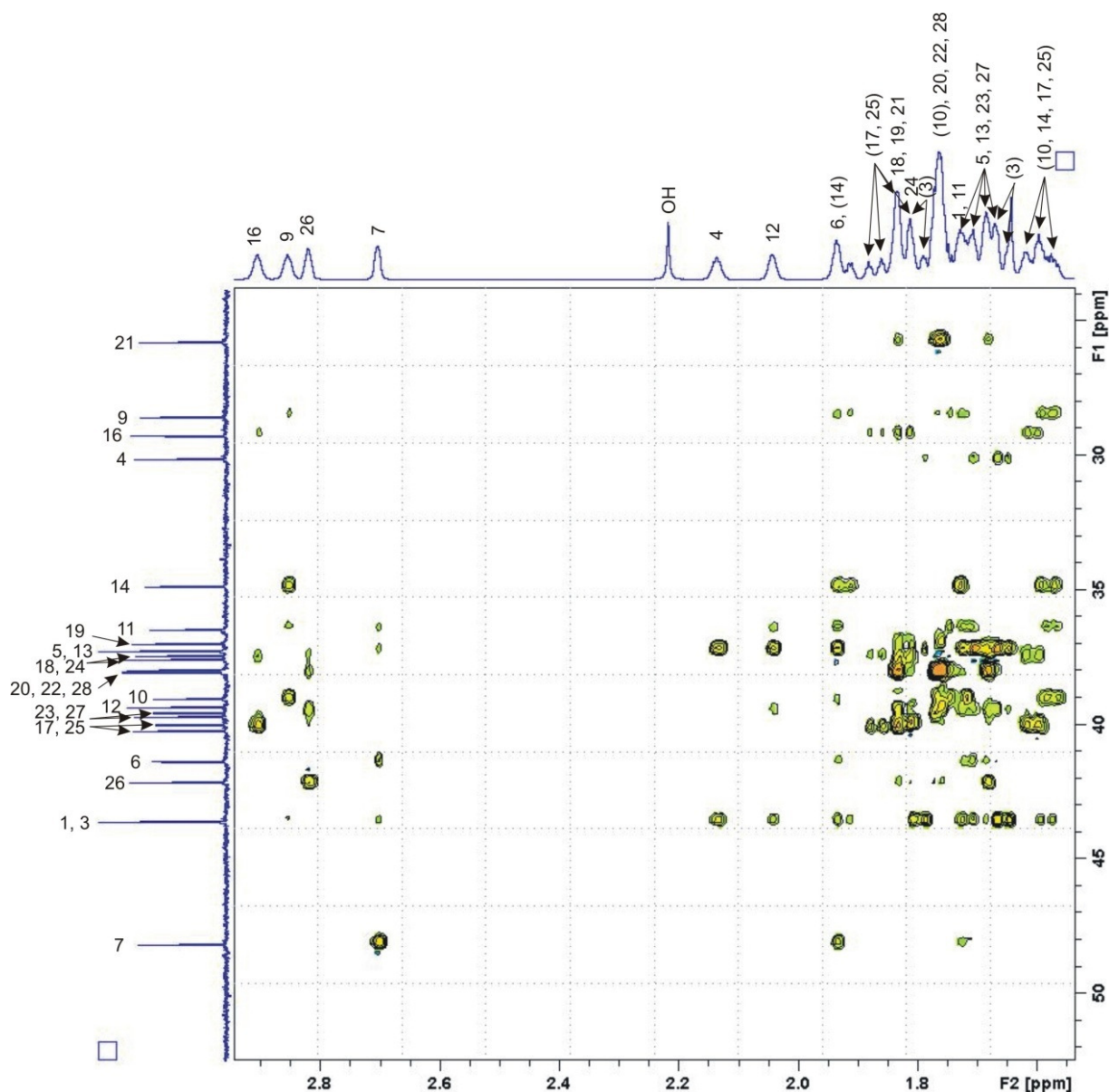


Figure 39. HSQC-TOCSY spectrum of **144**.

In the ^1H NMR spectrum, in accordance with HSQC-TOCSY spectral data, CH-1 corresponds to the correlation at 1.73 ppm with one-proton intensity, CH₂-3 – doublet of doublets at 1.64–1.82 ppm. Only second-order correlation signal of methine CH-7 is at 41.4 ppm (one-carbon intensity) of ^{13}C NMR spectrum and 1.94 ppm of the ^1H NMR spectrum (one-proton intensity), and corresponds to CH-6. Signal CH-1 in HSQC-TOCSY spectrum correlates with methine and methylene signals. Methylene signal at 34.8 ppm of ^{13}C NMR spectrum and 1.56–1.96 ppm of the ^1H NMR spectrum, which represents doublet of doublets, is consistent to CH₂-14. Signal of CH-12 belongs to the correlation of the ^{13}C NMR spectrum at 39.3 ppm, as well as signal at 2.05 ppm of the ^1H NMR spectrum with one-proton intensity. Correlation of methine carbon resonance at 43.6 ppm with the ^1H NMR spectrum at 2.14 ppm determines the signal as CH-4 (30.1 ppm, 1C). Correlation of signal CH-9 confirms the position of the signal

CH₂-14 and indicates the signal CH₂-10 at 39.0 ppm of the ¹³C NMR spectrum (1C) and 1.55–1.76 ppm of ¹H NMR one.

The signal of the ¹³C NMR spectrum at 25.8 ppm and the corresponding proton correlation at 1.84 ppm belong, analogously with the unsubstituted carbon and previously decoded spectrum of bromide **139**, to CH-21. Correlation of this signal in HSQC-TOCSY spectrum with three secondary carbon resonances at 38.0 ppm (one-carbon intensity each) can attribute these signals CH₂-20, CH₂-22 and CH₂-28. In ¹H NMR spectrum corresponding signal belongs to the complex multiplet at 1.76 ppm. Correlations of CH-26 with the signal of the ¹H NMR spectrum at 1.72 ppm and two signals of the ¹³C NMR spectrum at 39.5 and 39.7 ppm – indicate CH-23 and CH-27. Correlation of resonance CH-16 with the signals of the ¹³C NMR spectrum at 40.0 and 40.2 ppm, which correspond to two doublet of doublets of the ¹H NMR spectrum at 1.75–1.90 and 1.75–1.85 ppm, can attribute these signals CH₂-17 and CH₂-25. Common correlations of signals CH₂-20 and CH-17/25 can assign a group of signals of the ¹³C NMR spectrum 37.0, 37.4 and 37.6 ppm to C-18/24 and C-19 atoms. In the proton spectrum these signals correspond to the complex multiplet at 1.84 ppm.

At the end, there is only undefined methylene signal with two-carbon intensity and one methine with one-carbon intensity. Methine, undoubtedly, belongs to the CH-11 and situated at 36.5 ppm of the ¹³C NMR spectrum and 1.70 ppm of the proton spectrum. Methylene signal belongs to CH₂-5 and CH₂-13 (37.2 ppm, 2C). Proton correlations of these signals are in complex multiplet at 1.65–1.74 ppm. COSY spectral data confirms structure of alcohol **140** made on basis of HSQC-TOCSY. As full assignment of structure on basis of COSY data is impossible, only key correlations are marked, as those of CH-7, 9, 16 and 21 with hydrogen atoms in the cage as can be seen from Fig. 40.

Thus, by MW irradiation under phase transfer catalysis radical conditions we have synthesized and isolated as individual compounds two major products: 4-bromo-*anti*-diamantylidenediamantane (**143**) and *anti*-diamantylidenediamantan-2-ol (**144**). The structure of each of these compounds was confirmed by ¹H and ¹³C NMR spectral data and sets of 2D spectral data (¹H-¹H COSY, HSQC, HMBC and HSQC-TOCSY).

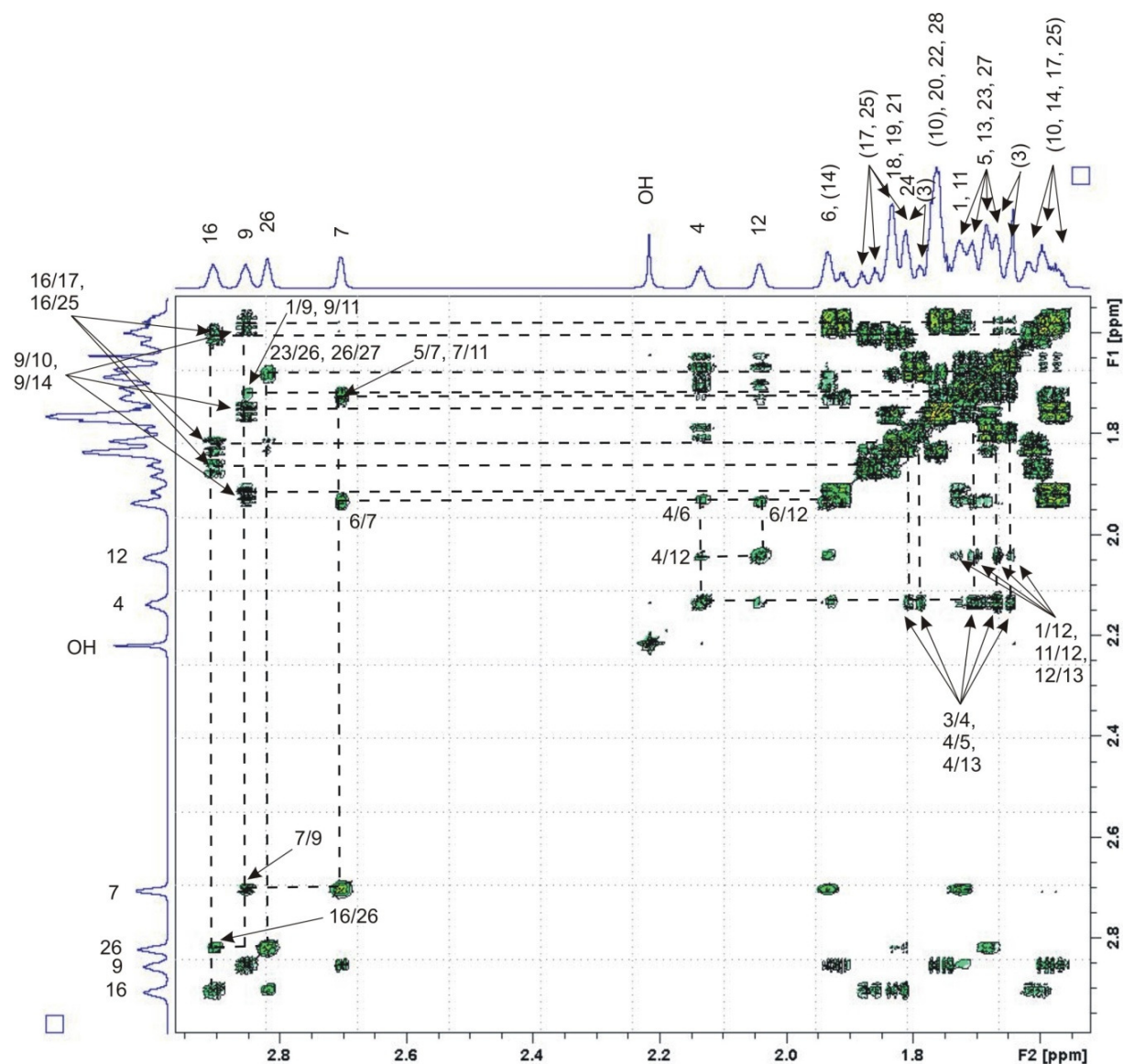
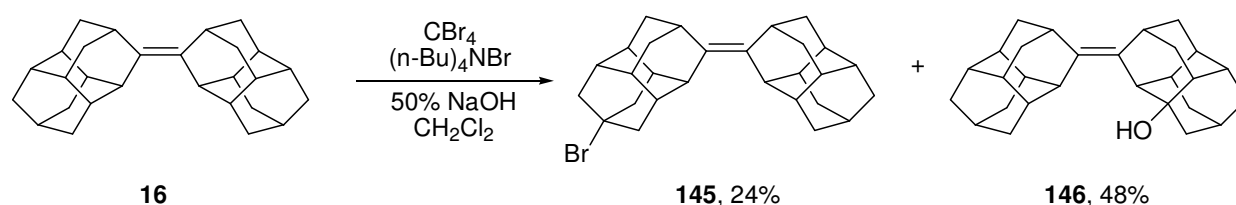


Figure 40. ^1H - ^1H COSY spectrum of **144**.

3.3.2. Functionalization of *syn*-diamantylidenediamantane (**16**) under PTC conditions

In the reaction of **16** under PTC conditions^[199] under MW gave the mixture of two main products, namely 4-bromo-*syn*-diamantylidenediamantane (**145**) and *syn*-diamantylidenediamantan-2-ol (**146**) (Scheme 63).



Scheme 63.

Products were separated by column chromatography on silica gel, similar to products of reaction of **16** under PTC conditions. Bromide **145** was eluted by pentane, a mixture of alcohols – by pentane : diethyl ether 1 : 1 mixture. Pure product **146** was obtained by recrystallization of last fractions from *n*-hexane.

Determination of the structure of the **145** is similar to the bromide **143**. The low-field group of signals of the ^1H NMR spectrum at 2.31–2.41 ppm with the intensity of 6H indicates apical substitution, as the only position where substituent surrounded by 6 hydrogen atoms. The ^{13}C NMR spectrum identifies 22 carbon atoms, which together with the DEPT and HSQC data give three quaternary, sixteen methine and six methylene carbon atoms (Fig. 41). Therefore, the signals at 131.3 and 135.2 ppm of ^{13}C NMR spectrum belong to the carbon atoms of the double bond, and the signal at 65.5 ppm – signal of the substituted quaternary carbon atom, which proves that functionalization took place at the tertiary carbon atom.

Structural fragment of C1-C14 is determined by set of 2D methods (^1H - ^1H COSY, HSQC, HMBC and HSQC-TOCSY).

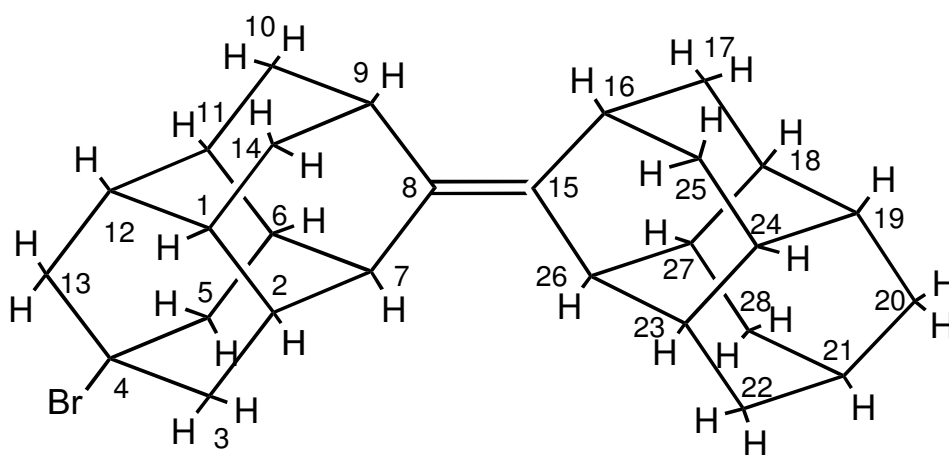


Figure 41. The structure of 4-bromo-*syn*-diamantylidenediamantane (**145**).

Doublet of doublets (2.31-2.41 ppm, 4H) and the corresponding signal of the ^{13}C NMR spectrum (49.3 ppm) and singlet (2.33 ppm, 2H) with the same signal at 49.3 ppm of ^{13}C NMR spectrum belong respectively to $\text{CH}_2\text{-3}/\text{CH}_2\text{-5}$ and $\text{CH}_2\text{-13}$. Correlation of these protons in the COSY spectrum (Fig. 43) indicates H-2/H-6 signal (1.79 ppm, 2H), which in the HSQC spectrum (Fig. 42) corresponds to the signal with two-carbon intensity at 43.0 ppm of ^{13}C NMR spectrum, as well as the H-12 signal (1.95 ppm, 1H) which is equal to one-carbon intensity signal at 40.8 ppm. Also, the primary correlation of signal H-12 in COSY spectrum allows assigning of the signal H-1/H-11 (1.84 ppm, 2H). Interaction of this signal in HSQC spectrum indicates C-1/C-11 at 35.7 ppm of the ^{13}C NMR spectrum (2C).

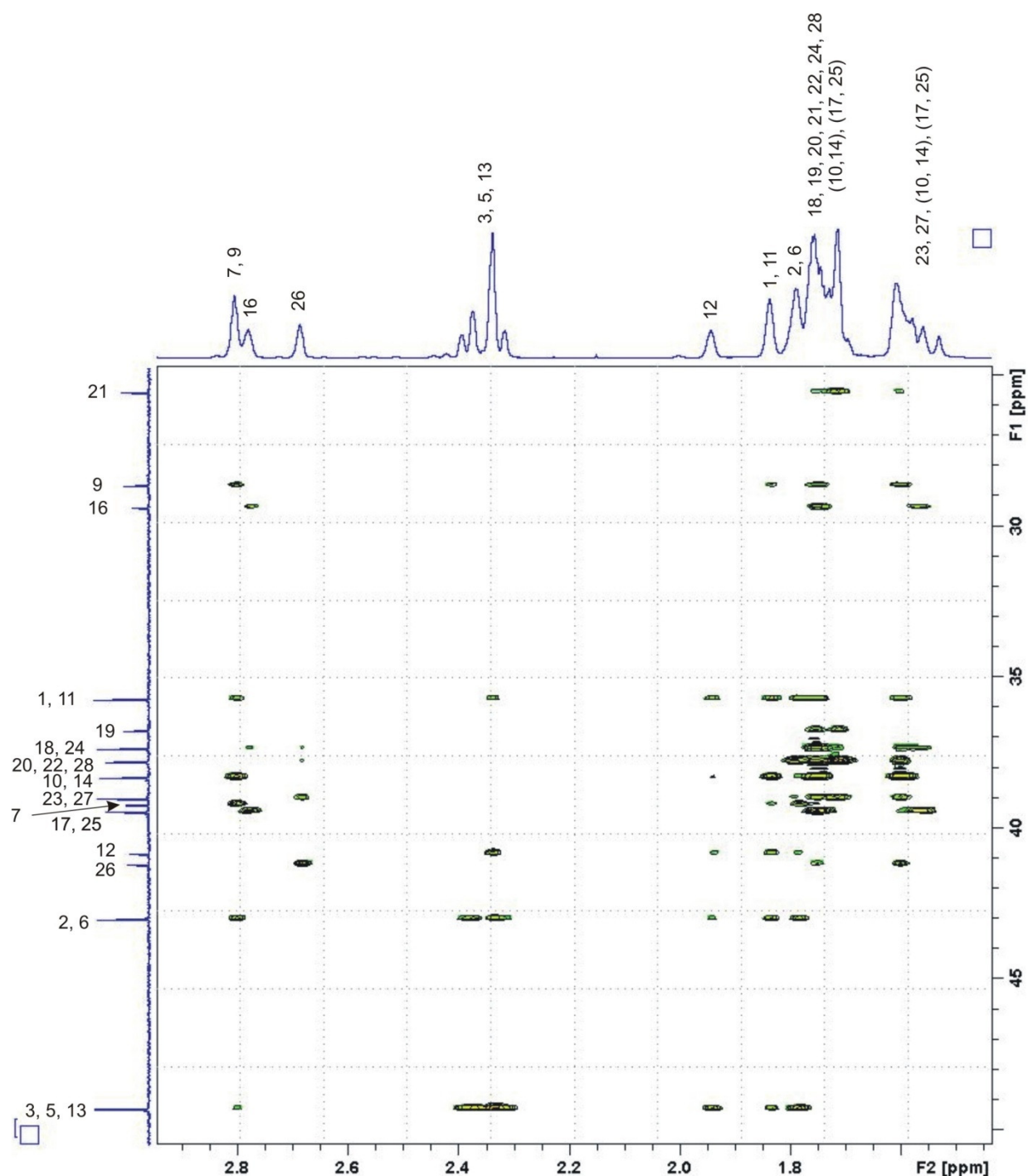


Figure 42. HSQC-TOCSY spectrum of **145**.

Analogously with previous spectra of **143** the second signal at 2.81 ppm (1H) and 28.6 ppm (1C) belongs to CH-9. H₂-10/H₂-14 signals are at 1.58–1.77 ppm (4H) with the corresponding C-10/C-14 resonances (38.3 ppm, 2C) according to ¹H–¹H COSY and HSQC-TOCSY spectral data.

Signals CH-16 and CH-26 are assigned in accordance with the spectrum of unsubstituted hydrocarbon, accordingly to COSY and HSQC-TOCSY spectra: correlation CH-16 is located at 2.78 ppm (1H) and 29.3 ppm (1C), CH-26 – at 2.70 ppm (1H) and 41.2 ppm (1C).

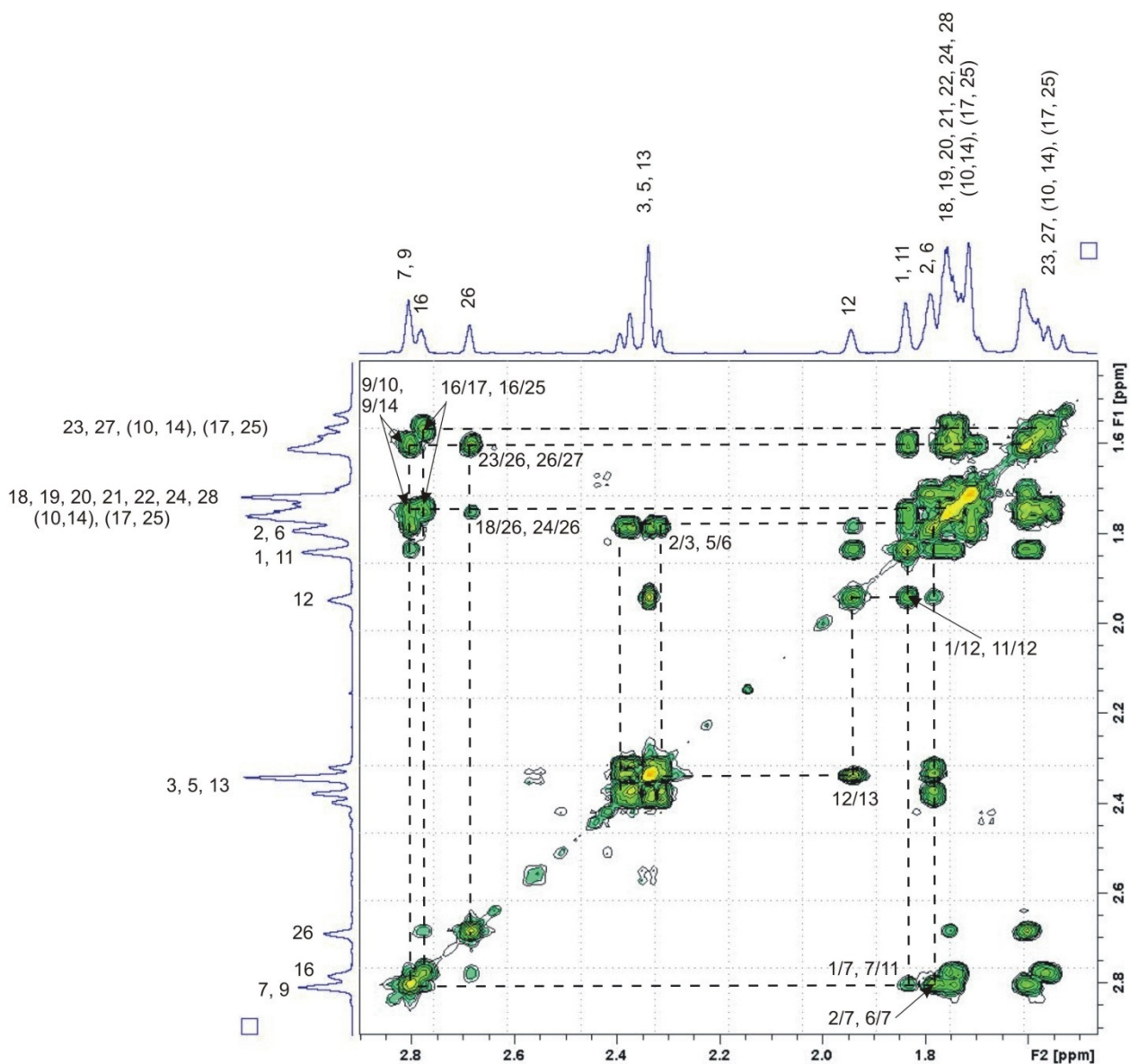


Figure 43. ^1H - ^1H COSY spectrum of **145**.

^1H - ^1H COSY spectrum allows assignation of signals H-23/H-27 with two-proton intensity at 1.60 ppm, hidden in a complex multiplet. Minor correlation signal of H-26 at 1.76 ppm of the ^1H NMR spectrum indicates H-18/H-24, as supported by data of HSQC-TOCSY and HMBC spectra. In the ^{13}C NMR spectrum signal of H-23/H-27 corresponds to the signal at 39.0 ppm (C-23/C-27); H-18/H-24 – to signal of 37.3 ppm (C-18/C-24). Correlation signal of COSY spectrum belonging to the H-16 signals at 1.53–1.76 ppm (with total four-proton intensity) as belonging to it in the HSQC spectrum signal 39.4 ppm (2C) indicates CH_2 -17/ CH_2 -25. From two resonances of tertiary carbon atoms, the resonance at 25.5 ppm (1C) is identified as C-21, analogously with **143**, and correlates in HSQC spectrum with one-proton intensity resonance at 1.79 ppm of ^1H NMR spectrum. The interaction of CH-21 in HSQC-TOCSY spectrum with the signals at 1.68–1.74 ppm of the ^1H NMR spectrum (6H) and signal 37.7 ppm (1C) and 37.8 ppm

(2C), defines them as CH₂-20 and CH₂-22/CH₂-28 respectively. Signal of spectrum which belongs to the tertiary carbon atom with correlation in HSQC at 1.76 ppm of the ¹H NMR spectrum is defined as CH-19. HMBC spectral data does not contradict to assignments which have been made for **145**.

Assigning of the structure of alcohol **146** is based on NMR spectral data, as in the previous cases. Comparison of spectral data from ¹³C NMR and DEPT experiments indicates presence of three quaternary carbon atoms, *i.e.*, two carbon atoms of the double bond (140.9 and 129.0 ppm) and carbon atom, near which substitution took place (71.0 ppm). The presence of 15 methine and 9 methylene resonances indicates C₁ symmetry of the substituted product (Fig. 44), while lower amount of methylene signals is due to overlapping of some correlations.

Further structure is defined by set of 2D spectral data (¹H-¹H COSY, NOESY, HSQC, and HSQC-TOCSY).

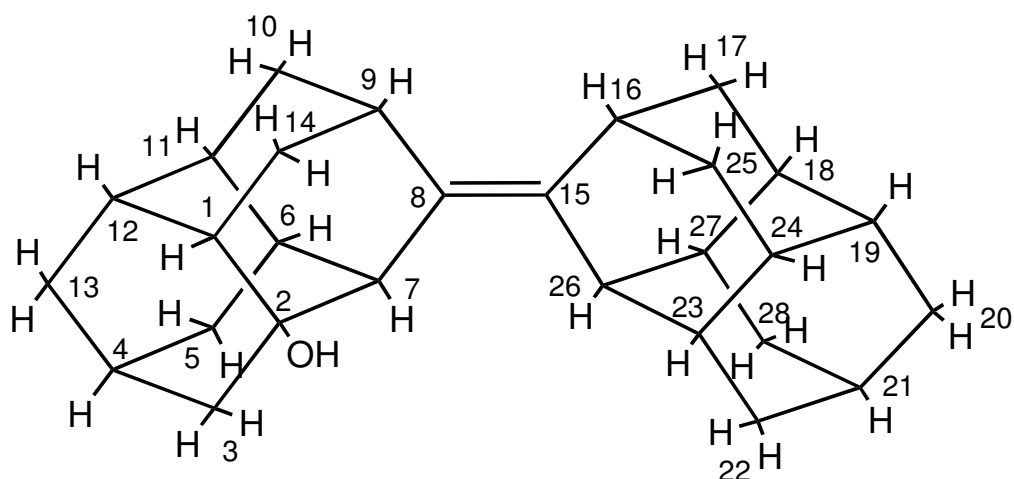


Figure 44. The structure of *syn*-diamantylidenediamantan-2-ol (**146**).

The signals of the ¹H NMR spectrum at 2.64 and 2.74 ppm (both of one-proton intensity) belong to CH-7 and CH-9, while signals at 2.71 (1H) and 2.83 ppm (1H) – to CH-26 and CH-16 respectively. Such conclusion can be based on ¹H-¹H COSY, NOESY, HMBS and HSQC-TOCSY spectral data. Thus, in HSQC-TOCSY spectrum the signals of ¹H NMR spectrum at 2.64 and 2.71 ppm correlate with methine signals at 47.7 and 41.3 ppm of the ¹³C NMR spectrum, signals of ¹H NMR spectrum at 2.74 and 2.83 ppm correlate with methine signals at 28.9 and 30.0 ppm of ¹³C NMR spectrum. Confirmation of the assignment can be found from HMBC spectral data, as well as assumption can be made about position at which substitution took place: signal of alcoholic proton at 2.11 ppm (1H) correlates with signals of ¹³C NMR spectrum at 71.0 (C-2), 47.7 (C-7) 43.6 (C-1) and 43.5 ppm (C-3).

By this assignment, according to HSQC-TOCSY spectral data, CH-1 corresponds to the resonance of 1.64 ppm of the ^1H NMR spectrum, CH₂-3 – to the doublet of doublets at 1.56–1.71 ppm. Correlation of CH-7 signal with proton resonance signal at 1.84 ppm can be assigned to CH-6, with carbon resonance signal at 41.4 ppm.

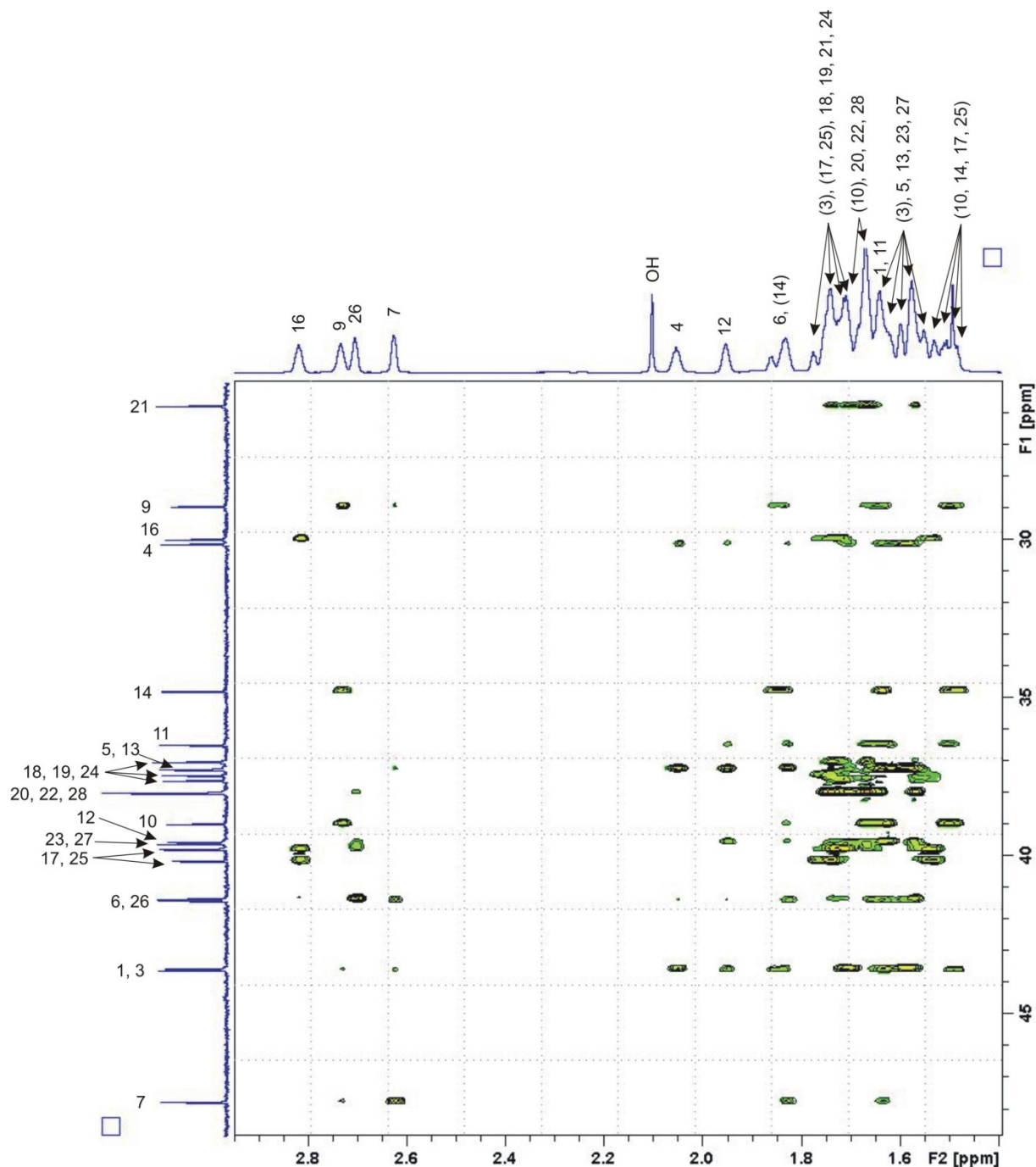


Figure 45. HSQC-TOCSY spectrum of **146**.

Signal of CH-6 in HSQC-TOCSY spectrum has two correlations apart from correlation with CH-7, *i.e.* with methylene signal at 37.2 ppm of ^{13}C NMR and 1.54–1.66 ppm of ^1H NMR spectra (CH₂-5) and methine signal at 36.5 ppm of ^{13}C NMR and 1.62 ppm of ^1H NMR spectra (CH-11).

Correlations of CH-9 in the HSQC-TOCSY spectrum allow also assignment of CH₂-14 (34.87 ppm of ¹³C NMR spectrum; 1.46–1.86 ppm of ¹H NMR spectrum, doublet of doublets) and CH₂-10 (39.0 ppm of ¹³C NMR spectrum; 1.46–1.68 ppm of ¹H NMR spectrum, doublet of doublets). Interaction of CH₂-14 with CH-1 proves this assignment. Correlation of CH-1 with signal at 39.5 ppm (1C) and 1.95 ppm (1H) indicates CH-12. Another correlation of CH₂-3 is with resonance at 2.06 ppm (1H) and 30.1 ppm (1C), which belong to CH-4. Last structure fragment of this cage by HSQC-TOCSY spectrum is CH₂-13 at 1.54–1.66 ppm of ¹H NMR spectrum and 37.2 ppm of ¹³C NMR spectrum (1C).

Correlations in HSQC-TOCSY spectrum of the CH-16 and CH-26 give starting points for determining the structure of the remaining cage fragment. Correlations of CH-16 with resonances at 39.8 and 40.1 ppm (one-carbon intensity each) can be related to CH₂-17/CH₂-25, with corresponding doublets of doublets in ¹H NMR spectrum at 1.52–1.74 and 1.52–1.78 ppm. Correlations of CH-26 with resonances at 39.6 and 39.7 ppm (one-carbon intensity each) relate to CH-23/CH-27, with corresponding signal at 1.56 ppm of ¹H NMR spectrum. From not assigned signals the one with one-carbon intensity at 25.8 ppm of ¹³C NMR spectrum and 1.74 ppm of ¹H NMR spectrum belongs to CH-21, analogously with the previously decoded spectral data; its complicated correlations with group of secondary carbon atoms at 1.62–1.72 ppm and relative carbon signals at 38.0 (2C) and 38.0 ppm (1C) can be assigned to CH₂-20/CH₂-22/CH₂-28. Remaining signals, situated at 37.0, 37.4 and 37.6 ppm (one-carbon intensity each) of ¹³C NMR spectrum with relative signals at 1.70–1.74 ppm of ¹H NMR spectrum – belong to CH-18/CH-19/CH-24.

¹H-¹H COSY spectral data (Fig. 46) confirms structure of alcohol **146** based on HSQC-TOCSY spectral data.

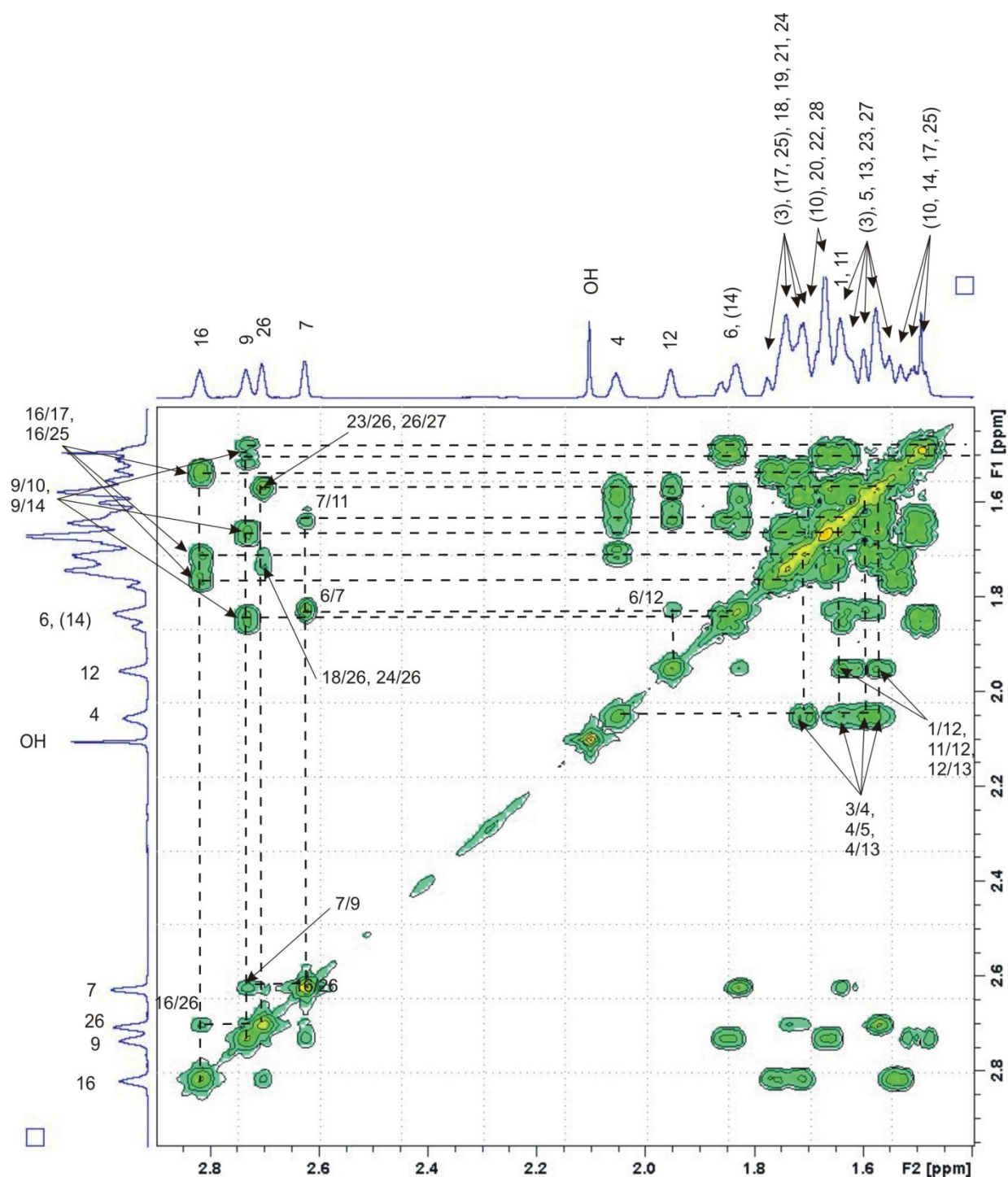
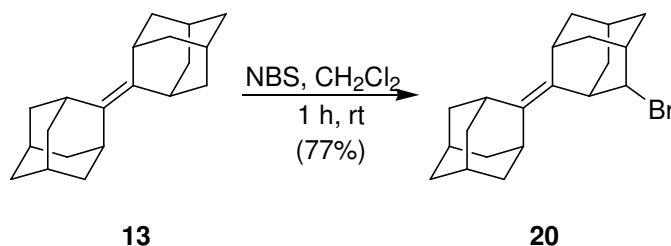


Figure 46. ^1H - ^1H COSY spectrum of **146**.

Thus, in a reaction of phase-transfer catalysis two major products were formed and isolated as individual compounds: 4-bromo-*syn*-diamantylidenediamantane (**145**) and *syn*-diamantylidenediamantan-2-ol (**146**). The structure of each of these compounds was confirmed by NMR spectral data of ^1H , ^{13}C and a set of 2D spectral data (^1H - ^1H COSY, HSQC, HMBC, and HSQC-TOCSY).

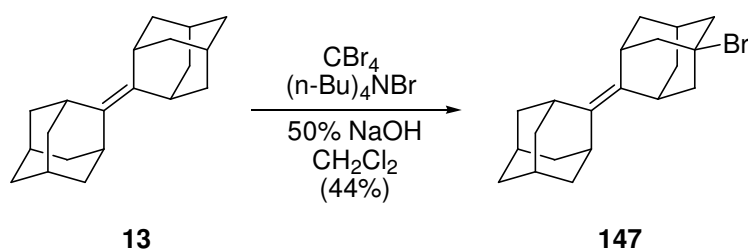
3.3.3. Functionalization of adamantylideneadamantane (**13**)



Scheme 64.

Reaction of **13** with *N*-bromosuccinimide was performed in refluxing methylene chloride as shown on the Scheme 64.^[77] Reaction was monitored by GC/MS, as despite the literature data, the quantitative yield in reaction is not always achieved in declared time. Unreacted **13** contaminates the target compound **20** and complicates the process of purification.

As it was reported before, **13** in the reaction with *N*-bromosuccinimide produces exclusively product of substitution of the secondary position. Such a result could only be explained by ionic mechanism of homoallylic halogenations, despite that NBS is traditionally involved into radical-chain reactions of halogenations. For the electron-rich olefins NBS serves as a source of halo-cation and whole addition reaction is driven by the electron density of the double bond. Additionally the normal reaction of olefins with NBS affords halogenation at the allylic position, while in **13** this path is unavailable due to steric hindrance.



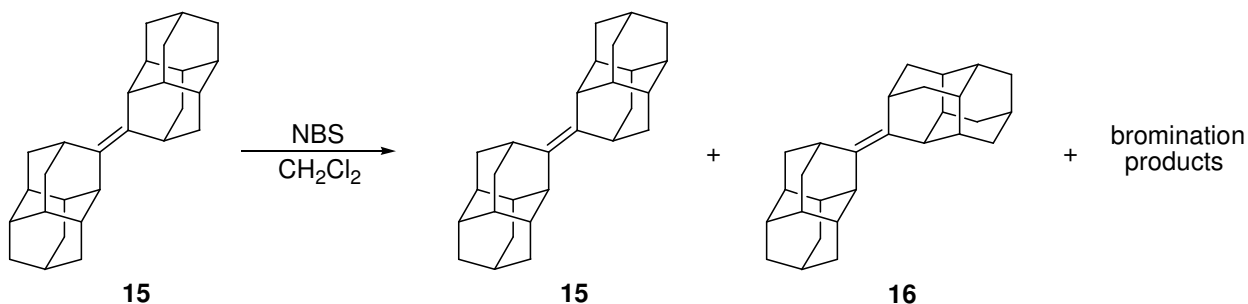
Scheme 65.

We found that reaction of **13** under PTC conditions (Scheme 65), similarly to **15** and **16**, afforded product of substitution at tertiary position, 5-bromoadamantylideneadamantane (**147**). Such substitution pattern indicates appearance of quaternary carbon atom signal in the APT vs DEPT spectrum of **147** at 67.0 ppm. Rest of the resonances belongs to two unequal quaternary carbons ($\delta_{\text{C}} = 129.0$ and 136.0 ppm) in addition to six methylene and five methine carbon atoms in agreement with product symmetry. To our surprise, as presence of bromine was proved by HRMS analysis, crystallographic data set could not resolve the structure of bromide, even proved

substitution at position 5 of the adamantylideneadamantane cage, due to the specific packing in the crystal of product.

3.3.4. Functionalization of *anti*-diamantylidenediamantane (**15**) with NBS

Reaction of **15** with *N*-bromosuccinimide was performed as shown on the Scheme 66, under conditions used for bromination of **13**.



Scheme 66.

Formation of the mixture of bromination products was expected due to the number of possible substitution positions near secondary carbon atom. However, after 24 h of reflux analysis by GC/MS indicated also isomerisation of the **15** into **16**. Proposed explanation is that since reaction of such sterically hindered olefins with NBS follows ionic mechanism, formation and decomposition of the bromonium derivative of the **15**, also causes deformation of the olefin with further conformation change, as isomers are close by energy.

Chapter 4. Conclusions and Outlook

As was presented in this doctoral thesis, a number of diamondoidyl ketones were synthesized and characterized. Methods of synthesis for diamantanedione-3,8 and diamantanedione-3,10 were developed, as well as optimization of the synthesis of C_5 -trishomocubane-8-one through newly developed approaches. Also triamantanone-16 was separated from the mixture of oxidation products of triamantane.

Two of reductive pairs for McMurry coupling were tested, namely titanium (III) chloride – lithium in DME and titanium (IV) chloride – zinc in THF. The second tested pair was found to be fully satisfying our needs in respect of simplicity, stability and reaction yields.

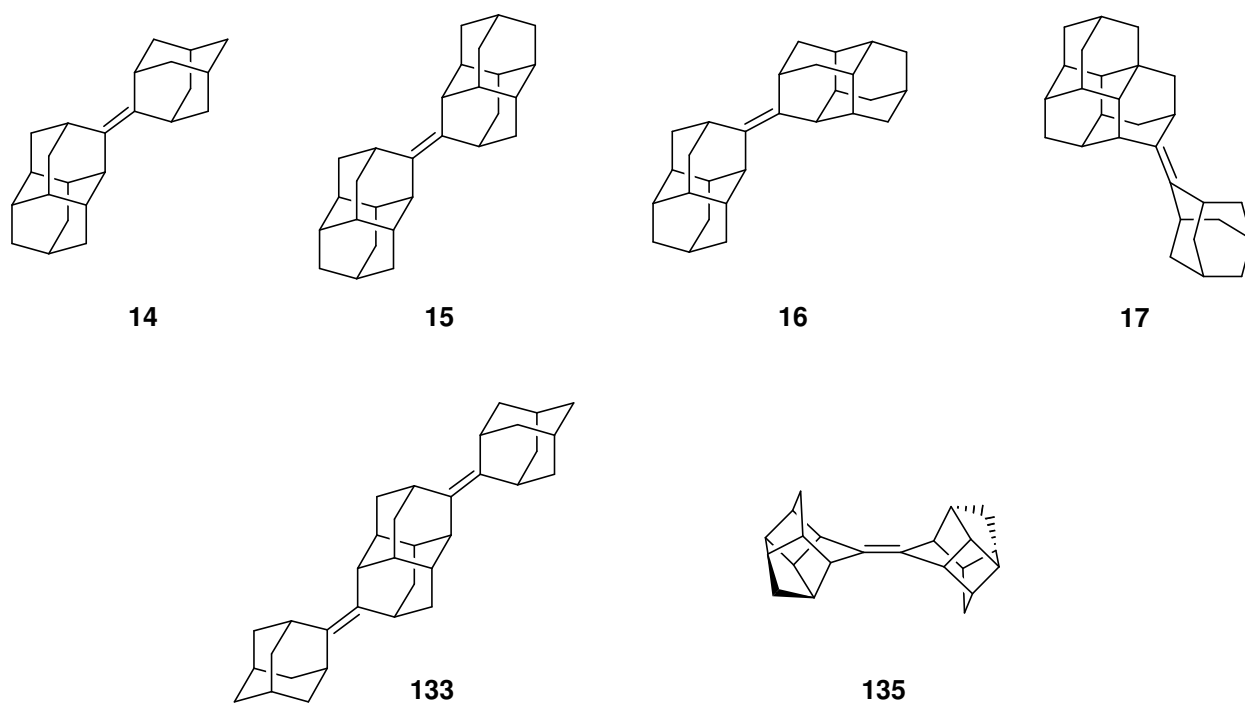


Figure 47. Synthesized coupled cage compounds.

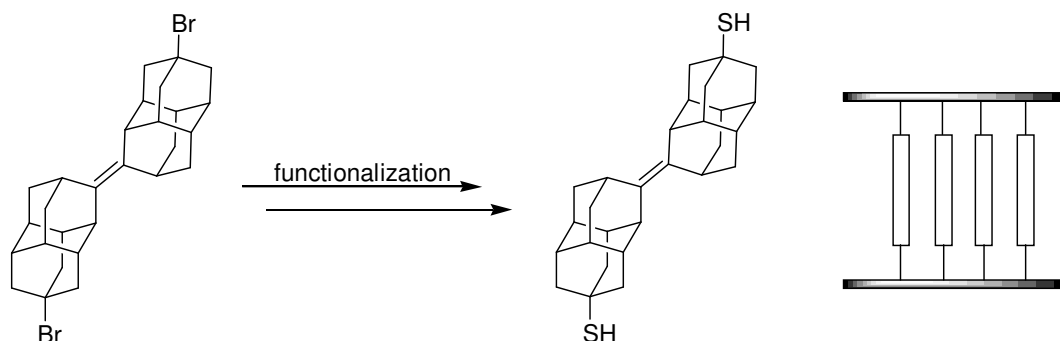
A number of new unsaturated coupled cage compounds, namely *anti*- and *syn*-diamantylidenediamantanes, adamantylidenediamantane-3, adamantylidenetriamantane-8, di(adamantylidene-2)diamantane-3,10, as well as C_i -*trans*- C_5 -8-trishomocubylidene- C_5 -8-trishomocubane, were synthesized in presence of titanium (IV) chloride – zinc, separated and characterized by analytical and computational methods. Individual stereoisomers of *anti*-, *syn*-diamantylidenediamantane and C_i -*trans*- C_5 -8-trishomocubylidene- C_5 -8-trishomocubane, were separated by fractional recrystallization from hexane. Alternatively the cross-coupled diamondoids separation on silica gel impregnated by silver nitrate was successfully applied.

In contrast to diamantanone, where two isomeric products were formed in equal amounts, reductive coupling of *C*₅-trishomocubane-8-one gives a mixture of stereoisomers and it was confirmed that *trans*-products are favored.

It was found by computational methods that terminal hydrogen atoms, neighboring to the carbon atoms of the double bond have destabilizing influence due to repulsive van der Waals interactions.

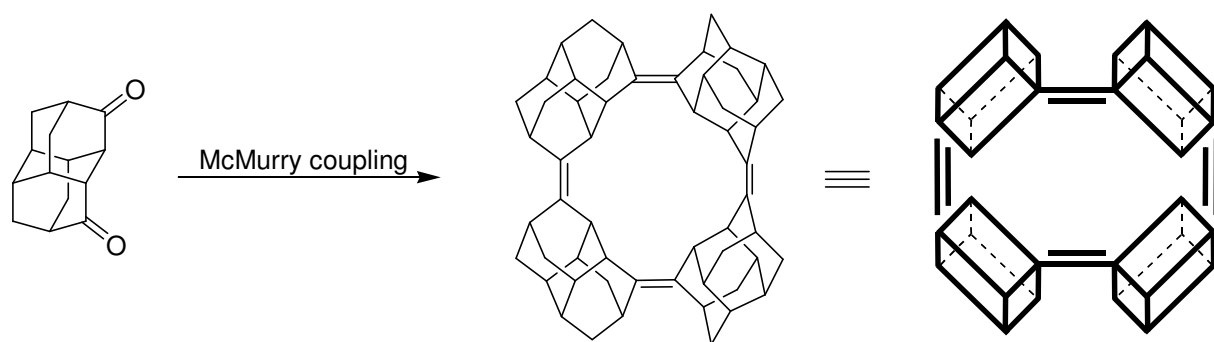
Functionalization of adamantylideneadamantane, *anti*- and *syn*-diamantylidenediamantanes under phase transfer catalytic conditions was performed and main components of the reaction mixture (4-bromo-*anti*- and 4-bromo-*syn*-diamantylidenediamantane as well as *anti*- and *syn*-diamantylidenediamantan-2-ol) were separated where tertiary carbon atom substituted products were formed.

Study of the structure/property relationships in synthesized nanodiamond family members opens avenues for studying their potential for molecular electronics. One of the next logical steps in our research would be conversion of substituted sterically hindered alkenes into thiols and self-assembling their monolayers on the metal surfaces. Functionalization of ketones and further introduction them into McMurry reaction would allow us to synthesize disubstituted coupled diamondoids in order to create conductive linkers between two surfaces.



Scheme 67.

We would also suggest to prepare a number of assembled molecules from cage ketone substrates with higher (2D- and 3D) topologies and sizes 1–5 nm, *e.g.*, ring-shaped nanodiamonds from diamantanediones. Also further study of synthetic properties of obtained compounds is under development.



Scheme 68. One of the possible structures as result of McMurry coupling of diamantanedione-3,8.

Chapter 5. Experimental part

5.1. Chemicals and solvents

Unless otherwise stated commercially available chemicals were used without further purification (Acros Organics, Fluka, Sigma-Aldrich, Merck, Alfa Aesar).

Solvents for synthesis, chromatography, recrystallization procedures were of the technical grade and distilled prior to use. Further purification of solvents described in Table 8.

Table 8.

Purification of solvents.

Solvent	Purification method
tetrahydrofurane	THF was predistilled from potassium hydroxide, refluxed over sodium and then distilled over sodium/benzophenone in argon flow
1,2-dimethoxyethane	DME was refluxed over sodium and then distilled over sodium/benzophenone in argon flow
methylene chloride	CH ₂ Cl ₂ was predistilled from CaCl ₂
diethyl ether	Et ₂ O was predistilled from potassium hydroxide and then distilled over sodium/benzophenone in argon flow
hexane	hexane was predistilled over KOH and for chromatography on silica gel impregnated with silver nitrate it was distilled over sodium/benzophenone

Air sensitive reactions were performed under argon, while for oxygen sensitive reagents additionally deoxygenized argon was used; glassware was flame dried in subsequent vacuum/argon flow.

For thin-layer chromatography silica gel 60 coated polyester sheets Macherey-Nagel Polygram Sil G/UV₂₅₄ were used. Column chromatography was performed using J.T. Baker silica gel with particle size 63–200 µm; flash column chromatography was performed using Merck silica gel with particle size 40–63 µm. Eluting mixtures read as volume : volume.

5.2. Instruments and methods

Proton nuclear magnetic resonance (¹H NMR) and carbon nuclear magnetic resonance (¹³C NMR) spectral data sets were recorded using Bruker AM 200, 400 or 600 spectrometer in 5 mm

NMR tubes at 298 K. Chemical shifts were measured in deuterated solvents and referred to TMS residual signals unless other stated.

GC/MS analyses were recorded using Quadrupol-MS HP MSD 5971 (EI) detector and HP 5890A gas chromatograph equipped with a J & W Scientific fused silica GC column (30 m \times 0.250 mm, 0.25 micron DB-5MS stationary phase: 5% phenyl and 95% methyl silicone) using He (4.6 grade) as carrier gas; T-program standard 60–250 °C (15 °C/min heating rate), injector and transfer line 250 °C.

High resolution mass spectra (HRMS) were recorded on a Thermo Finnigan MAT 95 sectorfield spectrometer.

Elemental analyses were performed on a Carlo Erba 1106 CHN analyzer.

Melting points were measured using a Büchi SMP 20 (< 190 °C), Bunsen burner melting point apparatus (> 190 °C) or Boethius apparatus and were not corrected.

5.3. General procedures

5.3.1. Preparation of basic pyrogallol solution for argon deoxygenation

To 125 mL of 60% aqueous solution of potassium hydroxide in 250 mL absorption flask 25 mL of freshly prepared 25% aqueous solution of pyrogallol A was added under argon. Solution has to be replaced afresh by necessity. For the best result two subsequent absorption flasks can be used.

5.3.2. Preparation of silica gel impregnated with 5% of silver nitrate

Solution of 5 g of silver nitrate into 5 mL of acetonitrile was added portionwise to 600 mL of hexane under vigorous stirring. Into this mixture 95 g of Merck silica gel with particle size 40–63 μ m was added carefully, suspension was stirred for 2 hours and hexane removed in vacuo. After silver nitrate was dissolved all operations were performed in darkened equipment.

5.3.3. *p*-Benzoquinone (123)^[200]

To the suspension of 20 g (0.182 mol) of hydroquinone (**124**) in 200 mL of distilled water in 500 mL 2-neck flask, equipped with reflux condenser and stirrer, 11 g of potassium bromate and 10 mL of 5% aqueous solution of sulfuric acid were added stepwise under intensive stirring. Reaction mixture was heated to 45 °C and kept until black color of intermediate quinhydrone

would change to bright yellow color of benzoquinone together with self-induced temperature rise to 70-75 °C. Reaction mixture was then cooled to 0 °C, filtered and precipitate was washed with ice water (2×15 mL) and dried in dark place to give 18.7 g (97%) of *p*-benzoquinone (**123**): m.p. 114-115 °C (lit.,^[200] 115 °C).

5.3.4. Cyclopentadiene (**125**)^[201]

Into 100-mL flask, equipped with Vigreux-column and distilling apparatus, 50 g of dicyclopentadiene was loaded and heated to 160-170 °C. Distilled at 38-46 °C cyclopentadiene (**125**) collected into flask, cooled with ice, and further stored in cold. As it is fastly dimerizing into dicyclopentadiene, fresh cyclopentadiene was prepared as needed.

5.4. Synthesis

5.4.1. Diamantanone (**113**)^[165, 168]

(1): To a suspension of 10 g (53.2 mmol) of diamantane (**2**) in 50 mL of methylene chloride in 250 mL 2-neck flask, equipped with stirrer, condenser and dropping funnel, fuming nitric acid (20 mL) was added dropwise on ice bath. Reaction mixture was stirred vigorously during the addition and after all nitric acid was added mixture was additionally stirred over ice bath for 30 min. After removal of ice bath reaction mixture was stirred until the solution became clear and then carefully 70 mL of distilled water was added and methylene chloride distilled off. Reaction mixture was then refluxed for 2 h and cooled under vigorous stirring. Product, as white solid, was obtained by filtration, washed on filter with water to pH 5–6 and dried to give 10.27 g (95%) of hydroxydiamantanes (**114**). No further purification was applied.

To a mixture of 37.5 mL of sulfuric acid (96–97%) and 1 mL of carbon tetrachloride in 100 mL flask, equipped with stirrer and reflux condenser, 5 g (24.5 mmol) of hydroxydiamantanes (**114**) was added under vigorous stirring. Reaction mixture was kept at 75-77 °C and stirred for 4 h, then cooled and poured on ca. 300 g of ice. Water layer was extracted with methylene chloride (4×75 mL), and then combined organic layer was washed with water (3×75 mL), saturated aqueous sodium bicarbonate (1×75 mL) and brine (1×75 mL), dried over anhydrous sodium sulfate and solvent removed in vacuo. Residue was purified by column chromatography on silica gel (pentane : diethyl ether = 2.5 : 1) to give 2.45 g (50%) of diamantanone (**113**): m.p. 247–249 °C (lit.,^[202] 249–250 °C). Spectral data identical to literature values.^[168]

(2): To a mixture of 60 mL of sulfuric acid (96-97%) and 40 mL of oleum (20%) in 250 mL flask, equipped with stirrer and reflux condenser, 10 g (53.2 mmol) of diamantane (**2**) was added under stirring. Reaction mixture was kept at 75-77 °C for 48 h, then cooled and poured on ca. 500 g of ice. Water layer was extracted with methylene chloride (5×100 mL), and then combined organic layer was washed with water (3×100 mL), saturated aqueous sodium bicarbonate (1×100 mL) and brine (1×100 mL), dried over anhydrous sodium sulfate and solvent was removed in vacuo, affording 9 g (90%) of diamantanone (**113**): m.p. 248–249 °C.

5.4.2. Triamantanones (**117** - **119**)^[167]

A mixture of 10.0 g (41.7 mmol) of triamantane (**3**) and 100 mL of sulfuric acid (96–97%) in 250 mL flask, equipped with stirrer and reflux condenser, was stirred at 78 °C for 4.5 h. The cooled solution was poured on ca. 500 g of ice and extracted with chloroform (5×100 mL), combined organic layer was washed with water (1×100 mL) and saturated solution of sodium bicarbonate (1×100 mL), dried over anhydrous sodium sulfate, filtered and solvent removed in vacuo. Oily residue was purified by column chromatography (pentane : ether = 2.5 : 1) to give 5.1 g (48%) of mixture of triamantanones (**117**-**119**). Further recrystallization of fractions, enriched with (**118**), from hexane afforded 0.056 g of triamantanone-8. Column chromatography on silica gel (methylene chloride : pentane = 4 : 1) afforded 0,042 g of triamantanone-16 (**119**): m.p. 216-217 °C.

Triamantanone-8 (118): ¹H NMR: δ = 2.48 (s, 1H, O=C–CH), 2.4 (s, 1H, O=C–CH), 1.90-2.0 (m, 4H), 1.58-1.85 (m, 13H), 1.52-1.57 (m, 1H), 1.44-1.49 (m, 1H), 1.24-1.28 (m, 1H) ppm; ¹³C NMR: δ = 217.8 (q, C=O), 55.8 (t), 47.4 (t), 46.0 (s), 45.7 (t), 45.6 (t), 44.2 (q), 43.6 (s), 38.3 (s), 37.6 (s), 37.2 (t), 37.2 (t), 37.1 (s), 37.0 (t), 36.8 (s), 34.7 (t), 27.3 (t) ppm; *m/z*: 255 (23), 254 (100), 226 (9), 135 (9), 131 (8), 130 (9), 129 (15), 128 (7), 117 (6), 92 (5), 91 (17), 86 (6), 84 (9), 79 (10), 77 (7), 51 (5); HR-MS: found 254.167 (calculated for C₁₈H₂₂O 254.167); Anal: calcd for C₁₈H₂₂O (254.37): C, 84.99; H, 8.72; found: C, 84.82; H, 8.86.

Triamantanone-16 (119): ¹H NMR: δ = 2.33 (t, 1H, O=C–CH), 1.92-2.04 (m, 5H), 1.87-1.91 (m, 1H), 1.77-1.86 (m, 9H), 1.69-1.76 (m, 2H) 1.61-1.68 (m, 4H) ppm; ¹³C NMR: δ = 218.1 (q, C=O), 49.4 (q), 48.4 (t), 44.9 (t), 38.7 (s), 37.7 (s), 37.4 (t), 37.2 (s), 37.1 (t), 35.8 (s), 35.0 (t), 34.1 (t), 26.9 (t) ppm; *m/z*: 255 (19), 254 (100), 227 (5), 226 (27), 135 (18), 134 (7), 131 (8), 130 (15), 129 (10), 128 (5), 117 (6), 115 (6), 105 (5), 92 (7), 91 (25), 66 (10), 77 (9); HR-MS: found 254.167 (calculated for C₁₈H₂₂O 254.167); Anal: calcd for C₁₈H₂₂O (254.37): C, 84.99; H, 8.72; found: C, 84.90; H, 8.65.

5.4.3. 9-Hydroxydiamantan-3-one (**115**)^[168]

(1): To a 3.75 mL of sulfuric acid (96–97%) in 10 mL flask, equipped with stirrer and reflux condenser, 0.25 g (0.11 mmol) of 4,9-dihydroxydiamantane (**116**) and 3 drops of carbon tetrachloride were added. Reaction mixture was stirred at 77 °C for 6 hours. The cooled solution was poured on ca. 25 g of ice and was extracted with chloroform (3×10 mL). The extract was washed with water (1×15 mL), saturated aqueous sodium hydrogen carbonate (1×15 mL), brine (1×15 mL) and dried over anhydrous sodium sulfate. Removal of solvent in vacuo afforded 0.19 g of mixture of products, which was purified by column chromatography on silica gel (pentane : diethyl ether = 2.5 : 1) yielding 0.06 g (26%) of diamantanone (**113**), 0.025 g (10%) of 9-hydroxydiamantan-3-one (**115**) as well as 0.06 g (22%) of mixture of chlorodiamantanones.

(2): To a 0.5 mL of sulfuric acid (96–97%) in 10 mL flask, equipped with stirrer and reflux condenser, 0.05 g (0.023 mmol) of 4,9-dihydroxydiamantane (**116**) was added. Reaction mixture was stirred at 77 °C for 6 hours. Analysis by GC/MS of the reaction mixture showed that starting material transformed into 9-hydroxydiamantan-3-one (**115**, 53%) and diketones (**120** and **121**, 6%). Quenching and separation of individual compounds was not performed.

(3): To a solution of 4 g (19.8 mmol) of diamantanone (**113**) in 50 mL of methylene chloride in 250 mL 2-neck flask, equipped with stirrer, reflux condenser and dropping funnel, 30 mL of fuming nitric acid was added dropwise on the ice bath. Reaction mixture was allowed to warm up in 30 min and stirred at ambient temperature for 48 h. Then 105 mL of dist. water added dropwise and methylene chloride distilled off. Reaction mixture refluxed for 8 h, cooled and extracted with methylene chloride (8×25 mL). Combined organic layer was washed with water (1×25 mL), saturated solution of sodium hydrogen carbonate (1×25 mL) and brine (1×25 mL), dried over anhydrous sodium sulfate, filtered and solvent removed in vacuo. Obtained solid rest was purified by column chromatography (hexane : ethyl acetate = 85 : 15) and recrystallized from benzene to give 3.5 g (81%) of **115**: m.p. 191–192 °C (lit.,^[168] 191–193 °C). Spectral data identical to literature values.^[168]

5.4.4. Dimantanediones (**120**, **121**)

A mixture of 3.5 g of 9-hydroxydiamantan-3-one (**115**) and 35 mL of sulfuric acid (96–97%) in 100 mL flask, equipped with stirrer and reflux condenser, was stirred at 76 °C for 7–10 days with control by GC/MS. After attaining stable conversion data reaction mixture was cooled,

poured on ca. 250 g of ice and extracted with chloroform (10×30 mL). Combined organic layer was washed with water (1×30 mL), saturated aqueous sodium bicarbonate (1×30 mL), brine (1×30 mL) and dried over anhydrous sodium sulfate. Removal of solvent in vacuo afforded 2.32 g of raw product, which was purified by column chromatography (hexane : diethyl ether = 2.5 : 1) yielding 0.62 g (18%) of diamantanediones (**120**, **121**), as well as 1.47 g (42%) of starting material, which was recovered and reused.

Diamantanedione-3,10 (120): ^1H NMR: δ = 2.69 (s, 2H), 2.59 (s, 2H), 2.0-2.22 (m, 12H) ppm; ^{13}C NMR: δ = 213.2 (q), 55.9 (t), 43.7 (t), 39.0 (t), 38.0 (s), 37.6 (s), 35.5 (t) ppm; m/z : 217 (15), 216 (100), 105 (5), 92 (6), 91 (10), 81 (6), 80 (6), 79 (14), 78 (6), 77 (7); HR-MS: found 216.116 (calculated for $\text{C}_{14}\text{H}_{16}\text{O}_2$ 216.115); Anal: calcd for $\text{C}_{14}\text{H}_{16}\text{O}_2$ (216.28): C, 77.75; H, 7.46; found: C, 77.82; H, 7.59.

Diamantanedione-3,8 (121): ^1H NMR: δ = 2.67 (s, 2H), 2.58 (s, 2H), 1.98-2.28 (m, 12H) ppm; ^{13}C NMR: δ = 215.1 (q), 54.1 (t), 43.0 (t), 38.1 (t), 36.5 (s) ppm; m/z : 217 (15), 216 (100), 131 (6), 119 (5), 117 (10), 95 (5), 92 (6), 91 (17), 79 (9), 77 (6); HR-MS: found 216.115 (calculated for $\text{C}_{14}\text{H}_{16}\text{O}_2$ 216.115); Anal: calcd for $\text{C}_{14}\text{H}_{16}\text{O}_2$ (216.28): C, 77.75; H, 7.46; found: C, 77.68; H, 7.60.

5.4.5. Tricyclo[6.2.1.0^{2,7}]undeca-4,9-diene-3,6-dione (**126**)

To a suspension of 15 g (0.139 mol) of *p*-benzoquinone (**123**) and 25 mL of ethanol in 100 mL 2-neck flask, equipped with magnetic stirred and reflux condenser, at 0 °C was added a solution of 11.2 mL (0.136 mol) of freshly distilled cyclopentadiene (**125**) in cold ethanol (10 mL). Cooling was then taken away and reaction mixture allowed to warm to room temperature and became clear. After 30 min of stirring reaction mixture was left overnight at low temperature. Formed crystalline precipitate was filtered, washed with cold ethanol (2×10 mL) and dried. Mother liquor was evaporated in vacuo until precipitation started and cooled overnight, filtered, precipitate was washed on filter with cold ethanol (2×5 mL) and dried. Obtained pale yellow crystals were combined to give 21.6 g (90%) of Diels-Alder adduct **126**: m.p. 76–78 °C (lit.,^[170] 76.0–78.5 °C). Spectral data identical to literature values.^[170]

5.4.6. Pentacyclo[5.4.0.0^{2,6}.0^{3,10}.0^{5,9}]undeca-8,11-dione (**127**)^[203]

Solution of 12 g (70 mmol) of Diels-Alder adduct **126** in 160 mL of ethylacetate was deoxygenated with argon and irradiated with for 6 h with a Hanovia medium-pressure Hg lamp (Duran filter). Then reaction mixture was evaporated in vacuo until precipitation occurred (ca. ¼

of starting volume) and cooled overnight. Filtration of crystalline precipitate afforded 10.5 g (87%) of colorless crystals of dione **127**: m.p. 243–244 °C (lit.,^[170] 245 °C). Spectral data identical to literature values.^[170]

5.4.7. Pentacyclo[5.4.0.0^{2,6}.0^{3,10}.0^{5,9}]undeca-8,11-dione 8-ethylene ketal (**128**)

To a solution of 8 g (46 mmol) of diketone **127** in 120 mL of benzene in 250 mL 2-neck flask, equipped with distilling trap and reflux condenser, 7.8 mL (~ 0.14 mol) of ethylene glycol and 100–150 mg of Dowex 60 was added. Reaction mixture was put onto preheated to 115–120 °C oil bath and refluxed for 75 min. After cooling the reaction mixture was filtered from Dowex 60, washed with water (2×50 mL) and dried over anhydrous sodium sulfate. Solvent was removed in vacuo to afford 9.53 g (95%) of monoethylene ketal **128**: m.p. 72–73 °C (lit.,^[171] 73.0–73.5 °C). Spectral data identical to literature values.^[171]

5.4.8. Pentacyclo[5.4.0.0^{2,6}.0^{3,10}.0^{5,9}]undecane-8-one ethylene ketal (**129**)

To the mixture of 0.42 g (7.5 mmol) of potassium hydroxide and 1 mL (20 mmol) of 98% hydrazine hydrate in 7.5 mL of diethylene glycol in 25 mL flask, equipped with stirrer and reflux condenser, 1 g (4.6 mmol) of ethylene ketal **128** was added. Reaction mixture was stirred at 150 °C for 1.5 h and then additionally at 200 °C for 3 h. The mixture was allowed to cool to ambient temperature, diluted with 10 mL of water and extracted with diethyl ether (4×30 mL). Combined organic layer was washed with 5% aqueous solution of hydrochloric acid (2×30 mL), saturated aqueous sodium bicarbonate (2×30 mL), water (2×50 mL) and dried over anhydrous sodium sulfate. Solvent was removed in vacuo to afford 0.49 g (42%) of ketal **129** as colorless oil: b.p. 180–186 °C (14 mm Hg). Spectral data identical to literature values.^[204]

5.4.9. Pentacyclo[5.4.0.0^{2,6}.0^{3,10}.0^{5,9}]undecane-8-one (**122**)

To the solution of 0.49 g (2.4 mmol) of ethylene ketal **129** in 3.5 mL of tetrahydrofuran in 100 mL flask, equipped with stirrer and reflux condenser, 18 mL of 10% aqueous sulfuric acid was added. Suspension was stirred at 80 °C for 3 hours and sulfuric acid was neutralized by pouring reaction mixture into 100 mL of 10% aqueous sodium bicarbonate. Water layer was extracted with methylene chloride (5×30 mL), combined organic layer was washed with water (3×50 mL) and dried over anhydrous sodium sulfate. Solvent was removed in vacuo and solid

rest was sublimed (2 mm Hg, 75–85 °C) to afford 0.29 g (75%) of *C*₅-trishomocubane-8-one (**122**): m.p. 194–195 °C (lit.,^[204] 194–195 °C). Spectral data identical to literature values.^[204]

5.4.10. 11-Hydroxypentacyclo[5.4.0.0^{2,6}.0^{3,10}.0^{5,9}]undecane-8-one ethylene ketal (**130**)

To a suspension of 1.6 g (42 mmol) of lithium aluminum hydride in 70 mL of dry diethyl ether in 2-neck 1 L flask, equipped with stirrer, reflux condenser and dropping funnel, solution of 9.5 g (43.6 mmol) of ketoketal **128** in 150–200 mL of dry diethyl ether was added dropwise. Reaction mixture was refluxed for 2–3 h and then under stirring and cooled with ice water quenched with saturated aqueous ammonium chloride solution. Organic layer was separated and water layer was additionally extracted with diethyl ether (3×50 mL). Combined organic layer was washed with brine (3×50 mL) and dried over anhydrous sodium sulfate. Solvent was removed in vacuo to afford 9.4 g (98%) of **130** as colorless, slowly crystallized at standing oil. For **130a**: m.p. 61–62 °C (lit.,^[205] 61.5–63.0 °C); **130b**: m.p. 44–47 °C (lit.,^[204] 45.0–46.0 °C).

endo-11-Hydroxypentacyclo[5.4.0.0^{2,6}.0^{3,10}.0^{5,9}]undecane-8-one ethylene ketal (**130a**):

¹H NMR: δ = 5.38 (d, 1H), 3.80–4.10 (m, 4H), 3.56–3.75 (m, 1H), 2.40–2.80 (m, 6H), 2.07–2.40 (m, 2H), 1.12 and 1.65 (AB system, 2H, *J* = 11 Hz) ppm; ¹³C NMR: δ = 115.8 (q, 1C), 72.4 (t, 1C), 65.6 (s, 1C), 63.0 (s, 1C), 47.2 (t, 1C), 46.8 (t, 1C), 44.7 (t, 1C), 43.6 (t, 1C), 39.9 (t, 1C), 39.3 (t, 1C), 39.1 (t, 1C), 38.9 (t, 1C), 35.0 (s, 1C) ppm; *m/z*: 220 (10), 159 (16), 158 (54), 141 (11), 132 (12), 131 (100), 130(69), 129 (44), 128 (21), 117 (21), 116 (27), 115 (33), 104 (13), 97 (12), 94 (11), 92 (12), 91 (83), 81 (14), 79 (16), 78 (33), 77 (27), 66 (16), 65 (22), 55 (15), 53 (17), 51 (15); HR-MS: found 220.109 (calculated for C₁₃H₁₆O₃ 220.110); Anal: calcd for C₁₃H₁₆O₃ (220.26): C, 70.89; H, 7.32; found: C, 70.77; H, 7.30.

exo-Hydroxypentacyclo[5.4.0.0^{2,6}.0^{3,10}.0^{5,9}]undecane-8-one ethylene ketal (**130b**):

¹H NMR: δ = 4.63 (t, 1H,), 3.65–3.85(m, 4 ppm; ¹³C NMR: δ = 122.3 (q, 1C), 81.3 (t, 1C), 68.0 (s, 1C), 62.3 (s, 1C), 54.8 (t, 1C), 53.3 (t, 1C), 45.2 (t, 1C), 44.5 (t, 1C), 43.5 (s, 1C), 42.7 (t, 1C), 42.4 (t,1C), 41.6 (t, 1C, overlapping) ppm; *m/z*: 220 (25), 175 (17), 158 (27), 154 (13), 141 (11), 132 (13), 131 (58), 130 (50), 129 (32), 128 (29), 127 (13), 126 (12), 125 (16), 119 (10), 117 (30), 116 (19), 115 (34), 113 (13), 112 (14), 105 (17), 104 (15), 103 (13), 99 (54), 97 (12), 95 (18), 94 (18), 92 (18), 91 (100), 89 (20), 87 (10), 86 (33), 83 (14), 82 (24), 82 (32), 79 (40), 78 (37), 77 (60), 73 (19), 68 (17), 67 (18), 66 (57), 65 (48), 63 (19), 55 (62), 54 (15), 53 (45), 52 (19), 51 (38), 50 (11); HR-MS: found 220.110 (calculated for C₁₃H₁₆O₃ 220.110); Anal: calcd for C₁₃H₁₆O₃ (220.26): C, 70.89; H, 7.32; found: C, 70.85; H, 7.43.

5.4.11. *exo*-11-Bromopentacyclo[5.4.0.0^{2,6}.0^{3,10}.0^{5,9}]undecane-8-one (131)

(1): A mixture of 7.8 g (35.5 mmol) of hydroxyketal **130a** and 120 mL of 48% hydrobromic acid in 250 mL 2-neck flask, equipped with stirrer and reflux condenser, was stirred at 80 °C for 3 h, then allowed to cool to ambient temperature and quenched in 120 mL of ice water. Obtained suspension was extracted with methylene chloride (3×75 mL), combined organic layer was washed with saturated aqueous sodium bicarbonate (1×50 mL), brine (2×50 mL) and dried over anhydrous sodium sulfate. Solvent was removed in vacuo and residue was purified by column chromatography on silica gel (hexane : ethyl acetate = 9 : 1) to give 3.76 g (44%) of desired product **131**: m.p. 82–83 °C (lit.,^[171] 84.5–85.3 °C). Spectral data identical to literature values.^[171]

(2): A mixture of 10.4 g (47.3 mmol) of hydroxyketal **130a** and 150 mL of 48% hydrobromic acid in 250 mL 2-neck flask, equipped with stirrer and reflux condenser, was kept at 60 °C for 24 h, allowed to cool to ambient temperature and poured in 150 mL of ice water. Dark coloured precipitate was filtered off, washed with water and dried. Purification by column chromatography on silica gel (hexane : ethyl acetate = 9 : 1) afforded 10.48 g (92%) of bromoketone **131**. Substance characteristics identical to values, obtained above.

5.4.12. *exo*-11-Bromopentacyclo[5.4.0.0^{2,6}.0^{3,10}.0^{5,9}]undecane-8-one ethylene ketal (132)

(1): To a solution of 3.7 g (15.5 mmol) of bromoketone **131** in 80 mL of benzene in 100 mL 2-neck flask, equipped with stirrer and distillation trap with reflux condenser, 1.7 mL (30 mmol) of ethylene glycol and 20–30 mg of Dowex 60 were added. Reaction mixture was refluxed for 5 h, then allowed to cool to ambient temperature, filtered from cationite and washed with water (2×50 mL). Organic layer was dried over anhydrous sodium sulfate and solvent was removed in vacuo to give 4.13 g (94%) of ketal **132** as colorless oil.

(2): To a solution of 8 g (36.3 mmol) of hydroxyketal **130a** in 180 mL of dry methylene chloride in 500 mL 2-neck flask, equipped with stirrer and reflux condenser, 20.96 g (80 mmol) of triphenylphosphine and 26.8 g (80.8 mmol) of carbon tetrabromide were added. Reaction mixture was refluxed for 5 h, then allowed to cool to 30–35 °C and 6–7 mL of methanol was added with subsequent reflux for 1 h additionally. Reaction mixture was allowed to cool to ambient temperature, filtered and solvent removed in vacuo. Residue was quenched by diethyl ether (3×75 mL) and to the combined ether solution 7–8 g of fine lithium iodide monohydrate

was added under stirring. Mixture was stirred for 3-4 h and precipitate was filtered off through silica gel, which was then additionally washed with diethyl ether (3×30 mL) and ether removed in vacuo. Residue was purified by column chromatography on silica gel (hexane : diethyl ether = 9 : 1) to give 9.8 g (95%) of ketal **132** as colorless oil.

exo-11-Bromopentacyclo[5.4.0.0^{2,6}.0^{3,10}.0^{5,9}]undecane-8-one ethylene ketal (132): ¹H NMR (CDCl₃): δ = 5.18 (s, 1H), 3.68-4.00 (m, 4H), 3.02-3.25 (m, 1H), 2.75-3.00 (m, 2H), 2.50-2.74 (m, 3H), 2.30-2.46 (m, 1H), 2.03-2.18 (m, 1H), 1.62 and 1.36 (dd, AB system, 2H, *J* = 11 Hz); ¹³C NMR: δ = 115.3 (q), 65.6 (s), 63.1 (s), 57.7 (t), 51.7 (t), 49.9 (t), 46.9 (t), 45.5 (t), 44.6 (t), 42.1 (t), 41.1 (t), 38.8 (t), 34.4 (s) ppm; *m/z*: 284 (10), 282 (10), 204 (14), 203 (100), 159 (8), 139 (6), 137 (8), 131 (11), 129 (9), 128 (8), 126 (5), 117 (20), 116 (7), 115 (15), 99 (13), 91 (19), 79 (8), 78 (7), 77 (12), 73 (7), 66 (7), 65 (11), 64 (6), 51 (7); HR-MS: found 282.025 (calculated for C₁₃H₁₅BrO₂ 282.026); Anal: calcd for C₁₃H₁₅BrO₂ (283.16): C, 55.14; H, 5.34; found: C, 55.23; H, 5.41.

5.4.13. Pentacyclo[5.4.0.0^{2,6}.0^{3,10}.0^{5,9}]undecane-8-one ethylene ketal (129)

To the solution of 4.2 g (14.8 mmol) of bromoketal **132** in 60 mL of dry tetrahydrofuran in 250 mL 2-neck flask, equipped with stirrer and reflux condenser, 3.5 mL of *tert*-butanol and 1.15 g (0.164 mol) of lithium wire were added. Reaction mixture was refluxed for 2 h, cooled to 30-40 °C, 1.75 mL of *tert*-butanol was added, and mixture refluxed 2 h additionally. After that flask was cooled on ice bath and excess of lithium was carefully destroyed by 20 mL of water. Received mixture was diluted with 150 mL of water and extracted by methylene chloride (3×75 mL). Combined organic layer was washed with water (1×75 mL) and dried over anhydrous sodium sulfate. Solvent was removed in vacuo to afford 2.9 g (97%) of ketal **129**. Substance characteristics identical to values, obtained above.^[204]

5.4.14. Adamantylideneadamantane (13)^[126, 179]

(1): A 50 mL 3-necked flame dried in argon flow flask, equipped with magnet stirrer, was fitted with 2 rubber septa and glass stopper. Anhydrous titanium (III) chloride (0.271 g, 1.76 mmol) was added into weighted flask in argon camera and flask connected to line with oxygen-free argon. One septum was replaced with dry reflux condenser, 15 mL of dry freshly distilled 1,2-dimethoxyethane was injected, followed by 0.1-0.15 g of washed lithium in small amount of dry hexane. Remaining septum was replaced with stopper and reaction mixture refluxed under argon for 1 h. Then 0.085 g (0.56 mmol) of adamantanone (**18**) was added as only reaction

mixture ceased to boil and it was refluxed for 24h additionally. Cooled reaction mixture was poured into 100 mL of water and 100 mL of methylene chloride was added. Organic layer was separated and water layer was extracted additionally with methylene chloride (3×30 mL). Combined organic layer was washed with water (2×30 mL), brine (1×30 mL) and dried over anhydrous sodium sulfate and solvent was removed in vacuo. Column chromatography purification (hexane) afforded 0.032 g (42%) of pure adamantylideneadamantane (**13**): m.p. 184–185 °C (lit.,^[71] 184–187 °C). Spectral data identical to literature values.^[71]

(2): A 100 mL 2-necked flame dried in argon flow flask, equipped with a magnet stirrer and reflux condenser with a bubble counter, was fitted with rubber septum and 50 mL of freshly distilled dry tetrahydrofuran was added through a septum in continuous argon flow. The solvent was cooled with an external ice bath and 2.5 mL (22.8 mmol) of titanium (IV) chloride was injected. The septum was removed and 3.06 g (47 mmol) of zinc powder was added in small portions. After the zinc addition the ice bath was removed and the reaction mixture was refluxed for 1 h. The reaction mixture was then cooled to ambient temperature and 1 mL of pyridine was added, followed by addition of a solution of 1.5 g (10 mmol) of adamantanone (**18**) in 15 mL of dry tetrahydrofuran. The resulting mixture was refluxed under argon for 12 h then was allowed to cool to ambient temperature and an external ice bath was applied. Reaction mixture was quenched by dropwise addition of 60 mL of a 10% solution of potassium carbonate. The dark blue slurry was transferred to a conical flask with 150 mL of diethyl ether and vigorously stirred for 15 min and then filtered. The residue on filter was washed with diethyl ether (3×75 mL) and then discarded. Mother liquor was separated and the aqueous layer was extracted with diethyl ether (2×75 mL). Combined organic layer was washed sequentially with water (1×70 mL), 5% solution of hydrochloric acid (2×50 mL), water (2×70 mL) and brine (1×50 mL). The organic layer was dried over anhydrous sodium sulfate and the solvent was removed in vacuo. The residue was purified by column chromatography (hexane) to afford 1.06 g (78%) of adamantylideneadamantane (**13**): m.p. 185–186 °C.

5.4.15. *anti*- and *syn*-Diamantylidenediamantanes (**15**, **16**)

Procedures (1) and (2) for synthesis of adamantylideneadamantane (**13**) were used. Ratio of reagents is presented in the tables below. For tetrahydrofuran in brackets the amount of dry tetrahydrofuran required for dissolving the diamantanone is given.

Table 9.

Ratio of reagents for synthesis of **15** and **16** by TiCl₃-Li coupling.

Ratio of reagents				Product mass, g	Yield, %
Diamantanone (113), g (mmol)	TiCl ₃ , g (mmol)	Li, g	DME, mL		
0.0886 (0.44)	0.271 (1.76)	0.15	15	0.038	46

Table 10.

Ratio of reagents for synthesis of **15** and **16** by TiCl₄-Zn coupling.

Ratio of reagents					Product mass, g	Yield, %
Diamantanone (113), g (mmol)	TiCl ₄ , mL (mmol)	Zn dust, g (mmol)	Pyridine, mL	THF, mL (mL)		
1.08 (5.34)	1.35 (12.3)	1.62 (24.9)	0.5	25 (7)	0.74	74

After reaction mixture work up the residue was purified by column chromatography (hexane) and pure *anti*- (**15**, m.p. 276 °C) and *syn*-diamantylidenediamantane (**16**, m.p. 245–248 °C) were isolated by fractional crystallization from hexane.

***anti*-Diamantylidenediamantane (15):** ¹H NMR (CDCl₃): δ = 2.84 (s, 2H), 2.73 (s, 2H), 1.7-1.81 (m, 24H), 1.65 (s, 4H), 1.56-1.62 (m, 4H) ppm; ¹³C NMR (CDCl₃): δ = 133.9 (q), 41.7 (t), 39.9 (s), 39.3 (t), 38.2 (s), 38.2 (s), 37.8 (t), 37.2 (t), 29.1 (t), 25.9 (t) ppm; *m/z*: 373 (29), 372 (100), 187 (19), 131 (5), 129 (6), 117 (5), 105 (7), 93 (6), 91 (13), 81 (5), 79 (7), 57 (5); HR-MS: found 372.282 (calculated for C₂₈H₃₆ 372.282); Anal: calculated for C₂₈H₃₆ (372.59): C, 90.26; H, 9.74; found: C, 90.23; H, 9.88.

***syn*-Diamantylidenediamantane (16):** ¹H NMR (CDCl₃): δ = 2.82 (s, 2H), 2.74 (s, 2H), 1.69-1.82 (m, 24H), 1.58-1.64 (m, 8H) ppm; ¹³C NMR (CDCl₃): δ = 133.9 (q), 41.3 (t), 39.8 (s), 39.3 (t), 38.2 (s, 2 signals overlapped), 37.8 (t), 37.2 (t), 29.4 (t), 25.9 (t) ppm; *m/z*: 373 (27), 372 (100), 187 (13), 91 (6); HR-MS: found 372.281 (calculated for C₂₈H₃₆ 372.282); Anal: calcd for C₂₈H₃₆ (372.59): C, 90.26; H, 9.74; found: C, 89.93; H, 9.96.

5.4.16. Adamantylidenediamantane-3 (14)

Procedures (1) and (2) for synthesis of adamantylideneadamantane (**13**) were used. Ratio of reagents is presented in the tables below. For tetrahydrofurane in brackets the amount of dry tetrahydrofurane required for dissolving the mixture of ketones is given.

Table 11.

Ratio of reagents for synthesis of **14** by TiCl₃-Li coupling.

Ratio of the ketones – 18 / 113	Ratio of reagents					Yield, g (%)
	18 , g (mmol)	113 , g (mmol)	TiCl ₃ , g (mmol)	Li, g	DME, mL	
1:1	0.056 (0.37)	0.075 (0.37)	0.46 (3.0)	0.17	20	0.067 (56)

Table 12.

Ratio of reagents for synthesis of **14** by TiCl₄-Zn coupling.

Ratio of the ketones – 18 / 113	Ratio of reagents						Yield, g (%)
	18 , g (mmol)	113 , g (mmol)	TiCl ₄ , mL (mmol)	Zn dust, g (mmol)	Pyridine, mL	THF, mL (mL)	
1:1	0.85 (5.7)	1.15 (5.7)	3.4 (0.031)	4.1 (63)	1.5	60 (15)	1.72 (95)
1:3.5	0.44 (2.9)	1.5 (10)	3.2 (0.029)	3.84 (35)	2	60 (15)	1.69 (95)
2:1	1.19 (8)	0.81 (4)	3.4 (0.031)	4.1 (63)	1.5	60 (15)	1.71 (94)
3.5:1	1.44 (9.6)	0.56 (2.8)	3.85 (0.035)	4.64 (71)	1.6	60 (15)	1.74 (97)
5:1	1.58 (10.5)	0.42 (0.42)	3.4 (0.031)	4.1 (63)	1.5	60 (15)	1.71 (95)

Obtained white solid is mixture of olefins – pure **14** was isolated by column chromatography on silica gel, impregnated with 5% of silver nitrate using hexane as eluent, m.p. 168–169 °C.

Adamantylidenediamantane-3 (14): ¹H NMR (CDCl₃): δ = 2.94 (s, 1H), 2.91 (s, 1H), 2.8 (s, 1H), 2.72 (s, 1H), 1.89-1.94 (m, 2H), 1.72-1.87 (m, 17H), 1.58-1.70 (m, 9H) ppm; ¹³C NMR (CDCl₃): δ = 133.7 (q), 133.4 (q), 41.4 (t), 39.8 (s), 39.8 (s), 39.7 (s), 39.2 (t), 38.2 (s), 38.2 (s), 37.8 (t), 37.4 (s), 37.2 (t), 32.2 (t), 31.8 (t), 29.2 (t), 28.6 (t), 26.0 (t) ppm; *m/z*: 321 (26), 320 (100), 277 (6), 268 (8), 263 (8), 254 (5), 202 (6), 187 (10), 135 (7), 133 (8), 132 (6), 131 (5), 129 (6), 119 (5), 117 (7), 111 (6), 105 (9), 97 (9), 95 (8), 93 (8), 92 (5), 91 (16), 85 (9), 83 (8), 81 (9),

79 (11), 77 (5), 71 (13), 69 (9), 67 (8), 57 (17), 55 (11), 43 (10), 41 (9); HR-MS: found 320.251 (calculated for $C_{24}H_{32}$ 320.250); Anal: calculated for $C_{24}H_{32}$ (320.51): C, 89.94; H, 10.06; found: C, 90.05; H, 10.15.

5.4.17. Adamantylidenetriamantane-8 (17)

Procedure (2) for synthesis of adamantylidenetriamantane (**13**) was used. Ratio of reagents is presented in the table below. For tetrahydrofuran in brackets the amount of dry tetrahydrofuran required for dissolving the mixture of ketones is given.

Table 13.

Ratio of reagents for synthesis of **17** by $TiCl_4$ -Zn coupling.

Ratio of reagents						
Adamantanone (18), g (mmol)	Triamantanone (118), g (mmol)	$TiCl_4$, mL (mmol)	Zn dust, g (mmol)	Pyridine, mL	THF, mL (mL)	Product mass, g Yield, %
0.033 (0.22)	0.056 (0.22)	0.11 (1)	0.135 (2.07)	0.1	2.2 (0.7)	0.042 51

Obtained white solid is mixture of olefins – 0.0043 g of **17**, as white solid, was isolated by column chromatography on silica impregnated with 5% of silver nitrate using hexane as eluent.

Adamantylidenetriamantane-8 (17): 1H NMR ($CDCl_3$): δ = 2.94 (s, 1H), 2.90 (s, 1H), 2.85 (s, 1H), 2.64 (s, 1H), 1.92 (s, 2H), 1.80-1.88 (m, 7H), 1.59-1.77 (m, 16H), 1.52-1.58 (m, 2H), 1.28-1.36 (m, 3H), 1.15-1.23 (m, 2H) ppm; ^{13}C NMR ($CDCl_3$): δ = 133.5 (q), 133.4 (q), 48.2 (t), 46.9 (s), 46.6 (t), 45.1 (s), 41.9 (t), 39.8 (s), 39.8 (s), 39.7 (s), 39.7 (s), 39.7 (s), 38.5 (s), 38.4 (t), 38.2 (t) 38.2 (s), 38.0 (t), 38.0 (s), 37.4 (s), 36.9 (t), 35.3 (t), 33.8 (q), 32.1 (t), 32.0 (t), 31.1 (t), 28.6 (t), 28.6 (t), 27.8 (t) ppm; m/z : 373 (31), 372 (100), 239 (22), 207 (10), 186 (10), 179 (10), 178 (10), 169 (10), 167 (17), 165 (21), 159 (11), 158 (13), 157 (10), 152 (10), 143 (28), 142 (10), 141 (34), 135 (17), 133 (23), 132 (12), 131 (34), 130 (14), 129 (70), 128 (45), 121 (14), 119 (34), 117 (43), 116 (22), 115 (27), 109 (13), 107 (22), 105 (69), 103 (12), 95 (14), 93 (43), 92 (15), 91 (94), 81 (31), 79 (58), 78 (10), 77 (18), 67 (20), 55 (18); HR-MS: found 372.284 (calculated for $C_{28}H_{36}$ 372.282); Anal: calculated for $C_{28}H_{36}$ (372.59): C, 90.26; H, 9.74; found: C, 9.13; H, 9.58.

5.4.18. Di(adamantylidene-2)diamantane-3,10 (**133**)

Procedure (2) for synthesis of adamantylideneadamantane (**13**) was used. Ratio of reagents is presented in the table below. For tetrahydrofuran in brackets the amount of dry tetrahydrofuran required for dissolving the mixture of ketones is given.

Table 14.

Ratio of reagents for synthesis of **133** by TiCl_4 -Zn coupling.

Ratio of reagents						Product mass, g	Yield, %
Adamantanone (18), g (mmol)	Diamantane-dione (120), g (mmol)	TiCl_4 , mL (mmol)	Zn dust, g (mmol)	Pyridine, mL	THF, mL (mL)		
1.43 (9.5)	0.4 (2)	2.86 (0.032)	3.5 (5.4)	1	72 (15)	1.04	87

For work up reaction mixture was cooled to ambient temperature and transferred into conical flask equipped with stirrer and ice bath with 120 mL of 10% solution of potassium carbonate. Dark blue slurry was stirred for 15 min with 200 mL of carbon disulfide and then filtered and residue on the filter was washed with carbon disulfide (5×50 mL). Combined mother liquor was separated from water and organic layer was washed with water (1×75 mL), 5% solution of hydrochloric acid (2×75 mL), brine (1×75 mL) and dried over anhydrous sodium sulfate. Carbon disulfide after filtration was distilled off and rests were additionally dried in vacuo to give 1.04g (87%) of mixture of olefins. Combined purification by column chromatography on hexane : tetrahydrofuran = 85 : 15 and hexane wash of **133** containing fractions afforded 0.14 g of pure di(adamantylidene-2)diamantane-3,10 (**133**) as white solid.

Di(adamantylidene-2)diamantane-3,10 (133**):** ^1H NMR (CDCl_3): δ = 2.95 (s, 2H), 2.89 (s, 2H), 2.80 (s, 2H), 2.76 (s, 2H), 1.76-1.95 (m, 20H), 1.59-1.72 (m, 16H) ppm; ^{13}C NMR (CDCl_3): δ = 133.7 (q), 133.5 (q), 41.2 (t), 40.0 (s), 39.9 (s), 39.9 (s), 39.7 (t), 37.7 (s), 32.5 (t), 32.2 (t), 29.5 (t), 29.0 (t) ppm; m/z : 454 (6), 453 (35), 452 (100), 269 (6), 268 (25), 226 (5), 225 (6), 135 (10), 133 (5), 93 (6), 91 (11), 79 (8); HR-MS: found 452.342 (calculated for $\text{C}_{34}\text{H}_{44}$ 452.344); Anal: calculated for $\text{C}_{34}\text{H}_{44}$ (452.71): C, 90.20; H, 9.80; found: C, 9.03; H, 86.

5.4.19. 8-Pentacyclo[5.4.0.0^{2,6}.0^{3,10}.0^{5,9}]undecylidene-8-pentacyclo[5.4.0.0^{2,6}.0^{3,10}.0^{5,9}]undecane (134 - 137)

Procedure (2) for synthesis of adamantylideneadamantane (**13**) was used. Reagents' ratio is presented in the table below. For tetrahydrofurane in brackets the amount of dry tetrahydrofurane required for dissolving of ketone is given.

Table 15.

Ratio of reagents for synthesis of **134-137** by TiCl₄-Zn coupling.

C ₅ -trishomocuban-8-one (122), g (mmol)	Reagents' ratios				Product mass, g	Yield, %
	TiCl ₄ , mL (mmol)	Zn dust, g (mmol)	Pyridine, mL	THF, mL (mL)		
2.4 (15)	3.75 (34)	4.5 (70.3)	2	60 (15)	2.0	93

For work up reaction mixture was cooled to ambient temperature and transferred into conical flask, equipped with stirrer and ice bath, with 120 mL of 10% solution of potassium carbonate. Dark blue slurry was stirred for 15 min with 200 mL of benzene, filtered and residue on the filter was washed with benzene (3×50 mL). Combined mother liquor was separated from water and organic layer was washed with water (1×100 mL), 5% solution of hydrochloric acid (2×100 mL), brine (1×100 mL) and dried over anhydrous sodium sulfate. Solvent was removed in vacuo and residue was purified by column chromatography on silica gel by hexane to give 2.0 g (93%) of olefin mixture (**134-137**). Individual **135** was obtained by fractional recrystallization from hexane, m.p. 230.5-231.5 °C.

C_i-trans-C₅-8-trishomocubylidene-C₅-8-trishomocubane (135): ¹H NMR (CDCl₃): δ = 2.95-3.02 (m, 2H), 2.55-2.68 (m, 8H), 2.27-2.36 (m, 4H), 2.12-2.17 (m, 2H), 1.29 and 1.69 (d and d, AB system, 4H, ^{AB}J = 12 Hz), 1.06 and 1.18 (dt and d, AB system, 4H, ^TJ = 1,6 Hz, ^{AB}J = 12,4 Hz) ppm; ¹³C NMR (CDCl₃): δ = 132.9 (q), 47.3 (t), 47.0 (t), 46.8 (t), 45.2 (t), 43.6 (t), 43.4 (t), 39.8 (t), 39.1 (t), 35.6 (s), 30.1 (s) ppm; *m/z*: 289 (17), 288 (71), 223 (20), 222 (68), 221 (11), 209 (39), 179 (10), 178 (12), 167 (13), 165 (22), 157 (16), 156 (63), 155 (45), 154 (11), 153 (19), 152 (16), 144 (12), 143 (79), 142 (31), 141 (45), 131 (11), 129 (35), 128 (55), 127 (16), 117 (12), 116 (11), 115 (53), 91 (40), 80 (10), 79 (100), 78 (24), 77 (62), 67 (18), 66 (25), 65 (24), 53 (10), 51 (14); HR-MS: found 288.187 (calculated for C₂₂H₂₄ 288.188); Anal: calculated for C₂₂H₂₄ (288.43): C, 91.61; H, 8.39; found: C, 91.68; H, 8.32.

5.4.20. Functionalization of *anti*-diamantylidenediamantane (**15**) under PTC conditions^[199]

(1): To a stirred solution of 0.088 g (0.237 mmol) of **15** in 1.1 mL of methylene chloride 0.2 g of carbon tetrabromide, 0.55 mL of 50% aqueous sodium hydroxide and 7 mg of tetra-*n*-butylammonium bromide were added. The reaction mixture was stirred for 14 days at r.t. and then filtered; the solid residue was washed with chloroform (3×5 mL) and diethyl ether (3×5 mL), and the combined organic layers were dried over anhydrous sodium sulfate. After removal of the solvents in vacuo, diamantylidenediamantane epoxide (**142**) was separated by column chromatography (hexane : ethyl acetate = 95 : 5) to yield 0.035 g (38%) of **142** as white solid, as well as 0.015 g (17%) of recovered **3**.

Diamantylidenediamantane epoxide (142): ¹H NMR (CDCl₃): δ = 1.92-1.99 (m, 4H), 1.88 (s, 2H), 1.65-1.85 (m, 30H) ppm; ¹³C NMR (CDCl₃): δ = 73.7 (q), 41.1 (t), 37.8 (s), 37.6 (t), 37.5 (s), 37.5 (s), 37.4 (s), 36.8 (t), 36.6 (t), 36.5 (t), 35.4 (s), 35.0 (t), 29.1 (t), 26.1 (t) ppm; *m/z*: 187 (25), 186 (100), 143 (5), 130 (8), 129 (9), 106 (5), 105 (6), 104 (5), 95 (7), 94 (9), 91 (9); HR-MS: found 388.277 (calculated for C₂₈H₃₆O 388.277); Anal: calculated for C₂₈H₃₆O (388.58): C, 86.54; H, 9.34; found: C, 86.58; H, 9.14.

(2): To a solution of 0.2 g (0.54 mmol) of **15** in 3.1 mL of methylene chloride 0.52 g of carbon tetrabromide, 1.1 mL of 50% solution of sodium hydroxide in water and 10 mg of tetra-*n*-butylammonium bromide were added. Reaction mixture was stirred for 4.5 hours at 70 °C (200W, microwave), then poured on water and extracted with methylene chloride (3×10 mL). Combined organic layer was washed with brine (1×10 mL) and dried over anhydrous sodium sulfate. Solvent was removed in vacuo and residue was subdued to column chromatography. Eluting with pentane afforded 0.056 g (23%) of bromide (**143**) with m.p. 251–252 °C, then eluent was changed to pentane : ether = 1 : 1 to afford 0.097 g (46%) of alcohol (**144**). Last fraction of alcohol was crystallized from hexane to afford pure *anti*-diamantylidenediamantan-2-ol (**144**): m.p. 280–282 °C.

***anti*-4-Bromodiamantylidenediamantane (143):** ¹H NMR (CDCl₃): δ = 2.88 (s, 1H), 2.83 (s, 2H), 2.74 (s, 1H), 2.34-2.42 (m, 6H), 1.98 (s, 1H), 1.88 (s, 2H), 1.85 (s, 2H), 1.78-1.83 (m, 8H), 1.72-1.76 (m, 6H), 1.66-1.55 (m, 8H) ppm; ¹³C NMR (CDCl₃): δ = 135.6 (q), 133.6 (q), 65.9 (q), 49.6 (s, 2 signals overlapped), 49.6 (s), 43.3 (t, 2 signals overlapped), 41.8 (t), 41.1 (t), 39.9 (t), 39.8 (s, 2 signals overlapped), 39.2 (t, 2 signals overlapped), 38.7 (s, 2 signals overlapped), 38.1 (s, 2 signals overlapped), 38.1 (s), 37.6 (t, 2 signals overlapped), 37.0 (t), 36.0 (t, 2 signals overlapped), 29.3 (t), 28.6 (t), 25.9 (t) ppm; *m/z*: 452 (20), 450 (20), 371 (19), 205 (10), 187 (18), 165 (15), 154 (23), 141 (11), 129 (17), 117 (21), 105 (28), 91 (100), 79 (87), 67

(35), 55 (40); HR-MS: found 450.193 (calculated for $C_{28}H_{35}Br$ 450.192); Anal: calculated for $C_{28}H_{35}Br$ (451.48): C, 74.49; H, 7.81; found: C, 74.58; H, 7.70.

anti-Diamantylidenediamantan-2-ol (144): 1H NMR ($CDCl_3$): δ = 2.91 (s, 1H), 2.86 (s, 1H), 2.82 (s, 1H), 2.71 (s, 1H), 2.22 (s, 1H), 2.14 (s, 1H), 2.05 (s, 1H), 1.90-1.96 (m, 2H), 1.85-1.90 (m, 1H), 1.80-1.85 (m, 5H), 1.66-1.80 (m, 16H), 1.65 (s, 2H), 1.55-1.63 (m, 4H) ppm; ^{13}C NMR ($CDCl_3$): δ = 140.8 (q), 129.0 (q), 71.1 (q), 48.2 (t), 43.6 (s, t, 2 signals overlapped), 42.1 (t), 41.4 (t), 40.2 (sec), 40.0 (s), 39.7 (t), 39.5 (t), 39.3 (t), 39.0 (s), 38.0 (s), 38.0 (s), 38.0 (s), 37.6 (t), 37.4 (t), 37.2 (s, 2 signals overlapped), 37.0 (t), 36.5 (t), 34.8 (s), 30.1 (t), 29.2 (t), 28.6 (t), 25.8 (t) ppm; m/z : 388 (100), 370 (17), 277 (6), 187 (18), 167 (10), 157 (10), 143 (12), 129 (23), 117 (19), 105 (30), 91 (77), 79 (48), 67 (31), 55 (35); HR-MS: found 388.277 (calculated for $C_{28}H_{36}O$ 388.276); Anal: calculated for $C_{28}H_{36}O$ (388.58): C, 86.54; H, 9.34; found: C, 86.70; H, 9.14.

5.4.21. Functionalization of *syn*-diamantylidenediamantane (16) under PTC conditions^[199]

To a solution of 0.2 g (0.54 mmol) of **16** in 3.1 mL of methylene chloride 0.52 g of carbon tetrabromide, 1.1 mL of 50% solution of sodium hydroxide in water and 10 mg of tetra-*n*-butylammonium bromide were added. Reaction mixture was stirred for 4.5 hours at 70 °C (200W, microwave), then poured on water and extracted with methylene chloride (3×10 mL). Combined organic layer was washed with brine (1×10 mL) and dried over anhydrous sodium sulfate. Solvent was removed in vacuo and residue was subdued to column chromatography. Eluting with pentane afforded 0.058 g (24%) of bromide (**145**) with m.p. 173 °C, then eluent was changed to pentane : ether = 1 : 1 to afford 0.1 g (48%) of alcohol (**146**). Last fraction of alcohol was crystallized from hexane to afford pure *syn*-diamantylidenediamantan-2-ol (**146**): m.p. 226–227 °C.

syn-4-Bromodiamantylidenediamantane (145): 1H NMR ($CDCl_3$): δ = 2.81 (s, 2H), 2.78 (s, 1H), 2.7 (s, 1H), 2.36-2.41 (d, 2H), 2.31-2.36 (d, 4H), 1.95 (s, 1H), 1.84 (s, 2H), 1.68-1.82 (m, 18H), 1.52-1.63 (m, 6H) ppm; ^{13}C NMR ($CDCl_3$): δ = 135.2 (q), 131.3 (q), 65.5 (q), 49.3 (s, 3 signals overlapped), 43.0 (t, 2 signals overlapped), 41.2 (t), 40.8 (t), 39.4 (s, 2 signals overlapped), 39.2 (t), 39.0 (t, 2 signals overlapped), 38.3 (s, 2 signals overlapped), 37.8 (s, 2 signals overlapped), 37.7 (s), 37.3 (t, 2 signals overlapped), 36.7 (t), 35.7 (t, 2 signals overlapped), 29.3 (t), 28.6 (t), 25.5 (t) ppm; m/z : 452 (15), 450 (15), 372 (64), 371 (75), 370 (46), 287 (12), 277 (17), 275 (16), 187 (50), 165 (16), 155 (17), 143 (25), 129 (52), 117 (20), 105 (63), 91 (100), 79 (45), 67 (22), 55 (29); HR-MS: found 450.193 (calculated for $C_{28}H_{35}Br$ 450.192); Anal: calculated for $C_{28}H_{35}Br$ (451.48): C, 74.49; H, 7.81; found: C, 74.43; H, 7.75.

***syn*-Diamantylidenediamantan-2-ol (146):** ^1H NMR (CDCl_3): δ = 2.83 (s, 1H), 2.74 (s, 1H), 2.71 (s, 1H), 2.64 (s, 1H), 2.22 (s, 1H), 2.11 (s, 1H), 2.06 (s, 1H), 1.95 (s, 1H), 1.81-1.88 (m, 2H), 1.46-1.79 (m, 27H) ppm; ^{13}C NMR (CDCl_3): δ = 140.9 (q), 129.0 (q), 71.0 (q), 47.7 (t), 43.6 (t), 43.5 (s), 41.4 (t), 41.3 (t), 40.1 (s), 39.8 (s), 39.7 (t), 39.6 (t), 39.5 (t), 39.0 (s), 38.0 (s), 38.0 (s, 2 signals overlapped), 37.6 (t), 37.4 (t), 37.2 (s), 37.2 (s), 37.0 (t), 36.5 (t), 34.8 (s), 30.1 (t), 30.0 (t), 28.9 (t), 25.8 (t) ppm; m/z : 388 (100), 370 (22), 277 (9), 187 (15), 167 (12), 155 (8), 141 (11), 129 (22), 117 (16), 105 (38), 91 (92), 79 (72), 67 (30), 55 (31); HR-MS: found 388.277 (calculated for $\text{C}_{28}\text{H}_{36}\text{O}$ 388.277); Anal: calculated for $\text{C}_{28}\text{H}_{36}\text{O}$ (388.58): C, 86.54; H, 9.34; found: C, 86.39; H, 9.26.

5.4.22. 4(e)-Bromoadamantylideneadamantane (20)^[77]

To a solution of 0.9 g (3.36 mmol) of adamantylideneadamantane (**13**) in 40 mL of methylene chloride in 100 mL flask, equipped with reflux condenser and stirrer, 5.56 g (31.2 mmol) of N-bromosuccinimide was added. Reaction mixture was stirred at reflux for 12 h, diluted with 10 mL of methylene chloride, washed with water (2×30 mL) and saturated solution of sodium thiosulfate (2×30 mL). Organic layer was dried over anhydrous sodium sulfate, filtered and solvent evaporated in vacuo. Residue was purified by column chromatography on hexane to afford 0.95 g (77%) of 4(e)-bromoadamantylideneadamantane (**20**): m.p. 129–130 °C (lit.,^[77] 130.5–131.5 °C). Spectral data identical to literature values.^[77]

5.4.23. Functionalization of adamantylideneadamantane (13) under PTC conditions^[199]

To a solution of 0.08 g (0.3 mmol) of **13** in 1.3 mL of methylene chloride 0.24 g of carbon tetrabromide, 0.66 mL of 50% solution of sodium hydroxide in water and 8 mg of tetra-*n*-butylammonium bromide were added. Reaction mixture was stirred for 3 hours at 70 °C (200 W, microwave) and then filtered, solid residue washed with dichloromethane (3×5 mL) and combined organic layer was dried over anhydrous sodium sulfate. After removal of solvent in vacuo, 0.045 g (44%) of 5-bromadamantylideneadamantane (**147**) with m.p. 125–127 °C was separated by column chromatography (hexane), as well as 0.042 g (52%) of adamantylideneadamantane (**13**) was recovered.

5-Bromadamantylideneadamantane (147): ^1H NMR (CDCl_3): δ = 3.07 (s, 2H), 2.87 (s, 2H), 2.45 (s, 2H), 2.27-2.45 (dd, 4H, J =11.9; 75.63 Hz), 2.13-2.18 (m, 1H), 1.9-1.95 (m, 2H), 1.79-1.89 (m, 8H), 1.61-1.71 (m, 6H) ppm; ^{13}C NMR (CDCl_3): δ = 136.0 (q), 129.0 (q), 66.9 (q), 50.7 (s), 49.0 (s), 39.5 (s), 39.5 (s), 37.5 (s), 37.2 (s), 35.7 (t), 33.0 (t), 32.1 (t), 28.4 (t), 28.3 (t)

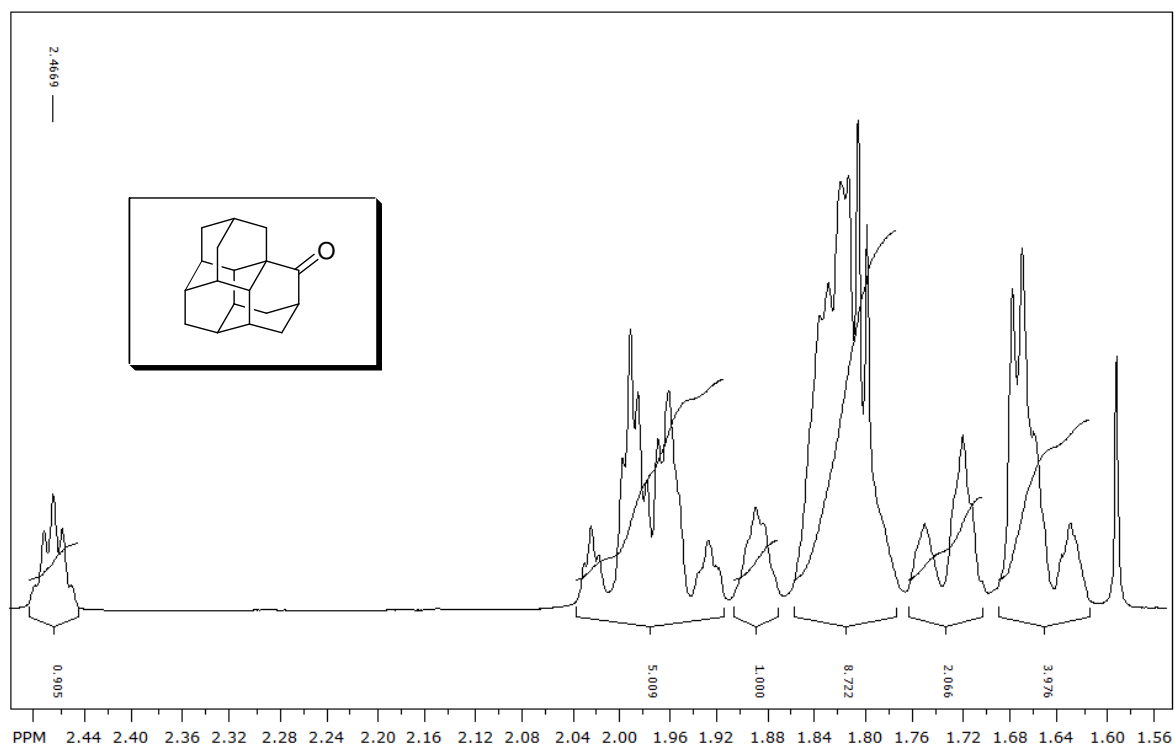
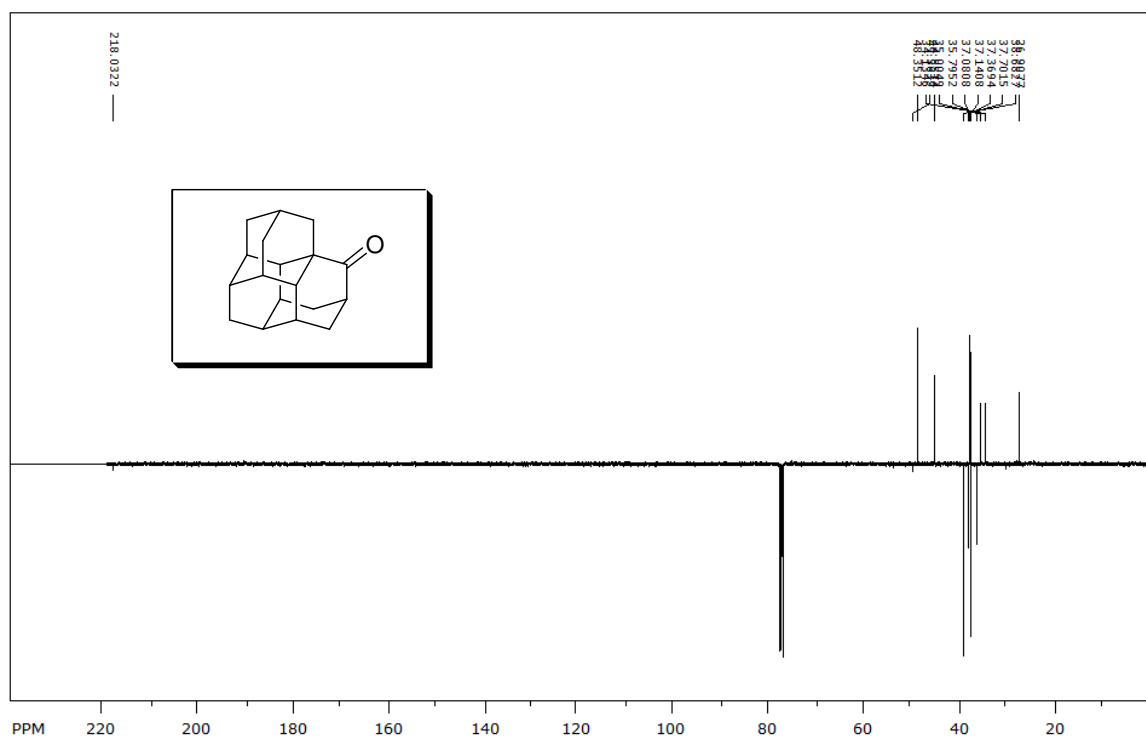
ppm; m/z : 348 (36), 346 (37), 268 (21), 267 (97), 225 (14), 212 (18), 211 (100), 135 (19), 129 (13), 119 (16), 117 (11), 105 (15), 93 (17), 91 (39), 81 (12), 79 (23), 77 (12), 67 (13), 55 (10), 41 (12); HR-MS: found 346.129 (calculated for $C_{20}H_{27}Br$ 346.129); Anal: calcd for $C_{20}H_{27}Br$ (347.33): C, 69.16; H, 7.84; found: C, 69.14; H, 7.91.

5.4.24. Functionalization of *anti*-diamantylidenediamantane (**15**) with NBS

To a solution of 0.026 g (0.07 mmol) of *anti*-diamantylidenediamantane (**15**) in 2 mL of methylene chloride in 10 mL flask, equipped with reflux condenser and stirrer, 0.12 g (0.7 mmol) of N-bromosuccinimide was added. Reaction mixture was stirred at reflux for 24 h and control by GC/MS proved presence of intractable mixture of bromides together with *anti*- and *syn*-diamantylidenediamantanes (**15**, **16**) as mixture = 2 : 3. Quench and separation of individual compounds was not performed.

APPENDIX

Appendix I. Spectral data of selected synthesized compounds

Figure A1. ^1H NMR spectrum of triamantanone-16 (**119**).Figure A2. APT spectrum of triamantanone-16 (**119**).

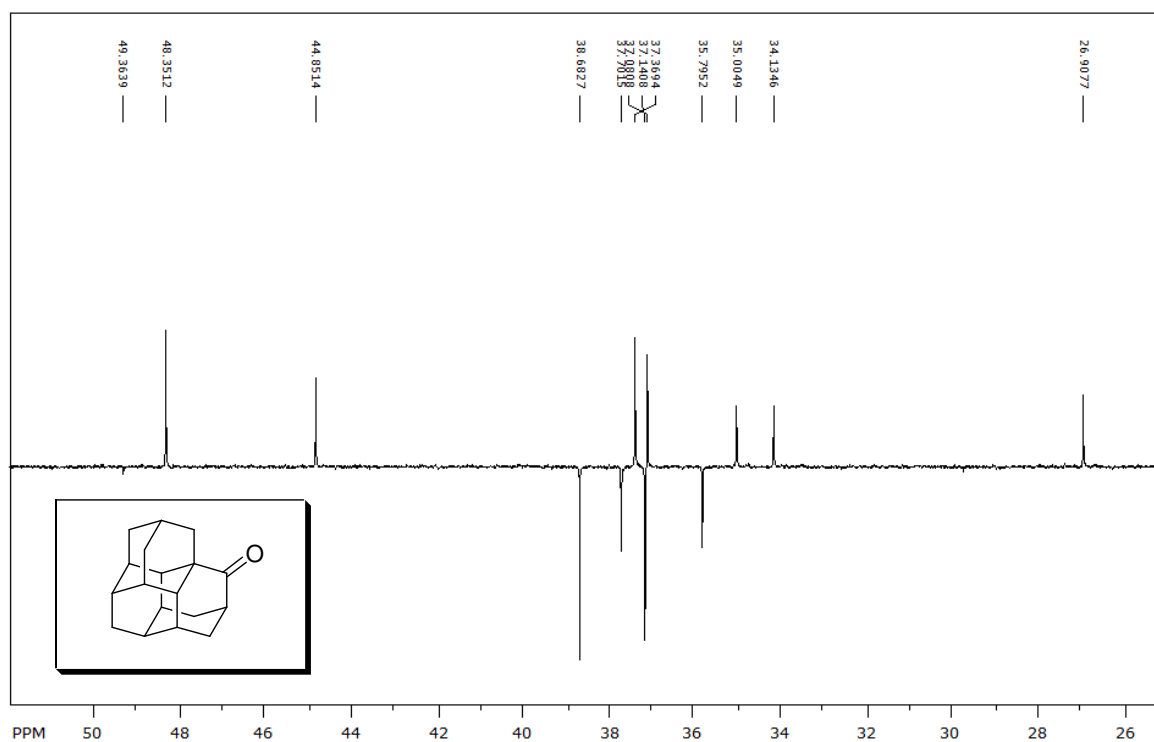


Figure A3. APT spectrum (part) of triamantanone-16 (**119**).

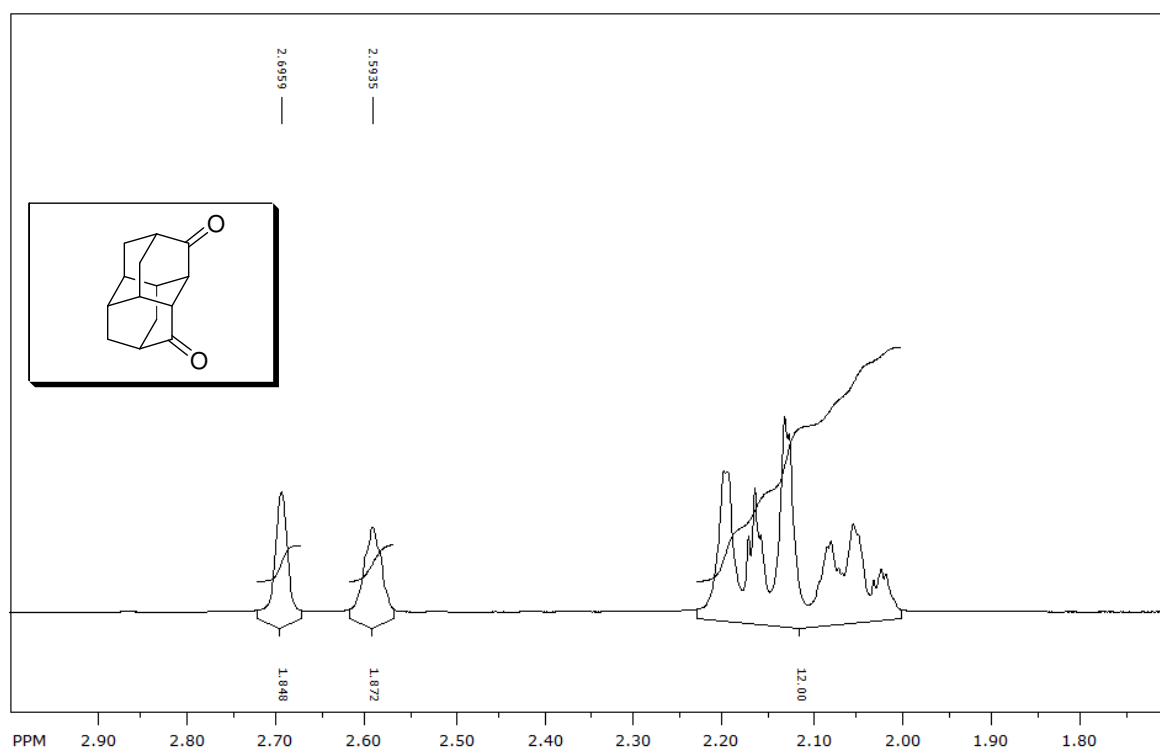


Figure A4. ^1H NMR spectrum of diamantanedione-3,8 (**121**).

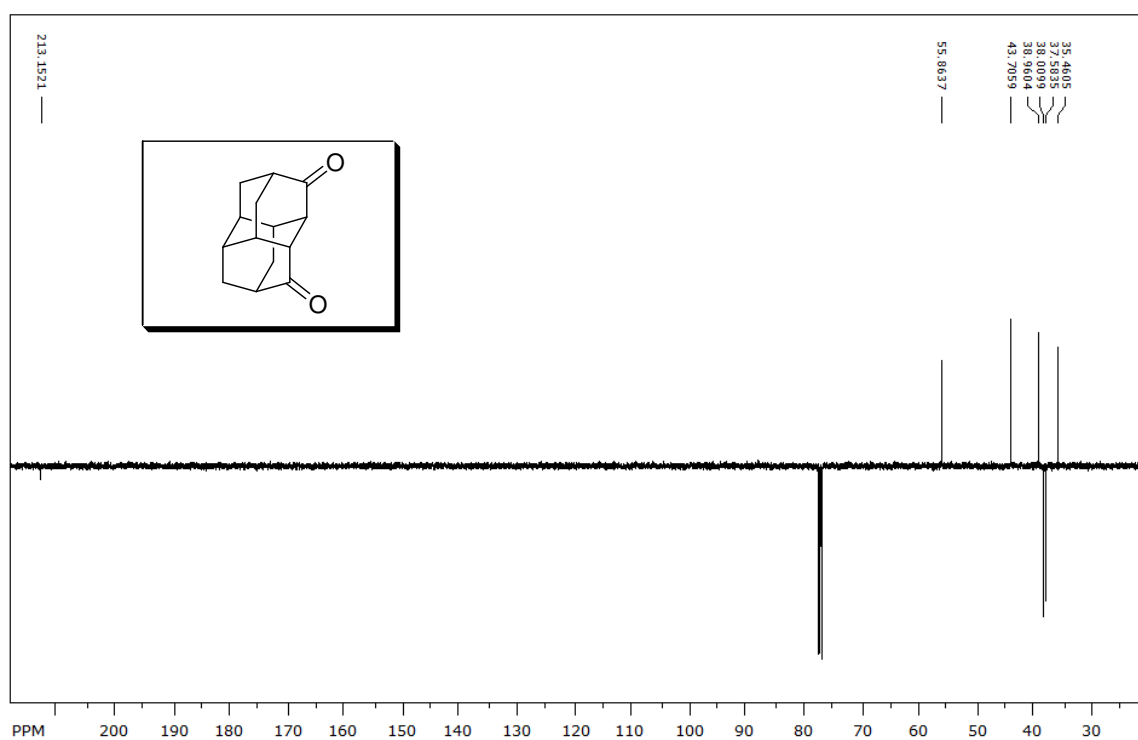


Figure A5. APT spectrum of diamantanedione-3,8 (**121**).

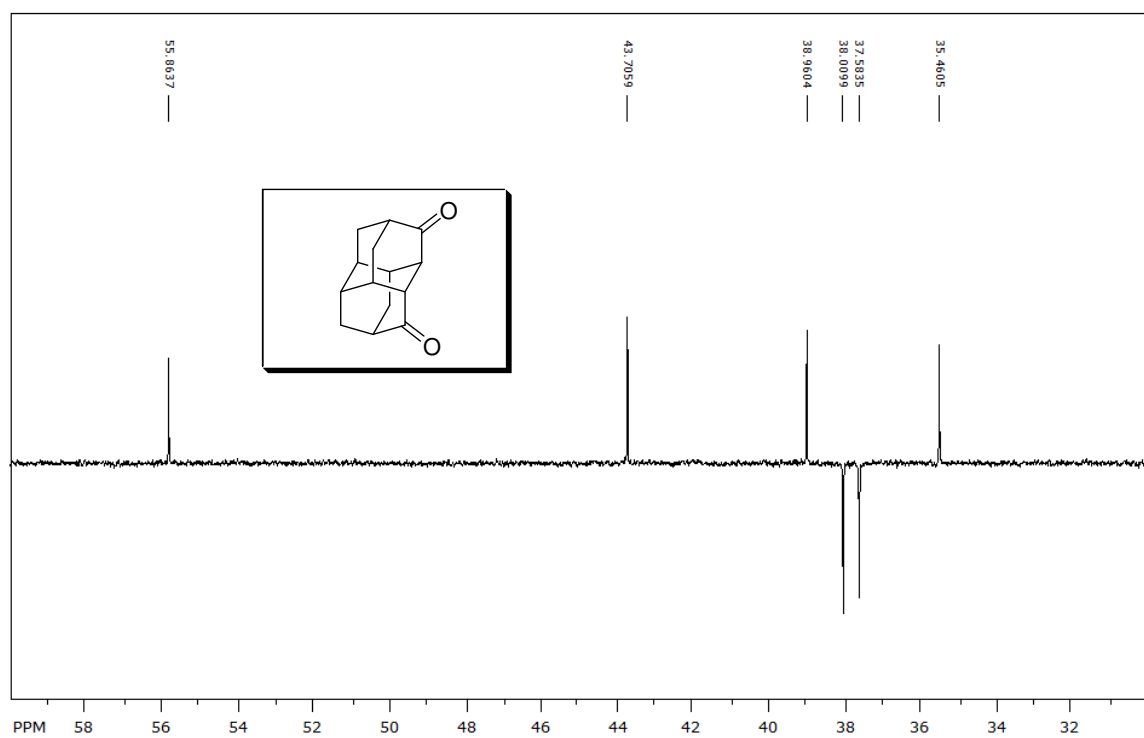


Figure A6. APT spectrum (part) of diamantanedione-3,8 (**121**).

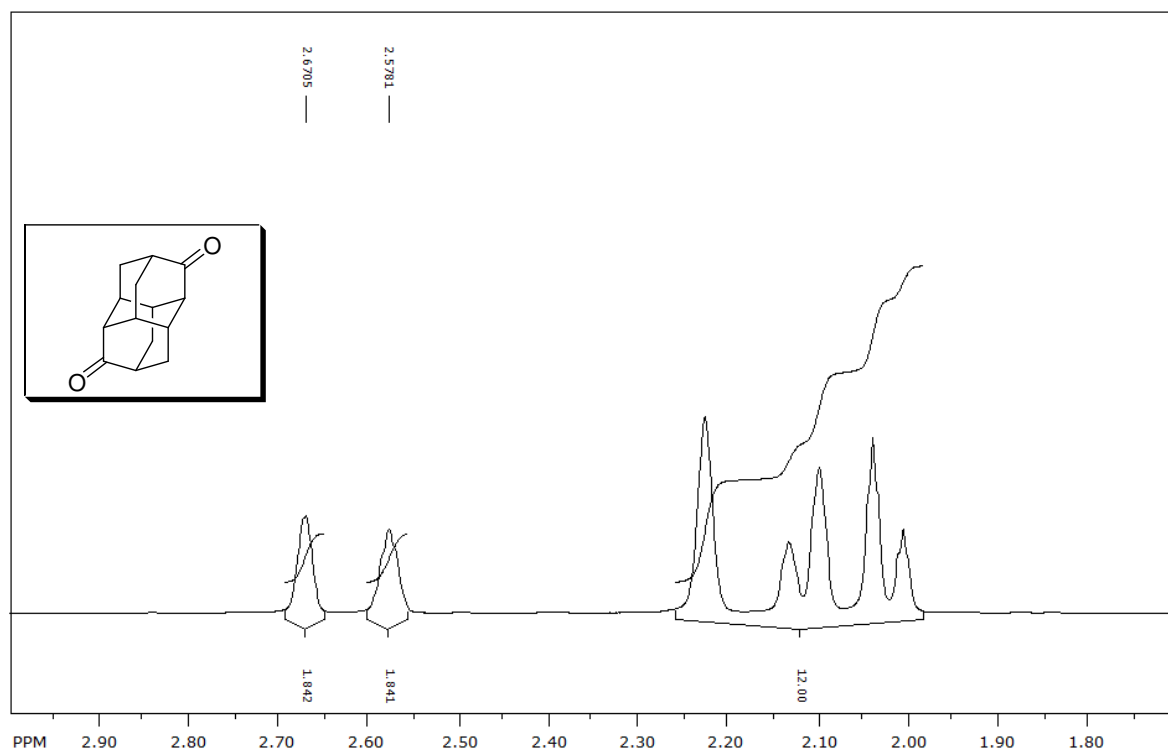


Figure A7. ^1H NMR spectrum of adamantanedione-3,10 (**120**).

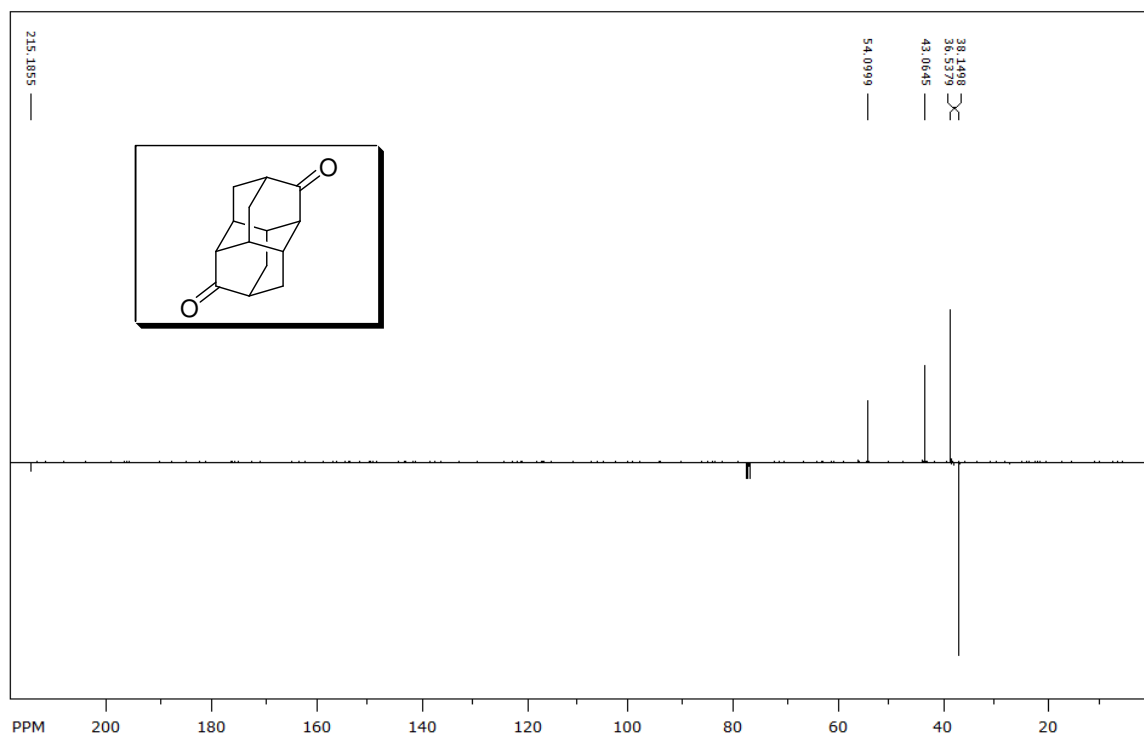


Figure A8. APT spectrum of adamantanedione-3,10 (**120**).

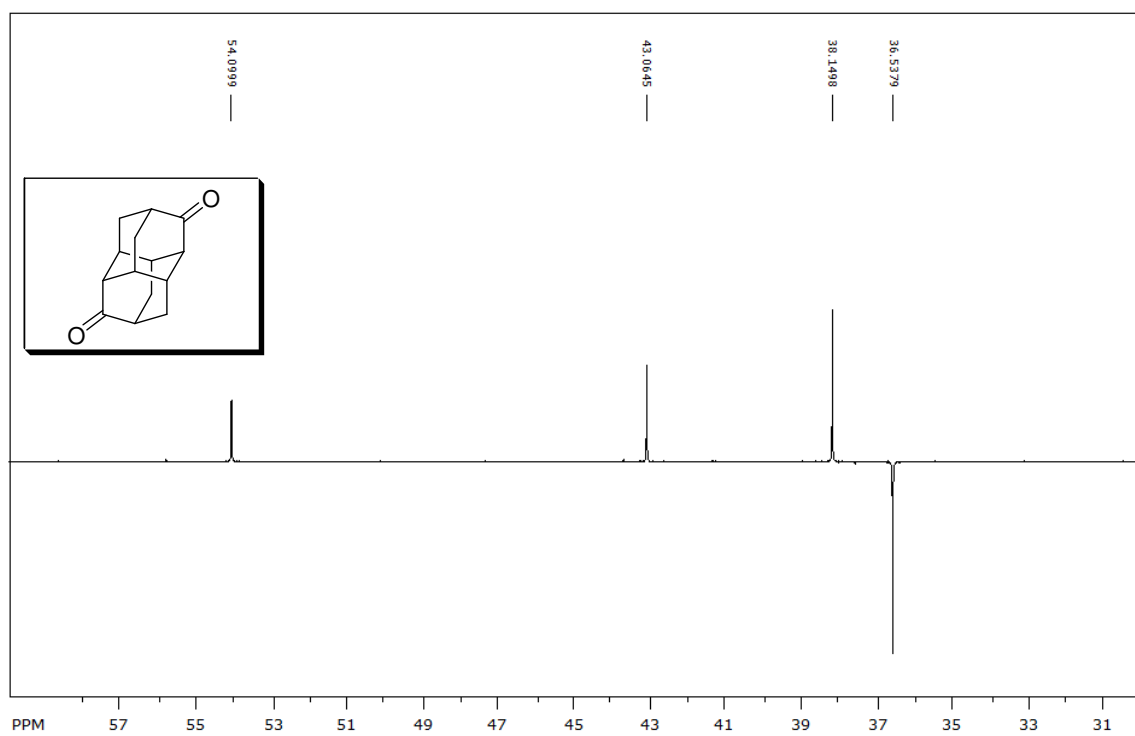


Figure A9. APT spectrum (part) of diamantanedione-3,10 (**120**).

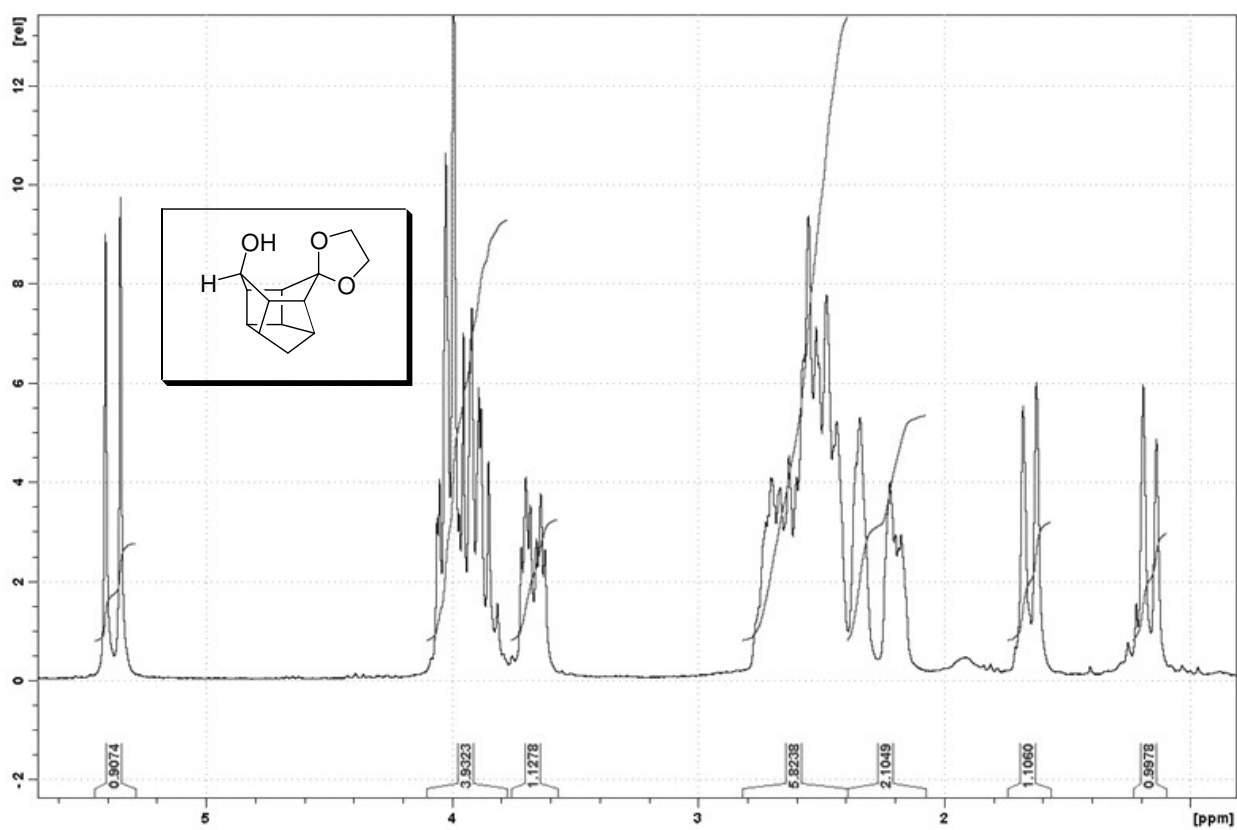


Figure A10. ¹H NMR spectrum of *endo*-11-hydroxypentacyclo[5.4.0.0^{2,6}.0^{3,10}.0^{5,9}]undecane-8-one ethylene ketal (**130a**).

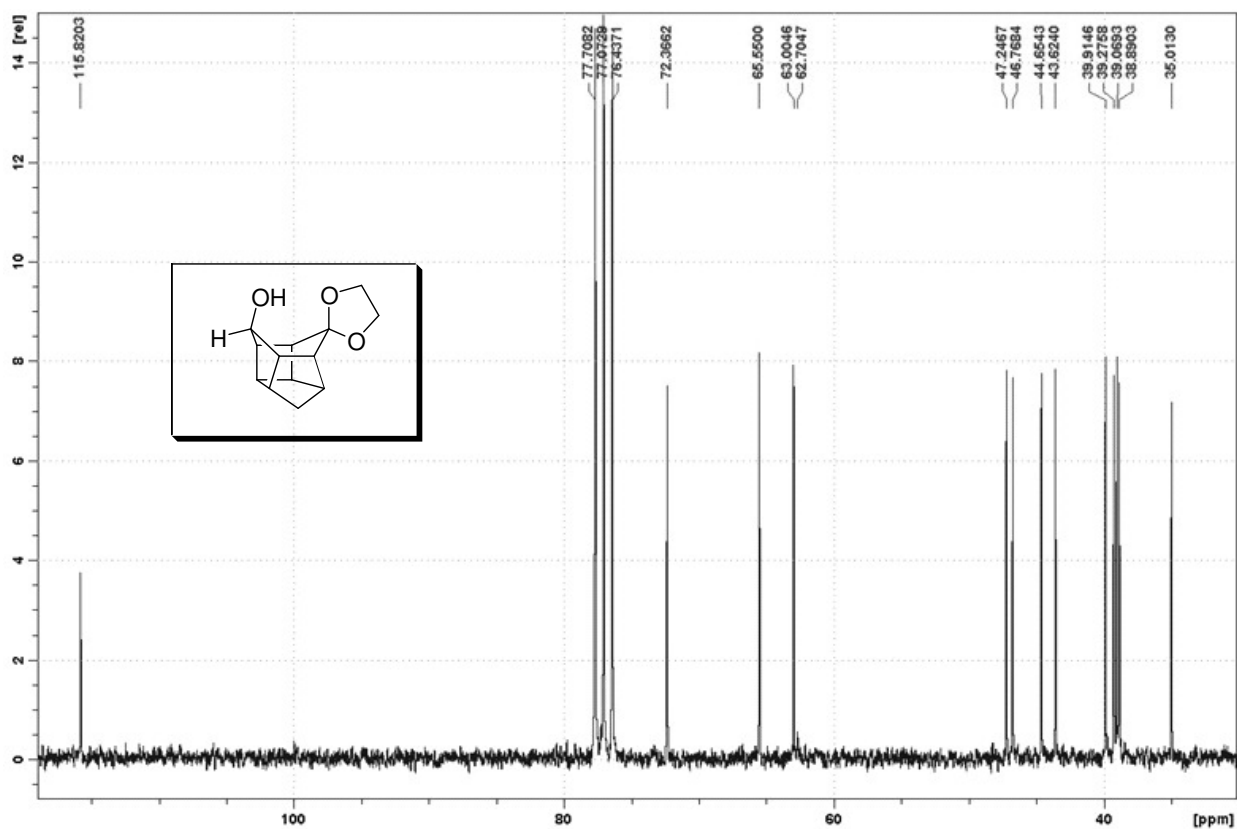
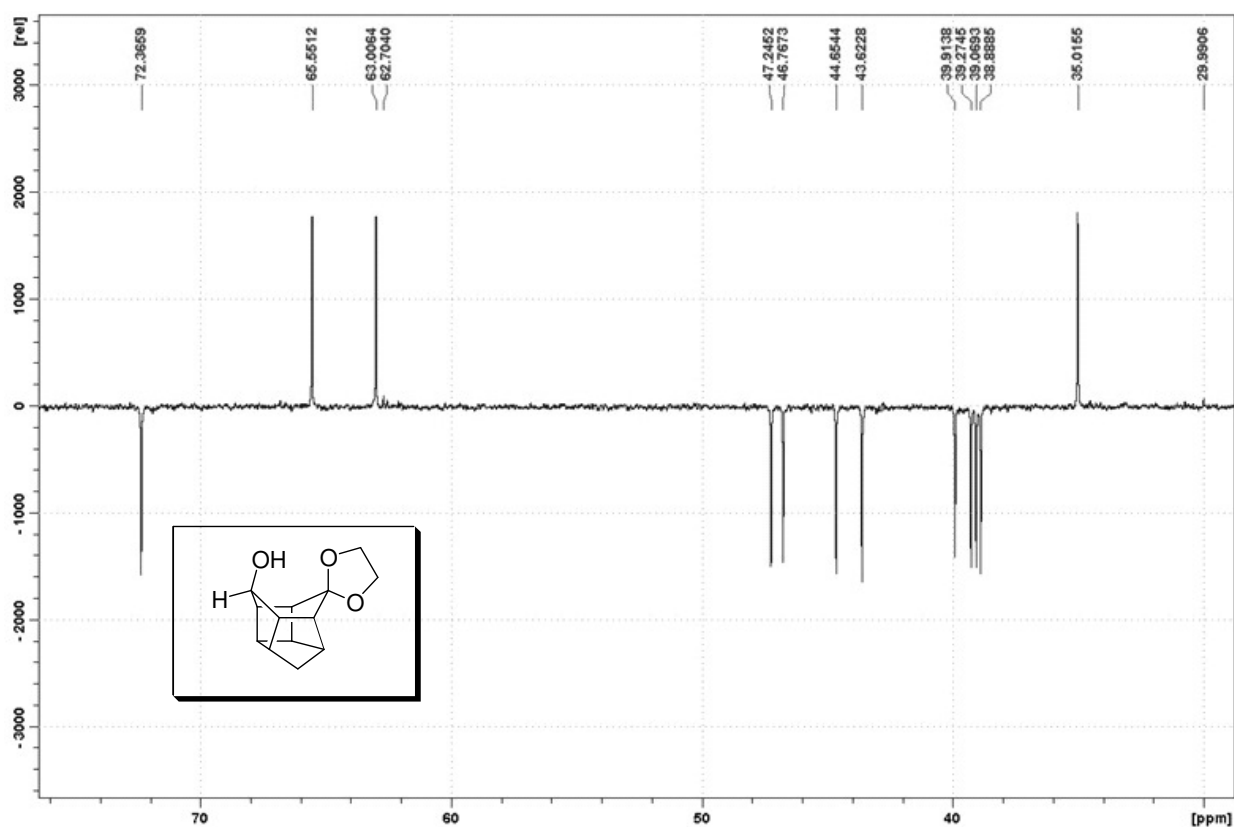


Figure A11. ¹³C NMR spectrum of *endo*-11-hydroxypentacyclo[5.4.0.0^{2,6}.0^{3,10}.0^{5,9}]undecane-8-one ethylene ketal (**130a**).



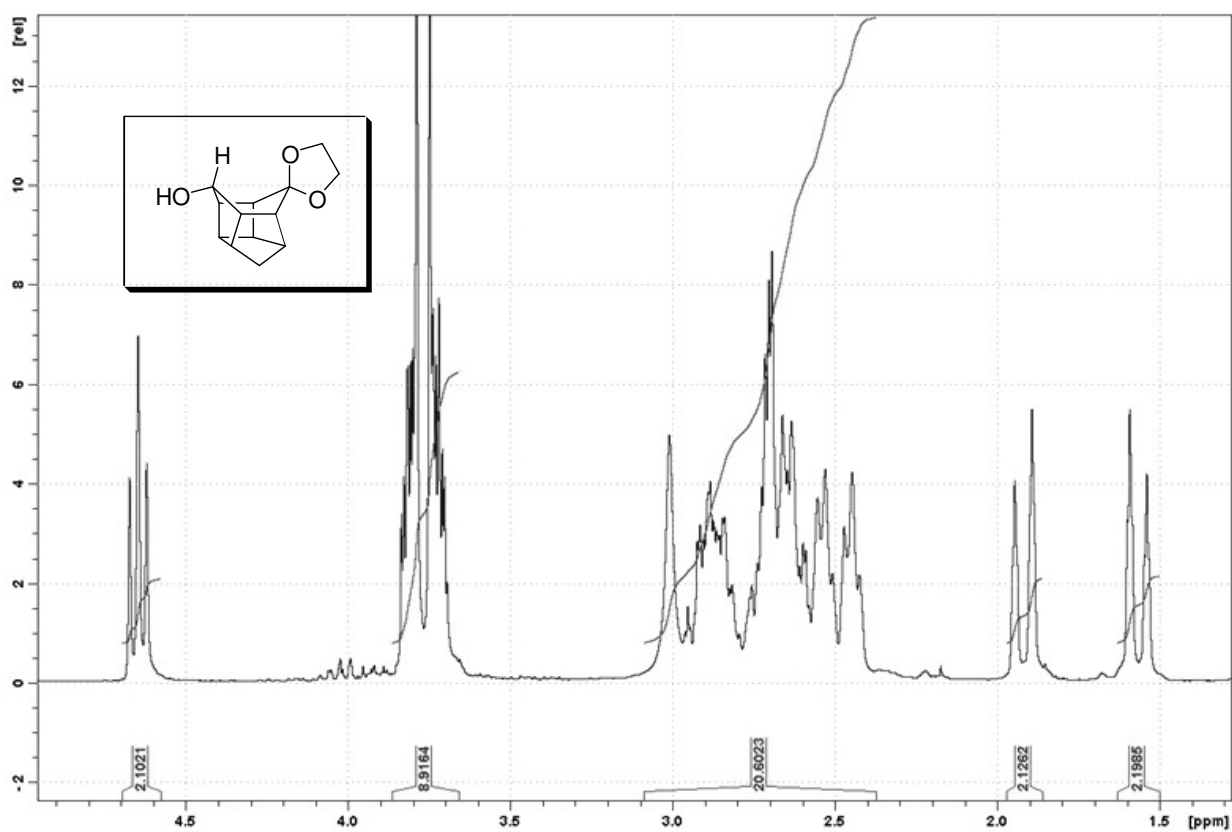


Figure A13. ^1H NMR spectrum of *exo*-11-hydroxypentacyclo[5.4.0.0^{2,6}.0^{3,10}.0^{5,9}]undecane-8-one ethylene ketal (**130b**).

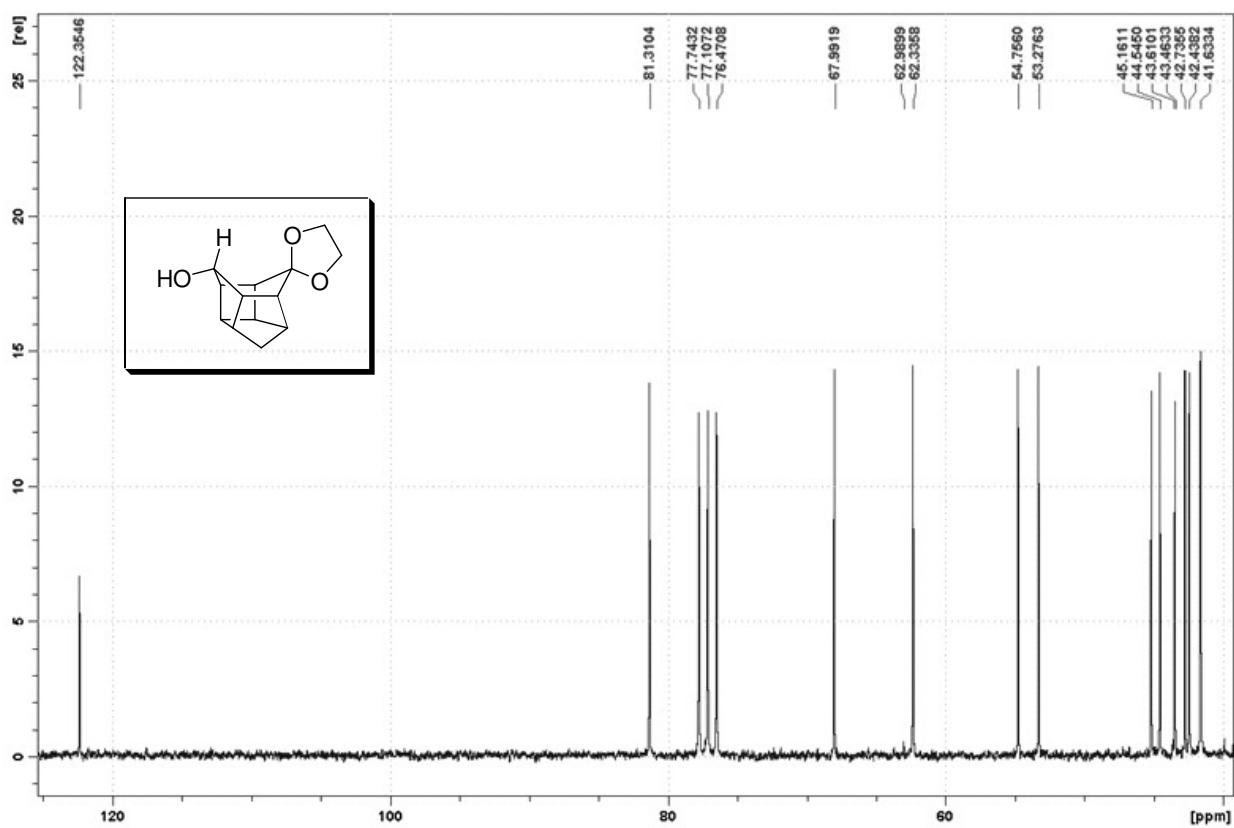


Figure A14. ^{13}C NMR spectrum of *exo*-11-hydroxypentacyclo[5.4.0.0^{2,6}.0^{3,10}.0^{5,9}]undecane-8-one ethylene ketal (**130b**).

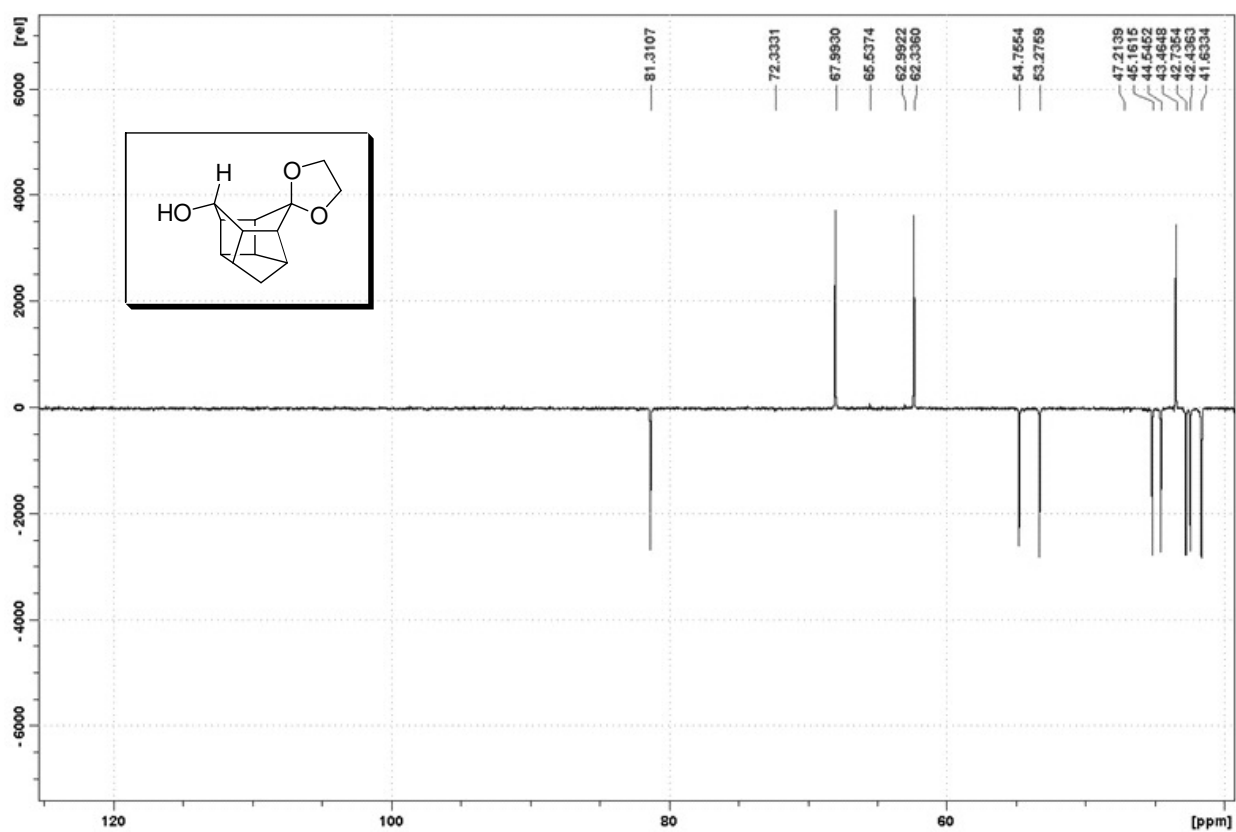


Figure A15. DEPT spectrum of *exo*-11-hydroxypentacyclo[5.4.0.0.0^{2,6}.0^{3,10}.0^{5,9}]undecane-8-one ethylene ketal (**130b**).

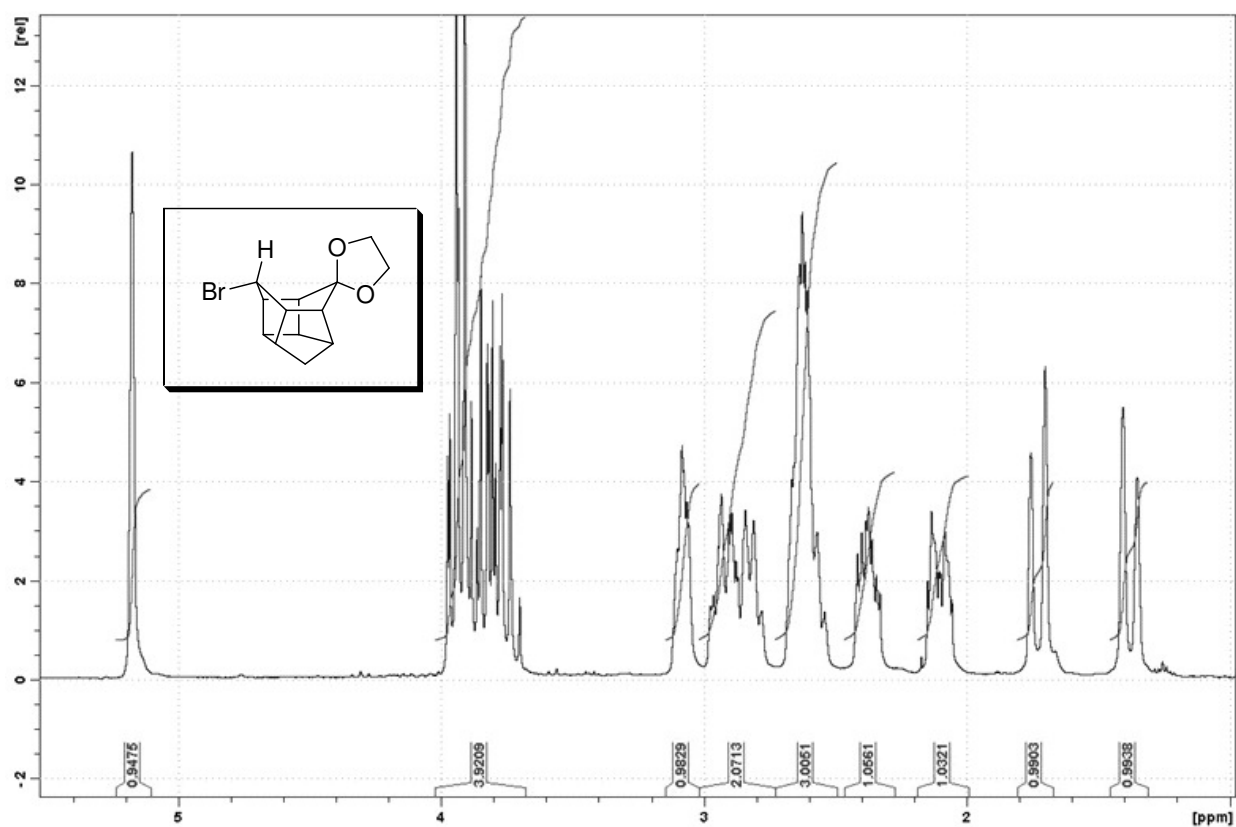


Figure A16. ^1H NMR spectrum of *exo*-11-bromopentacyclo[5.4.0.0^{2,6}.0^{3,10}.0^{5,9}]undecane-8-one ethylene ketal (132).

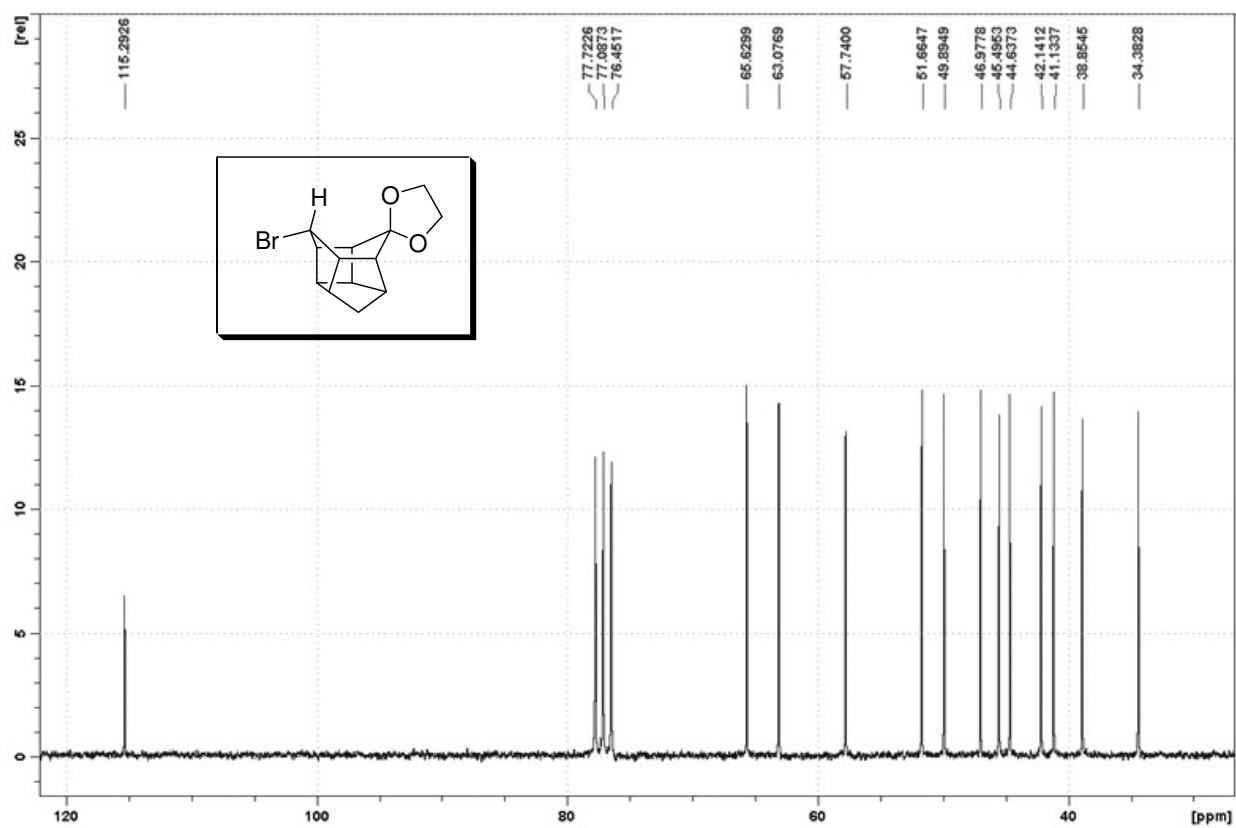


Figure A17. ^{13}C NMR spectrum of *exo*-11-bromopentacyclo[5.4.0.0^{2,6}.0^{3,10}.0^{5,9}]undecane-8-one ethylene ketal (132).

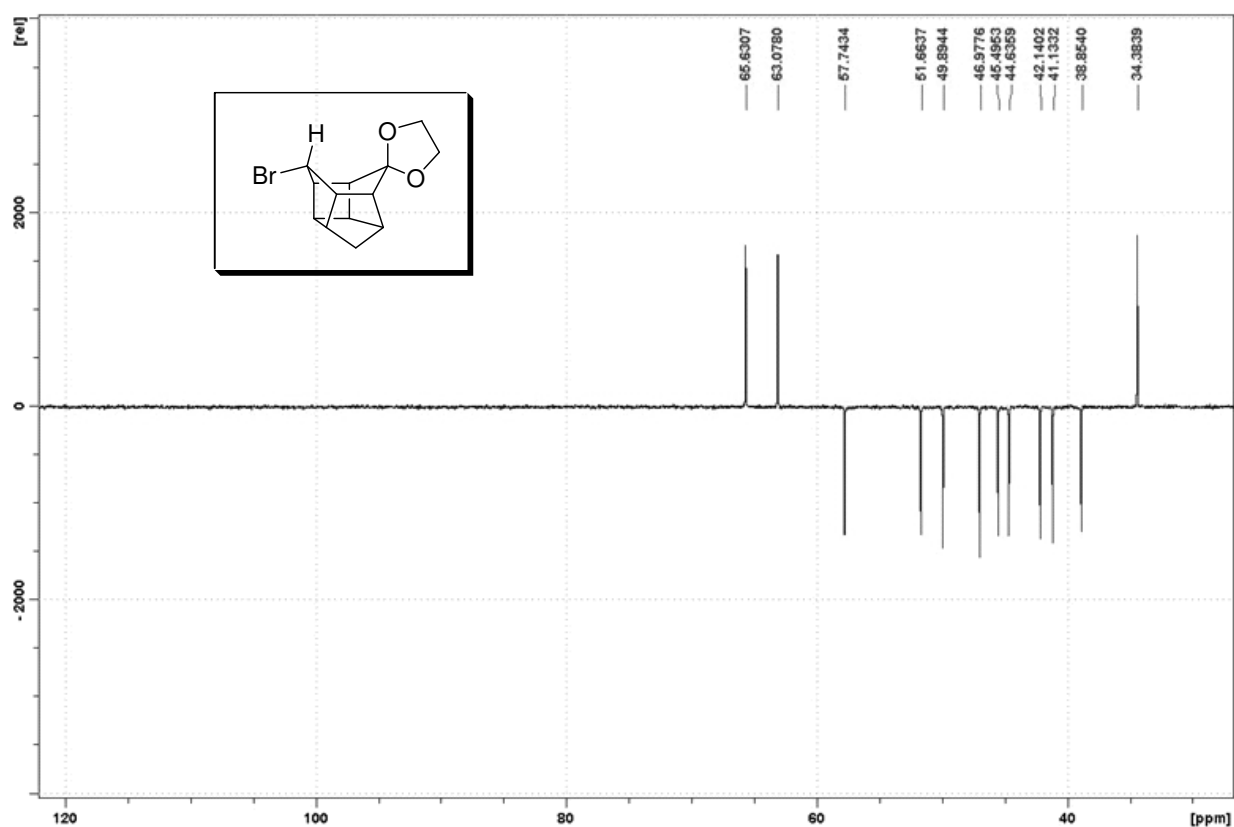


Figure A18. DEPT spectrum of *exo*-11-bromopentacyclo[5.4.0.0.0^{2,6}.0^{3,10}.0^{5,9}]undecane-8-one ethylene ketal (**132**).

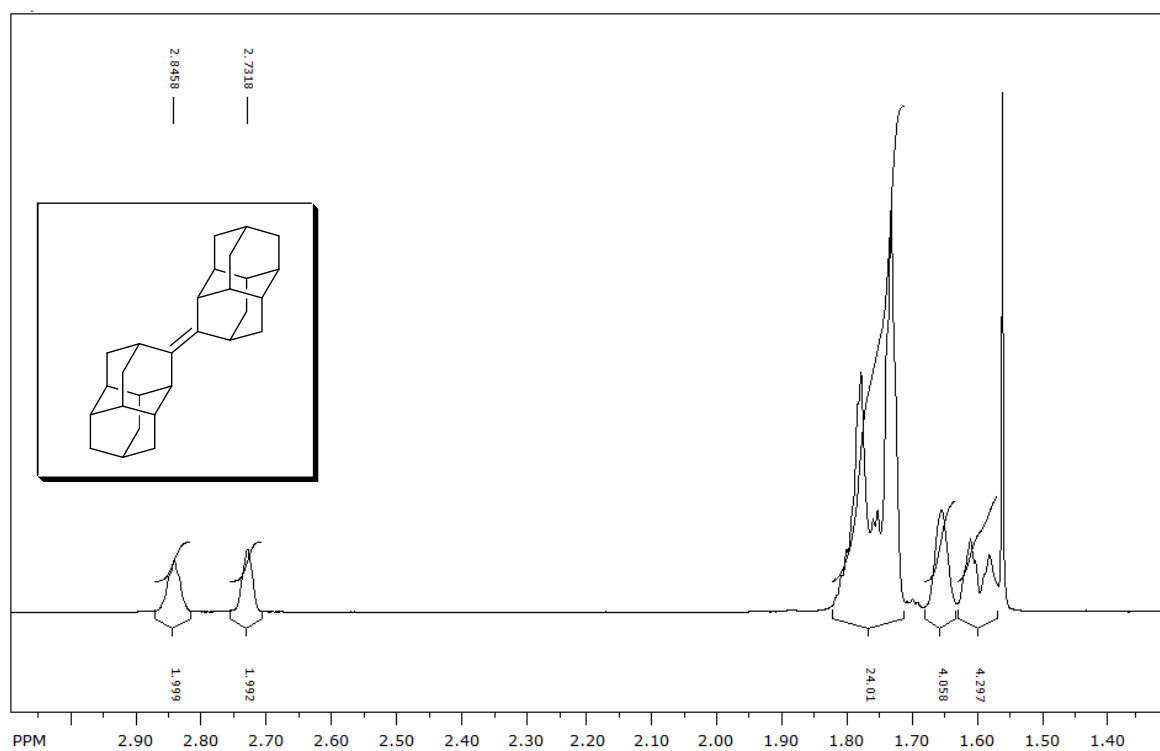


Figure A19. ¹H NMR spectrum of *anti*-diamantylidenediamantane (**15**).

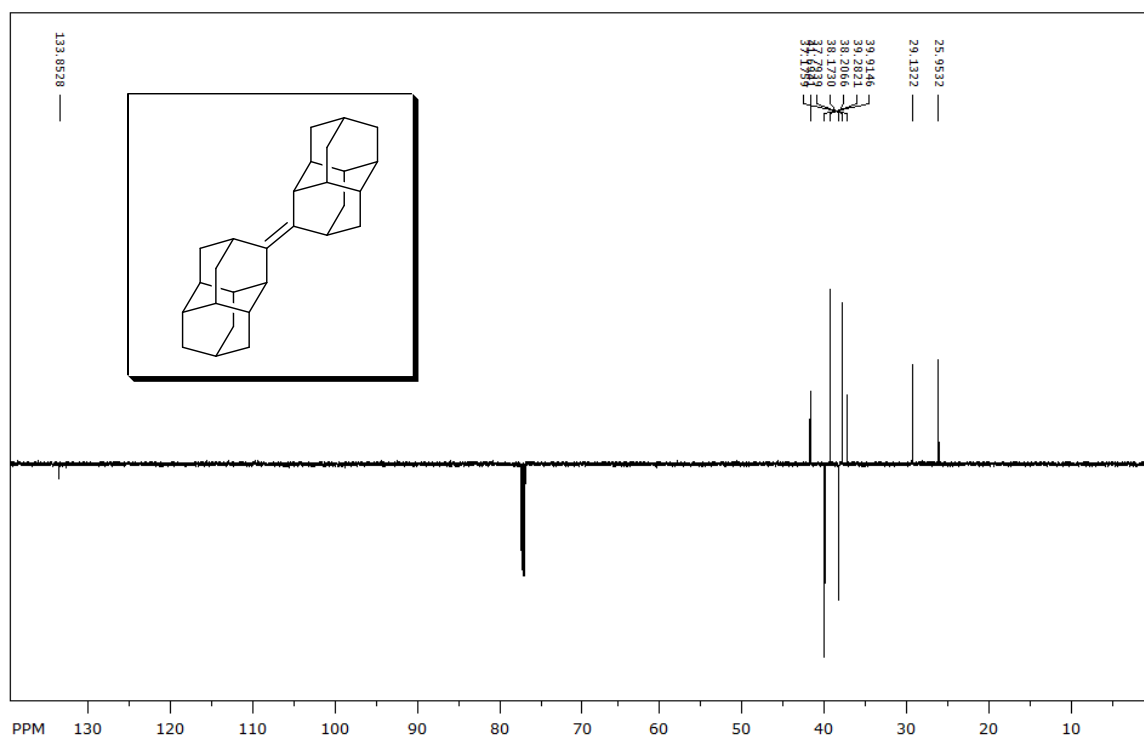


Figure A20. APT spectrum of *anti*-diamantylidenediamantane (**15**).

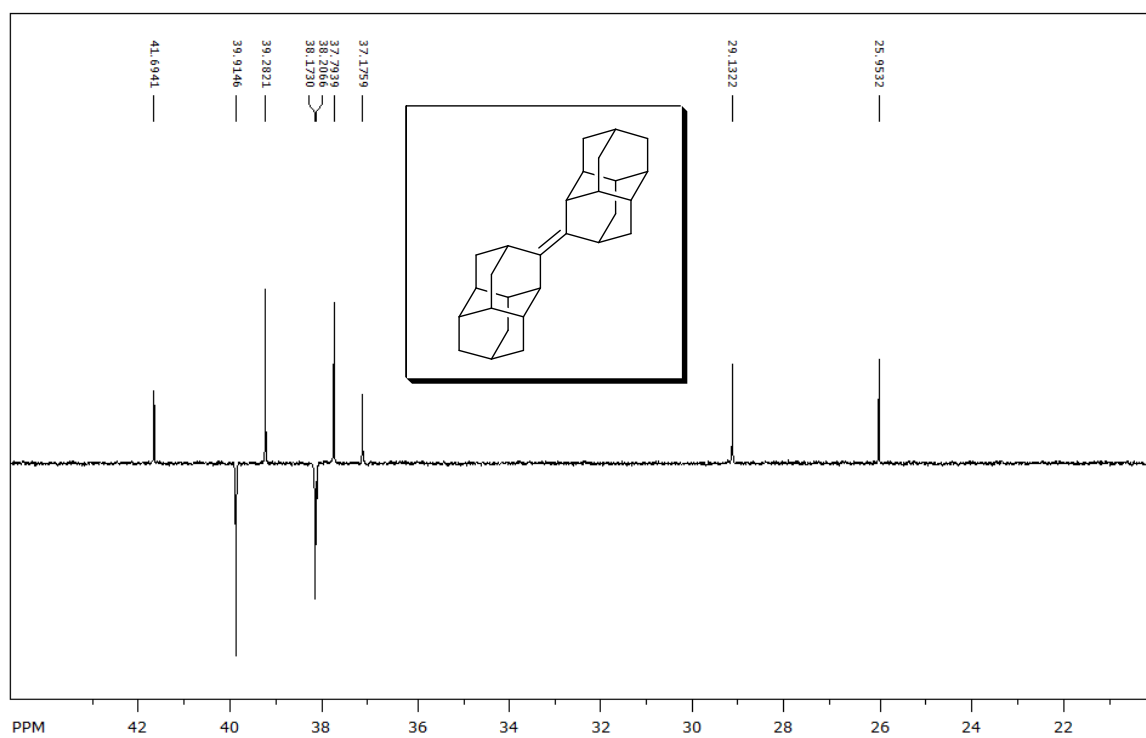


Figure A21. APT spectrum (part) of *anti*-diamantylidenediamantane (**15**).

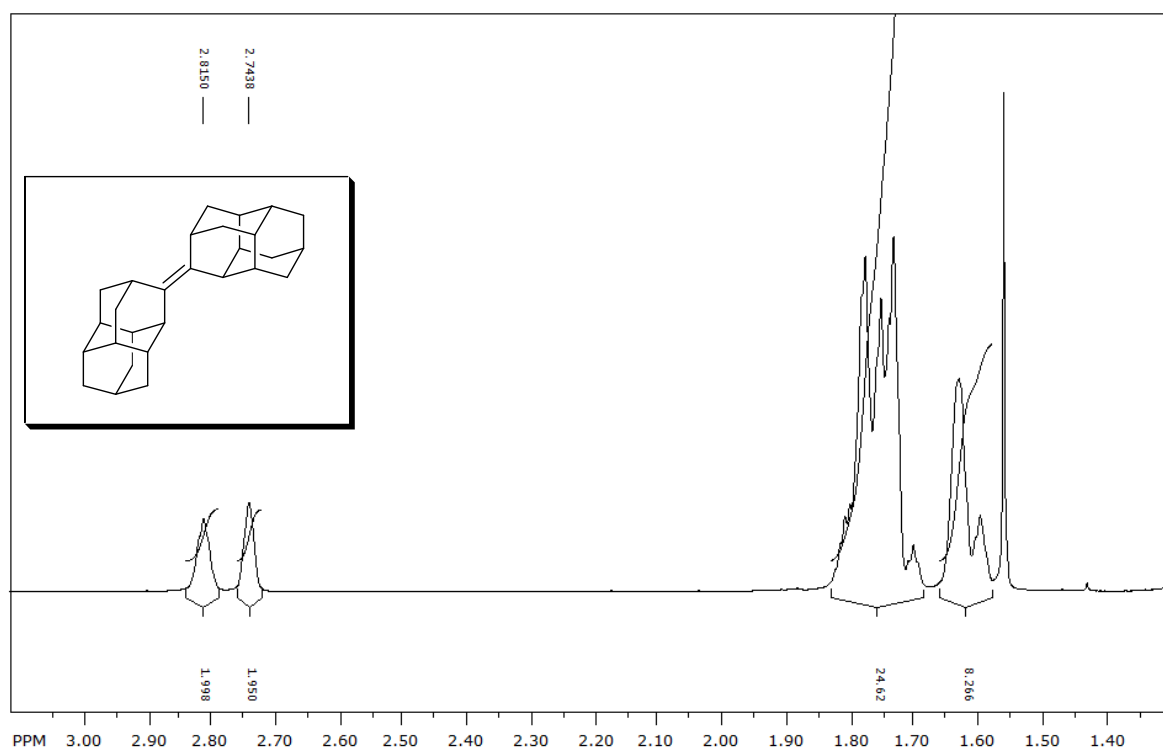


Figure A22. ¹H NMR spectrum of *syn*-diamantylidenediamantane (**16**).

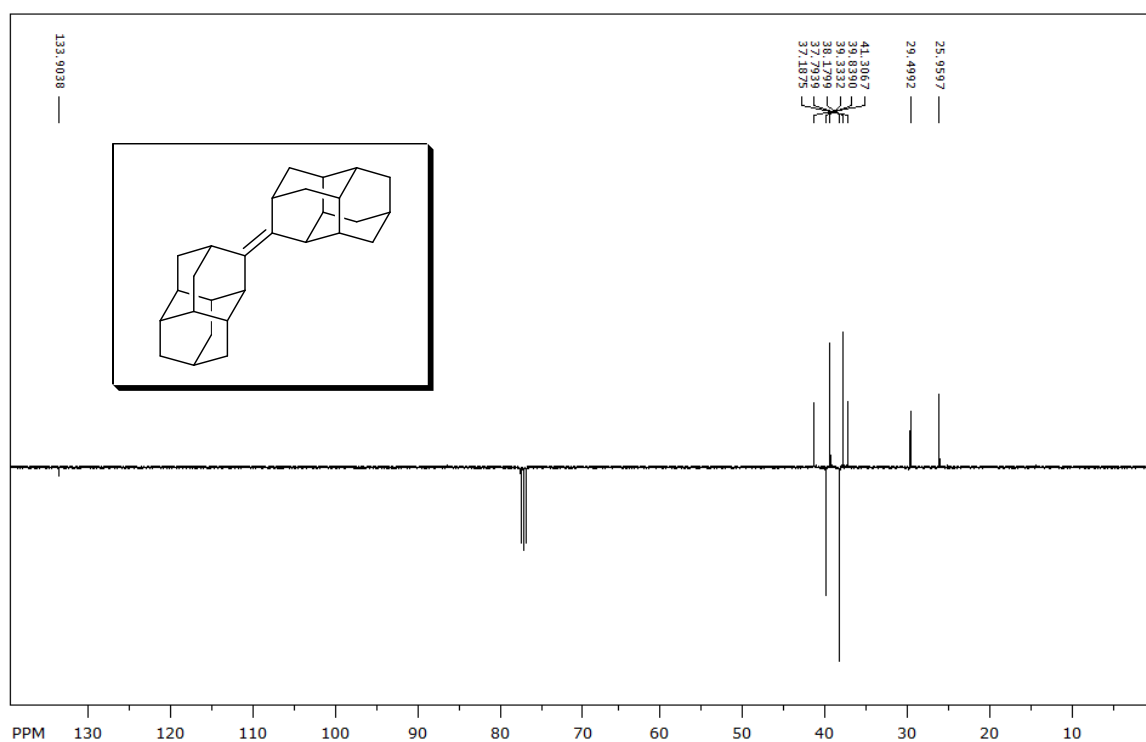


Figure A23. APT spectrum of *syn*-diamantylidenediamantane (**16**).

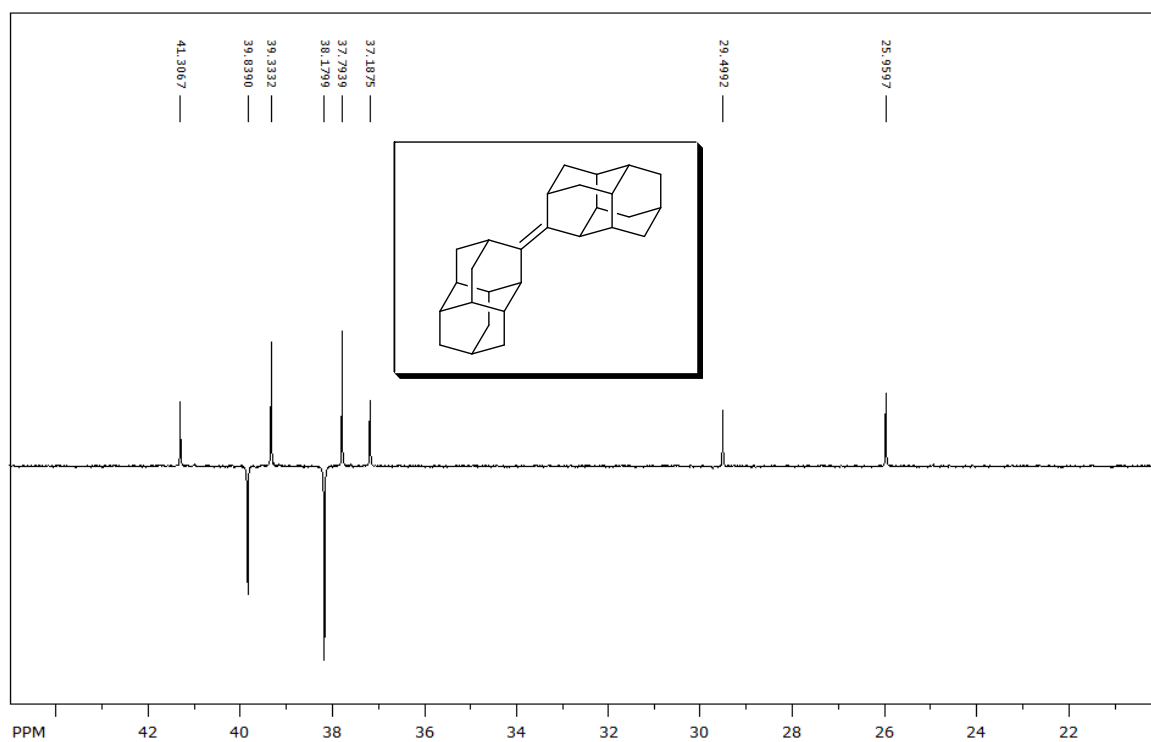


Figure A24. APT spectrum of *syn*-diamantylidenediamantane (**16**).

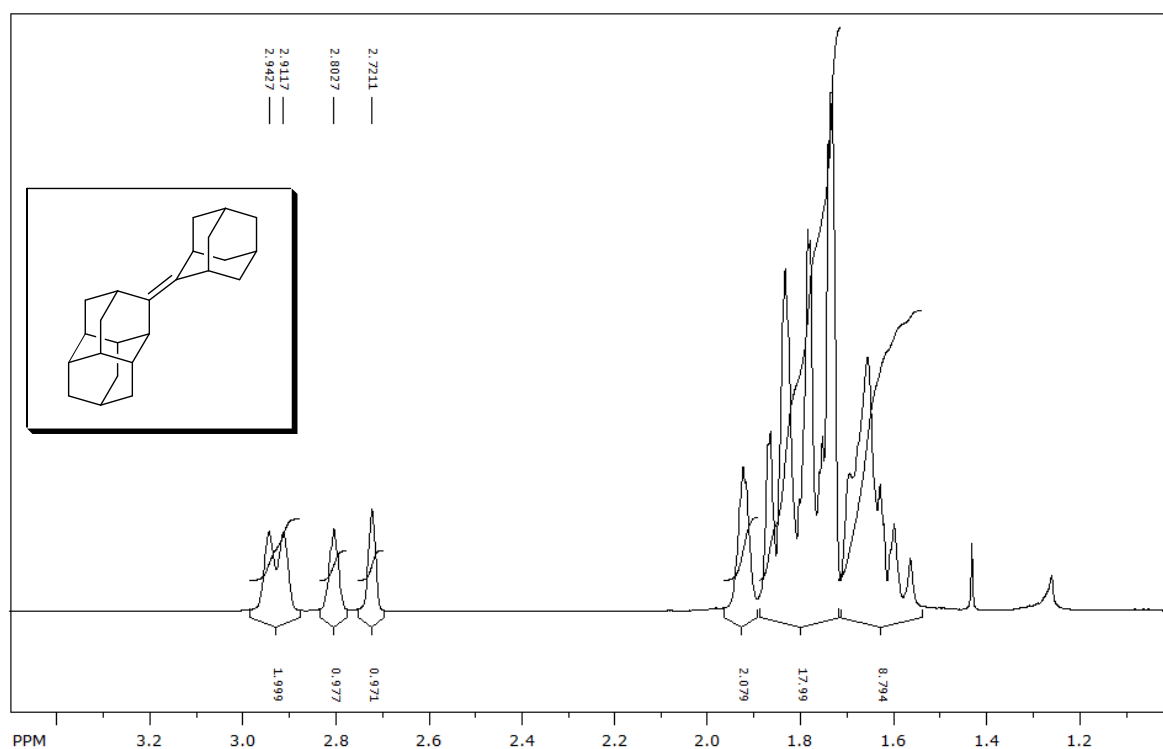


Figure A25. ¹H NMR spectrum of adamantylidenediamantane-3 (**14**).

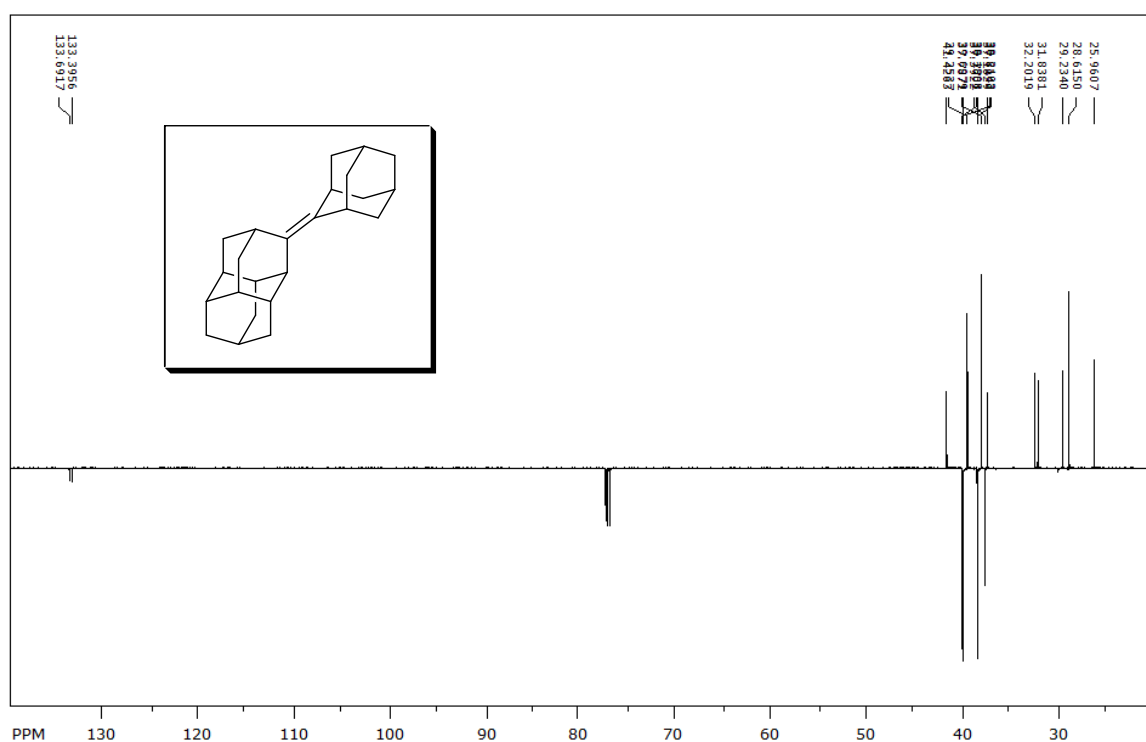


Figure A26. APT spectrum of adamantylidenediamantane-3 (**14**).

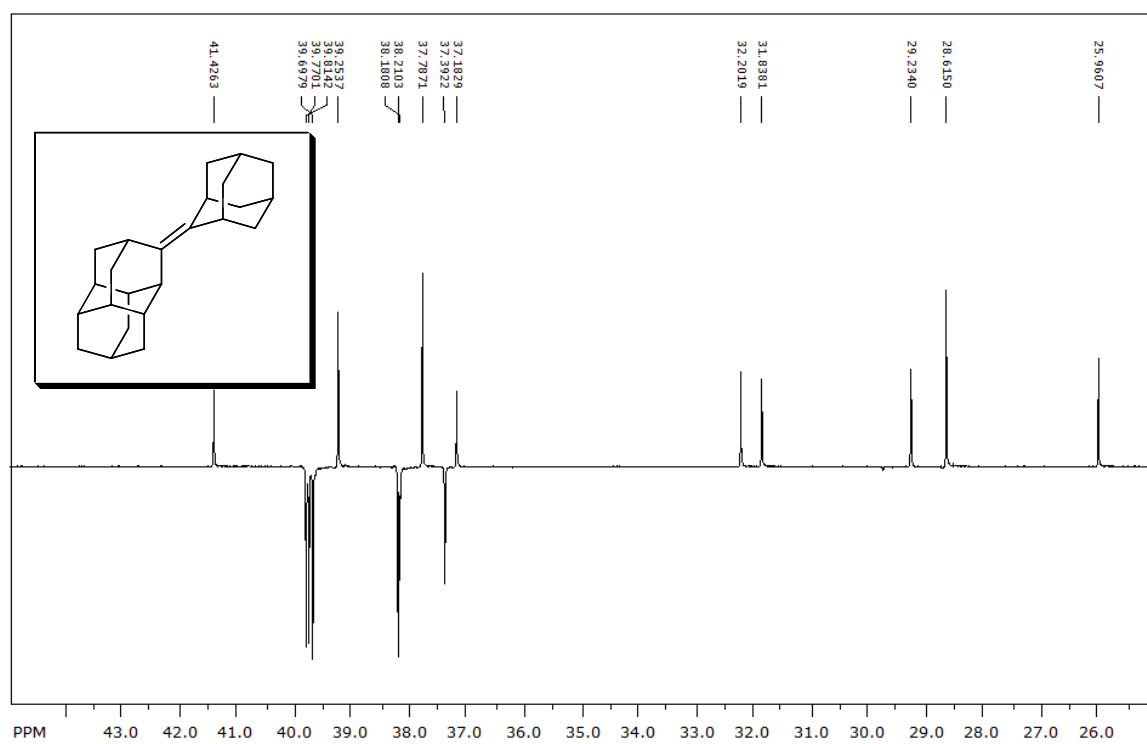


Figure A27. APT spectrum (part) of adamantylidenediamantane-3 (**14**).

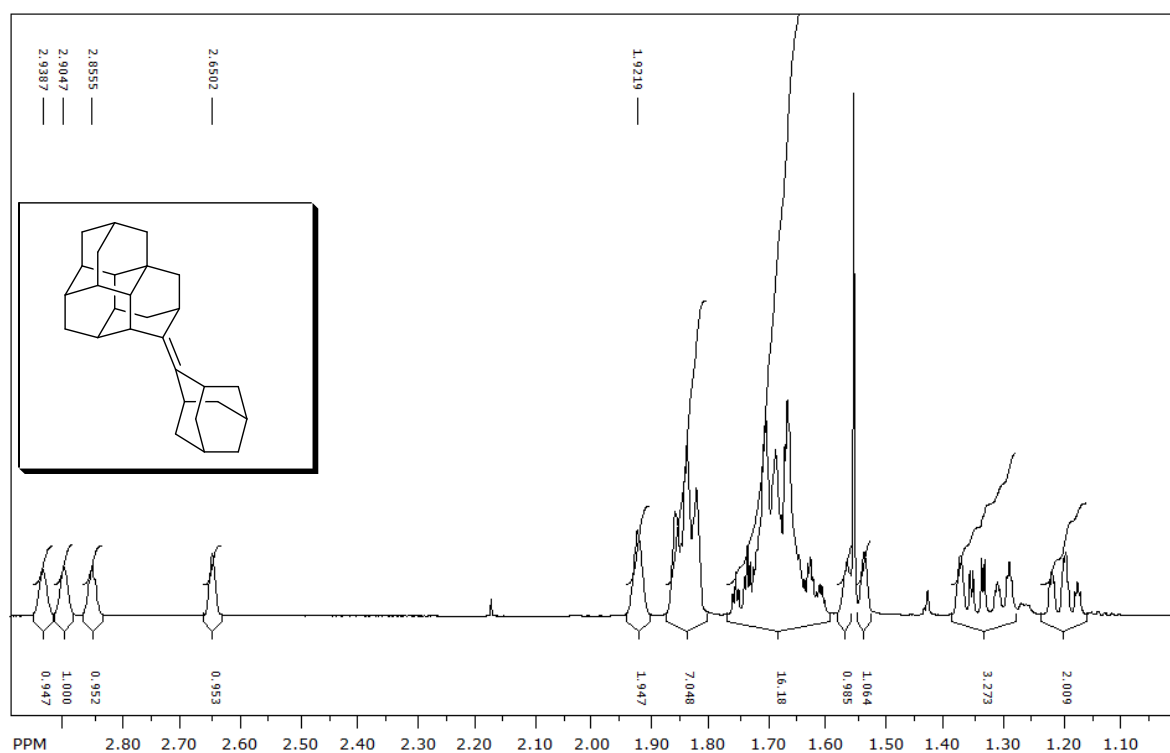
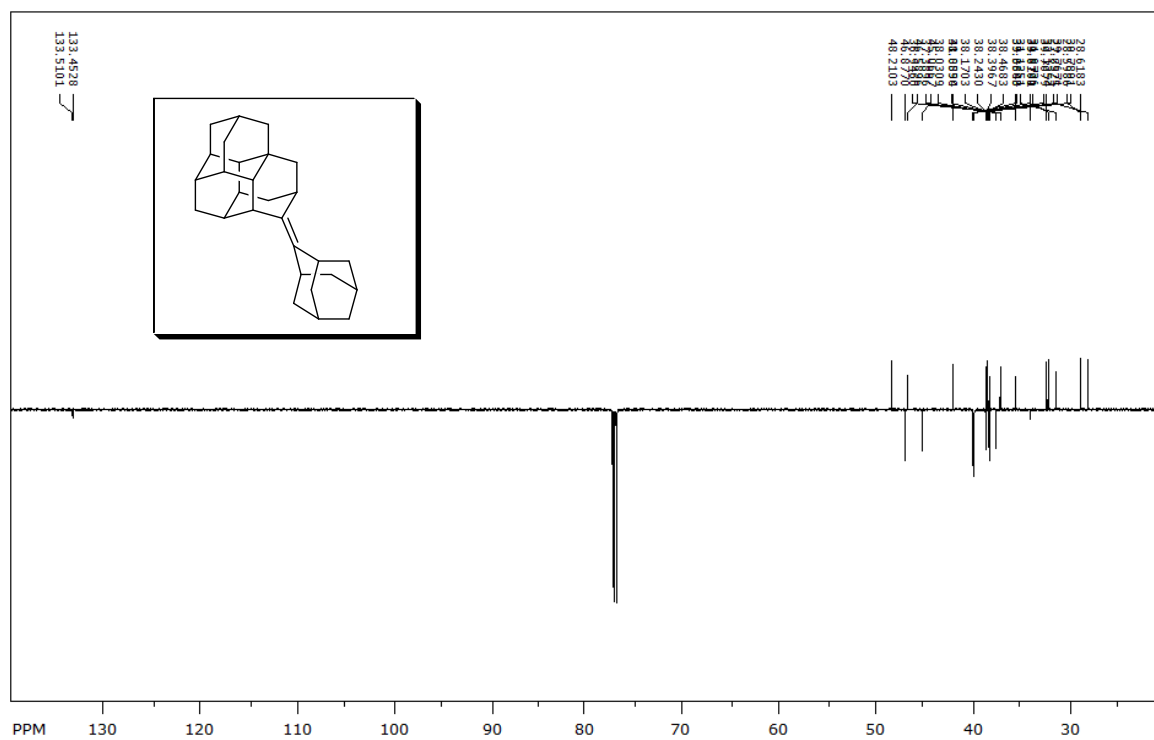


Figure A28. ¹H NMR spectrum of adamantyldenetriamantane-8 (**17**).



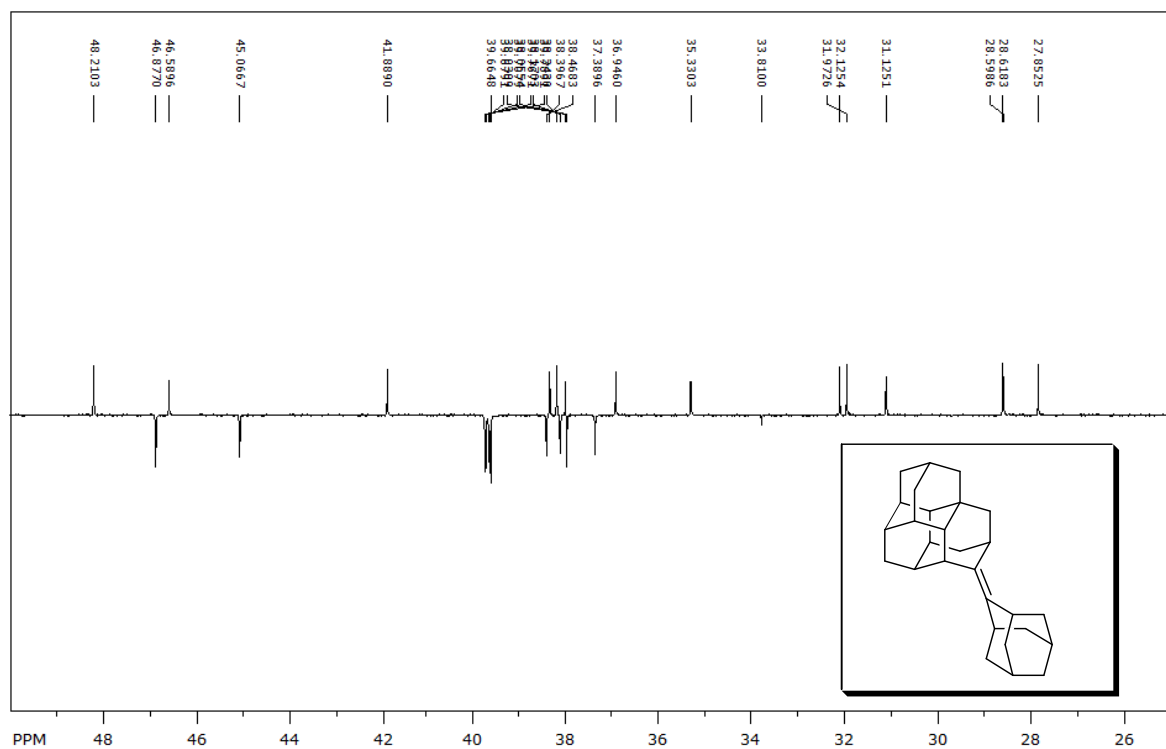


Figure A30. APT spectrum (part) of adamantylidenetriamantane-8 (**17**).

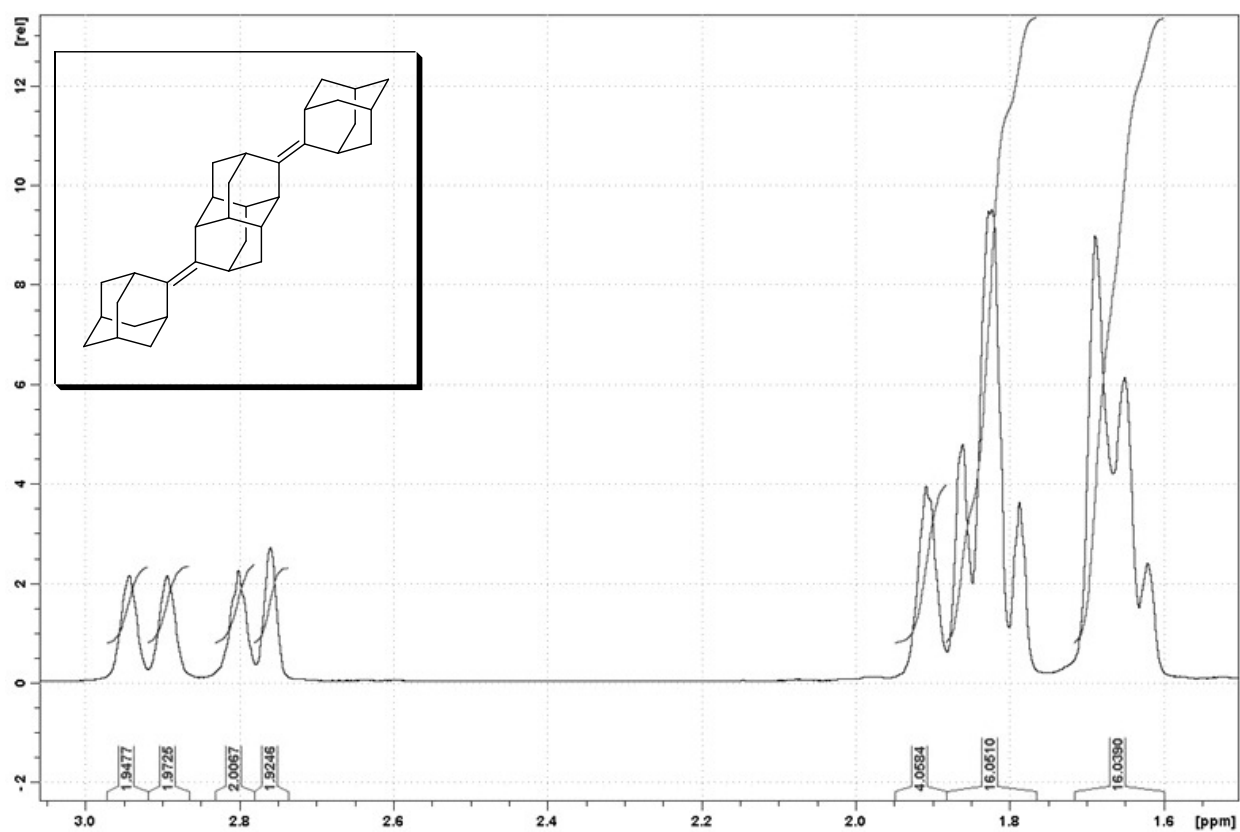


Figure A31. ¹H NMR spectrum of di(adamantylidene-2)diamantane-3,10 (**133**).

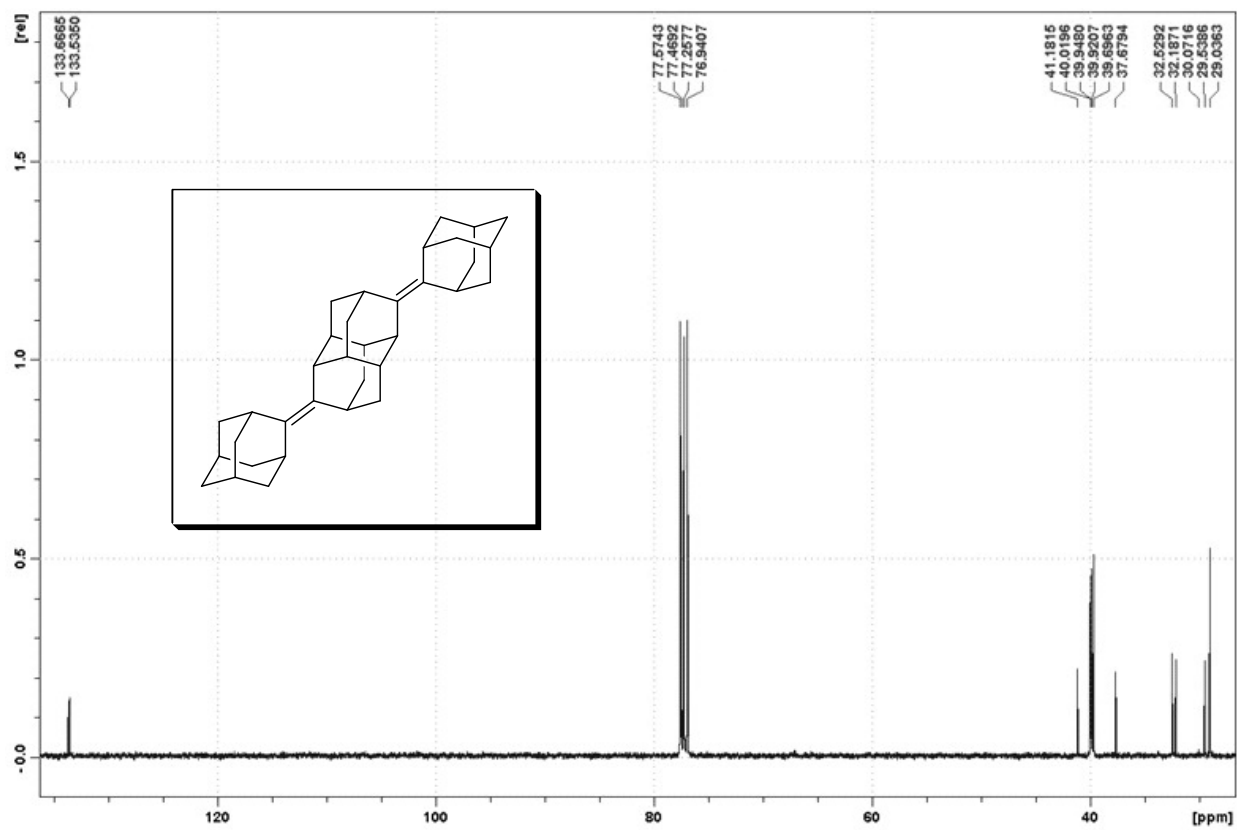


Figure A32. ¹³C NMR spectrum of di(adamantylidene-2)diamantane-3,10 (**133**).

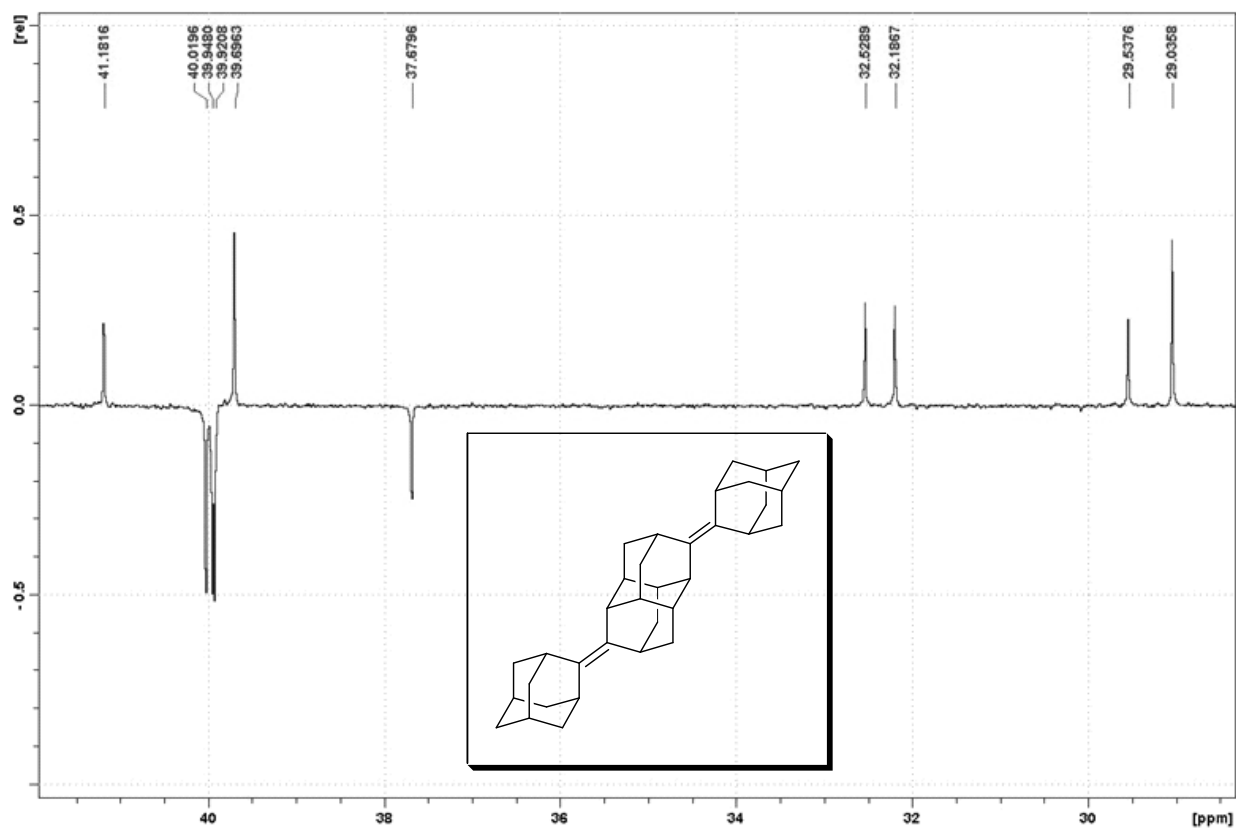


Figure A33. DEPT spectrum of di(adamantylidene-2)diamantane-3,10 (**133**).

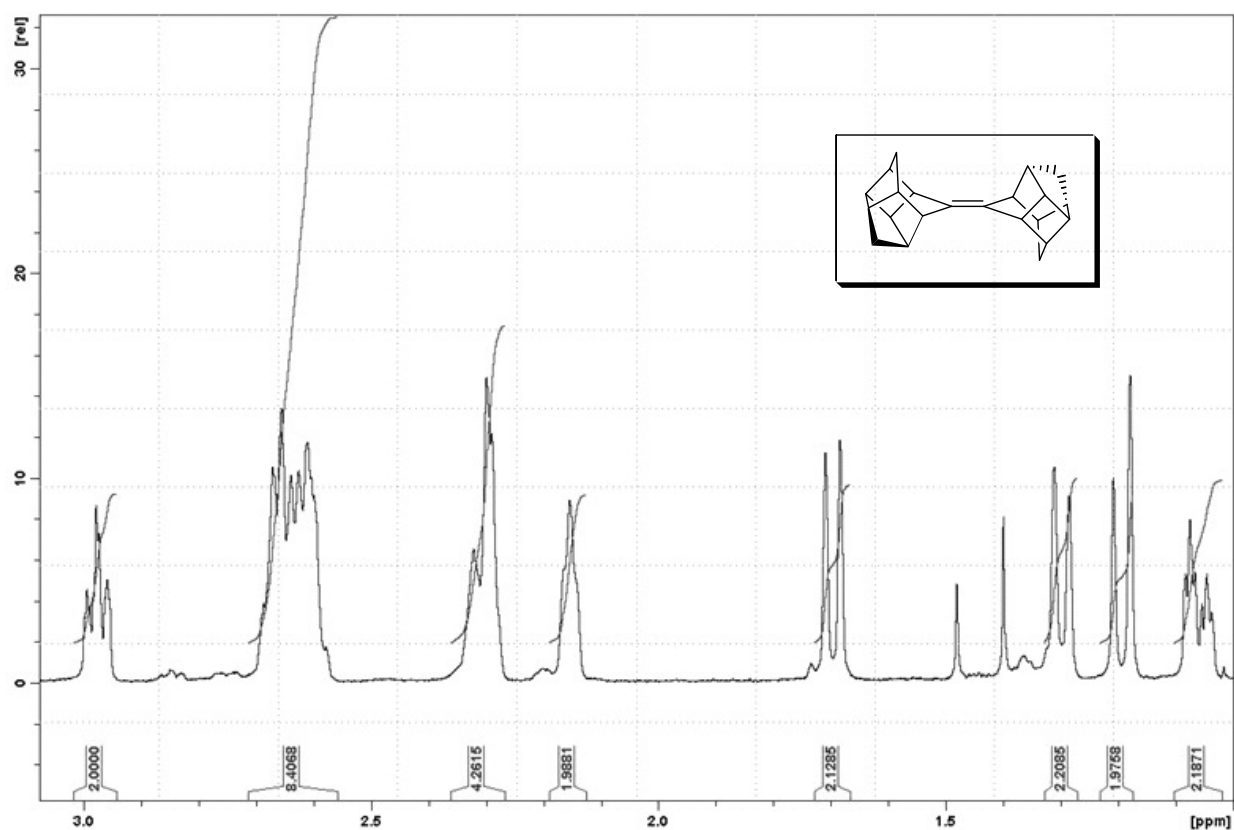


Figure A34. ^1H NMR spectrum of C_i -trans- C_S -8-trishomocubylidene- C_S -8-trishomocubane (135).

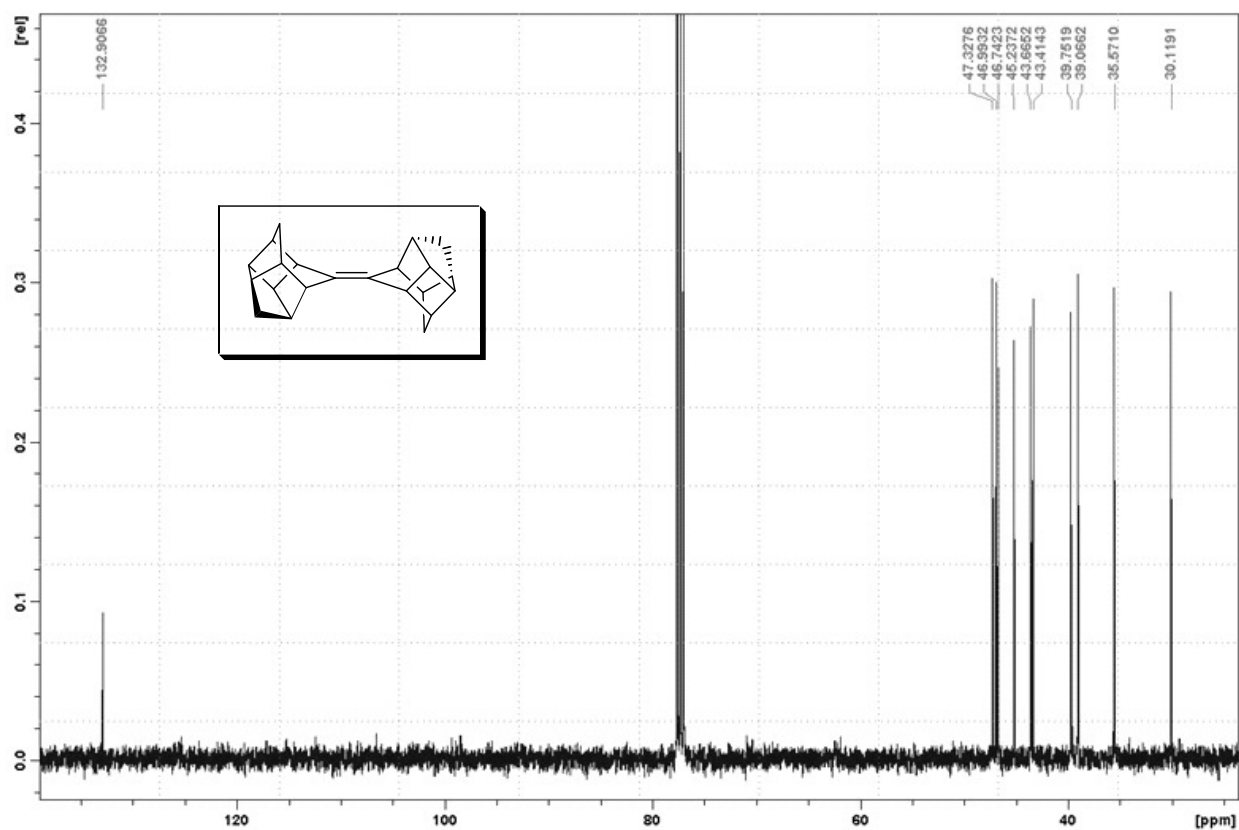


Figure A35. ^{13}C NMR spectrum of C_i -trans- C_S -8-trishomocubylidene- C_S -8-trishomocubane (135).

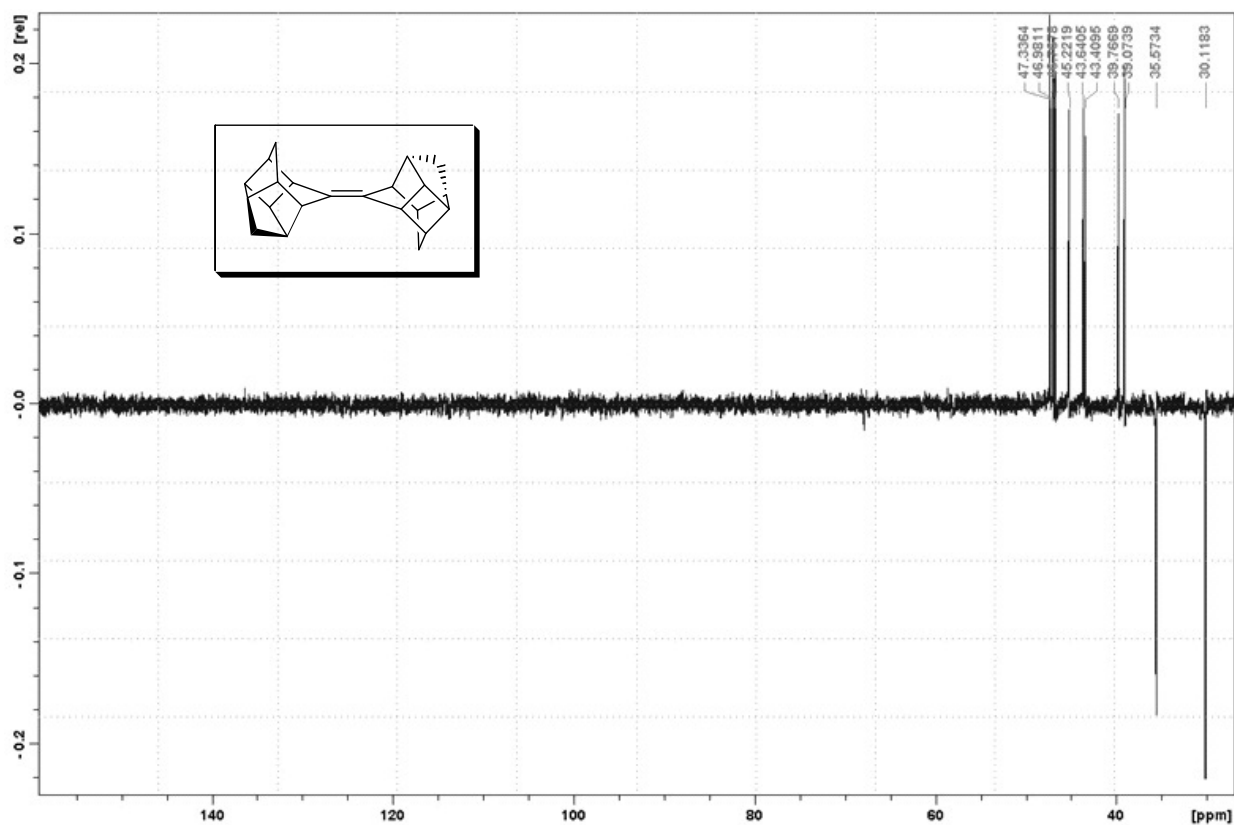


Figure A36. DEPT spectrum of C_i -*trans*- C_S -8-trishomocubylidene- C_S -8-trishomocubane (**135**).

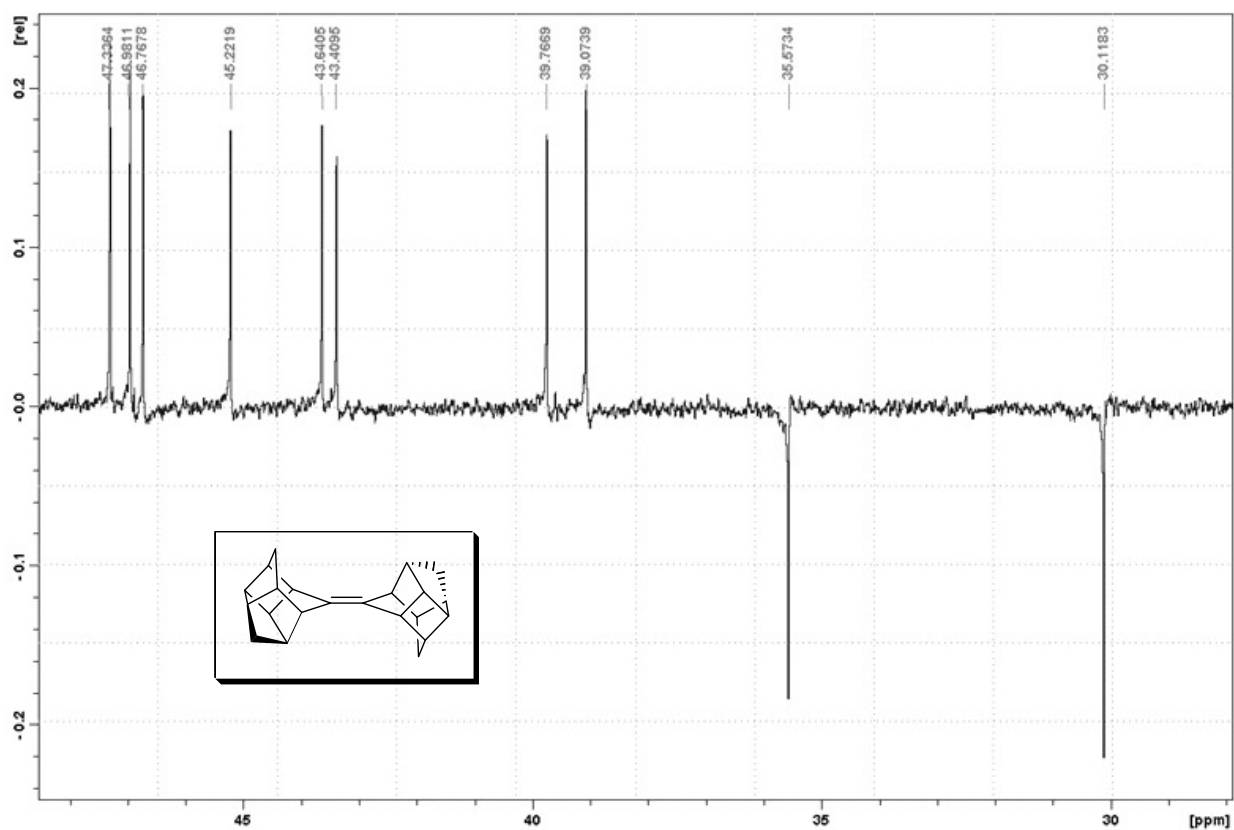


Figure A37. DEPT spectrum (part) of C_i -*trans*- C_S -8-trishomocubylidene- C_S -8-trishomocubane (**135**).

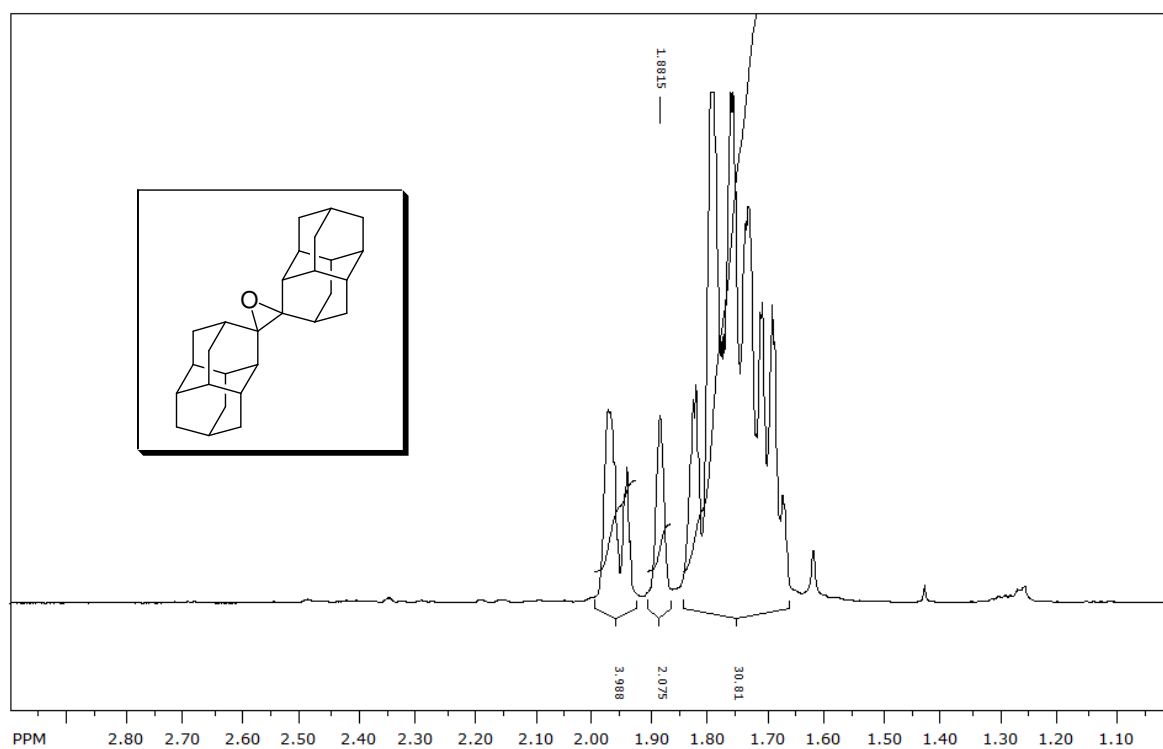


Figure A38. ^1H NMR spectrum of diadamantylidenediamantane epoxide (**142**).

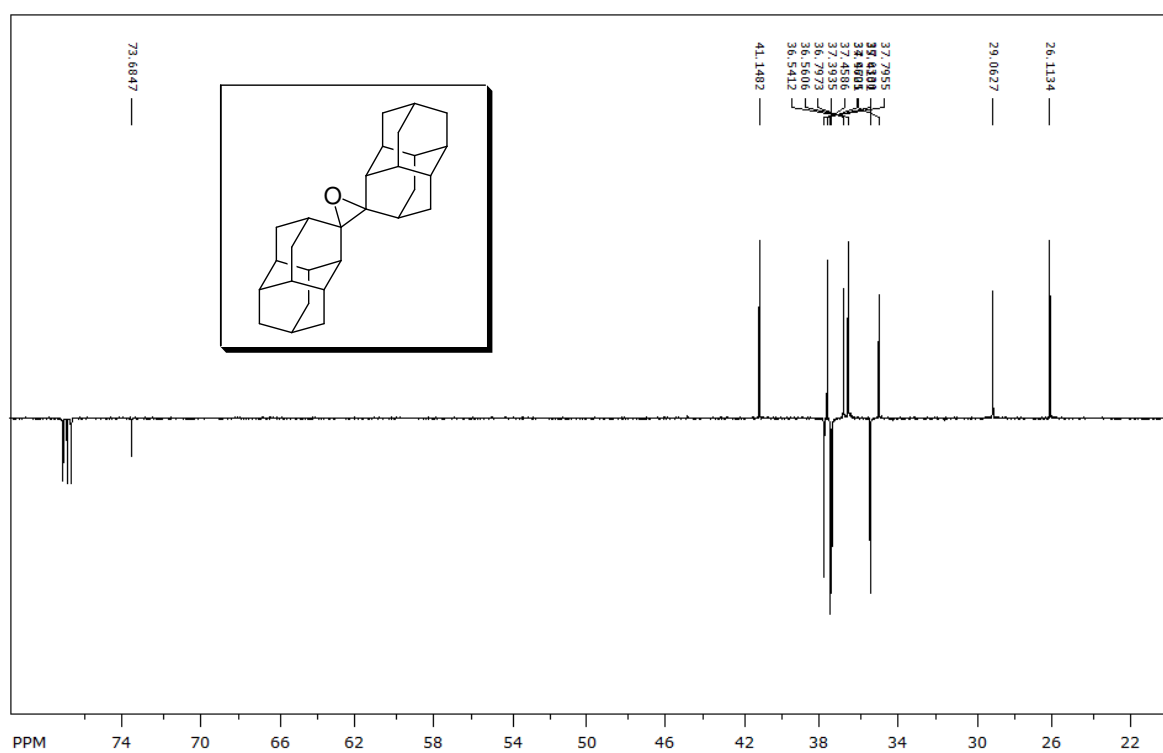


Figure A39. APT spectrum of diadamantylidenediamantane epoxide (**142**).

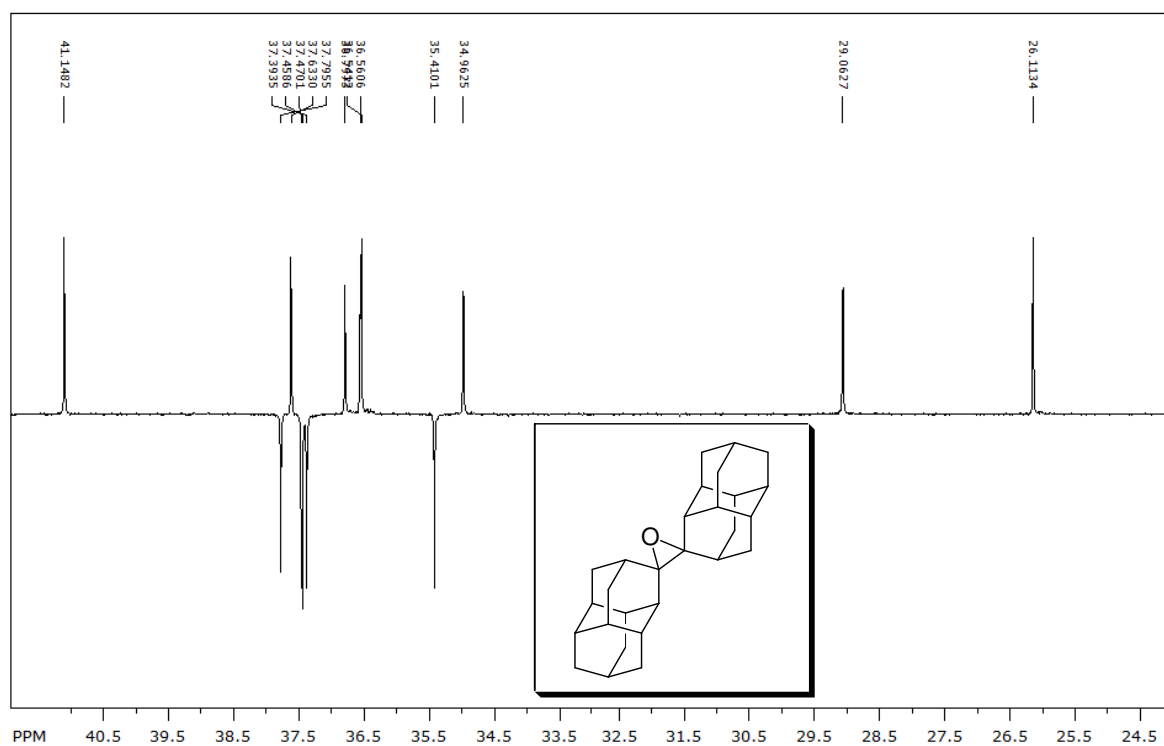


Figure A40. APT spectrum (part) of diadamantylidenediamantane epoxide (**142**).

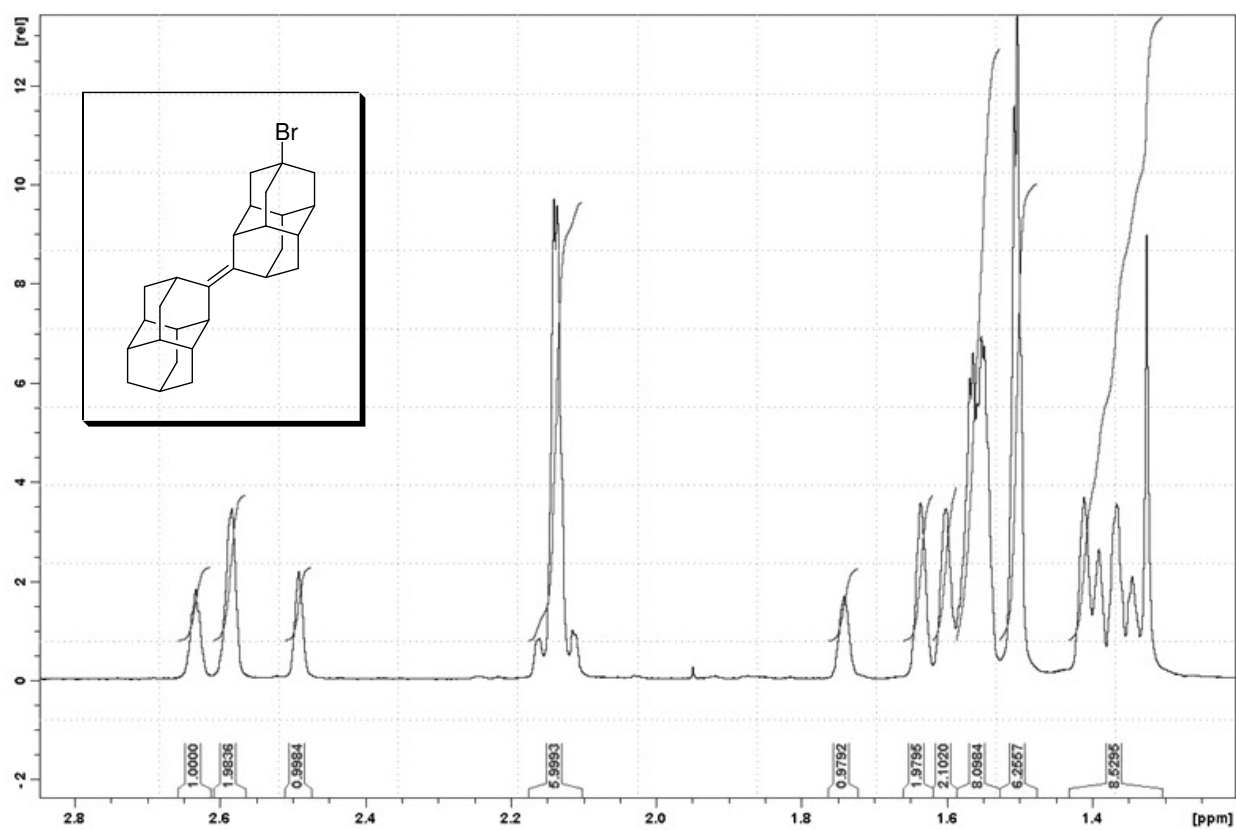


Figure A41. ^1H NMR spectrum of *anti*-4-bromodiamantylidenediamantane (**143**).

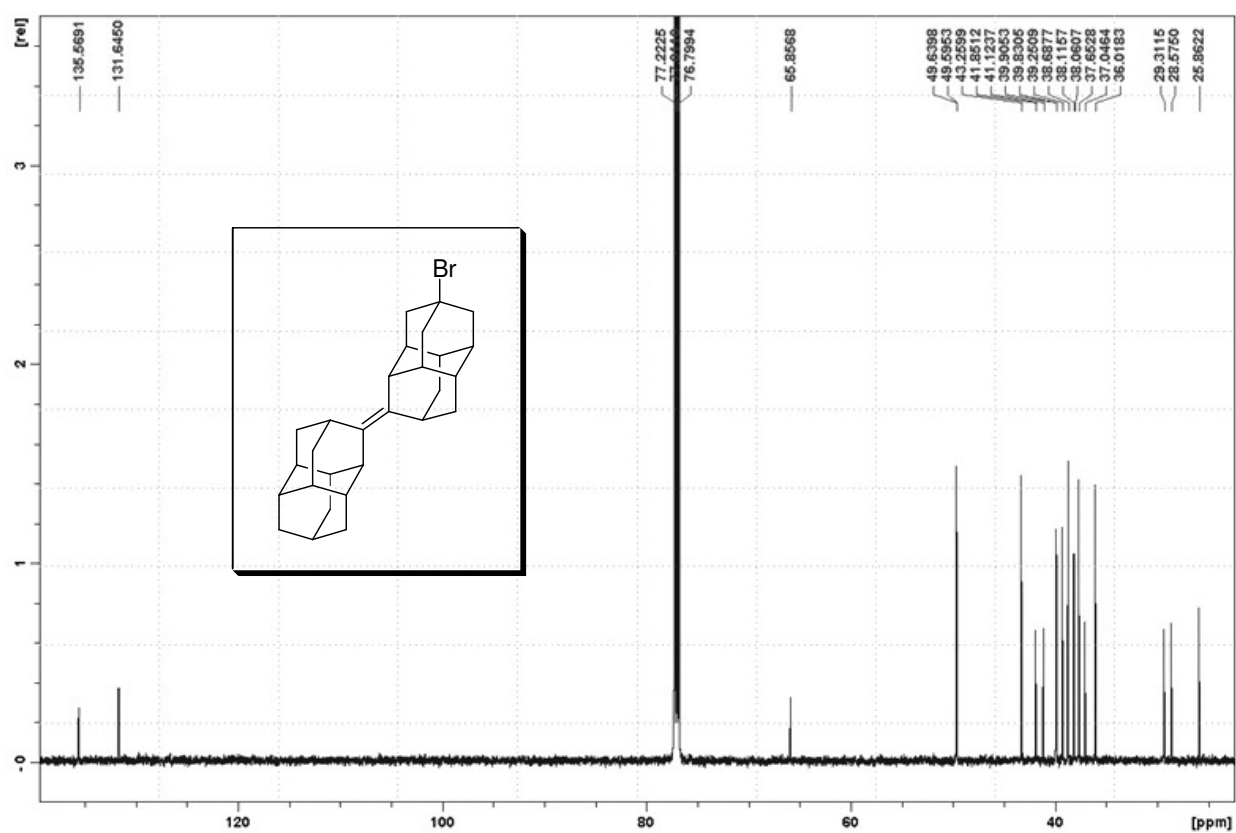


Figure A42. ^{13}C NMR spectrum of *anti*-4-bromodiamantylidenediamantane (**143**).

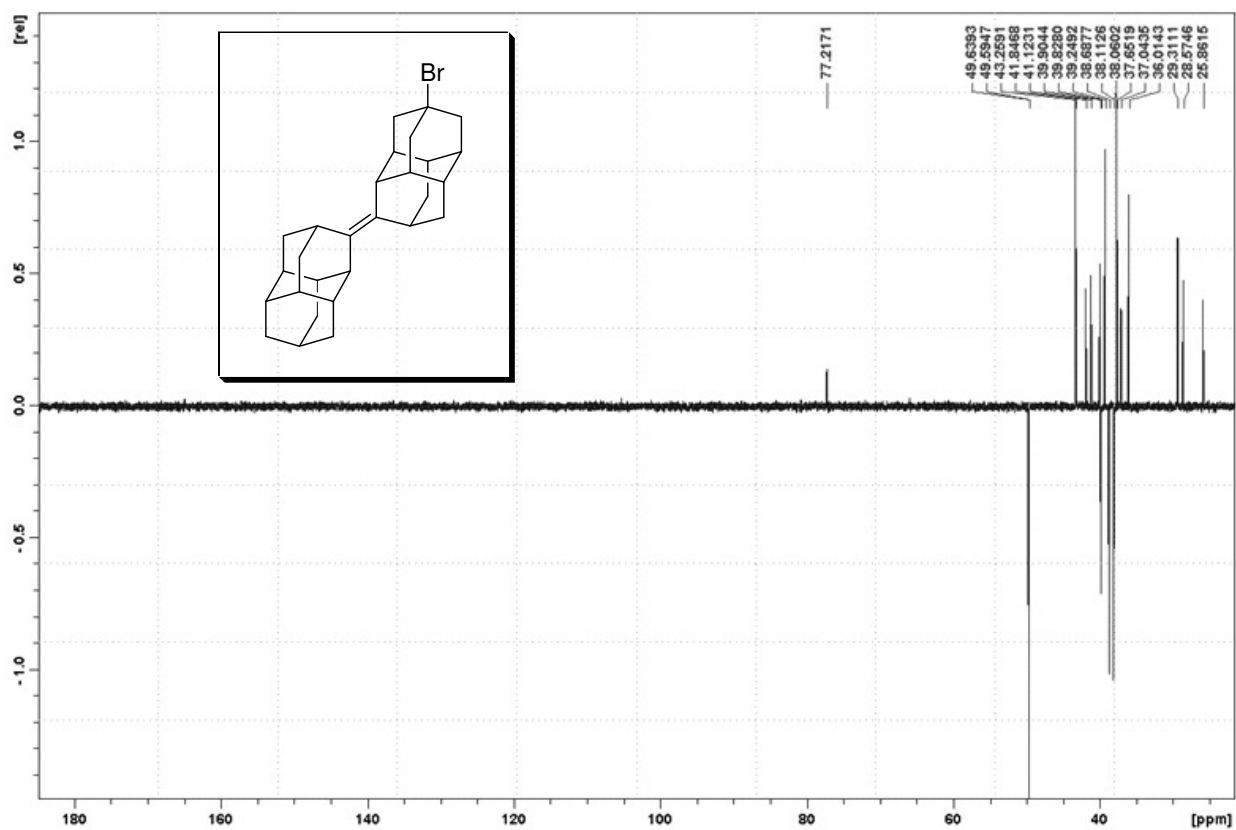


Figure A43. DEPT spectrum of *anti*-4-bromodiamantylidenediamantane (143).

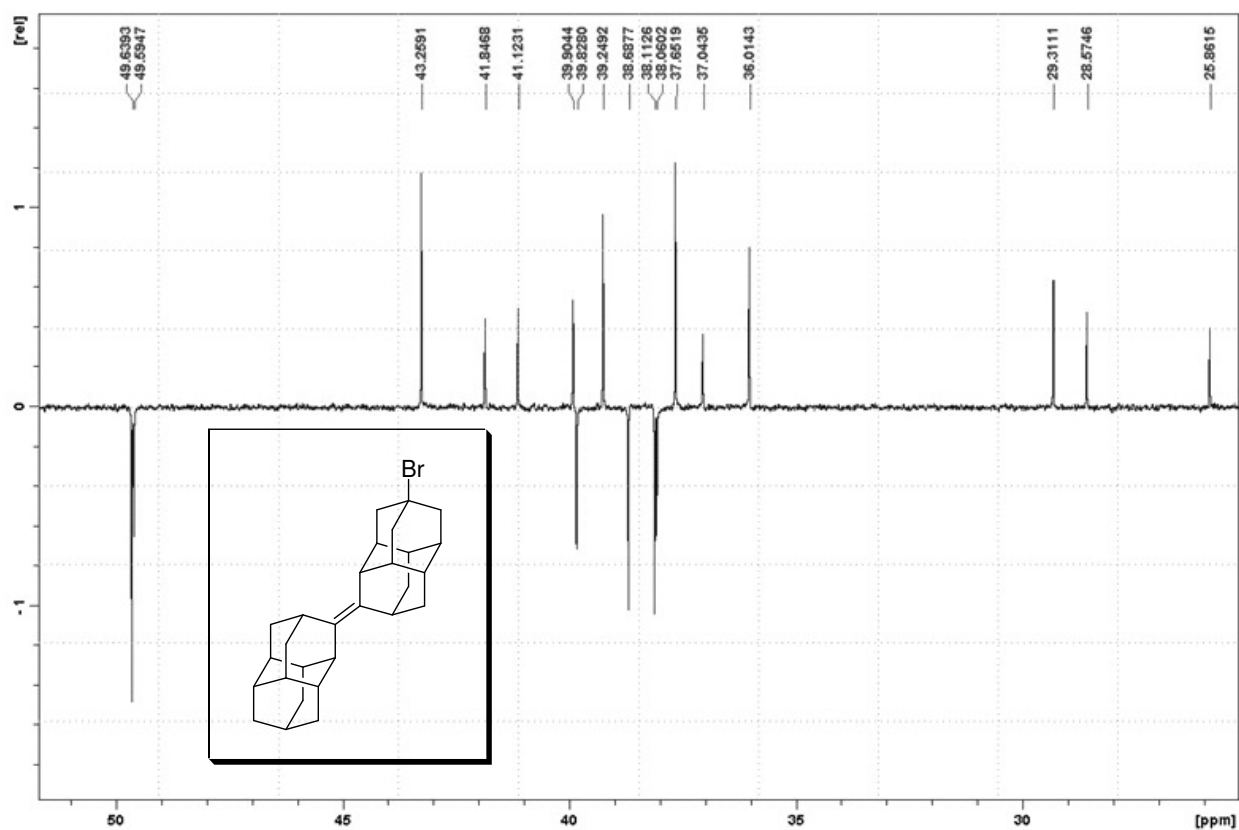


Figure A44. DEPT spectrum (part) of *anti*-4-bromodiamantylidenediamantane (143).

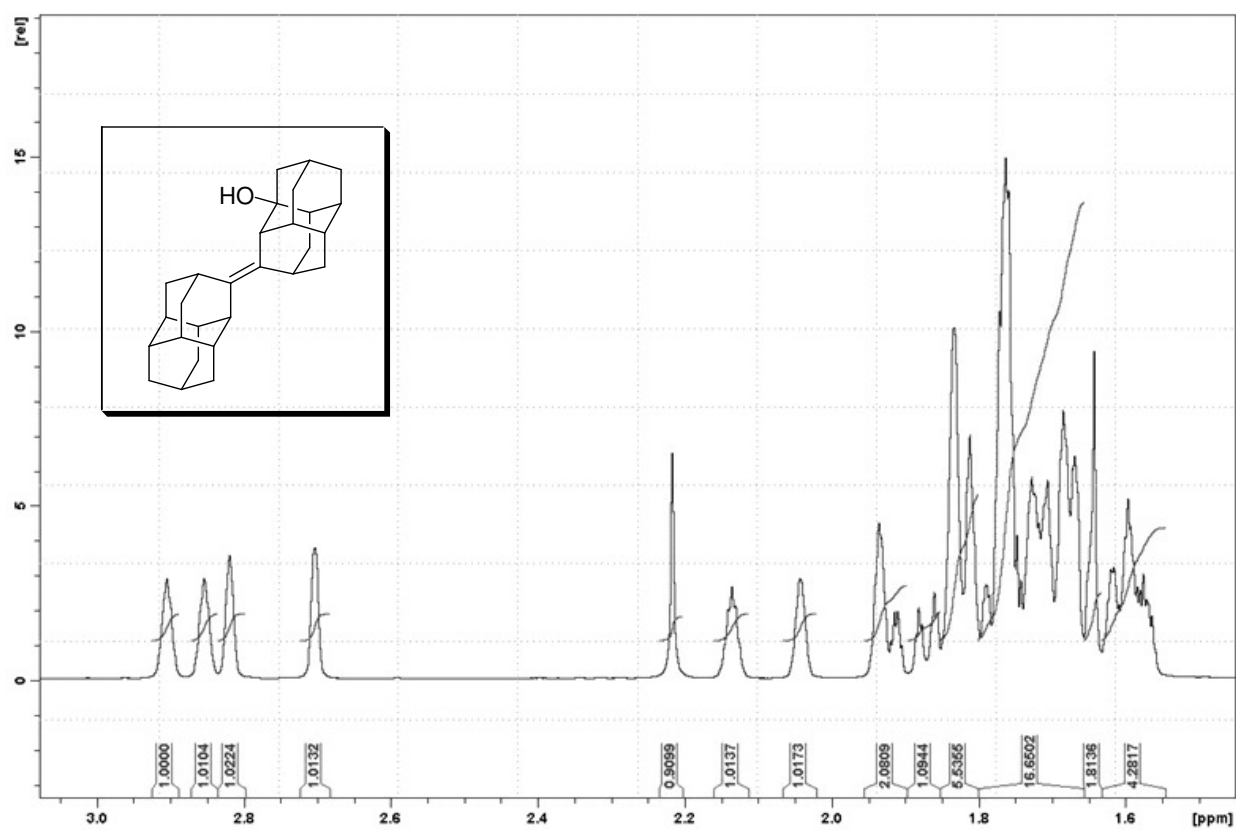


Figure A45. ^1H NMR spectrum of *anti*-diamantylidenediamantan-2-ol (**144**).

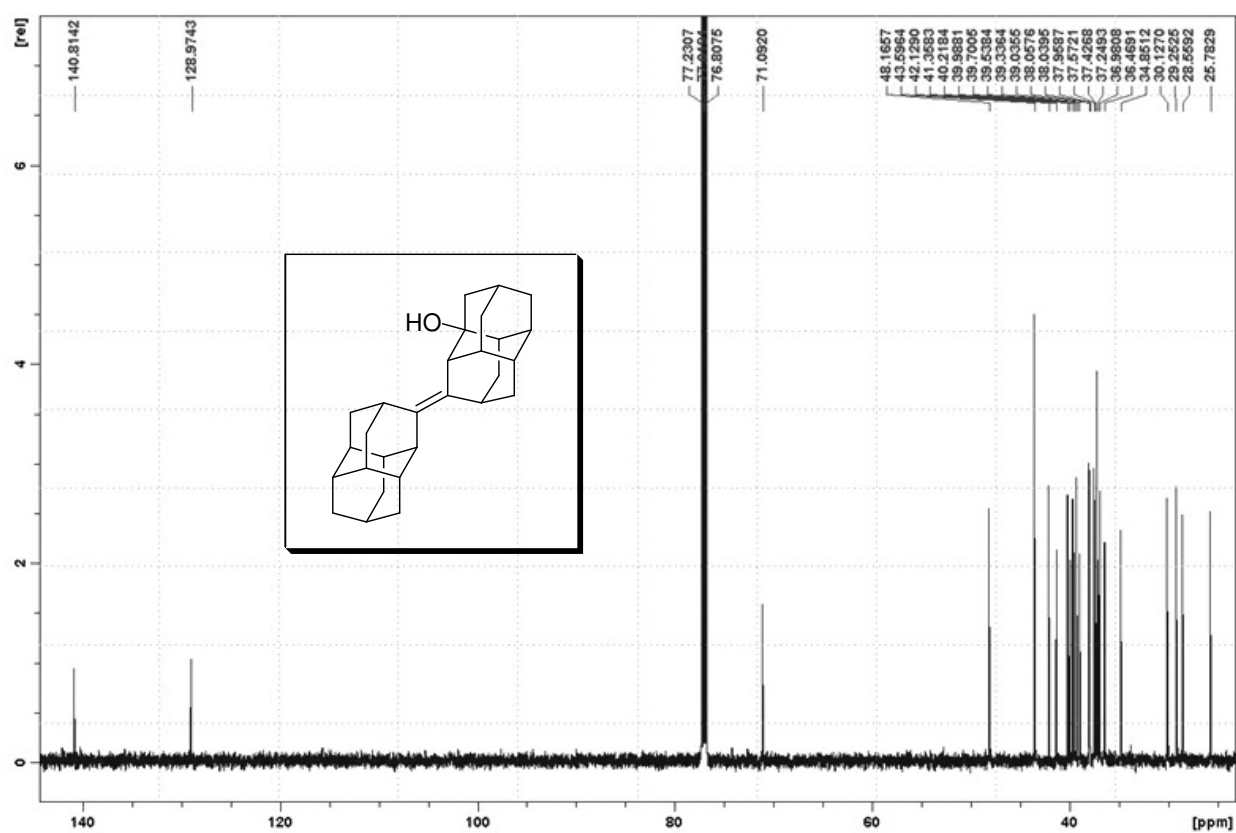
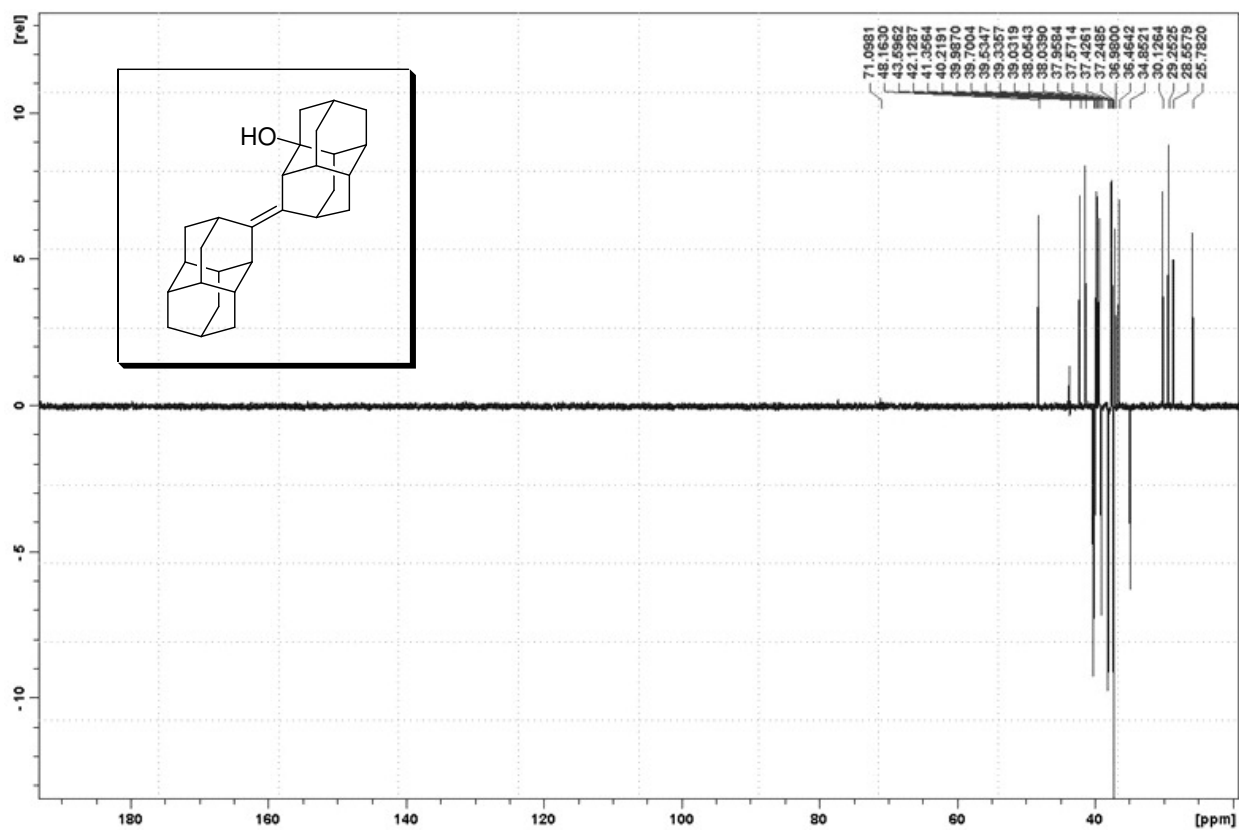


Figure A46. ^{13}C NMR spectrum of *anti*-diamantylidenediamantan-2-ol (**144**).



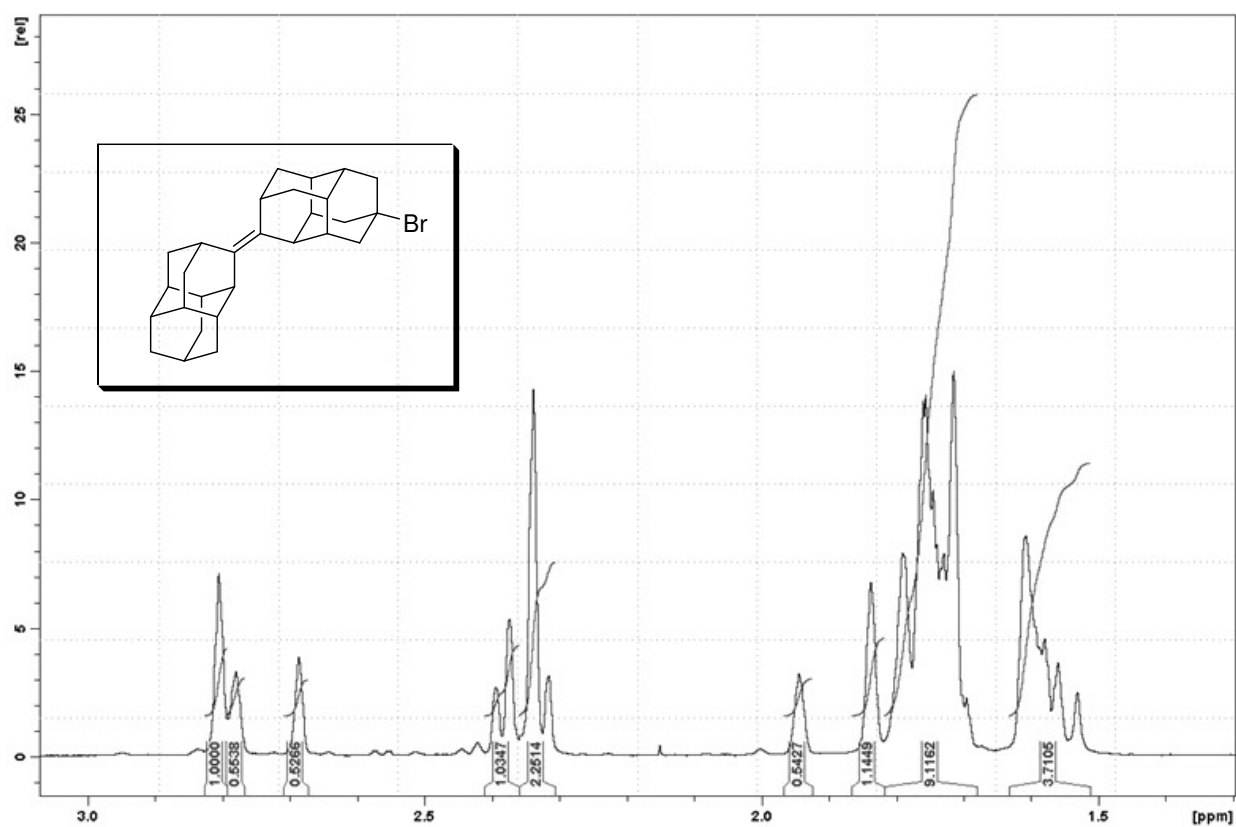


Figure A49. ^1H NMR spectrum of *syn*-4-bromodiamantylidenediamantane (**145**).

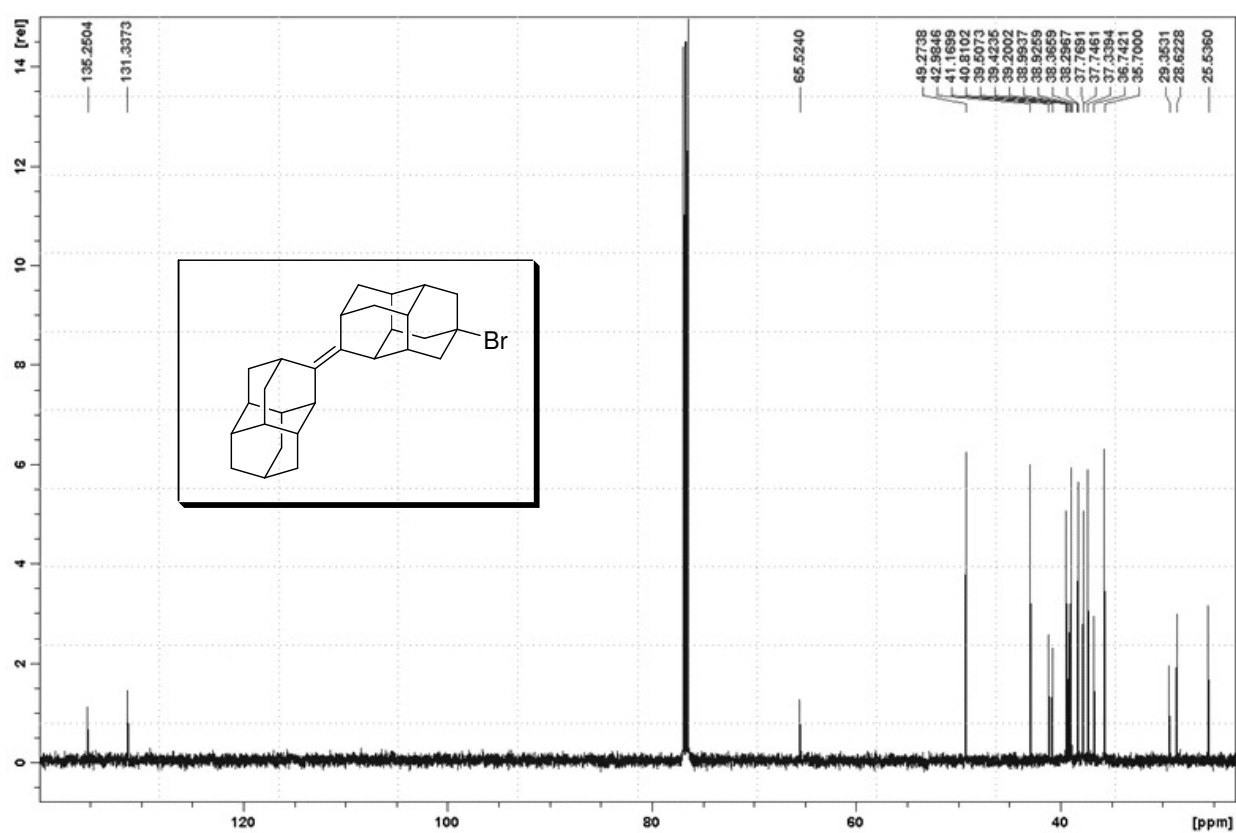


Figure A50. ^{13}C NMR spectrum of *syn*-4-bromodiamantylidenediamantane (**145**).

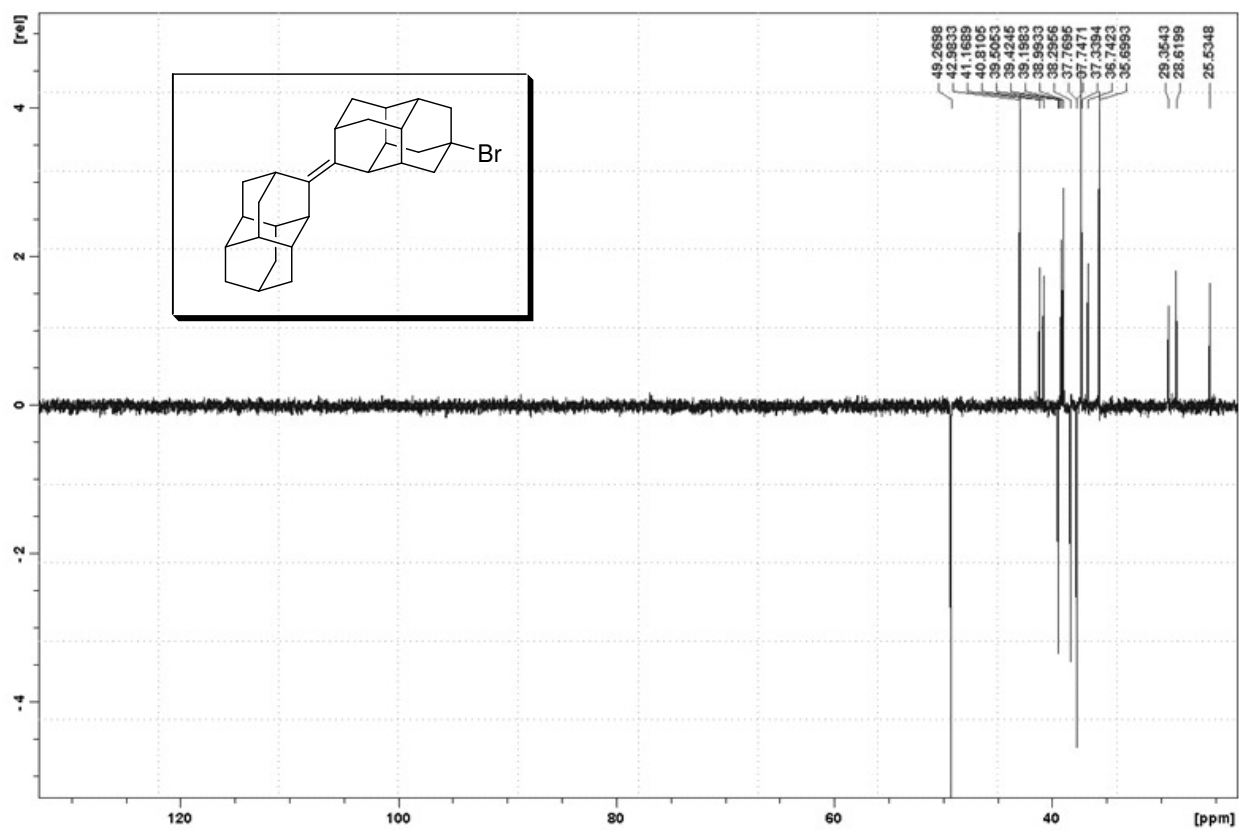


Figure A51. DEPT spectrum of *syn*-4-bromodiamantylidenediamantane (**145**).

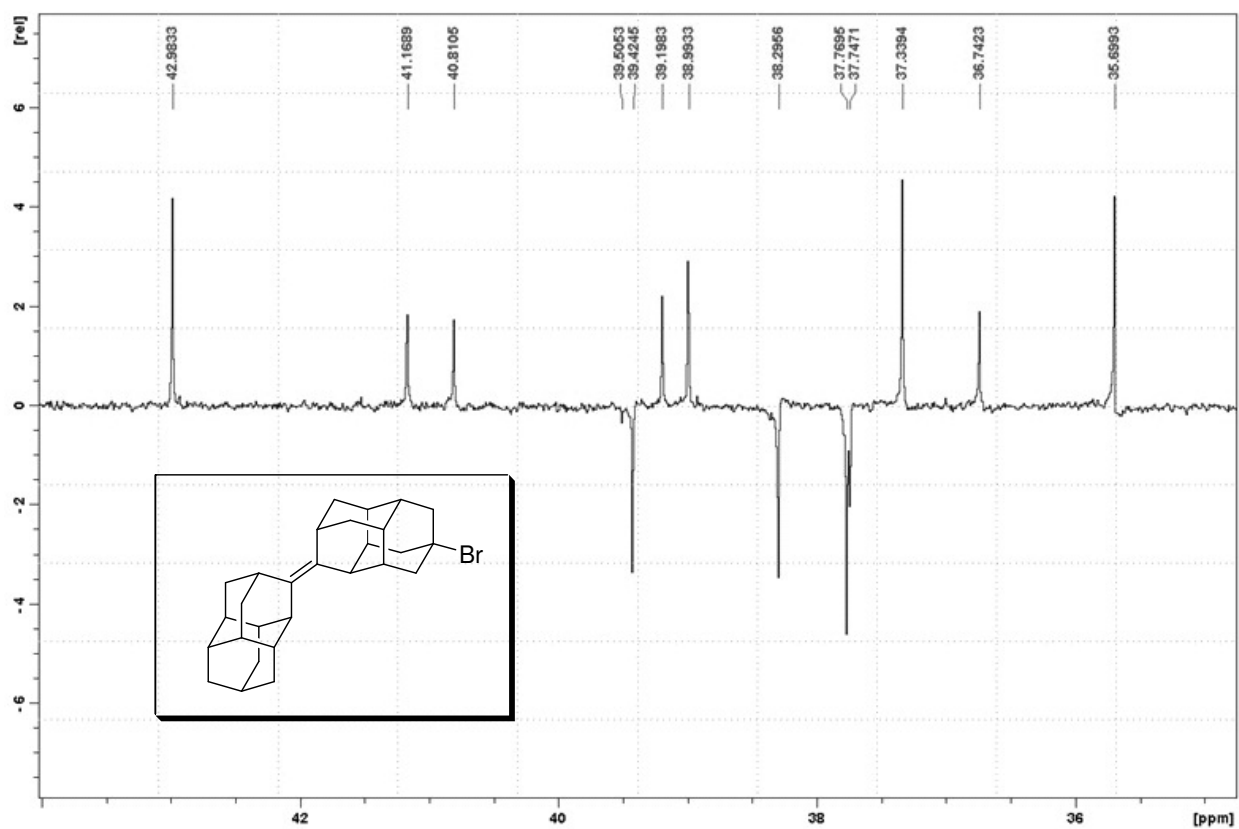


Figure A52. DEPT spectrum (part) of *syn*-4-bromodiamantylidenediamantane (**145**).

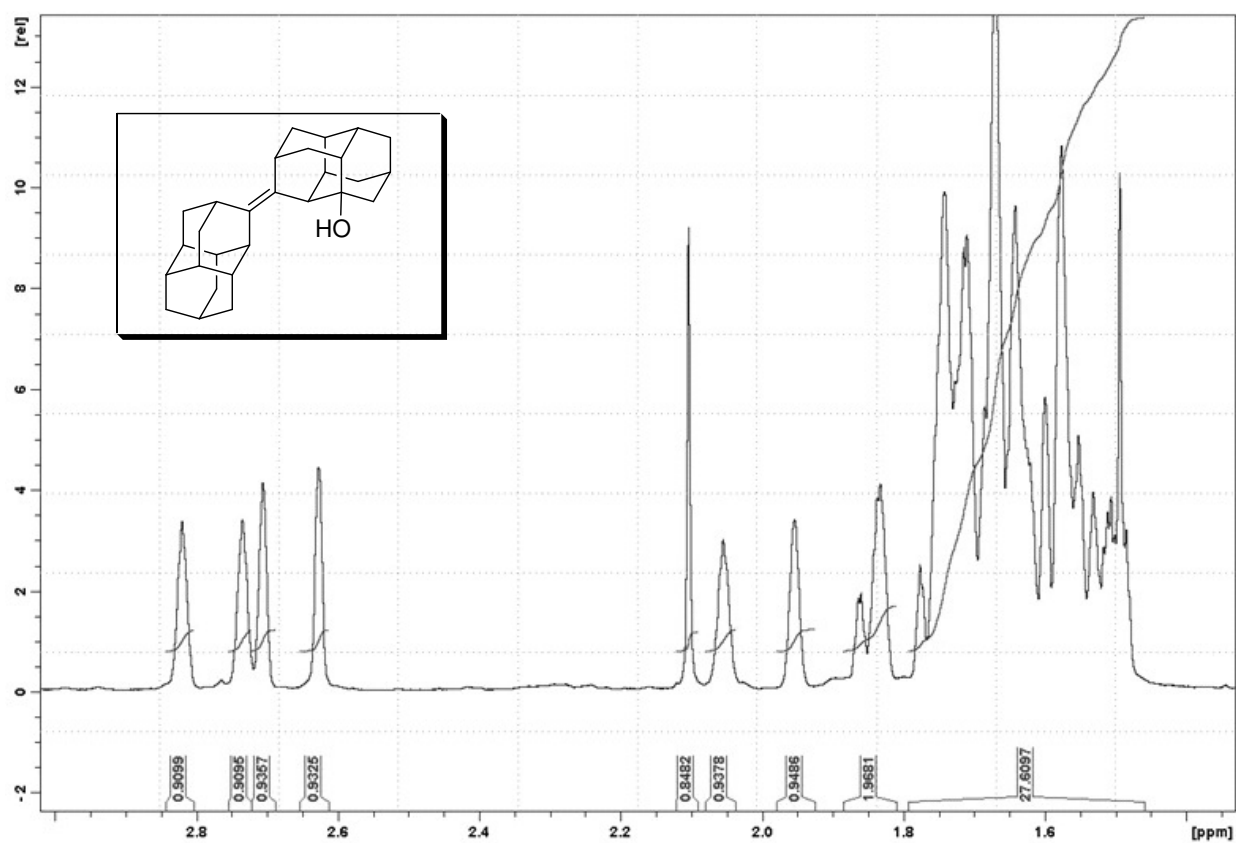


Figure A53. ^1H NMR spectrum of *syn*-diamantylidenediamantan-2-ol (**146**).

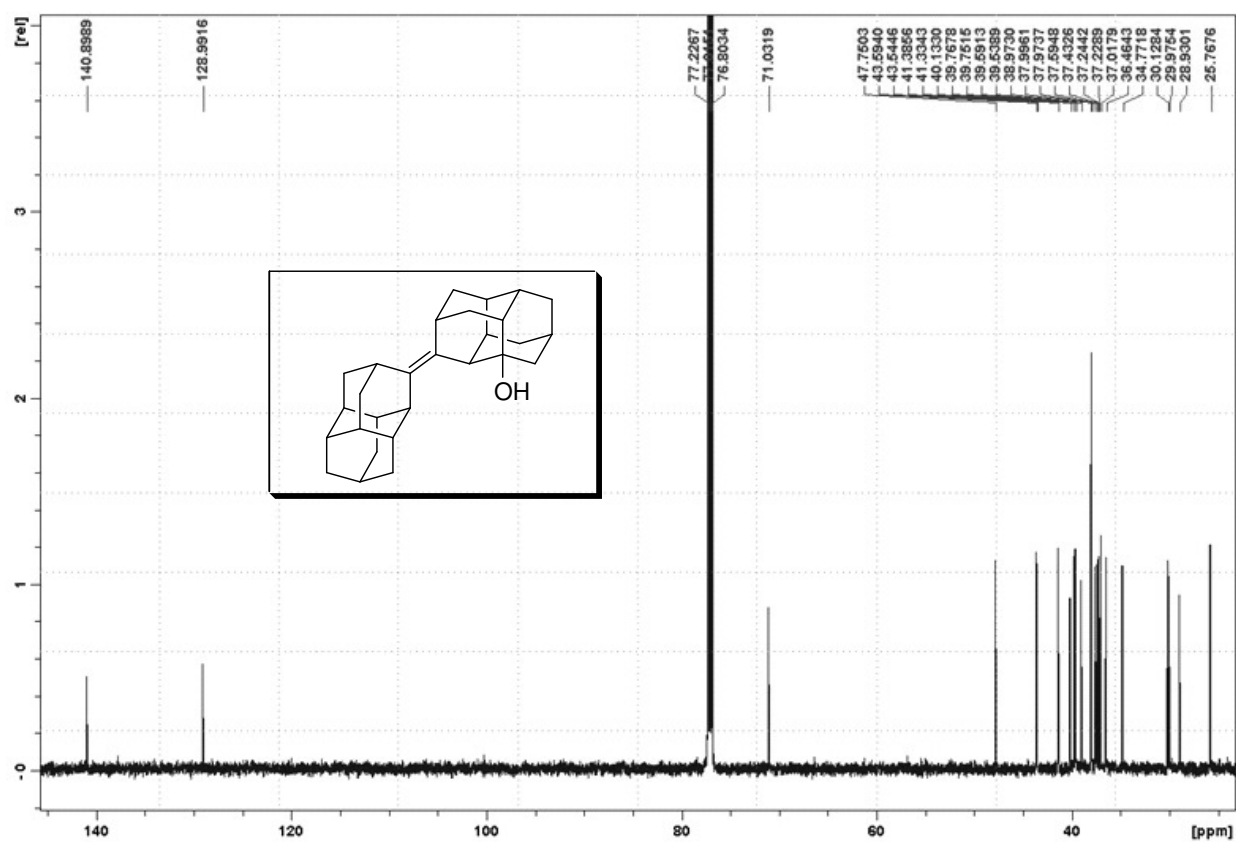


Figure A54. ^{13}C NMR spectrum of *syn*-diamantylidenediamantan-2-ol (**146**).

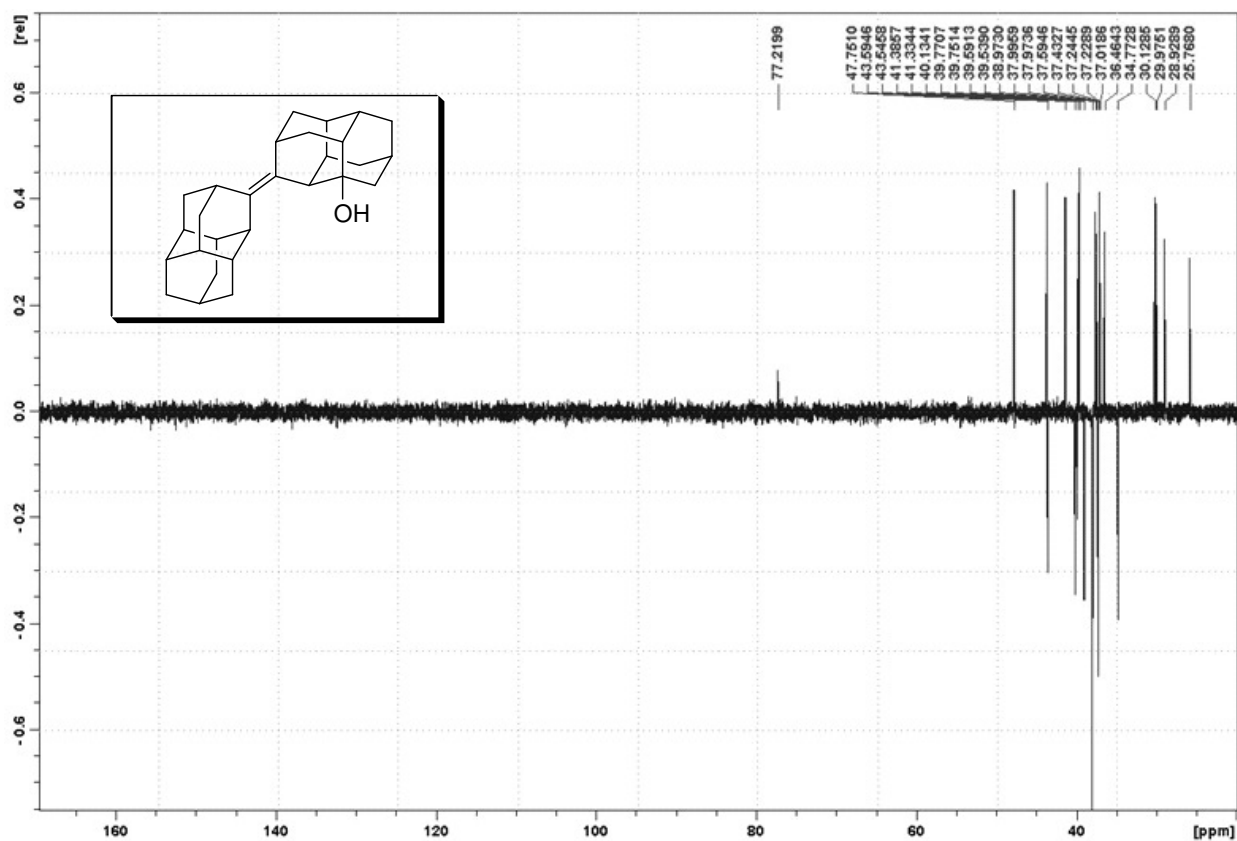


Figure A55. DEPT spectrum of *syn*-diamantylidenediamantan-2-ol (146).

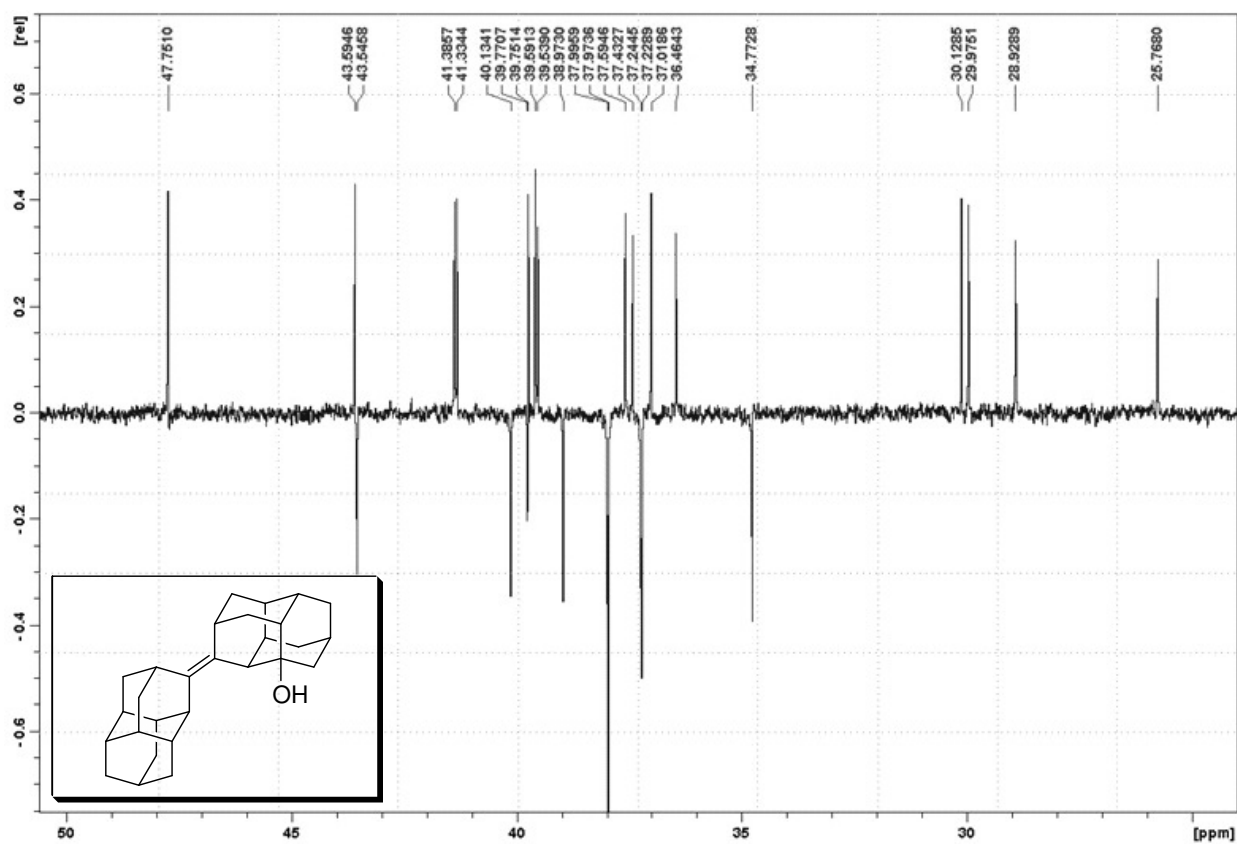


Figure A56. DEPT spectrum (part) of *syn*-diamantylidenediamantan-2-ol (146).

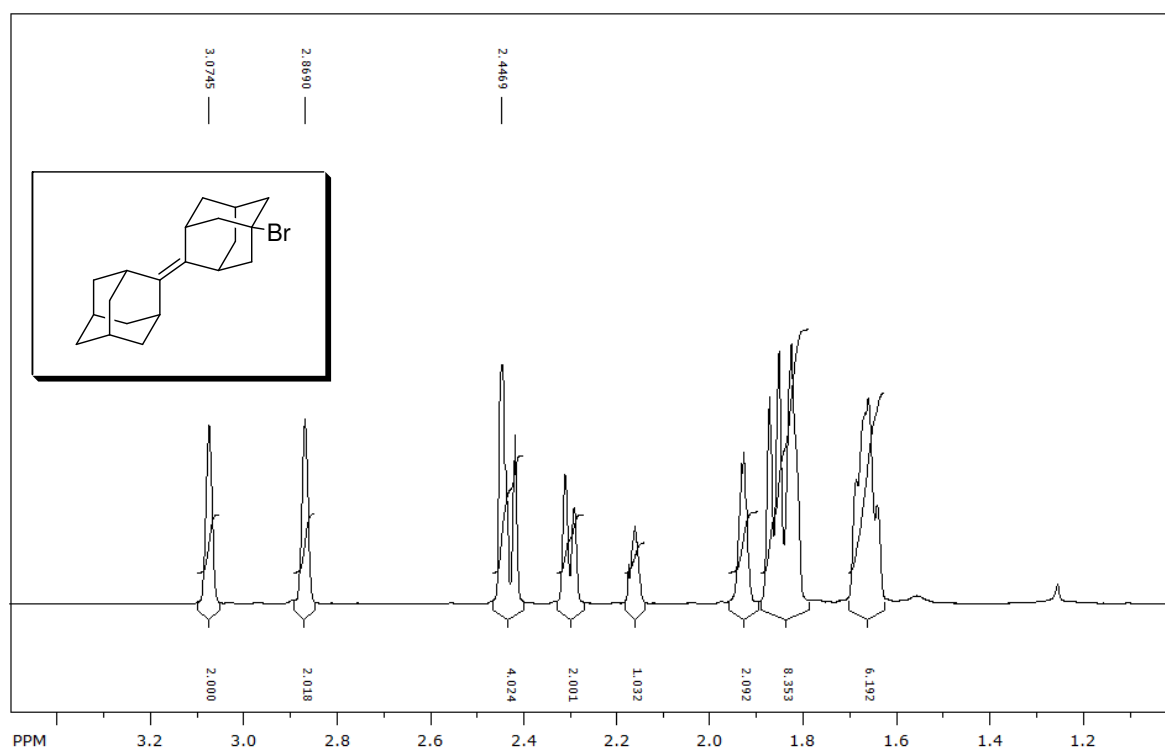


Figure A57. ¹H NMR spectrum of 5-bromoadamantylideneadamantane (**147**).

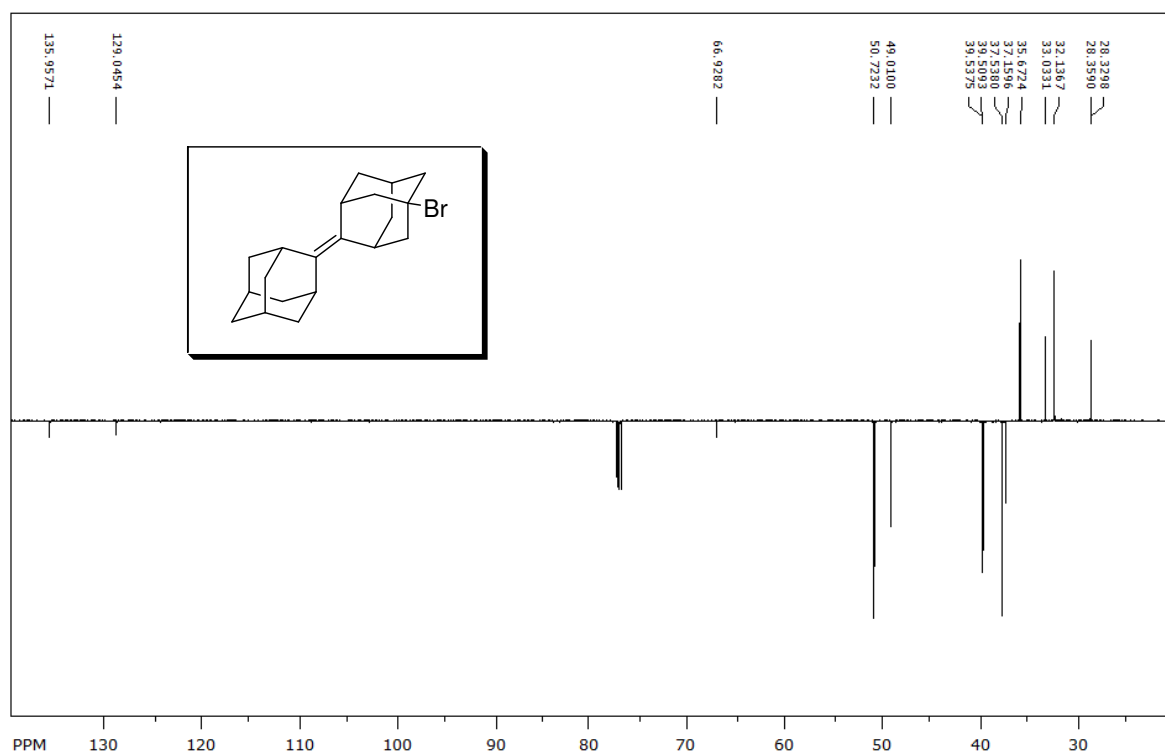


Figure A58. APT spectrum of 5-bromoadamantylideneadamantane (**147**).

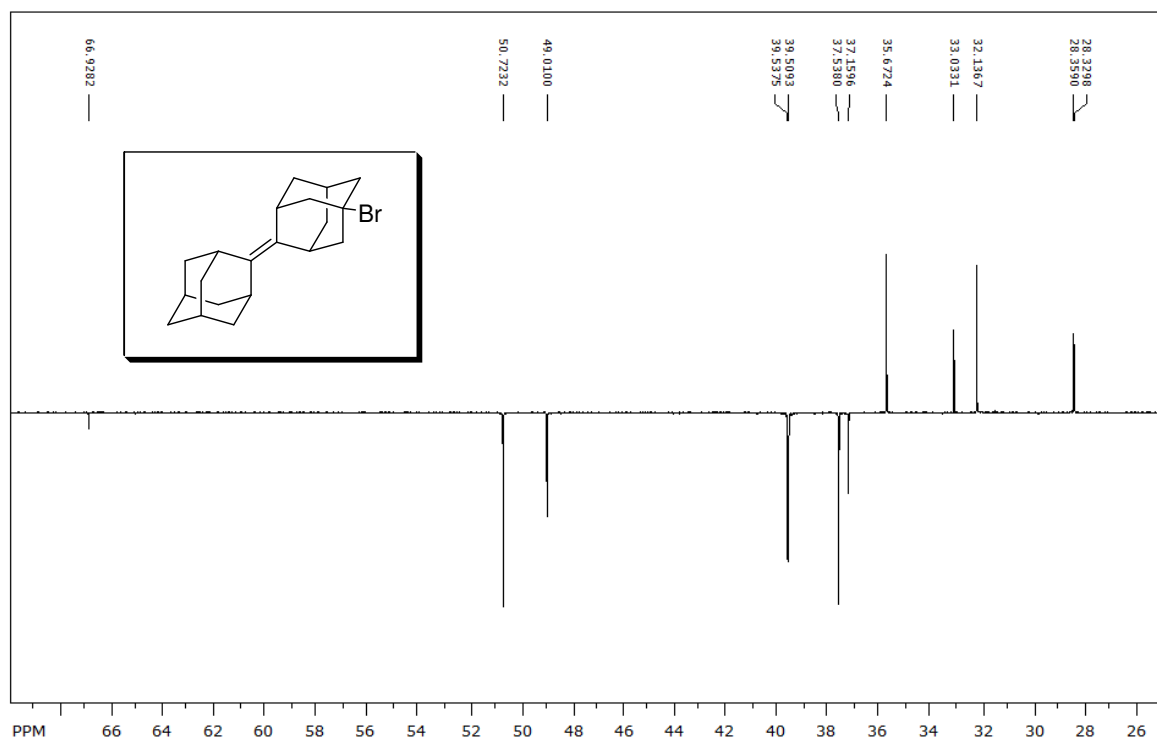


Figure A59. APT spectrum (part) of 5-bromoadamantylideneadamantane (**147**).

Appendix II. Crystal structures of selected synthesized compounds

X-Ray structure of *anti*-diamantylidenediamantane (**15**)

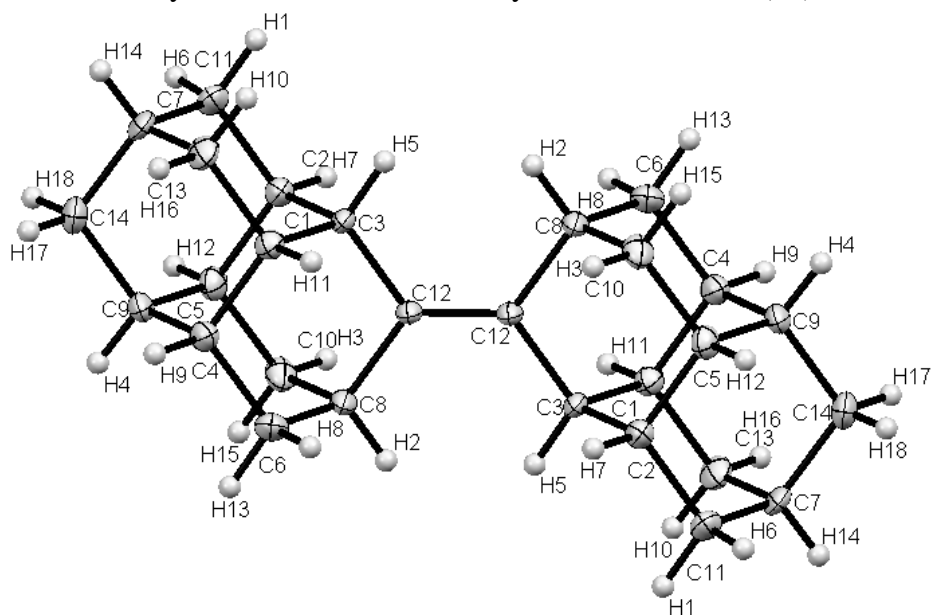


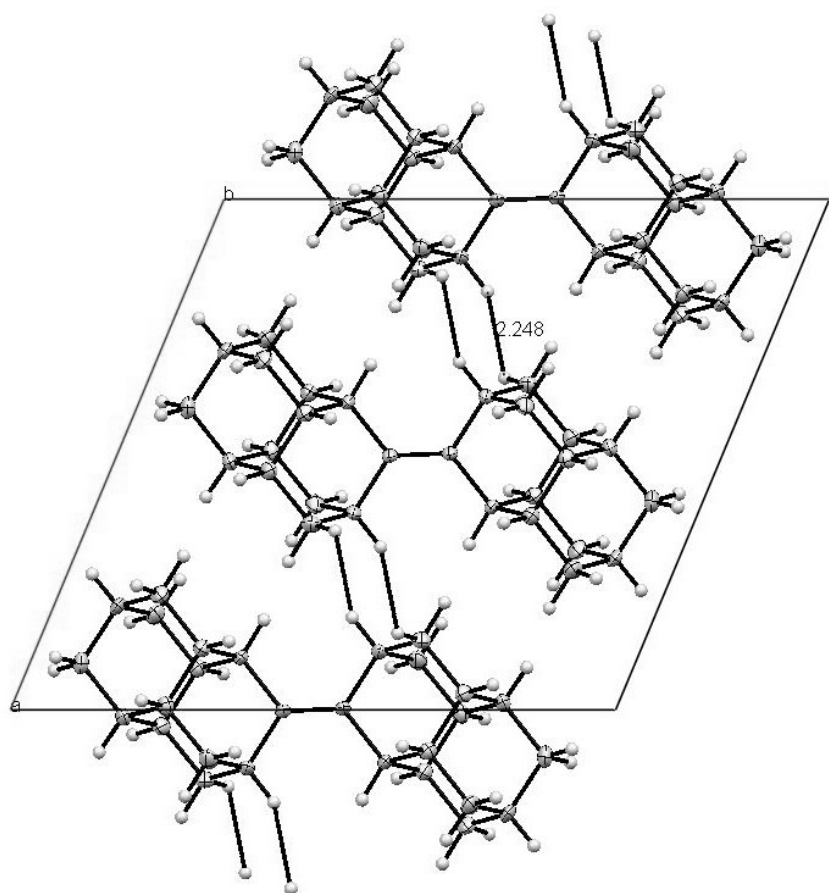
Figure A60. The crystal structure of *anti*-diamantylidenediamantane (**15**).

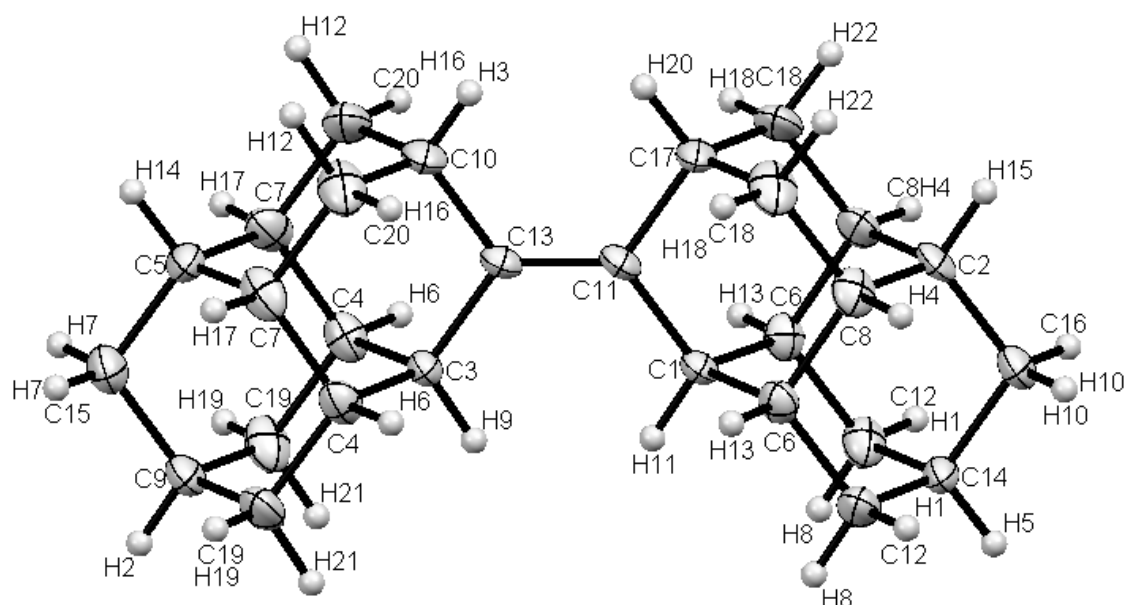
Table A1. Crystallographic key data of *anti*-diamantylidenediamantane (**15**).

Empirical formula	C ₁₄ H ₁₈ (C ₂₈ H ₃₆)
Formula weight; <i>M</i> [g mol ⁻¹]	186.30 (372.60)
Habitus	rectangle crystals
Color	colorless
Melting point [K]	549
Space group	P 2 ₁ /a
Unit cell dimensions:	<i>a</i> 12.2783(18) <i>b</i> 6.5650(7) <i>c</i> 13.424(2) <i>α</i> 90.00 <i>β</i> 112.714(17) <i>γ</i> 90.00
Volume; <i>V</i> [Å ³]	998.2(2)
Formula units/cell; <i>Z</i>	4
<i>F</i> (000)	408.0
Absorption coeff, mm ⁻¹	0.069
<i>T</i> [K]	293
<i>ρ</i> _{calcd} [g cm ⁻³]	1.240
2 θ _{max} [°]	56.29
Radiation wavelength, Å	Mo–K α (λ = 0.71073 Å)
Limits of <i>h</i> , <i>k</i> , <i>l</i>	-16 16; -7 8; -17 17
Reflections collected	8365
Unique reflections	2334
Number of parameters	199
<i>R</i> 1 [<i>I</i> > 2 σ (<i>I</i>)] (<i>R</i> _{all})	0.0550 (0.1088)
ω <i>R</i> 2 [<i>I</i> > 2 σ (<i>I</i>)] (<i>R</i> _{ref})	0.1425 (0.1676)
<i>R</i> -factor [%]	5.5
Goodness of fit on <i>F</i> ²	0.902
Residual electron density [e/Å ³]	0.06
Largest diff. peak and hole [e/Å ³]	0.34 and -0.32
<i>S</i>	0.902
<i>g</i> (weighting scheme)	0.1055

Table A2. Selected bond lengths and angles of *anti*-diamantylidenediamantane (**15**).

Bond	$d/\text{\AA}$	Bond	$d/\text{\AA}$
C(3) – C(12)	1.519(2)	C(3) – H(5)	0.99(3)
C(8) – C(12)	1.519(3)	C(8) – H(2)	0.98(2)
C(12) – C(12)	1.333(3)	H(2) – H(5)	1.97(4)
Angle	$\omega/^\circ$	H(3) – H(11)	3.73(4)
		H(7) – H(8)	3.75(4)
C(3) – C(12) – C(12)	125.0(2)		
C(8) – C(12) – C(12)	124.7(2)		

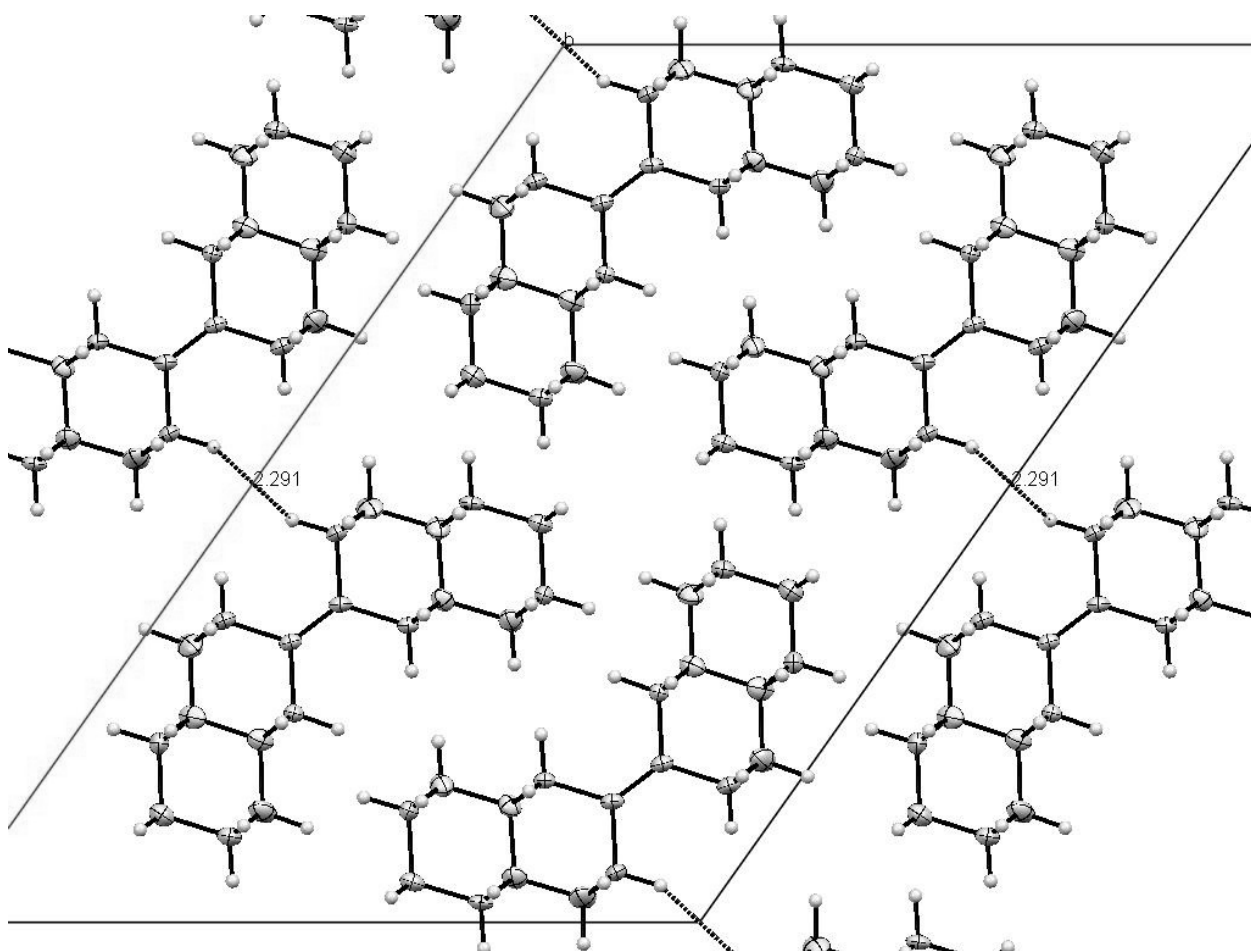
Figure A61. Packing and intermolecular distance in the crystal of *anti*-diamantylidenediamantane (**15**).

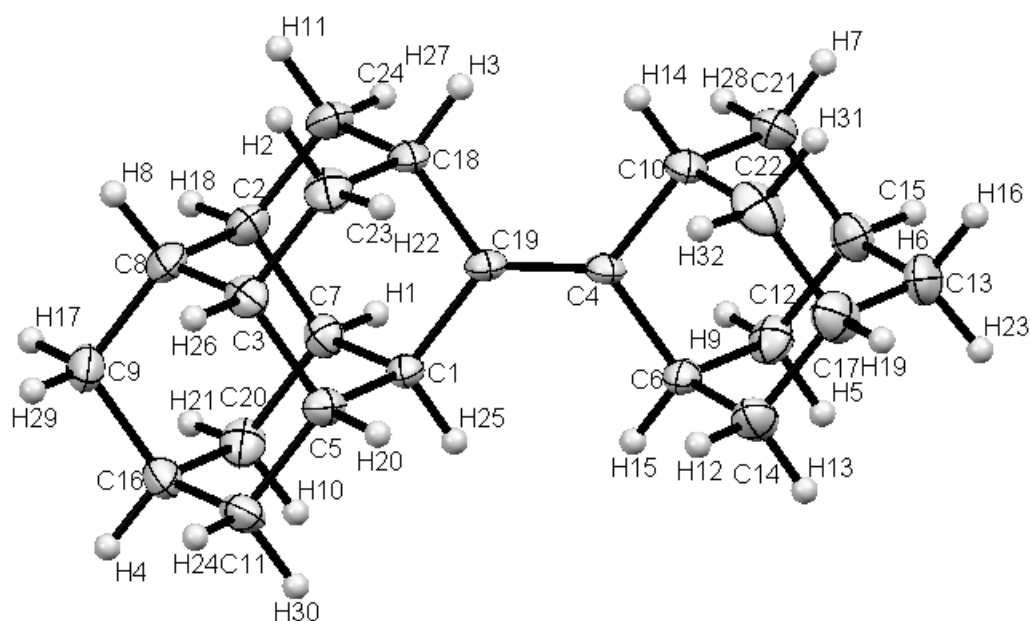
X-Ray structure of *syn*-diamantylidenediamantane (**16**)Figure A62. The crystal structure of *syn*-diamantylidenediamantane (**16**).Table A3. Crystallographic key data of *syn*-diamantylidenediamantane (**16**).

Empirical formula	C ₂₈ H ₃₆
Formula weight; <i>M</i> [g mol ⁻¹]	372.57
Habitus	rectangle crystal
Color	colorless
Melting point [K]	518-521
Space group	C 2/m
Unit cell dimensions:	<i>a</i> 22.980(3) <i>b</i> 6.6493(12) <i>c</i> 16.1980(19) <i>α</i> 90.00 <i>β</i> 125.389(10) <i>γ</i> 90.00
Volume; <i>V</i> [Å ³]	2017.74
Formula units/cell; <i>Z</i>	4
<i>F</i> (000)	816
Absorption coeff, mm ⁻¹	0.068
<i>T</i> [K]	293
<i>ρ</i> _{calcd} [g cm ⁻³]	1.226
2 θ max [°]	56.31
Radiation wavelength, Å	Mo-K α (λ = 0.71073 Å)
Limits of <i>h</i> , <i>k</i> , <i>l</i>	-27 30; -8 8; -20 20
Reflections collected	9258
Unique reflections	2467
Number of parameters	225
<i>R</i> 1 [<i>I</i> > 2 σ (<i>I</i>)] (<i>R</i> _{all})	0.0545 (0.1195)
<i>wR</i> 2 [<i>I</i> > 2 σ (<i>I</i>)] (<i>R</i> _{ref})	0.1349 (0.1737)
<i>R</i> -factor [%]	5.45
Goodness of fit on <i>F</i> ²	0.823
Residual electron density [e/Å ³]	0.05
Largest diff. peak and hole [e/Å ³]	0.29 and -0.27
<i>S</i>	0.823
<i>g</i> (weighting scheme)	0.0905

Table A4. Selected bond lengths and angles of *syn*-diamantylidenediamantane (**16**).

Bond	$d/\text{\AA}$	Bond	$d/\text{\AA}$
C(1) – C(11)	1.512(5)	C(1) – H(11)	0.98(3)
C(3) – C(13)	1.518(3)	C(3) – H(9)	1.00(3)
C(10) – C(13)	1.501(5)	C(10) – H(3)	0.90(4)
C(11) – C(13)	1.335(5)	C(17) – H(20)	0.99(5)
C(11) – C(17)	1.519(3)	H(3) – H(20)	1.96(8)
Angle	$\omega/^\circ$	H(6) – H(13)	3.82(5)
C(10) – C(13) – C(11)	124.9(3)	H(9) – H(11)	2.00(7)
C(13) – C(11) – C(17)	124.3(3)	H(16) – H(18)	3.73(5)
C(3) – C(13) – C(11)	124.6(3)		
C(13) – C(11) – C(1)	125.6(3)		

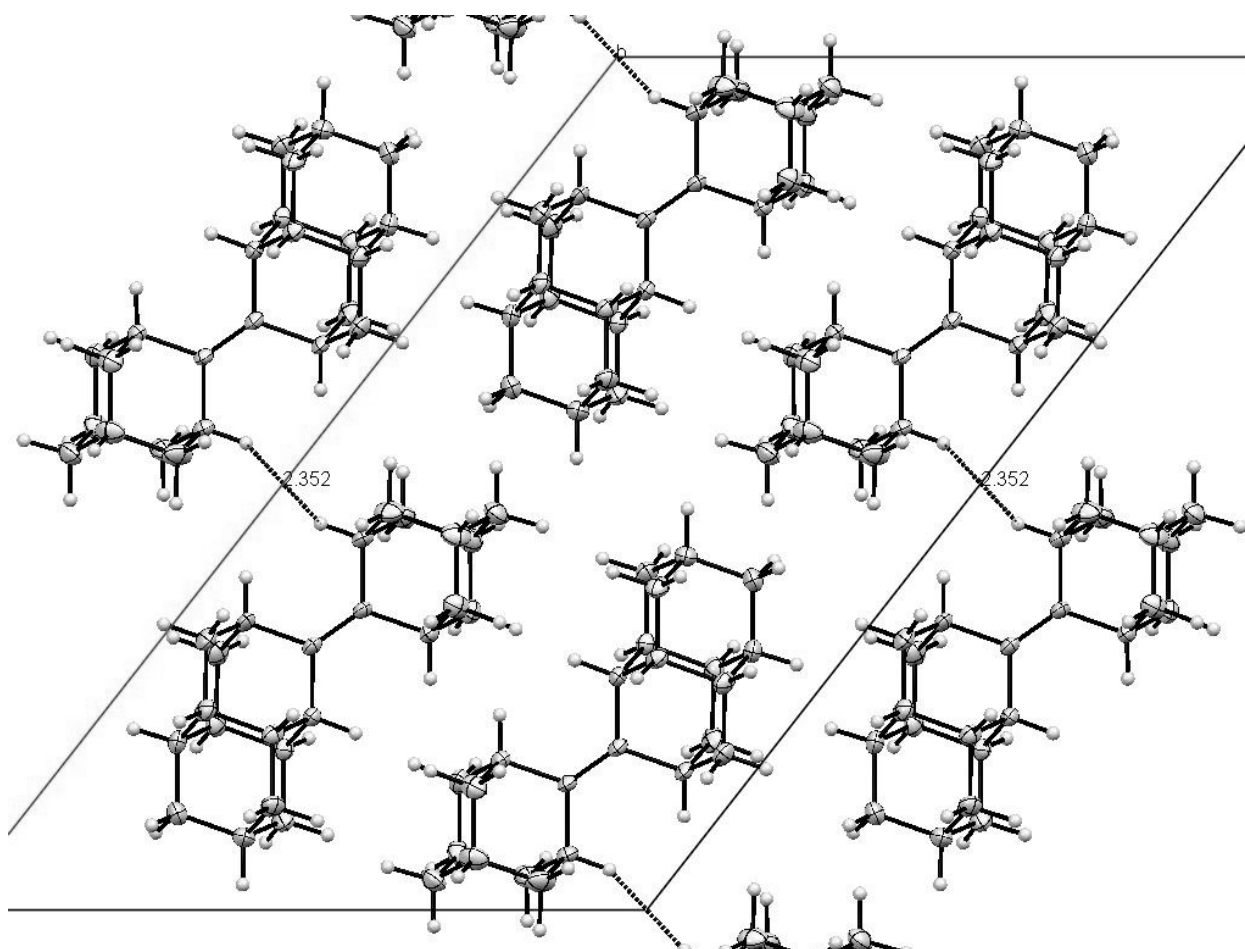
Figure A63. Packing and intermolecular distance in the crystal of *syn*-diamantylidenediamantane (**16**).

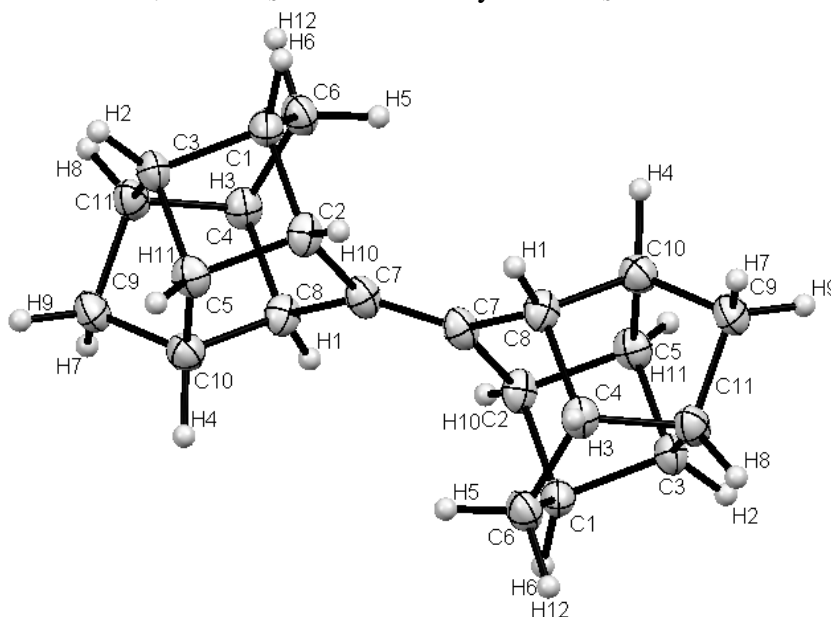
X-Ray structure of adamantylidenediamantane-3 (**14**)Figure A64. The crystal structure of adamantylidenediamantane-3 (**14**).Table A5. Crystallographic key data of adamantylidenediamantane-3 (**14**).

Empirical formula	C ₂₄ H ₃₂
Formula weight; <i>M</i> [g mol ⁻¹]	320.51
Habitus	rectangle crystals
Color	colorless
Melting point [K]	441-442
Space group	C2
Unit cell dimensions:	<i>a</i> 23.135(3) <i>b</i> 6.5721(7) <i>c</i> 14.9065(18) <i>α</i> 90.00 <i>β</i> 128.095(11) <i>γ</i> 90.00
Volume; <i>V</i> [Å ³]	1783.68
Formula units/cell; <i>Z</i>	4
<i>F</i> (000)	816.0
Absorption coeff, mm ⁻¹	0.077
<i>T</i> [K]	293
<i>ρ</i> _{calcd} [g cm ⁻³]	1.387
2 θ _{max} [°]	56.10
Radiation wavelength, Å	Mo-K α (λ = 0.71073 Å)
Limits of <i>h</i> , <i>k</i> , <i>l</i>	-30 30; -8 8; -19 19
Reflections collected	8160
Unique reflections	4305
Number of parameters	345
<i>R</i> 1 [<i>I</i> > 2 σ (<i>I</i>)] (<i>R</i> _{all})	0.0528 (0.0889)
ω <i>R</i> 2 [<i>I</i> > 2 σ (<i>I</i>)] (<i>R</i> _{ref})	0.1261 (0.1452)
<i>R</i> -factor [%]	5.28
Goodness of fit on <i>F</i> 2	0.818
Residual electron density [e/Å ³]	0.05
Largest diff. peak and hole [e/Å ³]	0.26 and -0.24
<i>S</i>	0.818
<i>g</i> (weighting scheme)	0.0759

Table A6. Selected bond lengths and angles of adamantylidenediamantane-3(**14**).

Bond	$d/\text{\AA}$	Bond	$d/\text{\AA}$
C(1) – C(19)	1.522(3)	C(1) – H(25)	0.99(3)
C(4) – C(6)	1.519(3)	C(6) – H(15)	0.96(3)
C(4) – C(10)	1.526(3)	C(10) – H(14)	0.96(3)
C(4) – C(19)	1.325(4)	C(18) – H(3)	0.98(2)
C(18) – C(19)	1.524(3)	H(1) – H(9)	3.89(6)
Angle	$\omega/^\circ$	H(3) – H(14)	1.98(5)
C(1) – C(19) – C(4)	124.8(2)	H(12) – H(20)	3.55(6)
C(4) – C(19) – C(18)	125.1(2)	H(15) – H(25)	1.98(6)
C(6) – C(4) – C(19)	125.3(2)	H(22) – H(32)	3.54(7)
C(10) – C(4) – C(19)	125.0(2)	H(27) – H(28)	3.78(7)

Figure A65. Packing and intermolecular distance in the crystal of adamantylidenediamantane-3 (**14**).

X-Ray structure of *C_i-trans-C₅-8-trishomocubylidene-C₅-8-trishomocubane (135)*Figure A66. The crystal structure of *C_i-trans-C₅-8-trishomocubylidene-C₅-8-trishomocubane (135)*.Table A7. Crystallographic key data of *C_i-trans-C₅-8-trishomocubylidene-C₅-8-trishomocubane (135)*.

Empirical formula	C ₂₄ H ₂₄
Formula weight; <i>M</i> [g mol ⁻¹]	288.41
Habitus	rectangle crystals
Color	colorless
Melting point [K]	503-504
Space group	P -1
Unit cell dimensions:	<i>a</i> 6.4007(11) <i>b</i> 6.6558(12) <i>c</i> 8.6661(16) <i>α</i> 80.31(2) <i>β</i> 86.24(2) <i>γ</i> 79.10(2)
Volume; <i>V</i> [Å ³]	357.14(11)
Formula units/cell; <i>Z</i>	1
<i>F</i> (000)	156
Absorption coeff, mm ⁻¹	0.075
<i>T</i> [K]	293
<i>ρ</i> _{calcd} [g cm ⁻³]	1.341
2 θ max [°]	56.02
Radiation wavelength, Å	Mo-K α (λ = 0.71073 Å)
Limits of <i>h</i> , <i>k</i> , <i>l</i>	-8 8; -7 8; -11 11
Reflections collected	3157
Unique reflections	1578
Number of parameters	148
<i>R</i> 1 [<i>I</i> > 2 σ (<i>I</i>)] (<i>R</i> _{all})	0.0964 (0.1149)
ω <i>R</i> 2 [<i>I</i> > 2 σ (<i>I</i>)] (<i>R</i> _{ref})	0.2560 (0.2648)
<i>R</i> -factor [%]	5.28
Goodness of fit on <i>F</i> ²	1.55
Residual electron density [e/Å ³]	0.082
Largest diff. peak and hole [e/Å ³]	0.44 and -0.47
<i>S</i>	1.55
<i>g</i> (weighting scheme)	0.0440

Table A8. Selected bond lengths and angles of *C_i-trans-C_S-8-trishomocubylidene-C_S-8-trishomocubane* (**135**).

Bond	<i>d</i> /Å	Bond	<i>d</i> /Å
C(1) – C(2)	1.558(5)	C(5) – C(6)	1.543(6)
C(1) – C(7)	1.581(6)	C(5) – C(9)	1.554(6)
C(1) – C(11)	1.523(6)	C(6) – C(7)	1.557(6)
C(2) – C(3)	1.548(6)	C(7) – C(8)	1.505(6)
C(2) – C(6)	1.558(6)	C(8) – C(8')	1.326(8)
C(3) – C(4)	1.522(6)	C(8) – C(9)	1.501(5)
C(3) – C(10)	1.547(6)	C(9) – C(10)	1.582(6)
C(4) – C(5)	1.535(6)	C(10) – C(11)	1.542(6)
Angle	ω/°	Angle	ω/°
C(2) – C(1) – C(11)	105.3(3)	C(5) – C(6) – C(7)	107.2(3)
C(7) – C(1) – C(11)	111.8(4)	C(1) – C(7) – C(6)	89.4(3)
C(2) – C(1) – C(7)	89.8(3)	C(1) – C(7) – C(8)	110.8(3)
C(1) – C(2) – C(3)	107.0(3)	C(6) – C(7) – C(8)	104.4(3)
C(1) – C(2) – C(6)	90.2(3)	C(8') – C(8) – C(7)	128.5(5)
C(3) – C(2) – C(6)	102.3(3)	C(8') – C(8) – C(9)	128.7(5)
C(2) – C(3) – C(4)	104.1(3)	C(7) – C(8) – C(9)	102.8(3)
C(2) – C(3) – C(10)	101.0(3)	C(5) – C(9) – C(8)	103.3(3)
C(4) – C(3) – C(10)	104.7(4)	C(5) – C(9) – C(10)	102.2(3)
C(3) – C(4) – C(5)	94.7(3)	C(8) – C(9) – C(10)	110.9(3)
C(4) – C(5) – C(6)	103.5(4)	C(3) – C(10) – C(9)	102.6(3)
C(4) – C(5) – C(9)	104.4(3)	C(3) – C(10) – C(11)	103.3(3)
C(6) – C(5) – C(9)	100.5(3)	C(9) – C(10) – C(11)	111.4(3)
C(2) – C(6) – C(5)	103.5(3)	C(1) – C(11) – C(10)	100.5(3)
C(2) – C(6) – C(7)	90.7(3)		

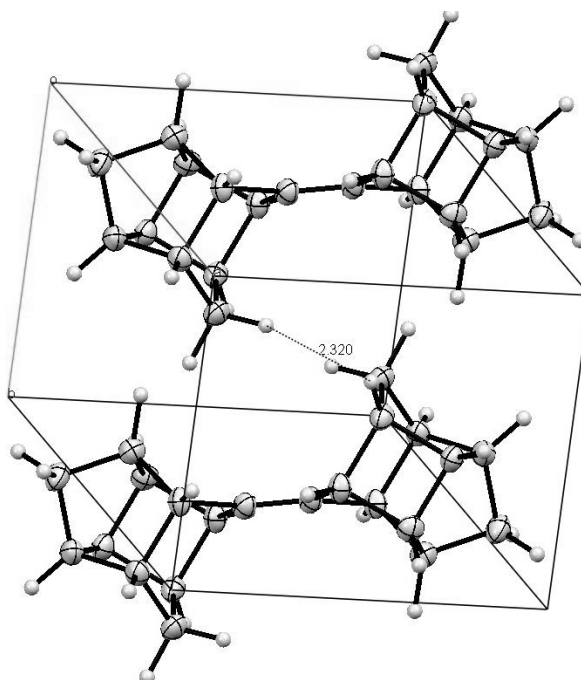
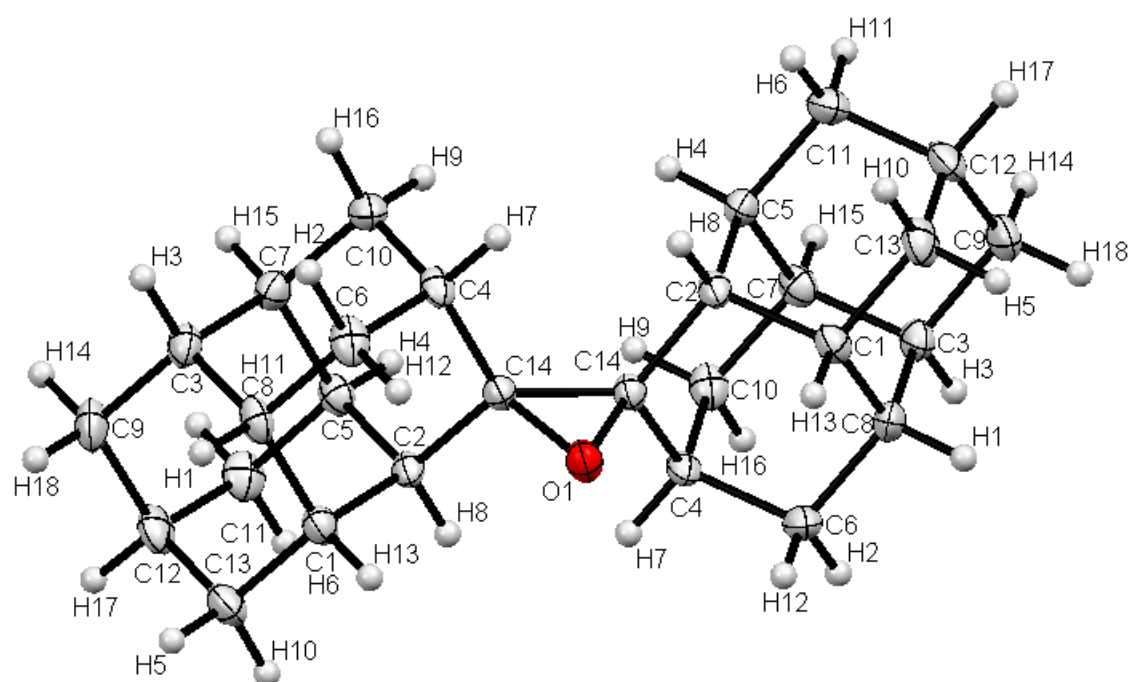


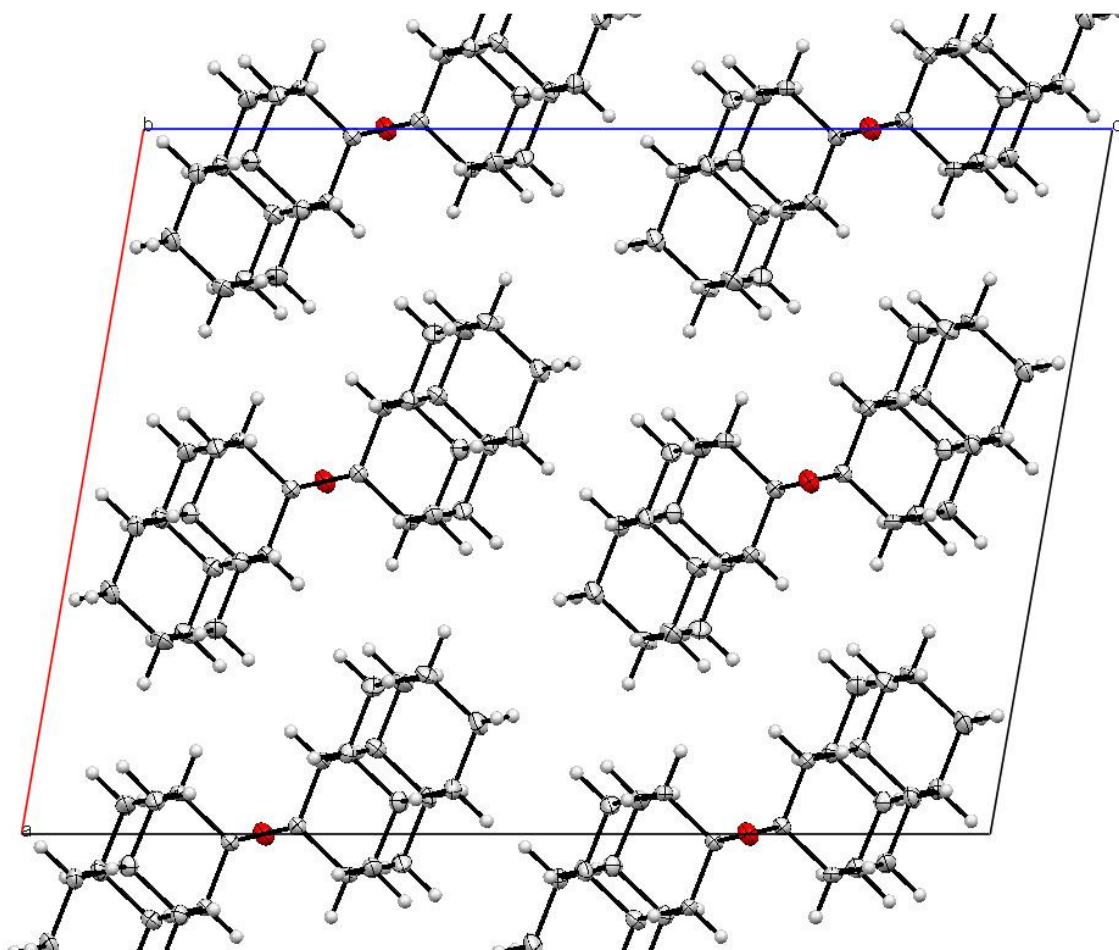
Figure A67. Packing and intermolecular distance in the crystal of *C_i-trans-C_S-8-trishomocubylidene-C_S-8-trishomocubane* (**135**).

X-Ray structure of diamantylidenediamantane epoxide (**142**)Figure A68. The crystal structure of diamantylidenediamantane epoxide (**142**).Table A9. Crystallographic key data of diamantylidenediamantane epoxide (**142**).

Empirical formula	C ₂₈ H ₃₆ O
Formula weight; <i>M</i> [g mol ⁻¹]	388.60
Habitus	rectangle crystals
Color	colorless
Space group	C 2/c
Unit cell dimensions:	<i>a</i> 15.2770(15) <i>b</i> 6.4285(4) <i>c</i> 20.700(2) <i>α</i> 90.00 <i>β</i> 99.842(12) <i>γ</i> 90.00
Volume; <i>V</i> [Å ³]	2002.99
Formula units/cell; <i>Z</i>	4
<i>F</i> (000)	847.9
Absorption coeff, mm ⁻¹	0.075
<i>T</i> [K]	293
<i>ρ</i> _{calcd} [g cm ⁻³]	1.289
2 θ _{max} [°]	54.03
Radiation wavelength, Å	Mo–K α (λ = 0.71073 Å)
Limits of <i>h</i> , <i>k</i> , <i>l</i>	-19 19; -7 8; -26 26
Reflections collected	7478
Unique reflections	2185
Number of parameters	204
<i>R</i> 1 [<i>I</i> > 2 σ (<i>I</i>)] (<i>R</i> _{all})	0.0525 (0.0892)
ω <i>R</i> 2 [<i>I</i> > 2 σ (<i>I</i>)] (<i>R</i> _{ref})	0.1325 (0.1512)
<i>R</i> -factor [%]	5.26
Goodness of fit on <i>F</i> ²	0.896
Residual electron density [e/Å ³]	0.06
Largest diff. peak and hole [e/Å ³]	0.42 and -0.21
<i>S</i>	0.896
<i>g</i> (weighting scheme)	0.0759

Table A10. Selected bond lengths and angles of diamantylidenediamantane epoxide (**142**).

Bond	<i>d</i> /Å	Bond	<i>d</i> /Å
C(4) – C(14)	1.527(2)	C(2) – H(8)	0.94(2)
C(2) – C(14)	1.515(2)	C(4) – H(7)	0.97(2)
C(14) – C(14)	1.478(2)	O(1) – C(14)	1.456(3)
Angle	$\omega/^\circ$		
C(2) – C(14) – C(14)	123.5(2)		
C(4) – C(14) – C(14)	122.7(2)		

Figure A69. Packing in the crystal of diamantylidenediamantane epoxide (**142**).

Appendix III. Cartesian coordinates of selected compounds (M06-2X/CC-pVTZ)**Adamantylidenediamantane-3 (14)**

H	2.89405	-1.25540	1.92059
H	2.89405	1.25540	1.92059
H	-2.38901	-1.25663	-3.34469
H	-2.38901	1.25663	-3.34469
C	-0.11882	0.00000	4.52373
C	-1.65100	-1.24756	2.99496
C	-1.65100	1.24756	2.99496
C	-1.50438	0.00000	3.87062
C	-0.56827	-1.25235	1.91400
C	-0.56827	1.25235	1.91400
C	1.05951	-1.25189	-3.32036
C	1.05951	1.25189	-3.32036
C	0.96204	0.00000	3.44063
C	-0.47194	0.00000	-4.85111
H	-0.00733	-0.88111	5.16184
H	-0.00733	0.88111	5.16184
H	-1.56536	-2.14851	3.60898
H	-1.56536	2.14851	3.60898
C	1.89908	-1.24944	1.46579
C	1.89908	1.24944	1.46579
C	-1.39360	-1.25163	-2.89128
C	-1.39360	1.25163	-2.89128
C	0.82790	1.25055	2.55394
C	0.82790	-1.25055	2.55394
C	-0.32014	1.25450	-3.98228
C	-0.32014	-1.25450	-3.98228
H	-2.64101	-1.26446	2.53035
H	-2.64101	1.26446	2.53035
H	-2.27582	0.00000	4.64327
H	-0.67297	-2.14224	1.28613
H	-0.67297	2.14224	1.28613
H	1.18616	-2.14961	-2.71002
H	1.18616	2.14961	-2.71002
H	0.93476	2.14290	3.17918
H	0.93476	-2.14290	3.17918
H	-0.42805	2.14621	-4.60331
H	-0.42805	-2.14621	-4.60331
C	-0.70333	0.00000	1.01915
C	1.21384	0.00000	-2.43963
C	1.74601	0.00000	0.58451
C	-1.23905	0.00000	-2.00977
C	0.36927	0.00000	-0.05088
C	0.13677	0.00000	-1.36954
H	1.81181	-2.14862	0.85058
H	1.81181	2.14862	0.85058
H	-1.30717	-2.14956	-2.27440
H	-1.30717	2.14956	-2.27440

H	-1.70124	0.00000	0.58427
H	2.20733	0.00000	-2.00157
H	2.53205	0.00000	-0.16474
H	-2.02595	0.00000	-1.26097
H	-1.45094	0.00000	-5.33788
H	1.95277	0.00000	3.90595
H	0.28500	0.00000	-5.64021
H	1.84274	1.25830	-4.08403
H	1.84274	-1.25830	-4.08403

anti-Diamantylidenediamantane (**15**)

H	2.93281	1.25645	-2.30182
H	2.93281	-1.25645	-2.30182
H	-2.93281	1.25645	2.30182
H	-2.93281	-1.25645	2.30182
C	0.24153	0.00000	-5.23912
C	-0.24153	0.00000	5.23912
C	-1.45743	1.24846	-3.90048
C	-1.45743	-1.24846	-3.90048
C	1.45743	1.24846	3.90048
C	1.45743	-1.24846	3.90048
C	-1.21094	0.00000	-4.75279
C	1.21094	0.00000	4.75279
C	-0.50767	1.25313	-2.70140
C	-0.50767	-1.25313	-2.70140
C	0.50767	1.25313	2.70140
C	0.50767	-1.25313	2.70140
C	1.18985	0.00000	-4.03885
C	-1.18985	0.00000	4.03885
H	0.42747	0.88071	-5.86028
H	0.42747	-0.88071	-5.86028
H	-0.42747	0.88071	5.86028
H	-0.42747	-0.88071	5.86028
H	-1.29879	2.14876	-4.50054
H	-1.29879	-2.14876	-4.50054
H	1.29879	2.14876	4.50054
H	1.29879	-2.14876	4.50054
C	1.89144	1.24999	-1.96728
C	1.89144	-1.24999	-1.96728
C	-1.89144	1.24999	1.96728
C	-1.89144	-1.24999	1.96728
C	0.95461	-1.25114	-3.17300
C	0.95461	1.25114	-3.17300
C	-0.95461	-1.25114	3.17300
C	-0.95461	1.25114	3.17300

H	-2.49475	1.26642	-3.55503
H	-2.49475	-1.26642	-3.55503
H	2.49475	1.26642	3.55503
H	2.49475	-1.26642	3.55503
H	-1.88652	0.00000	-5.61028
H	1.88652	0.00000	5.61028
H	-0.68511	2.14238	-2.08945
H	-0.68511	-2.14238	-2.08945
H	0.68511	2.14238	2.08945
H	0.68511	-2.14238	2.08945
H	1.13398	-2.14303	-3.78165
H	1.13398	2.14303	-3.78165
H	-1.13398	-2.14303	3.78165
H	-1.13398	2.14303	3.78165
C	-0.74555	0.00000	-1.82842
C	0.74555	0.00000	1.82842
C	1.63666	0.00000	-1.10989
C	-1.63666	0.00000	1.10989
C	0.19433	0.00000	-0.64111
C	-0.19433	0.00000	0.64111
H	1.73126	2.14872	-1.36646
H	1.73126	-2.14872	-1.36646
H	-1.73126	2.14872	1.36646
H	-1.73126	-2.14872	1.36646
H	-1.78701	0.00000	-1.51183
H	1.78701	0.00000	1.51183
H	2.32759	0.00000	-0.27251
H	-2.32759	0.00000	0.27251
H	-2.22722	0.00000	4.38812
H	2.22722	0.00000	-4.38812

syn-Diamantylidenediamantane (**16**)

H	2.78793	1.25666	-3.05027
H	2.78793	-1.25666	-3.05027
H	2.78793	-1.25666	3.05027
H	2.78793	1.25666	3.05027
C	-0.63599	0.00000	-5.08654
C	-0.63599	0.00000	5.08654
C	-1.87672	1.24837	-3.31478
C	-1.87672	-1.24837	-3.31478
C	-1.87672	-1.24837	3.31478
C	-1.87672	1.24837	3.31478
C	-1.88647	0.00000	-4.20206
C	-1.88647	0.00000	4.20206

C	-0.62161	1.25308	-2.44034
C	-0.62161	-1.25308	-2.44034
C	-0.62161	-1.25308	2.44034
C	-0.62161	1.25308	2.44034
C	0.61807	0.00000	-4.21062
C	0.61807	0.00000	4.21062
H	-0.63690	0.88072	-5.73491
H	-0.63690	-0.88072	-5.73491
H	-0.63690	-0.88072	5.73491
H	-0.63690	0.88072	5.73491
H	-1.89773	2.14874	-3.93501
H	-1.89773	-2.14874	-3.93501
H	-1.89773	-2.14874	3.93501
H	-1.89773	2.14874	3.93501
C	1.88730	1.25000	-2.42961
C	1.88730	-1.25000	-2.42961
C	1.88730	-1.25000	2.42961
C	1.88730	1.25000	2.42961
C	0.64251	-1.25113	-3.31373
C	0.64251	1.25113	-3.31373
C	0.64251	1.25113	3.31373
C	0.64251	-1.25113	3.31373
H	-2.77048	1.26630	-2.68504
H	-2.77048	-1.26630	-2.68504
H	-2.77048	-1.26630	2.68504
H	-2.77048	1.26630	2.68504
H	-2.78065	0.00000	-4.82827
H	-2.78065	0.00000	4.82827
H	-0.61520	2.14237	-1.80328
H	-0.61520	-2.14237	-1.80328
H	-0.61520	-2.14237	1.80328
H	-0.61520	2.14237	1.80328
H	0.63867	-2.14306	-3.94819
H	0.63867	2.14306	-3.94819
H	0.63867	2.14306	3.94819
H	0.63867	-2.14306	3.94819
C	-0.59750	0.00000	-1.53575
C	-0.59750	0.00000	1.53575
C	1.89069	0.00000	-1.53524
C	1.89069	0.00000	1.53524
C	0.64503	0.00000	-0.67000
C	0.64503	0.00000	0.67000
H	1.90707	2.14873	-1.80811
H	1.90707	-2.14873	-1.80811
H	1.90707	-2.14873	1.80811

H	1.90707	2.14873	1.80811
H	-1.50337	0.00000	-0.93230
H	-1.50337	0.00000	0.93230
H	2.79394	0.00000	-0.93307
H	2.79394	0.00000	0.93307
H	1.51077	0.00000	4.84405
H	1.51077	0.00000	-4.84405

C_i-trans-C₅-8-trishomocubylidene-C₅-8-trishomocubane (135)

C	1.47469	-0.34282	2.53865
C	-1.47469	0.34282	-2.53865
C	0.74971	0.73092	1.68686
C	-0.74971	-0.73092	-1.68686
C	0.02096	0.54614	4.01198
C	-0.02096	-0.54614	-4.01198
C	-0.27110	1.35182	2.72447
C	0.27110	-1.35182	-2.72447
C	-0.63341	-1.16669	1.47328
C	0.63341	1.16669	-1.47328
C	0.37145	-1.42191	2.63786
C	-0.37145	1.42191	-2.63786
C	-1.71155	0.97043	2.37700
C	1.71155	-0.97043	-2.37700
C	0.01749	-0.08785	0.65726
C	-0.01749	0.08785	-0.65726
C	1.51910	0.25341	3.94409
C	-1.51910	-0.25341	-3.94409
C	-1.64414	-0.54736	2.50471
C	1.64414	0.54736	-2.50471
C	-0.63157	-0.80845	3.65610
C	0.63157	0.80845	-3.65610
H	2.41381	-0.68631	2.11055
H	-2.41381	0.68631	-2.11055
H	1.41705	1.48298	1.27358
H	-1.41705	-1.48298	-1.27358
H	-0.35062	1.01141	4.92284
H	0.35062	-1.01141	-4.92284
H	-0.11327	2.42272	2.83988
H	0.11327	-2.42272	-2.83988
H	-0.99607	-2.02669	0.91886
H	0.99607	2.02669	-0.91886
H	0.72441	-2.43582	2.80532
H	-0.72441	2.43582	-2.80532
H	-2.01624	1.29924	1.38243
H	2.01624	-1.29924	-1.38243
H	-2.40327	1.39144	3.10927
H	2.40327	-1.39144	-3.10927
H	2.13430	1.15224	4.00862
H	-2.13430	-1.15224	-4.00862

H	1.85055	-0.46118	4.69907
H	-1.85055	0.46118	-4.69907
H	-2.60612	-1.05037	2.55908
H	2.60612	1.05037	-2.55908
H	-0.94273	-1.41427	4.50285
H	0.94273	1.41427	-4.50285

dl-D₃-trishomocubylidene-D₃-trishomocubane (**95**)

C	-0.73053	-0.23526	-4.08058
C	0.73053	0.23526	-4.08058
C	0.73053	-0.23526	4.08058
C	-0.73053	0.23526	4.08058
C	-0.72447	-1.03769	-2.73298
C	0.72447	1.03769	-2.73298
C	0.72447	-1.03769	2.73298
C	-0.72447	1.03769	2.73298
C	0.80120	-1.30332	-2.45896
C	-0.80120	1.30332	-2.45896
C	-0.80120	-1.30332	2.45896
C	0.80120	1.30332	2.45896
C	1.50094	-1.04603	-3.78730
C	-1.50094	1.04603	-3.78730
C	-1.50094	-1.04603	3.78730
C	1.50094	1.04603	3.78730
C	1.12425	-0.03227	-1.65006
C	-1.12425	0.03227	-1.65006
C	-1.12425	-0.03227	1.65006
C	1.12425	0.03227	1.65006
C	0.00000	0.00000	-0.65993
C	0.00000	0.00000	0.65993
H	-1.02410	-0.80804	-4.95795
H	1.02410	0.80804	-4.95795
H	1.02410	-0.80804	4.95795
H	-1.02410	0.80804	4.95795
H	-1.34301	-1.93017	-2.73024
H	1.34301	1.93017	-2.73024
H	1.34301	-1.93017	2.73024
H	-1.34301	1.93017	2.73024
H	1.02090	-2.23313	-1.93992
H	-1.02090	2.23313	-1.93992
H	-1.02090	-2.23313	1.93992
H	1.02090	2.23313	1.93992
H	1.32649	-1.81509	-4.54077
H	-1.32649	1.81509	-4.54077
H	-1.32649	-1.81509	4.54077
H	1.32649	1.81509	4.54077
H	2.57548	-0.90336	-3.66579
H	-2.57548	0.90336	-3.66579
H	-2.57548	-0.90336	3.66579
H	2.57548	0.90336	3.66579
H	2.14078	0.03223	-1.27079

H	-2.14078	-0.03223	-1.27079
H	-2.14078	0.03223	1.27079
H	2.14078	-0.03223	1.27079

meso-*D*₃-trishomocubylidene-*D*₃-trishomocubane (**104**)

C	0.00000	0.00000	0.65982
C	0.00000	0.00000	-0.65982
C	-0.94974	-0.60241	1.64994
C	-0.94974	-0.60241	-1.64994
C	0.94974	0.60241	1.64994
C	0.94974	0.60241	-1.64994
C	0.02091	1.26571	2.73308
C	0.02091	1.26571	-2.73308
C	-0.02091	-1.26571	2.73308
C	-0.02091	-1.26571	-2.73308
C	-1.39227	0.63270	2.45808
C	-1.39227	0.63270	-2.45808
C	1.39227	-0.63270	2.45808
C	1.39227	-0.63270	-2.45808
C	1.82949	-0.02941	3.78637
C	1.82949	-0.02941	-3.78637
C	-1.82949	0.02941	3.78637
C	-1.82949	0.02941	-3.78637
C	0.47469	0.60323	4.08053
C	0.47469	0.60323	-4.08053
C	-0.47469	-0.60323	4.08053
C	-0.47469	-0.60323	-4.08053
H	-1.75706	-1.22314	1.27015
H	-1.75706	-1.22314	-1.27015
H	1.75706	1.22314	1.27015
H	1.75706	1.22314	-1.27015
H	0.03492	2.35150	2.73063
H	0.03492	2.35150	-2.73063
H	-0.03492	-2.35150	2.73063
H	-0.03492	-2.35150	-2.73063
H	-2.09366	1.28068	1.93792
H	-2.09366	1.28068	-1.93792
H	2.09366	-1.28068	1.93792
H	2.09366	-1.28068	-1.93792
H	2.64118	0.68898	3.66531
H	2.64118	0.68898	-3.66531
H	-2.64118	-0.68898	3.66531
H	-2.64118	-0.68898	-3.66531
H	2.11394	-0.76539	4.53938
H	2.11394	-0.76539	-4.53938
H	-2.11394	0.76539	4.53938
H	-2.11394	0.76539	-4.53938
H	0.39906	1.24223	4.95803
H	0.39906	1.24223	-4.95803
H	-0.39906	-1.24223	4.95803
H	-0.39906	-1.24223	-4.95803

Adamantylideneadamantane (**13**)

H	-2.14872	-1.25914	-3.04758
H	-2.14872	1.25914	3.04758
H	2.14872	-1.25914	3.04758
H	2.14872	1.25914	-3.04758
H	-2.14872	-1.25914	3.04758
H	-2.14872	1.25914	-3.04758
H	2.14872	-1.25914	-3.04758
H	2.14872	1.25914	3.04758
C	1.24586	-1.25266	-2.43047
C	1.24586	1.25266	2.43047
C	-1.24586	-1.25266	2.43047
C	-1.24586	1.25266	-2.43047
C	1.24586	-1.25266	2.43047
C	1.24586	1.25266	-2.43047
C	-1.24586	-1.25266	-2.43047
C	-1.24586	1.25266	2.43047
C	0.00000	0.00000	-4.20101
C	0.00000	0.00000	4.20101
C	0.00000	1.25511	-3.31991
C	0.00000	-1.25511	3.31991
C	0.00000	1.25511	3.31991
C	0.00000	-1.25511	-3.31991
H	1.26519	-2.14977	-1.80693
H	1.26519	2.14977	1.80693
H	-1.26519	-2.14977	1.80693
H	-1.26519	2.14977	-1.80693
H	1.26519	-2.14977	1.80693
H	1.26519	2.14977	-1.80693
H	-1.26519	-2.14977	-1.80693
H	-1.26519	2.14977	1.80693
H	0.00000	2.14598	3.95110
H	0.00000	-2.14598	-3.95110
H	0.00000	2.14598	-3.95110
H	0.00000	-2.14598	3.95110
C	1.24599	0.00000	-1.53641
C	1.24599	0.00000	1.53641
C	-1.24599	0.00000	1.53641
C	-1.24599	0.00000	-1.53641
C	0.00000	0.00000	-0.66946
C	0.00000	0.00000	0.66946
H	2.14868	0.00000	-0.93284
H	2.14868	0.00000	0.93284
H	-2.14868	0.00000	0.93284
H	-2.14868	0.00000	-0.93284
H	0.88044	0.00000	4.84935
H	0.88044	0.00000	-4.84935
H	-0.88044	0.00000	-4.84935
H	-0.88044	0.00000	4.84935

Ethylene (**138**)

C	0.00000	0.00000	-0.66094
C	0.00000	0.00000	0.66094
H	-0.92224	0.00000	-1.22679
H	0.92224	0.00000	-1.22679
H	0.92224	0.00000	1.22679
H	-0.92224	0.00000	1.22679

Tetramethylethylene (**139**)

C	0.00000	0.00000	0.66801
C	0.00000	0.00000	-0.66801
C	1.24710	0.02943	1.51246
C	-1.24710	-0.02943	1.51246
C	-1.24710	0.02943	-1.51246
C	1.24710	-0.02943	-1.51246
H	-1.13345	-0.77362	2.30433
H	1.13345	0.77362	2.30433
H	1.13345	-0.77362	-2.30433
H	-1.13345	0.77362	-2.30433
H	-1.39725	0.93255	2.01009
H	1.39725	-0.93255	2.01009
H	1.39725	0.93255	-2.01009
H	-1.39725	-0.93255	-2.01009
H	-2.14841	-0.27254	0.95923
H	2.14841	0.27254	0.95923
H	2.14841	-0.27254	-0.95923
H	-2.14841	0.27254	-0.95923

Tetra-*iso*-propylethylene (**140**)

C	0.09731	0.00000	0.66387
C	-0.09731	0.00000	-0.66387
C	-1.46879	0.00000	-1.34506
C	1.46879	0.00000	1.34506
C	-1.05115	0.00000	1.66118
C	1.05115	0.00000	-1.66118
C	-1.05291	1.26365	2.52725
C	-1.05291	-1.26365	2.52725
C	1.05291	1.26365	-2.52725
C	1.05291	-1.26365	-2.52725
C	-2.28216	1.27792	-1.11134
C	-2.28216	-1.27792	-1.11134
C	2.28216	1.27792	1.11134
C	2.28216	-1.27792	1.11134
H	-1.26138	0.00000	-2.41537
H	1.26138	0.00000	2.41537
H	-1.98690	0.00000	1.11715
H	1.98690	0.00000	-1.11715
H	-1.91776	1.26371	3.19266

H	-1.91776	-1.26371	3.19266
H	1.91776	1.26371	-3.19266
H	1.91776	-1.26371	-3.19266
H	-1.09950	2.15893	1.90531
H	-1.09950	-2.15893	1.90531
H	1.09950	2.15893	-1.90531
H	1.09950	-2.15893	-1.90531
H	-0.16088	1.33470	3.15176
H	-0.16088	-1.33470	3.15176
H	0.16088	1.33470	-3.15176
H	0.16088	-1.33470	-3.15176
H	-3.16188	1.28424	-1.75778
H	-3.16188	-1.28424	-1.75778
H	3.16188	1.28424	1.75778
H	3.16188	-1.28424	1.75778
H	-1.68204	2.15756	-1.34722
H	-1.68204	-2.15756	-1.34722
H	1.68204	2.15756	1.34722
H	1.68204	-2.15756	1.34722
H	-2.62731	1.38266	-0.08429
H	-2.62731	-1.38266	-0.08429
H	2.62731	1.38266	0.08429
H	2.62731	-1.38266	0.08429

Tetra-*tert*-butylethylene (**141**)

C	0.00000	0.00000	-0.68504
C	0.00000	0.00000	0.68504
C	1.22515	-0.52331	1.52521
C	1.22515	0.52331	-1.52521
C	-1.22515	-0.52331	-1.52521
C	-1.22515	0.52331	1.52521
C	2.12317	1.46100	-0.69633
C	2.12317	-1.46100	0.69633
C	-2.12317	1.46100	0.69633
C	-2.12317	-1.46100	-0.69633
C	0.65795	1.49048	-2.59370
C	0.65795	-1.49048	2.59370
C	-0.65795	1.49048	2.59370
C	-0.65795	-1.49048	-2.59370
C	2.14028	-0.48981	-2.27897
C	2.14028	0.48981	2.27897
C	-2.14028	-0.48981	2.27897
C	-2.14028	0.48981	-2.27897
H	2.77295	2.01000	-1.37974
H	2.77295	-2.01000	1.37974
H	-2.77295	2.01000	1.37974
H	-2.77295	-2.01000	-1.37974
H	2.76864	0.95240	0.00677
H	2.76864	-0.95240	-0.00677
H	-2.76864	0.95240	-0.00677
H	-2.76864	-0.95240	0.00677

H	1.52017	2.18628	-0.14846
H	1.52017	-2.18628	0.14846
H	-1.52017	2.18628	0.14846
H	-1.52017	-2.18628	-0.14846
H	1.49949	1.94440	-3.11808
H	1.49949	-1.94440	3.11808
H	-1.49949	1.94440	3.11808
H	-1.49949	-1.94440	-3.11808
H	0.08171	2.29291	-2.13128
H	0.08171	-2.29291	2.13128
H	-0.08171	2.29291	2.13128
H	-0.08171	-2.29291	-2.13128
H	0.03752	1.00377	-3.33710
H	0.03752	-1.00377	3.33710
H	-0.03752	1.00377	3.33710
H	-0.03752	-1.00377	-3.33710
H	1.98275	-0.43750	-3.35574
H	1.98275	0.43750	3.35574
H	-1.98275	-0.43750	3.35574
H	-1.98275	0.43750	-3.35574
H	1.98932	-1.51996	-1.97824
H	1.98932	1.51996	1.97824
H	-1.98932	-1.51996	1.97824
H	-1.98932	1.51996	-1.97824
H	3.18965	-0.24803	-2.10233
H	3.18965	0.24803	2.10233
H	-3.18965	-0.24803	2.10233
H	-3.18965	0.24803	-2.10233

Appendix IV. List of Symbols and Abbreviations

°	grade
°C	degree Celsius
1D and 2D	single and two dimension spectral data
APT	Attached Proton Test spectrum
<i>ca.</i>	about
COSY	Correlation Spectroscopy
CVD	Chemical Vapor Deposition
d	doublet (in proton spectral data sets)
dd	doublet of doublets (in proton spectral data sets)
DEPT	Distortionless Enhancement by Polarization Transfer
DFT	Density Functional Theory
DME	dimethoxyethane
dt	doublet of triplets (in proton spectral data sets)
<i>e.g.</i>	<i>exempli gratia</i>
GC/MS	Gas chromatography/mass spectrometry
HMBC	Heteronuclear multiple-bond correlation spectroscopy
HR-MS	High Resolution Mass Spectrographer
HSQC	Heteronuclear single-quantum correlation spectroscopy
Hz	hertz
<i>i.e.</i>	<i>id est</i>
<i>in situ</i>	in the reaction mixture
<i>J</i>	indirect dipole dipole coupling
m	multiplet (in proton spectral data sets)
<i>m/z</i>	mass-to-charge ratios
mp	melting point
MW	microwave
NBS	N-bromosuccinimide
NEA	Negative Electron Affinity
NMR	Nuclear Magnetic Resonance
NOESY	Nuclear Overhauser effect Spectroscopy
<i>p-</i>	<i>para-</i>
ppm	parts-per-million
PTC	Phase Transfer Catalysis
Py	pyridine
q	quaternary (in carbon spectral data sets)

s	singlet (in proton spectral data sets)
s	secondary (in carbon spectral data sets)
t	triplet (in proton spectral data sets)
t	tertiary (in carbon spectral data sets)
THF	tetrahydrofurane
TMS	tetramethylsilane
TOCSY	Total Correlation Spectroscopy
TS	transition structure
<i>vs</i>	<i>versus</i>
Å	angstrom
δ	chemical shift

References

- [1] G. F. Cerofolini, G. Arena, C. M. Camalleri, C. Galati, S. Reina, L. Renna, D. Mascolo, *Nanotechnology* **2005**, *16*, 1040.
- [2] W. Ho, *J. Chem. Phys.* **2002**, *117*, 11033.
- [3] N. R. Greiner, D. S. Phillips, J. D. Johnson, F. Volk, *Nature* **1988**, *333*, 440.
- [4] J. C. Angus, A. Argoitia, R. Gat, Z. Li, M. Sunkara, L. Wang, Y. Wang, *Phil. Trans. R. Soc. Lond. A* **1993**, *342*, 195.
- [5] P. Badziag, W. S. Verwoerd, W. P. Ellis, N. R. Greiner, *Nature* **1990**, *343*, 244.
- [6] Y. K. Chang, H. H. Hsieh, W. F. Pong, M. H. Tsai, F. Z. Chien, P. K. Tseng, L. C. Chen, T. Y. Wang, K. H. Chen, D. M. Bhusari, J. R. Yang, S. T. Lin, *Phys. Rev. Lett.* **1999**, *82*, 5377.
- [7] J. Y. Raty, G. Galli, C. Bostedt, T. W. van Buuren, L. J. Terminello, *Phys. Rev. Lett.* **2003**, *90*, 0374011.
- [8] T. van Buuren, L. N. Dinh, L. L. Chase, W. J. Siekhaus, L. J. Terminello, *Phys. Rev. Lett.* **2004**, *80*, 3803.
- [9] C. Bostedt, T. van Buuren, T. M. Willey, N. Franco, L. J. Terminello, C. Heske, T. Möller, *App. Phys. Lett.* **2004**, *84*, 4056.
- [10] H. Kato, S. Yamasaki, H. Okushi, *App. Phys. Lett.* **2005**, *86*, 222111.
- [11] X. Blase, C. Adessi, D. Connetable, *Phys. Rev. Lett.* **2004**, *93*, 237004.
- [12] K. W. Lee, W. E. Pickett, *Phys. Rev. Lett.* **2004**, *93*, 237003.
- [13] J. E. Butler, I. Oleynik, *Phil. Trans. R. Soc. A* **2008**, *366*, 295.
- [14] A. Badzian, T. Badzian, *Ceram. Int.* **1996**, *22*, 223.
- [15] F. Cleri, P. Keblinski, L. Colombo, D. Wolf, S. R. Phillpot, *Europhys. Lett.* **1999**, *46*, 671.
- [16] S. Osswald, G. Yushin, V. Mochalin, S. O. Kucheyev, Y. Gogotsi, *J. Am. Chem. Soc.* **2006**, *128*, 11635.
- [17] B. Slepetz, I. Laszlo, Y. Gogotsi, D. Hyde-Volpe, M. Kertesz, *Phys. Chem. Chem. Phys* **2010**, *12*, 14017.
- [18] O. A. Shenderova, G. McGuire, **2006**, 203.
- [19] D. M. Gruen, O. A. Shenderova, A. Y. Vul, *Ultrananocrystalline diamond : synthesis, properties, and applications*, **2005**.
- [20] A. A. Fokin, P. R. Schreiner, *Mol. Phys.* **2009**, *107*, 823.
- [21] O. A. Shenderova, V. V. Zhirnov, D. W. Brenner, *Crit. Rev. Solid State Mater. Sci.* **2002**, *27*, 227.

- [22] S. Gupta, A. M. Scuttler, J. Farmer, *J. Appl. Phys.* **2010**, *107*, 104308.
- [23] A. V. Karabutov, V. D. Frolov, V. I. Konov, *Diam. Relat. Mater.* **2001**, *10*, 840.
- [24] J. Ristein, *Diam. Relat. Mater.* **2000**, *9*, 1129.
- [25] J. Ristein, F. Maier, M. Riedel, J. B. Cui, L. Ley, *Phys. Stat. Sol. A* **2000**, *181*, 65.
- [26] Y. Liu, Z. Gu, J. L. Margrave, V. N. Khabashesku, *Chem. Mater.* **2004**, *16*, 3924.
- [27] T. Tsubota, O. Hirabayashi, S. Ida, S. Nagaoka, M. Nagata, Y. Matsumoto, *Phys. Chem. Chem. Phys.* **2002**, *4*, 806
- [28] A. Kruger, Y. Liang, G. Jarre, J. Stegk, *J. Mater. Chem.* **2006**, *16*, 2322.
- [29] T. Nakamura, M. Ishihara, T. Ohana, Y. Koga, *Chem. Comm.* **2003**, 900.
- [30] A. Krüger, Y. Liang, G. Jarre, J. Stegk, *J. Mater. Chem.* **2006**, *16*, 2322.
- [31] R. Lin, Z. A. Wilk, *Fuel* **1995**, *74*, 1512.
- [32] J. E. Dahl, S. G. Liu, R. M. K. Carlson *Science* **2003**, *299*, 96.
- [33] H. Schwertfeger, A. A. Fokin, P. R. Schreiner, *Angew. Chem. Int. Ed.* **2008**, *47*, 1022.
- [34] Z. Wang, C. Yang, B. Hollebone, M. Fingas, *Environ. Sci. Technol.* **2006**, *40*, 5636.
- [35] D.-M. Shen, M. M. Wu, *US5345020 Pat.* **1994**.
- [36] D.-M. Shen, M. M. Wu, *US5367097 Pat.* **1994**.
- [37] J. E. Dahl, R. M. K. Carlson, S. Liu, *US7061073 Pat.* **2006**.
- [38] S. Liu, J. E. Dahl, R. M. K. Carlson *US7304190 Pat.* **2007**.
- [39] J. E. Dahl, R. M. K. Carlson, S. Liu, *US7306671 Pat.* **2007**.
- [40] G. C. McIntosh, M. Yoon, S. Berber, D. Tománek, *Phys. Rev. B* **2004**, *70*, 045401.
- [41] R. M. K. Carlson, J. E. Dahl, S. Liu, *US7309476 Pat.* **2007**.
- [42] D. Lässig, J. Lincke, R. Gerhardt, H. Krautscheid, *Inorg. Chem.* **2012**, *51*, 6180–6189.
- [43] M. J. Zaworotko, *Chem. Soc. Rev.* **1994**, 283.
- [44] N. N. Adarsh, P. Dastidar, *Chem. Soc. Rev.* **2012**, *41*, 3039.
- [45] S. D. Karlen, R. Ortiz, O. L. Chapman, M. A. Garcia-Garibay, *J. Am. Chem. Soc.* **2005**, *127*, 6554.
- [46] J. Voskuhl, M. Waller, S. Bandaru, B. A. Tkachenko, C. Fregonese, B. Wibbeling, P. R. Schreiner, B. J. Ravoo, *Org. Biomol. Chem.* **2012**, *10*, 4524.
- [47] A. A. Spasov, T. V. Khamidova, L. I. Bugaeva, I. S. Morozov, *Pharm. Chem. J.* **2000**, *34*, 1.
- [48] H. Enomoto, A. Sawa, H. Suhara, N. Yamamoto, H. Inoue, C. Setoguchi, F. Tsuji, M. Okamoto, Y. Sasabuchi, M. Horiuchi, M. Ban, *Bioorg. Med. Chem. Lett.* **2010**, *20*, 4479.
- [49] W. E. Heyd, L. T. Bell, J. R. Heystek, P. E. Schurr, C. E. Day, *J. Med. Chem.* **1982**, *25*, 1101.

- [50] A. A. Fokin, A. Merz, N. A. Fokina, H. Schwertfeger, S. L. Liu, J. E. P. Dahl, R. K. M. Carlson, P. R. Schreiner, *Synthesis* **2009**, 909.
- [51] J.-J. Wanga, K.-T. Huang, Y.-T. Chern, *Anti-Cancer Drugs* **2004**, *15*, 277.
- [52] C. Sinkel, S. Agarwal, N. A. Fokina, P. R. Schreiner, *J. Appl. Polym. Sci.* **2009**, *114*, 2109.
- [53] Y. Wang, B. A. Tkachenko, P. R. Schreiner, A. Marx, *Org. Biomol. Chem.* **2011**, *9*, 7482.
- [54] A. Nitzan, M. A. Ratner, *Science* **2003**, *300*, 1384.
- [55] A. Schnurpfeil, M. Albrecht, *Theor. Chem. Acc.* **2007**, *117*, 29.
- [56] A. A. Fokin, E. D. Butova, L. V. Chernish, N. A. Fokina, J. E. P. Dahl, R. M. K. Carlson, P. R. Schreiner, *Org. Lett.* **2007**, *9*, 2541.
- [57] J. M. Buriak, *Chem. Rev.* **2002**, *102*, 1271.
- [58] V. N. Mochalin, O. A. Shenderova, D. Ho, Y. Gogotsi, *Nat. Nanotech.* **2012**, *7*, 11.
- [59] L. Lai, A. S. Barnard, *Nanoscale* **2011**, *3*, 2566.
- [60] L. Lai, A. S. Barnard, *J. Phys. Chem. C* **2011**, *115*, 6218.
- [61] D. Hea, L. Shao, W. Gong, E. Xie, K. Xub, G. Chen, *Diam. Relat. Mater.* **2000**, *9*, 1600.
- [62] K. Subramanian, W. P. Kang, J. L. Davidson, B. K. Choi, M. Howell, *Diam. Relat. Mater.* **2006**, *15*, 1994.
- [63] N. D. Drummond, A. J. Williamson, R. J. Needs, G. Galli, *Phys. Rev. Lett.* **2005**, *95*, 096801.
- [64] T. M. Willey, J. D. Fabbri, J. R. I. Lee, P. R. Schreiner, A. A. Fokin, B. A. Tkachenko, N. A. Fokina, J. E. P. Dahl, R. M. K. Carlson, A. L. Vance, W. Yang, L. J. Terminello, T. van Buuren, N. A. Melosh, *J. Am. Chem. Soc.* **2008**, *130*, 10536.
- [65] W. A. Clay, Z. Liu, W. Yang, J. D. Fabbri, J. E. Dahl, R. M. K. Carlson, Y. Sun, P. R. Schreiner, A. A. Fokin, B. A. Tkachenko, N. A. Fokina, P. A. Pianetta, N. Melosh, Z.-X. Shen, *Nano Lett.* **2009**, *9*, 57.
- [66] T. M. Willey, J. R. I. Lee, J. D. Fabbri, D. Wang, M. H. Nielsen, J. C. Randel, P. R. Schreiner, A. A. Fokin, B. A. Tkachenko, N. A. Fokina, J. E. P. Dahl, R. M. K. Carlson, L. J. Terminello, N. A. Melosh, T. van Buuren, *J. Electron Spectrosc. Relat. Phenom.* **2009**, *172*, 69.
- [67] S. Roth, D. Leuenberger, J. Osterwalder, J. E. Dahl, R. M. K. Carlson, B. A. Tkachenko, A. A. Fokin, P. R. Schreiner, M. Hengsberger, *Chem. Phys. Lett.* **2010**, *495*, 102.
- [68] T. M. Willey, C. Bostedt, T. van Buuren, J. E. Dahl, S. G. Liu, R. M. K. Carlson, L. J. Terminello, T. Möller, *Phys. Rev. Lett.* **2005**, *95*, 113401.
- [69] T. J. Hingston, M. R. Sambrook, K. Porfyrakis, G. A. D. Briggs, *Tetr. Lett.* **2006**, *47*, 7413.

- [70] A. Salomon, D. Cahen, S. Lindsay, J. Tomfohr, V. B. Engelkes, C. D. Frisbie, *Adv. Mater.* **2003**, *15*, 1881.
- [71] H. W. Geluk, *Synthesis* **1970**, 652.
- [72] P. D. Bartlett, M. S. Ho, *J. Am. Chem. Soc.* **1974**, 96.
- [73] T. Okazaki, K. Ogawa, T. Kitagawa, K. Takeuchi, *J. Org. Chem.* **2002**, *67*, 5981.
- [74] D. H. R. Barton, B. J. Willis, *J. Chem. Soc., Perk. Trans.* **1972**, *1*.
- [75] A. P. Schaap, G. R. Faler, *J. Org. Chem.* **1973**, *38*, 3061.
- [76] J. H. Wieringa, J. Strating, H. Wynberg, *Tetr. Lett.* **1970**, *11*.
- [77] E. W. Meijer, R. M. Kellogg, H. Wynberg, *J. Org. Chem.* **1982**, *47*, 2005.
- [78] C. Walling, B. B. Jacknow, *J. Am. Chem. Soc.* **1960**, 82.
- [79] C. Walling, W. Thaler, *J. Am. Chem. Soc.* **1961**, 83.
- [80] J. C. Hummelen, T. M. Luider, H. Wynberg, *Methods Enzymol.* **1986**, *133*.
- [81] H. Wynberg, H. Numan, *J. Am. Chem. Soc.* **1977**, 99.
- [82] G. A. Tolstikov, B. M. Lerman, T. A. Belogaeva, *Izv. AN SSSR Ser. Chem.* **1988**.
- [83] J. E. McMurry, M. P. Fleming, *J. Am. Chem. Soc.* **1974**, *96*, 4708.
- [84] J. E. McMurry, *Acc. Chem. Res.* **1983**, *16*, 405.
- [85] T. Mukaiyama, T. Sato, J. Hanna, *Chem. Lett.* **1973**.
- [86] S. Tyrlik, I. Wolochowicz, *Bull. Soc. Chim. Fr.* **1973**, 2147.
- [87] J. E. McMurry, M. P. Fleming, K. L. Kees, L. R. Krepski, *J. Org. Chem.* **1978**, *43*.
- [88] X.-F. Duan, J. Zeng, J.-W. Lii, Z.-B. Zhang, *J. Org. Chem.* **2006**, *71*.
- [89] H. Hopf, C. Mlynek, *J. Org. Chem.* **1990**, 55.
- [90] R. Dams, M. Malinowski, H. J. Geise, *Bull. Soc. Chim. Belg.* **1982**, *91*.
- [91] J. E. McMurry, M. P. Fleming, *J. Org. Chem.* **1976**, *41*.
- [92] J. E. McMurry, L. R. Krepski, *J. Org. Chem.* **1976**, *41*.
- [93] J. E. McMurry, T. Lectka, J. G. Rico, *J. Org. Chem.* **1989**, *54*, 3748.
- [94] A. Fürstner, A. Hupperts, A. Ptock, E. Janssen, *J. Org. Chem.* **1994**, *59*.
- [95] A. Fürstner, D. N. Jumbam, *Tetrahedron* **1992**, *48*.
- [96] S. Rele, S. Chattopadhyay, S. K. Nayak, *Tetr. Lett.* **2001**, *42*.
- [97] N. Stühr-Hansen, *Tetr. Lett.* **2005**, *46*.
- [98] S. K. Nayak, A. Banerji, *J. Org. Chem.* **1991**, *56*.
- [99] P. G. Taylor, *Mechanisms and Synthesis*, **2002**.
- [100] R. Dams, M. Malinowski, I. Westdorp, H. J. Geise, *J. Org. Chem.* **1982**, *47*.
- [101] E. J. Corey, R. L. Danheiser, S. Chandrasekaran, *J. Org. Chem.* **1976**, *41*.
- [102] H. Idriss, K. G. Pierce, M. A. Barteau, *J. Am. Chem. Soc.* **1994**, *116*.
- [103] L. E. Aleandri, S. Becke, B. Bogdanovic, D. J. Jones, *J. Organomet. Chem.* **1994**, *472*.

- [104] B. Bogdanovic, A. Bolte, *J. Organomet. Chem.* **1995**, 502.
- [105] M. Stahl, U. Pidun, G. Frenking, *Angew. Chem. Int. Ed.* **1997**, 36, 2234.
- [106] C. Villiers, M. Ephritikhine, *Angew. Chem. Int. Ed.* **1997**, 36, 2380.
- [107] C. Villiers, A. Vandaïs, M. Ephritikhine, *J. Organomet. Chem.* **2001**, 617-618, 744.
- [108] J. E. McMurry, J. G. Rico, *Tetr. Lett.* **1989**, 30.
- [109] M. Bandini, P. G. Cozzi, S. Morganti, A. Umani-Ronchi, *Tetr. Lett.* **1999**, 40.
- [110] A. Chatterjee, T. H. Bennur, N. N. Joshi, *J. Org. Chem.* **2003**, 68.
- [111] Y.-G. Li, Q.-S. Tian, J. Zhao, Y. Feng, M.-J. Li, T. You, *Tetrahedron: Asymmetry* **2004**, 15.
- [112] J. E. McMurry, D. D. Miller, *J. Am. Chem. Soc.* **1983**, 105.
- [113] H. M. Walborsky, H. H. Wüst, *J. Am. Chem. Soc.* **1982**, 104, 5807.
- [114] T. Mukaiyama, Y. Ogawa, K. Kuroda, J.-I. Matsuo, *Chem. Lett.* **2004**, 33.
- [115] U. Eilitz, C. Bottcher, J. Sieler, S. Gockel, A. Haas, K. Burger, *Tetrahedron* **2001**, 57.
- [116] A. Detsi, M. Koufaki, T. Calogeropoulou, *J. Org. Chem.* **2002**, 67.
- [117] I. Columbus, S. Biali, *J. Org. Chem.* **1994**, 59.
- [118] J. E. McMurry, G. J. Haley, J. R. Matz, J. C. Clardy, J. Mitchell, *J. Am. Chem. Soc.* **1986**, 108.
- [119] S. J. Emond, P. Debroy, R. Rathore, *Org. Lett.* **2008**, 10.
- [120] G. A. Tolstikov, B. M. Lerman, T. A. Belogaeva, *Synth. Comm.* **1991**, 21.
- [121] D. Lenoir, R. M. Frank, *Tetr. Lett.* **1978**.
- [122] D. Lenoir, R. M. Frank, F. Cordt, A. Gieren, V. Lamm, *Chem. Ber.* **1980**, 113.
- [123] D. Lenoir, *Synthesis* **1977**.
- [124] R. S. Villasenor, C. R. Johnson, *Org. Synth.* **1981**, 60.
- [125] G. A. Olah, G. K. S. Prakash, *Synthesis* **1976**.
- [126] A. P. Marchand, G. M. Reddy, M. N. Deshpande, W. H. Watson, A. Nagl, O. S. Lee, E. Osawa, *J. Am. Chem. Soc.* **1990**, 112, 3521.
- [127] B. A. Vastine, M. B. Hall, *J. Am. Chem. Soc.* **2007**, 129, 12068.
- [128] C. I. Herrerías, X. Yao, Z. Li, C.-J. Li, *Chem. Rev.* **2007**, 107, 2546.
- [129] M. Newcomb, P. H. Toy, *Acc. Chem. Res.* **2000**, 33, 449.
- [130] M. Costas, K. Chen, L. Que, Jr., *Coordin. Chem. Rev.* **2000**, 200-202, 517.
- [131] R. N. Austin, H.-K. Chang, G. J. Zylstra, J. T. Groves, *J. Am. Chem. Soc.* **2000**, 122, 11747.
- [132] N. A. Fokina, B. A. Tkachenko, J. E. P. Dahl, R. M. K. Carlson, A. A. Fokin, P. R. Schreiner, *Synthesis* **2012**, 2012, 259.

- [133] A. A. Fokin, P. A. Gunchenko, A. A. Novikovskiy, T. E. Shubina, B. V. Chernyaev, J. E. P. Dahl, R. M. K. Carlson, A. G. Yurchenko, P. R. Schreiner, *Eur. J. Org. Chem.* **2009**, 2009, 5153.
- [134] N. A. Fokina, B. A. Tkachenko, M. A., M. Serafin, J. E. P. Dahl, R. M. K. Carlson, A. A. Fokin, P. R. Schreiner, *Eur. J. Org. Chem.* **2007**, 4738.
- [135] A. A. Fokin, B. A. Tkachenko, N. A. Fokina, H. Hausmann, M. Serafin, J. E. P. Dahl, R. M. K. Carlson, P. R. Schreiner, *Chem. Eur. J.* **2009**, 15, 3851.
- [136] H. Schwertfeger, C. Würtele, M. Serafin, H. Hausmann, R. M. K. Carlson, J. E. P. Dahl, P. R. Schreiner, *J. Org. Chem.* **2008**, 73, 7789.
- [137] J. Strating, J. H. Wieringa, H. Wynberg, *J. Chem. Soc. D* **1969**, 907.
- [138] H. Slebocka-Tilk, R. G. Ball, R. S. Brown, *J. Am. Chem. Soc.* **1985**, 107, 4504.
- [139] R. S. Brown, R. Gedy, H. Slebocka-Tilk, J. M. Buscher, K. R. Kopecky, *J. Am. Chem. Soc.* **1984**, 106.
- [140] I. Roberts, G. E. Kimball, *J. Am. Chem. Soc.* **1937**, 59.
- [141] S. M. Islam, R. A. Poirier, *J. Phys. Chem. A* **2008**, 112, 152.
- [142] G. Bellucci, R. Bianchini, C. Chiappe, F. Marioni, R. Ambrosetti, R. S. Brown, H. Slebocka-Tilk, *J. Am. Chem. Soc.* **1989**, 111, 2640.
- [143] G. Bellucci, R. Bianchini, C. Chiappe, R. Ambrosetti, D. Catalano, A. J. Bennet, H. Slebocka-Tilk, G. H. M. Aarts, R. S. Brown, *J. Org. Chem.* **1993**, 58, 3401.
- [144] C. Chiappe, A. D. Rubertis, A. Jaber, D. Lenoir, C. Wattenbach, C. S. Pomelli, *J. Org. Chem.* **2002**, 67, 7066.
- [145] C. Chiappe, H. Detert, D. Lenoir, C. Pomelli, M. F. Ruasse, *J. Am. Chem. Soc.* **2003**, 125, 2864.
- [146] W. A. Nugent, *J. Org. Chem.* **1980**, 45, 4533.
- [147] T. Mori, R. Rathore, S. V. Lindeman, J. K. Kochi, *Chem. Comm.* **1998**, 927.
- [148] G. A. Olah, P. Schilling, P. W. Westerman, H. C. Lin, *J. Am. Chem. Soc.* **1974**, 96.
- [149] J. Bolster, R. M. Kellogg, *J. Chem. Soc., Chem. Comm.* **1978**.
- [150] Y. Sugihara, K. Onda, M. Sato, T. Suzuki, *Tetr. Lett.* **2010**, 51, 4110.
- [151] I. A. Abu-Yousef, D. N. Harpp, *Tetr. Lett.* **1995**, 36, 201.
- [152] I. A. Abu-Yousef, D. N. Harpp, *J. Org. Chem.* **1997**, 62, 8366.
- [153] J. Nakayama, Y. Tajima, P. Xue-hua, Y. Sugihara, *J. Am. Chem. Soc.* **2007**, 129, 7250.
- [154] A. P. Marchand, V. Vidyasagar, W. H. Watson, A. Nagl, R. P. Kashyap, *J. Org. Chem.* **1991**, 56.
- [155] H. Keul, *Chem. Ber.* **1972**, 108.

- [156] Y. Dong, J. Chollet, H. Matile, S. A. Charman, F. C. K. Chiu, W. N. Charman, B. Scoreaux, H. Urwyler, J. Santo Tomas, C. Scheurer, C. Snyder, A. Dorn, X. Wang, J. M. Karle, Y. Tang, S. Wittlin, R. Brun, J. L. Vennerstrom, *J. Med. Chem.* **2005**, *48*, 4953.
- [157] J. H. Wieringa, J. Strating, H. Wynberg, W. Adam, *Tetr. Lett.* **1972**.
- [158] H. Numan, J. H. Wieringa, H. Wynberg, J. Hess, A. Vos, *Chem. Comm.* **1977**.
- [159] Y. Maeda, Y. Niino, T. Kondo, M. Yamada, T. Hasegawa, T. Akasaka, *Chem. Lett.* **2011**, *40*, 1431.
- [160] Y. Chen, A. J. H. Spiering, S. Karthikeyan, G. W. M. Peters, E. W. Meijer, R. P. Sijbesma, *Nat. Chem.* **2012**, *4*, 559.
- [161] D. M. Vriezema, M. Comellas Aragones, J. A. A. W. Elemans, J. J. L. M. Cornelissen, A. E. Rowan, R. J. M. Nolte, *Chem. Rev.* **2005**, *105*, 1445.
- [162] K. Srinivasan, B. C. Gibb, *Chem. Comm.* **2008**, 4640.
- [163] A. Guerrero, R. Herrero, E. Quintanilla, J. Z. Dávalos, J.-L. M. Abboud, P. B. Coto, D. Lenoir, *Chem. Phys. Chem.* **2010**, *11*, 713.
- [164] W. L. Yang, J. D. Fabbri, T. M. Willey, J. R. I. Lee, J. E. Dahl, R. M. K. Carlson, P. R. Schreiner, A. A. Fokin, B. A. Tkachenko, N. A. Fokina, W. Meevasana, N. Mannella, K. Tanaka, X. J. Zhou, T. van Buuren, M. A. Kelly, Z. Hussain, N. A. Melosh, Z.-X. Shen, *Science* **2007**, *316*, 1460.
- [165] A. A. Fokin, B. A. Tkachenko, P. A. Gunchenko, D. V. Gusev, P. R. Schreiner, *Chem. Eur. J.* **2005**, *11*, 7091.
- [166] H. W. Geluk, L. M. A. Schlatmann, *Tetrahedron* **1968**, *24*, 5361.
- [167] A. A. Fokin, T. S. Zhuk, A. E. Pashenko, P. O. Dral, P. A. Gunchenko, J. E. P. Dahl, R. M. K. Carlson, T. V. Koso, M. Serafin, P. R. Schreiner, *Org. Lett.* **2009**, *11*, 3068.
- [168] T. Courtney, D. E. Johnston, M. A. McKervery, J. J. Rooney, *J. Chem. Soc., Perk. Trans.* **1972**, 2691.
- [169] Z. Kafka, L. Vodicka, M. Hajek, *Fresenius Z. Anal. Chem.* **1984**, *318*, 354.
- [170] A. P. Marchand, R. W. Allen, *J. Org. Chem.* **1974**, 39.
- [171] P. E. Eaton, L. Cassar, R. A. Hudson, D. R. Hwang, *J. Org. Chem.* **1976**, *41*.
- [172] A. P. Marchand, G. V. Madhava Sharma, G. S. Annapurna, P. R. Pednekar, *J. Org. Chem.* **1987**, 52.
- [173] M. Nakazaki, K. Naemura, *J. Org. Chem.* **1977**, 42.
- [174] M. Nakazaki, K. Naemura, S. Nakahama, *J. Org. Chem.* **1978**, 43.
- [175] A. P. Marchand, Y. Wang, C. Ren, V. Vidyasagar, D. Wang, *Tetrahedron* **1996**, 52.
- [176] T. G. Dekker, D. W. Oliver, A. Venter, *Tetr. Lett.* **1980**, 21.

- [177] A. M. Aleksandrov, A. V. Turov, M. Y. Kornilov, V. P. Kuhar, *Zh. Org. Khim.* **1991**, 37, 2566.
- [178] J. C. McKennis, L. Brener, J. S. Ward, R. Pettit, *J. Am. Chem. Soc.* **1971**, 93.
- [179] M. P. Fleming, J. E. McMurry, *Org. Synth.* **1981**, 60.
- [180] S. C. Swen-Walstra, G. J. Visser, *J. Chem. Soc. D* **1971**, 82.
- [181] F. P. DiSanzo, P. C. Uden, S. Siggia, *Anal. Chem.* **1980**, 52, 906.
- [182] R. R. Heath, J. H. Tumlinson, R. E. Doolittle, A. T. Proveaux, *J. Chromatogr. Sci.* **1975**, 13, 380.
- [183] J.-L. M. Abboud, I. Alkorta, J. Z. Davalos, *J. Phys. Org. Chem.* **2001**, 14, 839.
- [184] F. A. Carey, *Organic Chemistry, 5th Ed.*, **2004**.
- [185] P. R. Schreiner, L. V. Chernish, P. A. Gunchenko, E. Y. Tikhonchuk, H. Hausmann, M. Serafin, S. Schlecht, J. E. P. Dahl, R. M. K. Carlson, A. A. Fokin, *Nature* **2011**, 477, 308.
- [186] S. Grimme, C. Mück-Lichtenfeld, G. Erker, G. Kehr, H. Wang, H. Beckers, H. Willner, *Angew. Chem. Int. Ed.* **2009**, 48, 2592.
- [187] S. Grimme, *J. Comput. Chem.* **2006**, 27 1787.
- [188] Y. Zhao, D. G. Truhlar, *Theor. Chem. Acc.* **2008**, 120, 215.
- [189] S. Grimme, J. Antony, S. Ehrlich, H. Krieg, *J. Chem. Phys.* **2010**, 132, 154104.
- [190] M. J. Frisch, G. W. Trucks, H. B. Schlegel, G. E. Scuseria, M. A. Robb, J. R. Cheeseman, J. A. Montgomery Jr., T. Vreven, K. N. Kudin, J. C. Burant, J. M. Millam, S. S. Iyengar, J. Tomasi, V. Barone, B. Mennucci, M. Cossi, G. Scalmani, N. Rega, G. A. Petersson, H. Nakatsuji, M. Hada, M. Ehara, K. Toyota, R. Fukuda, J. Hasegawa, M. Ishida, T. Nakajima, Y. Honda, O. Kitao, H. Nakai, M. Klene, X. Li, J. E. Knox, H. P. Hratchian, J. B. Cross, V. Bakken, C. Adamo, J. Jaramillo, R. Gomperts, R. E. Stratmann, O. Yazyev, A. J. Austin, R. Cammi, C. Pomelli, J. W. Ochterski, P. Y. Ayala, K. Morokuma, G. A. Voth, P. Salvador, J. J. Dannenberg, V. G. Zakrzewski, S. Dapprich, A. D. Daniels, M. C. Strain, O. Farkas, D. K. Malick, A. D. Rabuck, K. Raghavachari, J. B. Foresman, J. V. Ortiz, Q. Cui, A. G. Baboul, S. Clifford, J. Cioslowski, B. B. Stefanov, G. Liu, A. Liashenko, P. Piskorz, I. Komaromi, R. L. Martin, D. J. Fox, T. Keith, M. A. Al-Laham, C. Y. Peng, A. Nanayakkara, M. Challacombe, P. M. W. Gill, B. Johnson, W. Chen, M. W. Wong, C. Gonzalez, J. A. Pople, Gaussian 03, Revision D.02; Gaussian, Inc, Wallingford CT, **2004**.
- [191] R. A. Pascal, C. M. Wang, G. C. Wang, L. V. Koplitz, *Cryst. Growth Des.* **2012**, 12, 4367.
- [192] N. C. Craig, P. Groner, D. C. McKean, *J. Phys. Chem. A* **2006**, 110, 7461.

- [193] J. L. Carlos, S. H. Bauer, *J. Chem. Soc., Faraday Trans. 2* **1974**, 70, 171.
- [194] G. Casalone, T. Pilati, M. Simonetta, *Tetr. Lett.* **1980**, 21, 2345.
- [195] O. Ermer, *Angew. Chem. Int. Ed.* **1983**, 22, 998.
- [196] O. Klein, H. Hopf, J. Grunenberg, *Eur. J. Org. Chem.* **2009**, 2009, 2141.
- [197] H. M. Sulzbach, E. Bolton, D. Lenoir, P. v. R. Schleyer, H. F. Schaefer, *J. Am. Chem. Soc.* **1996**, 118, 9908.
- [198] P. R. Schreiner, O. Lauenstein, E. D. Butova, P. A. Gunchenko, I. V. Kolomitsin, A. Wittkopp, G. Feder, A. A. Fokin, *Chem. Eur. J.* **2001**, 7, 4996.
- [199] P. R. Schreiner, O. Lauenstein, I. V. Kolomitsyn, N. Suad, A. A. Fokin, *Angew. Chem. Int. Ed.* **1998**, 37, 1895.
- [200] A. I. Vogel, *Practical Organic Chemistry*, 5th Ed., **1996**.
- [201] R. B. Moffet, *Org. Synth.* **1952**, 32, 41.
- [202] T. M. Gund, M. Nomura, V. Z. Williams Jr., P. v. R. Schleyer, C. Hoogzand, *Tetr. Lett.* **1970**, 11, 4875.
- [203] R. C. Cookson, E. Crundwell, R. R. Hill, J. Hude, *J. Chem. Soc.* **1964**, 3062.
- [204] T. G. Dekker, D. W. Oliver, *S. Afr. J. Chem.* **1979**, 32.
- [205] J. C. Barborak, D. Khoury, W. F. Maier, P. v. R. Schleyer, E. C. Smith, W. F. Smith, C. Wyrick, *J. Org. Chem.* **1979**, 44, 4761.

Acknowledgements

I would like to express my gratitude to all those people who supported me and contributed into this work.

At first of all, I would like to thank my supervisor Prof. Dr. Peter R. Schreiner, Ph. D. for giving me this excellent opportunity to work in his group, scientific supervision, encouragement and support.

I would like to thank Prof. Dr. Andrey A. Fokin, D. Sc. for his knowledge and valuable advices in both experimental and theoretical chemistry of cage compounds.

Special thanks to Dr. Nataliya A. Fokina, Ph. D. and Dr. Boryslav Tkachenko, Ph. D. for support, late evening solvent and compound loans and talks about chemistry or not. You kept me running every day. Thanks to Dr. Hartmut Schwertfeger, my lab neighbor and fellow-in-need. Would there be anything in the world you could not handle by just a few calls?

Many thanks to our group members, who donated their valuable time to me: Dipl.-Chem. Mareike M. Machuy, Dr. Adelina Nemirowski, Dr. Zhiguo Zhang, Dipl.-Chem. Volker Lutz, Dr. Christian E. Müller, Dipl.-Chem. Christian Kleiner, Dr. Parham Rooshenas, Dipl.-Chem. Katharina M. Lippert, Dr. Lucas Wanka, Dr. Mike Kotke, Dr. Torsten Weil, Dr. Shadi Amiri, Dr. Ekaterina Butova.

I would like to thank Dr. Heike Hausmann and Antonie Pospiech for time spent for my NMR experiments – and there've been a lot; Dr. Erwin Röker and Beatrix Todt for HR-MS, GC/MS and GC experiments; Dr. M. Serafin for X-Ray analysis and deciphering of my compounds; Rainer Schmidt and Anike Mertz for the HPLC separations; Roland Meurer for the elemental analyses; Volker Erb for constant flow of chemicals and Jürgen Merthe for glassware.

I would like to thank also my Kiev colleagues: Dr. Pavel A. Gunchenko, Nguyen Duc Lan Anh, Alexander E. Pashenko, Olga V. Kovalenko, Tetyana V. Shamota, Dr. Lesya V. Chernysh.

The financial support by Deutscher Akademischer Austauschdienst (DAAD) and Deutsche Forschungsgemeinschaft (DFG) is gratefully acknowledged. Many thanks I owe to Justus-Liebig

Universität, Giessen and National Technical University of Ukraine “Kiev Polytechnic Institute” for support and workspace.

And at last but not least I would like to thank my family. Words are poor, but feeling is great.